Working towards a plant-produced Bovine papillomavirus vaccine: Expression of BPV1 virus-like particles and pseudovirions in *Nicotiana benthamiana*

Inge Pietersen

PTRING009

Dissertation presented for the degree of

Master of Science

In the Department of Molecular and Cell Biology

University of Cape Town

April 2019

Full Name: Inge Pietersen

Student Number: PTRING009

Course: MCB5005W

Plagiarism Declaration

I, Inge Pietersen, declare that this dissertation, submitted for the degree of Master of Science at the University of Cape Town under the supervision of Dr. Inga Hitzeroth, Dr. Albertha van Zyl, and Prof. Ed Rybicki, is my own work.

I have used the Harvard convention for citation and referencing, and this dissertation has been submitted to the TurnItIn module. I confirm that my supervisor has seen my report and any concerns revealed by such have been resolved with my supervisor.

Signature:

Signed by candidate

Date:

14 April 2019

Acknowledgements

Thank you to my supervisor, Dr. Inga Hitzeroth, and my co-supervisors, Dr. Alta van Zyl and Prof. Ed Rybicki, for all the wonderful opportunities, advice, freedom, and encouragement throughout this project – I have learnt a tremendous amount! Thank you also to Dr. Ann Meyers for always being available for friendly assistance and support.

Thank you to Guven Edgu and Markus Sacks for the warm hospitality in Germany, for teaching me the plant-cell pack method, and for introducing me to Bananaweizen. Thank you also to the Fraunhofer IME for the exchange research opportunity.

Thank you to Mohammed “Mo” Jaffer for the TEM training and assistance.

Thank you to Megan Hendriks and Faezah Davids for tissue culture training, and to Rosie Meggersee for help with biopanning.

Thank you to Prof. Rainer Fischer for the pTRA vectors, to Dr. Neil Christensen for the monoclonal antibodies, and to Dr. John Schiller’s group for the pSheLL and pYSEAP plasmids.

Thank you to Ryan Sweke for compiling the particle analysis script, general computer advice, climbs, and fireside physics lectures.

Thank you to the Council for Scientific Research (CSIR) and the Poliomyelitis Research Foundation (PRF) for providing funding for this project.

Thank you to my lab mates and lab friends at the Biopharming Research Unit for the wonderful work environment and comradery. Thank you especially to Francisco “Sensei” Pera, for helping me find my feet in the lab, and for all the science and non-science/nonsense discussions in the years to follow; Aleyo, for your endless advice, encouragement, help, and the many laugh and vent sessions; and Corrie, for all the hikes, climbs, potjies, and weekend adventures that made my time in Cape Town a treat.

Thank you to my dear friends Jannah, Bianca, and Rusty, for your love, support, and shared adventures – my life is a happier place with you in it.

Thank you to my family, for your love, support, and encouragement. Thank you especially to my mom for all our long phone calls, for listening to, but not taking my complaints too seriously, for always providing perspective, and for encouraging me to work to where my limits are, and to my dad for your empathy, sympathy, and great scientific and academic advice.

In memory of Terry Pratchett. Your stories have brought magic to my life and have inspired me beyond words. In spite of my best efforts, no dragons, faeries, or Feegles were produced in this study, but I hope it still makes for an interesting read.

“Universities are very familiar with bright, qualified school-leavers who arrive and then go into shock on finding that biology or physics isn’t quite what they’ve been taught so far. ‘Yes, but you needed to understand that,’ they are told, ‘so that now we can tell you why it isn’t exactly true.’ Discworld teachers know this, and use it to demonstrate why universities are truly storehouses of knowledge: students arrive from school confident that they know very nearly everything, and they leave years later certain that they know practically nothing. Where did the knowledge go in the meantime? Into the university, of course, where it is carefully dried and stored.” – Terry Pratchett (The Science of Discworld)

Table of Contents

1 Chapter 1: Literature Review 13

1.1 Literature Review 13

1.1.1 Introduction 13

1.1.2 Bovine papillomaviruses 14

1.1.3 Viral Structure and Classification 15

1.1.4 Virus Life Cycle 19

1.1.5 Bovine papillomavirus epidemiology and pathology 22

1.1.6 Global and Local Prevalence and Importance of BPV: 29

1.1.7 Economic and Agricultural Impacts 30

1.1.8 Equine Industry: 31

1.1.9 Tourism and Wildlife Conservation: 32

1.1.10 BPV as a model for HPV (and vice versa) 34

1.1.11 Treatment of BPV Infections 35

1.1.12 Prevention of BPV Infections: BPV Vaccines and Vaccine Candidates 37

1.1.13 Plant Expression Systems 42

1.1. Project Aims and Objectives: 45

2 Chapter 2: Expression Optimisation and Production of BPV1 VLPs in Plants 47

2.1 Introduction 47

2.1.1 Plant Expression Systems for the Production of Recombinant Proteins 47

2.2 Materials and Methods: 50

2.2.1 Construct Design and Generation of Recombinant *Agrobacterium* 50

2.2.2 Small-scale Expression Studies in *N. benthamiana* 56

2.2.3 Evaluation of L2 expression 59
2.2.4 Large-scale expression of BPV1 L1 and L1/L2 VLPs in *N. benthamiana* 60
2.2.5 Protein analysis of purified BPV VLPs 62
2.3 Results: 63
2.3.1 Generation and Confirmation of Constructs for Plant Expression 63
2.3.2 Optimisation of L1 Expression in Tobacco Plants 67
2.3.3 Antibody detection of BPV proteins 72
2.3.4 Evaluation of L2 expression 74
2.3.5 Mass Spectrometry 75
2.3.6 Large-scale purification of putative BPV1 L1 and L1/L2 VLPs in *N. benthamiana* . 77
2.4 Discussion 82
2.5 Conclusions and Future Work 86
3 Chapter 3: Expression and Optimisation of Plant-Produced PsVs 88
3.1 Introduction 88
3.1.1 Therapeutic vaccines 90
3.2 Materials and Methods: 93
3.2.1 Transient expression of BPV1 PsVs in *N. benthamiana* 93
3.2.2 Optimisation of PsVs Expression and Purification: 93
3.2.3 Quantification and analysis of PsV expression and activity 100
3.2.4 Pseudovirion neutralisation studies and antibody comparison 103
3.3 Results: 106
3.3.1 Purification of PsVs 106
3.3.2 Optimisation studies 113
3.3.3 Quantification and analysis of PsV expression and activity 127

3.4 Discussion 133
3.4.1 *In planta* production of BPV1 PsVs 133
3.4.2 Optimisation of PsV purifications: optimisation of density gradient centrifugation 135
3.4.3 Optimisation of PsV expression 137
3.4.4 Detection and Quantification of BPV1 PsVs and VLPs 138
3.4.5 Testing the immunogenic potential of BPV1 VLPs and PsVs 142
3.4.6 Analysis of PsV formation and stability 144
3.5 Conclusions and Future Work 147
4 Chapter 4: Discussion and Conclusions 149
4.1 General Discussion 149
4.2 Conclusions and Future Work 152
References: 155

Abstract:

Working towards a plant-produced Bovine papillomavirus vaccine: Expression of BPV1 virus-like particles and pseudovirions in plants

Inge Pietersen

April 2019

Bovine papillomaviruses (BPVs) are DNA viruses implicated in several diseases and cancers of considerable veterinary and agricultural importance in cattle, horses, as well as several wild animal species, leading to their economic depreciation through the deterioration of their function and appearance. As BPV is widespread, easily transmissible, and infection often occurs asymptomatically, it is imperative that interventions are carried out to mitigate the threat of outbreaks occurring in livestock. There is a demand for prophylactic vaccines to immunise animals routinely and from a young age so as to prevent infection from occurring, as there is currently no fully effective treatment against established disease. Virus-like particles (VLPs) have in recent years been adopted as safe and efficacious vaccine antigens, and pseudovirions (PsVs) as experimental vaccines and vectors for therapeutic agents. Prophylactic VLP-based candidate vaccines against BPV types 1, 2, and 4 have previously been produced, yet these produce antibodies which are largely type-specific, and are expensive and not widely available in developing countries, where food security and the use of cattle for meat, dairy, leather products, as well as draft animals, is often essential for survival. Plant-based expression systems for the production of biopharmaceuticals, such as vaccines, offer several advantages over traditional protein expression systems, chief of which is a reduction in production costs, improved biosafety features, and a potential for rapid scalability.

BPV1 is one of the most virulent BPV types and, as the most prevalent type, is responsible for the majority of BPV-related diseases. To address the lack of a cheap and readily-available vaccine, BPV1 VLPs and PsVs were expressed in *N. benthamiana* plants as a prelude to producing a candidate prophylactic and therapeutic vaccine. Expression of L1 and L1/L2 VLPs was successful, as was the encapsidation of a reporter gene plasmid into the L1/L2 VLPs, demonstrating the first successful *in planta* production of BPV PsVs. Several approaches to optimise VLP and PsV purification and expression were also explored, and significant increases in both protein expression levels and numbers of VLPs and PsVs was observed through the application of each of the following techniques: increasing acetosyringone induction concentrations from 200 µM to 500 µM; a brief heat-shock treatment of plants 2 days post agroinfiltration (dpi); and extending the harvesting time of plant biomass from 4dpi to 6dpi. Furthermore, purification and concentration of BPV1 particles was further enhanced through centrifugation of clarified plant extract on an iodixanol density gradient prepared with a 3M NaCl buffer. PsVs produced through these methods were shown to be capable of pseudo-infecting and expressing the reporter gene in mammalian HEK293TT cells, and neutralisation of the PsVs by different monoclonal antibodies was also demonstrated.

These findings highlight the potential use of BPV PsVs for a diverse range of functions, including their potential use as dual prophylactic-therapeutic vaccines, capable of delivering therapeutics or DNA vaccines to specific tissues, as well as their ability to be used as model organisms for the study of HPV and other PVs.

List of Abbreviations:

(k)Da	(kilo) Dalton
n	nano-
µ	micro-
m	milli-
m	meter
r	radius
d	diameter
bp	base pairs
=	equals/is
g	grams
g	gravitational force
L	litre/s
M	molar
h	hour/s
min	minute/s
s	second/s
rpm	revolutions per minute
v/v	volume per volume
w/v	weight per volume
F	fraction
dpi	days post infiltration
M	molecular marker
℃	degrees Celsius
V	Volts
Amp	Ampere
Ω	Ohm (resistance)

O/N	Overnight
OD	Optical density
Agrobacterium	*Agrobacterium tumefaciens*
AHS	African Horse Sickness Virus
BCIP	5-bromo-4-chloro-3-indolyl-phosphate
BPV(s)	Bovine papillomavirus(es)
BSA	Bovine serum albumin
CP	Capsid/coat protein
CsCl	Caesium chloride
DIVA	Differentiating Infected from Vaccinated Animals
DNA	Deoxyribonucleic acid
DPBS	Dulbeco's phosphate buffered saline
EDTA	Ethylenediaminetetraacetic acid
ELISA	Enzyme-linked immunosorbent assay
EtBr	Ethidium bromide
HPV(s)	Human papillomavirus(es)
HS	High salt
GC	Guanine and cytosine
IPTG	Isopropyl b-D-1-thiagalactopyranoside
LB	Luria broth
LB_A	LB media containing Ampicillin
LB_{RCK}	LB media containing Rifampicin, Carbenicillin, and Kanamycin
MAb(s)	Monoclonal antibodies
NAb(s)	Neutralising antibodies
NaOAc	Sodium acetate
ORF	Open reading frame

PA	Polyacrylamide
PAb(s)	Polyclonal antibodie(s)
PBS	Phosphate-buffered saline
PCR	Polymerase Chain Reaction
PEG	Polyethylene glycol
pNPP	p-Nitrophenyl phosphate
PsV(s)	Pseudovirion(s)
PV(s)	Papillomavirus(es)
RuBisCO	Ribulose-1,5-bisphosphate carboxylase/oxygenase
SDS	Sodium dodecyl sulphate
SEAP	Secreted embryonic alkaline phosphatase
TEM	Transmission Electron Microscopy
TSP	Total Soluble Protein
UTR	Untranslated region
VLP(s)	Virus-like particle(s)

1 Chapter 1: Literature Review

1.1 Literature Review

1.1.1 Introduction

Cutaneous papillomas, or warts, have been present in both animals and humans for centuries. The term papilloma, which originates from the Latin word for nipple, “papilla”, and the Greek suffix of “oma”, meaning tumour, refers to the nipple-like nodule created by warts or tumours on the skin (Araldi *et al.*, 2015). A viral aetiology of papillomas was established by Ciuffo in 1907, with Bovine papillomavirus (BPV) being the first virus recognised to be associated with papilloma formation, in 1955 (Ciuffo, 1907; Karamanou *et al.*, 2010). The transforming ability of BPV was discovered in 1963, and in 1982 the full BPV type 1 genome was sequenced, assembled, and published (Chen *et al.*, 1982; Araldi *et al.*, 2017). BPV belongs to the *Papillomaviridae* (PV) family, a group of hundreds of small dsDNA viruses, which are widespread and infect a broad range of animals (Nasir *et al.*, 2007; Araldi *et al.*, 2017). A growing body of work has revealed that nearly all mammalian species are prone to one or more papillomaviruses, and over 50 mammalian species have been shown to be infected with at least one type of species-specific papillomavirus. This includes humans, as well as many domestic and wild animal species (Borzacchiello and Roperto, 2008; Campo and Roden, 2010).

Papillomaviruses are usually highly species-specific, and appear to have co-evolved with their host species (Van Doorslaer, 2013; Munday, 2014; Trewby *et al.*, 2014). This theory is supported by the clustering of PVs infecting closely related host species, and the phylogenetic divergence of PVs correlating with divergence of their host species (Van Doorslaer, 2013). This theory is further supported by the similarity in GC (guanine and cytosine) content between PVs and their hosts’ genomes, as well as similarities in the replicative mechanisms adopted by PVs and their hosts (Van Doorslaer, 2013; Trewby *et al.*, 2014). Papillomaviruses are generally also cell-type specific: the majority are strictly epitheliotropic, although some may also infect dermal

fibroblasts (Borzacchiello *et al.*, 2003; Jelinek and Tachezy, 2005; van Dyk *et al.*, 2009). It is due to the high species specificity of PVs that BPVs, among other animal PVs, have often been used as models for the study of HPV infections, to determine their interactions with their hosts and environmental co-factors (Borzacchiello and Roperto, 2008).

1.1.2 Bovine papillomaviruses

There have been approximately 180 human PVs and over 160 animal PVs characterised, 23 of which are bovine in origin (Koch *et al.*, 2018). Bovine papillomaviruses, also referred to as *Bos Taurus* papillomaviruses (BPVs), are viral pathogens which infect the epithelial surfaces of cattle and equids, where they are associated with the formation of both benign warts and malignant tumours (Campo, 2002b; de Villiers *et al.*, 2004). Cattle (*Bos taurus*) are the natural and most common hosts for infection by BPVs, in which these viruses induce exophytic (outward growing) papillomas of the cutaneous or mucosal epithelia (Campo, 1997; Doorbar, 2005).

Like other PVs, BPVs are largely species-specific, and generally infect only their natural hosts, even under experimental conditions. The only known exceptions of papillomaviruses crossing species barriers and infecting non-host species are BPV1 and, to a lesser extent, BPV2, which infect not only cattle and other ruminants, but commonly infect horses and other equids (Chambers *et al.*, 2003; Bocaneti *et al.*, 2016; Lunardi *et al.*, 2016). There is also recent evidence suggesting that BPV-5 and-13 are also capable of infecting other species such as horses (Lunardi *et al.*, 2013; Bocaneti *et al.*, 2016). In bovines, BPV1 and-2 are aetiological agents of papillomas, which usually regress spontaneously. In horses, however, BPV1 and-2 cause persistent, locally invasive, fibroblastic skin tumours, known as sarcoids (Chambers *et al.*, 2003; Nasir *et al.*, 2007), and it has recently been found that BPV2 is also capable of infecting sheep (Mazzuchelli-de-Souza *et al.*, 2018; Roperto *et al.*, 2018). In addition to the aforementioned animals, papillomatosis associated with BPV infection also afflicts various wild animals. In South Africa, BPV1 and-2 have been found in tumours of giraffes (*Giraffa camelopardalis*), Cape mountain zebra (*Equus zebra zebra*), African buffalo (*Syncerus caffer*), and sable antelope (*Hippotragus niger*) (van Dyk *et al.*,

2009; Williams *et al.*, 2011), and evidence of BPV has also been found in lesions of water buffalo (*Bubalis bubalis*) (Silvestre *et al.*, 2009; Roperto *et al.*, 2013) and bison (*Bison bonasus*) (van Dyk *et al.*, 2009).

1.1.3 Viral Structure and Classification

1.1.3.1 Viral Structure:

Bovine papillomaviruses, like other PVs, have non-enveloped isometric capsids that are approximately 50-60nm in diameter (Figure 1.1) (Chen *et al.*, 2000). These paracrystalline structures are often formed within the nuclei of infected cells, and capsids consist of two protein types: these are L1, the major capsid protein, and L2, the minor capsid protein, which is present at roughly 1/30th the abundance of L1, although the precise ratio is unknown and probably variable (Buck *et al.*, 2008; Buck *et al.*, 2013). These two proteins can form T=1 pentamers, which consist of an association of 1 x L2 and 5 x L1 proteins. When 72 of these pentameric capsomeres assemble, they form the T=7 quasi-icosahedral viral capsid (Kirnbauer *et al.*, 1996; Modis *et al.*, 2002). An atomic model of this structure has shown that the L1 protein is exposed on the viral surface, which indicates its role in infection and immunogenicity (Modis *et al.*, 2002; Wolf *et al.*, 2010). The L1 protein facilitates viral binding to the cell surface, by interacting with the cell surface heparan sulphate proteoglycans (Chen *et al.*, 2000; Wolf *et al.*, 2010). As the main role of the L2 minor capsid protein is to bind to viral DNA and induce virion assembly, its presence is most abundant in mature papillomas, and it has only been detected as a nuclear antigen in the different epithelial and mucosal layers (Borzacchiello and Roperto, 2008; Buck *et al.*, 2008). However, it appears that L2 may also play a role in infectivity. This has been demonstrated in studies of animals vaccinated with L2, which demonstrate the ability of the L2 protein to confer immunogenicity (Karanam *et al.*, 2009; Jagu *et al.*, 2011; Lima *et al.*, 2014; Hainisch *et al.*, 2017).

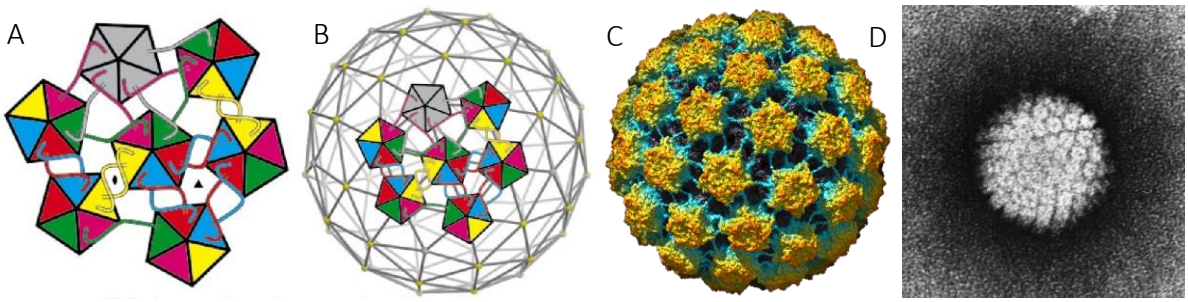

Figure 1.1 Bovine papillomavirus structure.

Diagram illustrating packaging of pentamer packaging and the C-terminal arm interchange in papillomaviruses. Pentamers (/capsomeres) consist of 5 copies of monomeric L1 protein, assembled in a circular complex arranged around a single copy of the L2 minor capsid protein in the middle. In papillomaviruses the L1 C-terminal arm invades its neighbouring pentamer, around which it wraps and inserts back into its pentamer of origin (Buck *et al.*, 2008). Pentamers are arranged in T=1 icosahedral particles, which consist of 12 pentamers, illustrated in **Figure 1.1.A.** In these particles, pentamers are centred along 5-fold symmetry axes, and the arm-to-arm interactions are distinct from those in the virion. Six sets of the T=1 particles assemble into the full T=7 icosahedral lattices, which consist of 72 copies of the L1/L2 pentamers. Models of the self-assembled full viral capsid are depicted in **Figure 1.1.B** and **C**. **Figure 1.1.D** shows an electron microscopy image of a T=7 PV virion. **Figure 1.1.A, B.,** and **C.** were sourced with permission from Wolf *et al.* (2010), and **Figure 1.1.D** was obtained from Wikimedia Commons at [https://en.wikipedia.org/wiki/File:Papilloma_Virus_%28HPV%29_EM.jpg, Accessed 22.04.2018].

Encapsidated within the capsid assemblage is the covalently closed circular double-stranded BPV genome. The BPV genome is composed of between 7300-8000 nucleotides, which are complexed with cellular histones and condensed into a minichromosome (Chen *et al.*, 2000; Bocaneti *et al.*, 2016). The genomes of PVs are functionally divided into domains on the basis of transforming capabilities, and consists of three different regions: **1**.) the long control region (LCR), which contain the elements required for replication of viral DNA; **2**.) the open reading frame (ORF) region, corresponding to early genes (E1 and E2) which encode for proteins associated with transcription and cell transformation, as well as "adaptive proteins", E5 and/or E6 and/or E7, that are associated with uncontrolled cell proliferation and transformation processes; and **3**.) the late gene region, encoding for the viral capsid proteins, L1 and L2 (Doorbar, 2005; Van Doorslaer, 2013; Wilson *et al.*, 2013).

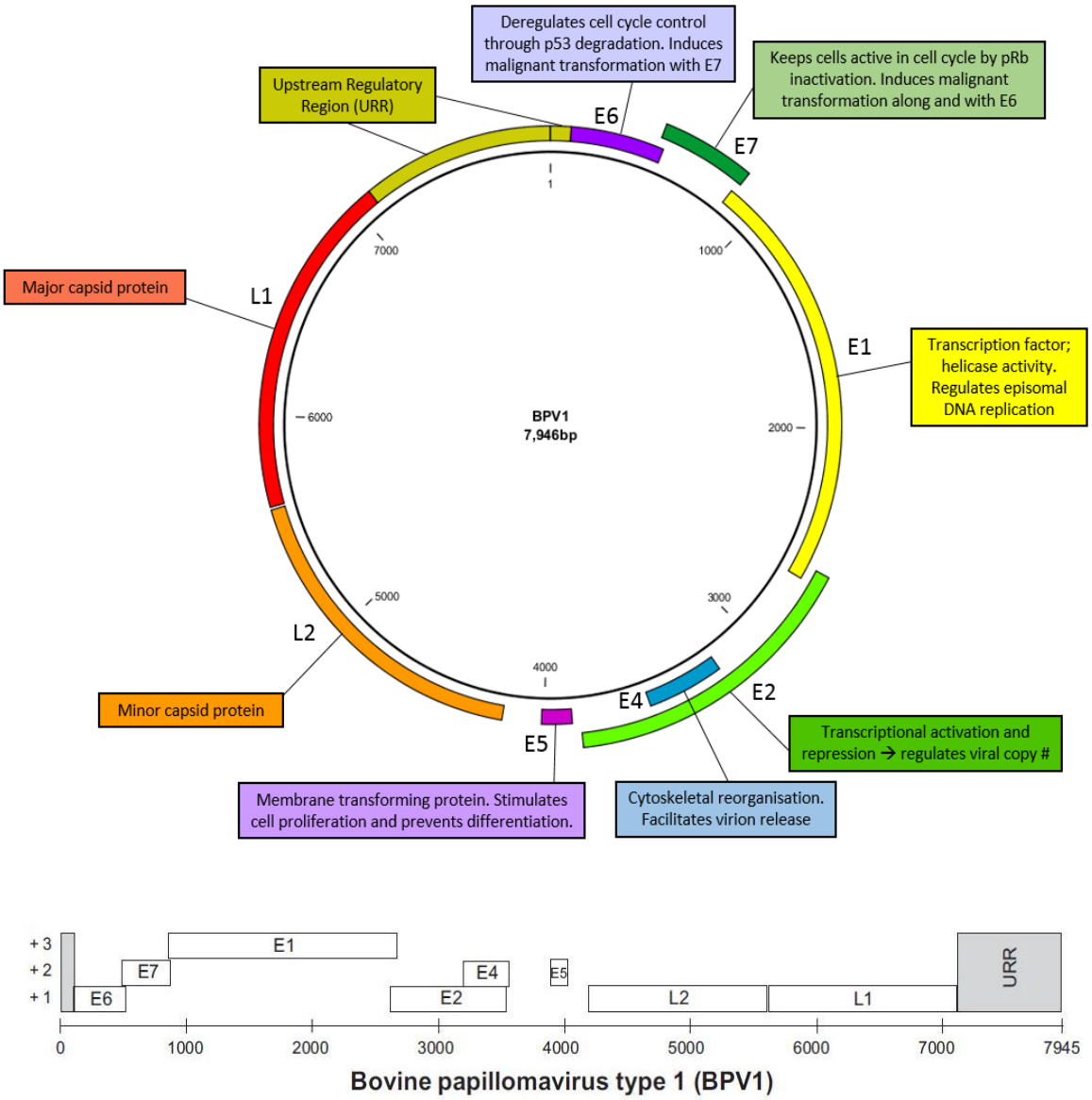

Figure 1.2. Schematic of BPV1 genome and functions

Figure 1.2.A. depicts a circularised BPV1 genome, with gene functions annotated on the figure. This figure was modified from Christensen *et al.* (2017). **Figure 1.2.B.**, obtained with permission from Rector and Van Ranst (2013), illustrates a linearised form of the BPV1 genome, and indicates the overlapping reading frames in which the various BPV1 proteins are expressed.

1.1.3.2 Classification of Bovine papillomaviruses:

Papillomaviruses are classified by genomic properties rather than serological differences, and are therefore defined by genotypes (Bernard *et al.*, 2010). To date, 23 different BPV types (BPV1 – BPV23) have been identified (https://pave.niaid.nih.gov), associated with different

histopathological lesions (da Silva *et al.*, 2016; Bauermann *et al.*, 2017). These BPVs have been genetically characterised by sequence analysis of a highly conserved L1 region, using the degenerate primer pairs (FAP59/FAP64 or MY09/MY11) which were initially designed for HPV detection, and which have been used for the identification and characterisation of most PV types in affected species (Daudt *et al.*, 2018). Following genetic characterisation, the BPV types have been further classified phylogenetically into five genera. 1.) *Xipapillomaviruses* (*Xi*-PVs), which contains the largest number of BPVs, and consists of the purely epitheliotropic BPV3,-4,-6,-9,-10,-11, and-15, two species of BPV12, and three currently unclassified types, BPV17,-20, and-23. The genomes of BPV3,-4, and-6, lack the E6 ORF, which has been replaced with E5. 2.) The *Deltapapillomaviruses* (*Delta*-PVs), which include BPV1, -2, -13, and -14, are associated with fibropapillomas (benign tumours of the epithelium and underlying derma) in cattle, and equine sarcoids in equids. These are the most prevalent and economically important BPVs, due to their ability to infect various species. 3.) *Epsilonpapillomaviruses* (*Epsilon*-PVs), which comprises of BPV5 and -8; 4.) *Dyoxipapillomaviruses* (*Dyoxi*-PVs), which contains only BPV-7, and are phylogenetically distant from the other BPV types; and three new BPV types, BPV16,-18, and-22, which were classified into 5.) the *Dyokappapapillomavirus* (*Dyokappa*-PV) genus. Two other recent additions, BPV19 and-21, are currently not classified within the existing genera (Bernard *et al.*, 2010; Hatama, 2012; Lunardi *et al.*, 2013; da Silva *et al.*, 2016; Lunardi *et al.*, 2016; Bauermann *et al.*, 2017; Daudt *et al.*, 2018).

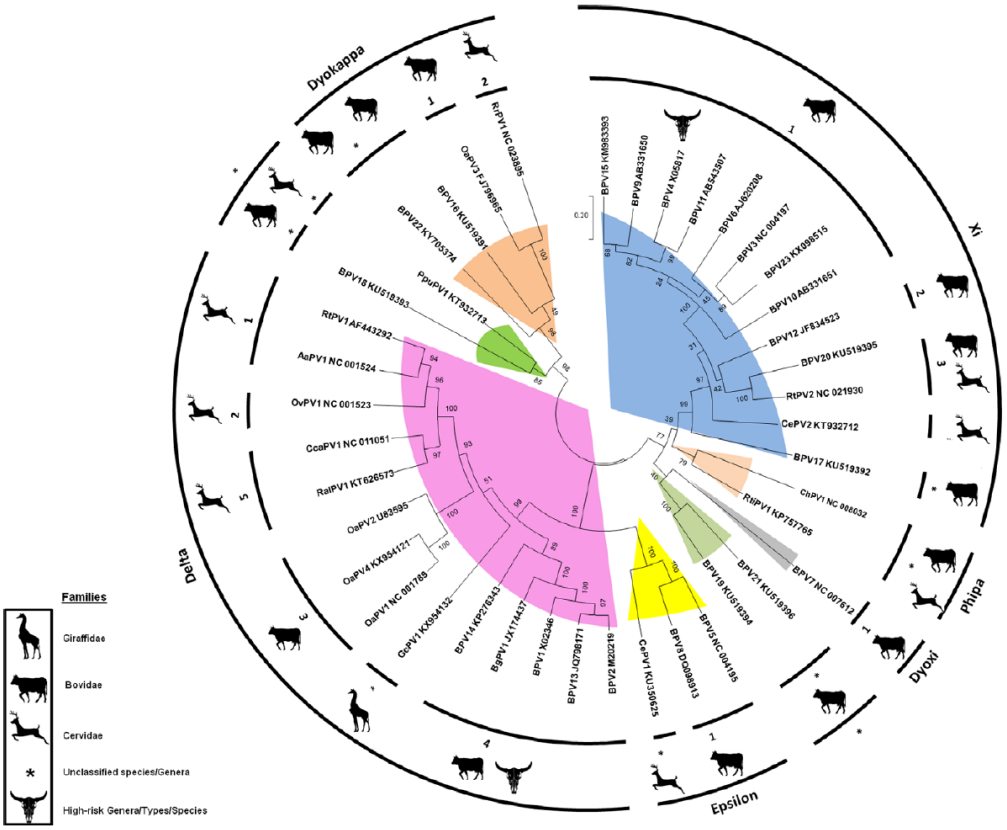

Figure 1.3. Phylogenetic tree showing the evolutionary relationship between Ruminantia PVs, based on their L1 gene sequences.

Tree topology of 41 nucleotide sequences, drawn to scale, with substitutions per site indicated by branch lengths. Positions containing gaps and missing data were excluded from analysis and a total of 1307 positions were included in the final data set. The tree was obtained by applying Neighbour-Join and BioNJ algorithms to a matrix of pairwise distances estimated through the maximum composite likelihood (MCL) approach, and then selecting the highest log likelihood value, after an initial heuristic search was performed. Evolutionary rate differences among the sites were evaluated using a discrete Gamma distribution to divide these sites in 5 categories. MEGA7 was used to conduct evolutionary analyses.

Obtained with permission/modified from (Daudt *et al.*, 2018).

1.1.4 Virus Life Cycle

Papillomaviruses are genetically heterogeneous but have a similar biology (Brandt, 2016). Host-specific PVs have a specified tropism for stratified squamous epithelial cells, and infect the epithelia of humans and animals, upon which they cause hyperproliferative lesions referred to

as warts or papillomas (Cerqueira and Schiller, 2017). Replication of the bovine papillomavirus, as with other PVs, is tightly associated with the maturation and differentiation of keratinocytes, which form the outer layer of the epidermis, as well as other epithelial surfaces of the genitals, oral cavity, and oesophagus (Campo, 1997). This process is traditionally divided into two phases: the early phase, during which replication of the viral genome occurs, and the late phase, in which capsid protein expression and viral assembly takes place (Doorbar, 2005; Cerqueira and Schiller, 2017).

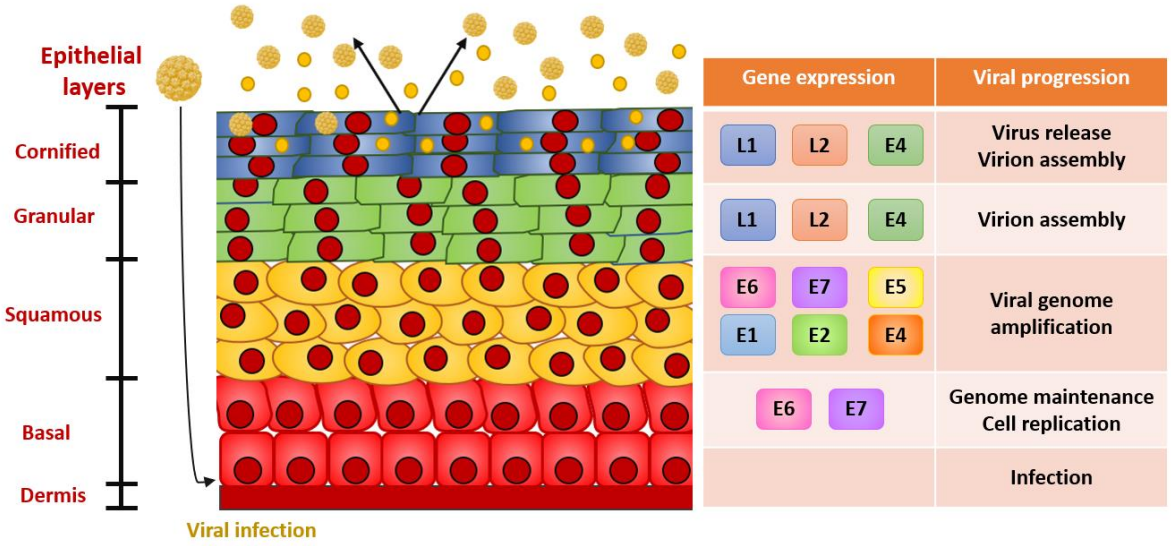

Figure 1.4. Progression of PV life cycle and differential protein expression.

This figure depicts the organisation of the double-stranded DNA BPV genome, and the phases of protein expression linked with the differentiation of the epithelial cells. The genome is divided into the early (E) region, which codes for replication proteins E1, E2, E4, E5, E6, and E7; the late (L) region, coding structural proteins L1 and L2, which are expressed at the most differentiated epithelial layers, in the granular and cornified cells; and long control region (LCR), which contains elements required for viral replication. This image was modified from Araldi *et al.* (2017).

In order to establish a persistent infection, the virus must infect the mitotically active basal cell layer, within which steady-state replication of the viral genome can take place. This process is demonstrated in Figure 1.4. The vegetative replication of the genome for viral proliferation and dissemination, characterised by high copy number amplification, occurs only after the division of

the cell, and once the daughter cell has moved into the upper layers of the epithelium and initiated differentiation (Cerqueira and Schiller, 2017). The early phase therefore initiates as the virus infects the basal keratinocyte cells, to which it is exposed through abrasions or wounds. While in the basal and suprabasal layers, the genome expresses its early genes, E1 and E2. These genes encode for the proteins involved in cell transformation and viral replication, and can subvert cellular proliferation, leading to cell transformation. The E1 protein plays a role in viral replication, though it is unclear whether it also contributes to the pathogenesis of viral infection (Campo *et al.*, 1994; Peh *et al.*, 2002). The E2 protein is active in both viral DNA replication, as well as transcriptional control of the viral genes, including that of the E2 gene itself (Borzacchiello and Roperto, 2008). Bovine papillomavirus' transcriptional control depends largely on the interactions between 12 sites in the LCR and E2 protein, which is essential for the BPV life cycle. There are also several cellular transcription factors which maintain a delicate balance in their interactions with the LCR, and which regulate the expression of viral genes. Should this balance be disturbed, an increase in the transcription and expression of viral genes occurs, which results in a neoplastic state (Campo, 1997; Nasir *et al.*, 2007). Studies of E2 in *in vitro* systems have demonstrated the ability of the E2 protein to induce apoptosis, yet it is unknown whether it is also capable of inducing programmed cell death *in vivo* (Nasir *et al*., 2007; Yuan *et al*., 2010). The E4 ORF encodes for a set of small proteins generated by alternative splicing and posttranslational modifications, which are expressed in the granular layer. These proteins, which interact with the filamentous cytokeratin network, are prolific within papillomas, composing up to 30% of the total protein. While the functions of these interactions are not yet fully understood, it has been suggested that the E4 proteins interfere with proper keratinocyte differentiation, to favour viral DNA replication and virion assembly (Doorbar, 2013). The E5, E6, and E7 proteins are expressed within the deep layers of papillomas, and E7 throughout the lesions (Borzacchiello *et al.*, 2006; DiMaio and Petti, 2013). These proteins are all capable of cell transformation, overcoming cell cycle controls through the activation of growth factor receptors (E5), and the inactivation of suppressor proteins p53 and p105Rb, by E6 and E7 respectively (Tomita *et al.*, 2007; Tomaic, 2016). The relative significance of these proteins, and their roles in cell transformation, vary between the different PV types (Peh *et al.*, 2002).

1.1.5 Bovine papillomavirus epidemiology and pathology

1.1.5.1 Bovine papillomas

Papillomas are caused by species-specific papillomaviruses (Araldi *et al.*, 2017). Infection by *Delta-PVs* first leads to the transformation of sub-epithelial fibroblasts, followed by epidermal hyperplasias and papillomatosis, while *Xi-PVs* lead only to the transformation of the epithelial component, and *Epsilon-PVs* cause both fibropapillomas and epithelial papillomas (Jelinek and Tachezy, 2005; Borzacchiello and Roperto, 2008). These warts are often morphologically distinct and caused by different BPVs, and immunity to one does not necessarily confer immunity to others, except occasionally in the case of BPV1 and BPV2 (Shafti-Keramat *et al.*, 2009; Lima *et al.*, 2014; Hainisch *et al.*, 2017). Research on the molecular epidemiology of BPVs has found correlations between the viral type and specific lesions or tissue tropism, and it is only bovine *Delta-PVs* that are known to infect both epithelial and mesenchymal tissue, and which show cross-species infection (Roperto *et al.*, 2013; Bocaneti *et al.*, 2016; Roperto *et al.*, 2016a; Roperto *et al.*, 2016b).

In cattle, warts can occur on almost any part of the body, though these occur most commonly on the head, neck, shoulders, and occasionally on the back or abdomen (Campo, 1997; Borzacchiello and Roperto, 2008; Bocaneti *et al.*, 2016). Four BPV types are known to produce skin lesions, with types 1 and 2 responsible for the majority of warts found on the heads and necks of cattle, although warts may also occur in other areas like the vaginal mucosa, teats, penis, and gastrointestinal (GI) tract in the case of BPV2 (Borzacchiello *et al.*, 2003; Borzacchiello and Roperto, 2008; Hatama, 2012). When there are numerous lesions, these may be sufficiently characteristic to confirm the diagnosis, yet a definitive diagnosis requires the identification of the virus through molecular techniques, such as polymerase chain reaction (PCR), or its cytopathic effects on the individual cells (Araldi *et al.*, 2017; Palanivel *et al.*, 2017). Warts appear roughly two months after exposure. They are usually self-limiting and tend to regress spontaneously and drop off after several months, although they may sometimes persist for over a year (Campo, 1997). The degree and period of the lesions depend on the viral type, the area affected, and the degree of susceptibility of the host. In younger animals, multiple papillomas over various

epithelial and mucosal areas are often seen, whereas in older animals, single papillomas are most frequently found although these may not always be due to viral infection (Campo, 2002b; Campo and Roden, 2010). A persistent form of cutaneous papillomatosis with smaller papillomas may also sometimes be found in herds of older cattle (Campo *et al.*, 1994; Campo, 1997; Ugochukwu *et al.*, 2018). Papillomatosis may become a heard problem when a large group of young, susceptible animals become infected. When fibropapillomas, such as those characteristic of BPV1 and-2, affect the venereal regions, they may cause pain, disfiguration, and infection of the penis of young bulls, or dystocia (obstructed labour) when the vaginal mucosa of heifers is affected (Borzacchiello and Roperto, 2008; Monke *et al.*, 2018; Moroni *et al.*, 2018).

Co-infection with one or multiple types of BPV is often reported in cattle, with various combinations or simultaneous presence of different BPVs found within a single lesion. An impaired immune response is believed to predispose hosts to such co-infections (Carvalho *et al.*, 2013; Bocaneti *et al.*, 2016; Roperto *et al.*, 2016b). In a study by Carvalho *et al.* (2013), PV co-infections were detected in 90% of the samples examined from cattle with a high incidence of cutaneous papillomas. There is further evidence that δ-PVs and ξ-PVs co-infections frequently occur in both domestic and wild ruminants, and BPV14 was recently detected in cutaneous warts alongside BPV2 and BPV3 (da Silva *et al.*, 2016; Savini *et al.*, 2016). These findings suggest that, like human PVs, phylogenetically related and unrelated BPVs are capable of co-infecting their hosts. While the implications of this discovery are yet to be elucidated, it has been suggested that the joint interactions of the different BPV types may act in a synergistic manner to transform cells (Roperto *et al.*, 2016a). It has further been proposed that the simultaneous infection by certain BPV types may interfere with the biological behaviour of bovine bladder tumours, in a manner similar to what has been reported for human cervical cancer, in which type-specific interactions between the genotypes in multiple infections may either reduce or increase rates of high-risk cervical lesions and cancers. Specifically, there seemed to be a reduced risk of squamous cervical cancer development in co-infections of high-risk and low-risk HPV types, suggesting that intergenomic competition, superinfection exclusion, or a more effective immune response triggered by the multiple infections may interfere with the progression to invasive cervical cancer

(Salazar *et al.*, 2015; Sundström *et al.*, 2015; Roperto *et al.*, 2016a; Roperto *et al.*, 2016b; Biryukov *et al.*, 2018).

1.1.5.2 Bovine cancers

While the majority of BPV infections are asymptomatic or result in minor lesions that regress within a few months following infection, BPVs also have oncogenic potential (Borzacchiello and Roperto, 2008). Occasionally, BPV-induced lesions may persist and become malignant, progressing to squamous cell cancer or, less frequently, adenocarcinoma (a malignant tumour formed in the mucus-secreting glands in epithelial tissue). This occurs particularly with mucosal lesions, or in the presence of environmental co-factors or carcinogens. Several papillomaviruses are consistently associated with neoplastic progression and cancers, and these are classified as 'high-risk' viruses (Borzacchiello and Roperto, 2008; Campo and Roden, 2010; Pesavento *et al.*, 2018).

The development of such malignancies in the presence of carcinogens has been demonstrated experimentally in studies of cancers in the urinary bladder and upper alimentary tract of cattle, which showed a strong correlation with the feeding of cattle on bracken fern (genus *Pteridium*) (Campo *et al.*, 1992; Campo *et al.*, 1994; Roperto *et al.*, 2008). Bracken is thought to be the only higher plant which causes cancers in animals, as it contains immunosuppressive, mutagenic, clastogenic and carcinogenic chemicals such as ptaquiloside and quercetin, which is a co-carcinogen of BPV4 *in vivo* (Jarrett *et al.*, 1990; Roperto *et al.*, 2016a). Cattle consuming bracken often develop upper alimentary tract cancer, in the case of BPV4, and urinary bladder cancers, which are occasionally associated with BPV1, and more commonly with BPV2 and BPV13 (Borzacchiello and Roperto, 2008; Roperto *et al.*, 2013; Roperto *et al.*, 2016b). In a study by Campo *et al.* (1992), BPV2 was found in 69% of experimental bladder cancers, and in half of the naturally occurring cases. A further study by Borzacchiello *et al.* (2003) found a strong association of BPV2 with urinary bladder cellular abnormalities. These findings suggest that BPV2 plays a role in bladder oncogenesis. A recent study by Roperto *et al.* (2016a) also revealed the presence of

BPV14 DNA in bovine bladder tumours. The BPV14 DNA was isolated either on its own, or in combination with other *Delta*-PVs. These findings indicate that BPV14 could also be involved in bladder neoplasias, as it possesses an E5 oncoprotein capable of inducing cell proliferation. Furthermore, the presence of BPV14 in Europe suggests that it, like other *Delta*-PVs has a global distribution (Roperto *et al.*, 2016a; Roperto *et al.*, 2016b). This is a significant problem, especially in regions where bracken is endemic, such as large areas of Scotland and New Zealand, on which cattle, ovines, and other ungulates regularly graze.

1.1.5.2.1 Equine Sarcoids

Bovine papillomaviruses also play a role in the aetiology and pathology of equine sarcoids. In 1936, Jackson coined the term "equine sarcoid" to describe a characteristic fibroblastic neoplasm which was distinct from the neoplasms of papillomas, fibromas, and fibrosarcomas, and occurred in the skin of horses, donkeys, and mules (Chambers *et al.*, 2003). These mainly affect young- to middle-aged horses between 2-6 years old, of all types and breeds. Equine sarcoids are local, aggressive, non-metastasising, and non-regressing fibroblastic skin tumours, and are the most prevalent skin tumours in horses worldwide, representing ~70% of all skin tumours of horses and up to 90% of all equine tumours (Ashrafi *et al.*, 2008; Bogaert *et al.*, 2008; van Dyk *et al.*, 2009; Koch *et al.*, 2018).

Sarcoids may occur as single or multiple lesions of various forms and sizes, ranging from small wart-like lesions to large, ulcerated fibrous growths (Chambers *et al.*, 2003; Bogaert *et al.*, 2010). The histological resemblance of equine sarcoids to fibrotic sections of bovine fibropapillomas led researchers to suspect the aetiology and involvement of BPVs in equine sarcoid formation. This association was confirmed by the intradermal inoculation of cell-free extract from cattle warts into healthy horses, which subsequently developed sarcoid lesions (Chambers *et al.*, 2003; Yuan *et al.*, 2007). These results have further been confirmed by the consistent identification of BPV DNA and various viral genes expressed in sarcoids (Bogaert *et al.*, 2010; Lunardi *et al.*, 2013). Through various molecular techniques, such as Southern blot hybridisation and PCR, researchers

have detected BPV DNA in 86-100% of equine sarcoids examined (Yuan *et al.*, 2007; Bocaneti *et al.*, 2016).

Equine sarcoids are classified into 6 clinical types; occult, verrucous, nodular, fibroblastic, mixed, and malevolent, and histopathological analysis may be required for diagnosis and to distinguish these from other skin lesions (Chambers *et al.*, 2003; van Dyk *et al.*, 2009). PCR techniques are used for the analysis of both benign and malignant PV-associated lesions, and these techniques have been used to determine the role of BPV in the formation of equine sarcoids (van Dyk *et al.*, 2009). Most equine sarcoids are found to contain viral DNA of either BPV1 or-2, or both, and both BPV types have been detected in horses, donkeys, and mules, as well as in captive zebras (*Equus burchelli boehmi*) in Mexico and the USA (Lohr *et al.*, 2005). In South Africa BPV has also been associated with sarcoids of Cape mountain zebra, giraffes, sable antelope, and African buffalo (van Dyk *et al.*, 2009; Williams *et al.*, 2011). The frequency of BPV1 and-2 recovered from sarcoids varies over diverse geographic areas, and while BPV1 is more common in horses in Europe and Australia, BPV2 is more prevalent in horses in the USA and Canada (Lunardi *et al.*, 2013).

While it is still unclear what the immune response to equine sarcoids in horses are, several possible immune evasion mechanisms have been described (O'Brien and Saveria Campo, 2002; Chambers *et al.*, 2003). These mechanisms may contribute to the persistence and progression of PV-associated disease, and it has been suggested that the genetic predisposition may explain why certain animals succumb to disease even though BPV may also be present in unaffected animals (Bogaert *et al.*, 2005; Daudt *et al.*, 2016; Gaynor *et al.*, 2016). In a study by Carr *et al.* (2001), it was discovered that BPV DNA was present in 98% of equine sarcoid tissue and in 63% of normal skin from sarcoid-positive animals. These findings differ from earlier results where normal skin and other tissues from sarcoid-affected horses were consistently negative when tested for BPV DNA (Martens *et al.*, 2000; Carr *et al.*, 2001). In a different study by Bogaert *et al.* (2005), BPV DNA was found on the normal skin of 44% of sarcoid-unaffected horses living in close

proximity with affected horses. In a later study, this group also demonstrated the presence of BPV DNA on the normal skin of 73% of horses in contact with cattle, and showed that 30% of horses which had no contact with either clinical sarcoid or cattle, were positive for BPV DNA (Bogaert *et al.*, 2008). It has therefore been proposed that genetic predisposition, and/or environmental factors, may explain why certain animals succumb to disease, while others do not. These findings also demonstrate the ubiquity of BPV DNA, and how easily and frequently the viral material is transmitted.

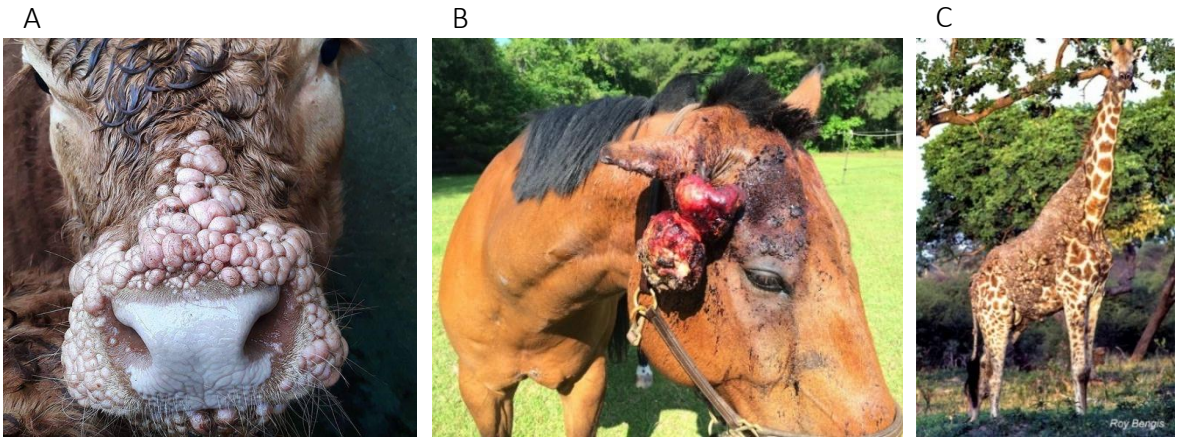

Figure 1.5. Images of animals afflicted with BPV-associated lesions and warts.

A) A domestic cow (*Bos taurus)* with multiple papillomas on its face. B.) A horse severely afflicted by equine sarcoids on its face. These sarcoids typically appear at sites of previous injury. Unlike bovine papillomas of cattle, sarcoids often persist, may be resistant to therapeutic interventions, and frequently reappear after surgical excisions. C.) A giraffe in the Kruger National Park (South Africa) severely infested with tumours on its back. Depending on how severe and where the lesions are located, sarcoids may severely limit the mobility of the animal. Images obtained from A: Life of a Vet Student Blog (n.d.) B: Michael Porter (2014, and C: Roy Bengis (African Wildlife Diseases).

1.1.5.3 Epidemiology of BPV:

BPVs are capable of infecting hosts through cuts or abrasions and inducing the formation of papillomas through targeting of the keratinocyte. Viral growth and maturation is paired with the maturation of cells from the basal to the surface layers, as discussed previously (see section 1.1.4 and 1.1.5). The virus is mainly spread from infected animals by direct contact with uninfected animals, with infection usually occurring through skin abrasions. It has also been suggested that

when infected animals scratch themselves against walls or fences to relieve the irritation caused by the warts, that viral material is shed and can infect other animals when they scratch against or lick the fences, infecting their mouth and alimentary tract (Bocaneti *et al.*, 2016; Palanivel *et al.*, 2017). Cattle are the natural hosts and main reservoir for infection by the virus, and instruments such as milking equipment, halters, ropes, tagging and tattooing tools, and scratching surfaces may serve as potential sources for infection. PV virions may survive in the environment for several weeks or months, especially if protected by pieces of tissue, such as wart fragments or pieces of tissue on halters (Thomas, 2013).

Calves (weanlings and yearlings) are most susceptible to BPV infection and wart formation, due to their undeveloped immune systems, and most cattle under 2 years of age are afflicted with warts (Borzacchiello and Roperto, 2008). These usually regress spontaneously as the immune system recognises and overcomes disease, and few cattle over the age of 2 years have warts (Endecott, 2014). Calves are frequently infected by BPV through small cuts and abraded skin, and often inadvertently infected during tattooing or ear tagging, and tattoos are often overgrown with warts (Morter, 2016). Warts generally appear within 1-6 months of infection, and often spread from the ear to other sites on the head and neck. Warts are also sometimes found on the teats of lactating cows, where they may spread to the mouth, head, and necks of suckling calves (Lunardi *et al.*, 2016; Dagalp *et al.*, 2017). In older animals, warts are generally restricted to animals with an underlying immune deficiency or stress.

It is not yet fully understood how BPV infection of horses and the development of equine sarcoids occurs. In BPV-induced lesions of cattle, whole infectious virus particles are formed, yet thus far no such particles have been detected in equine sarcoids. It is therefore thought that non-productive infection occurs in equines; however, some sarcoids have been found to contain BPV1 DNA complexed with the L1 capsid protein, which might be indicative of virion precursors, and could potentially present a source for infection even without particle formation (Brandt *et al.*, 2008; Hartl *et al.*, 2011). It has been suggested that direct or indirect contact with infected horses

and cattle might result in infection, and there is a growing body of evidence that transmission by insects may also play a role in the transmission of BPV, both within herds of the same species, and between horses and cattle (Bogaert *et al.*, 2005; Finlay *et al.*, 2009; Haspeslagh *et al.*, 2018). Contact with the virus alone, however, is not sufficient for infection and tumoral proliferation, and skin trauma, the immunological status, and genetic constitution of the individual animal are all relevant factors (Chambers *et al.*, 2003; Nasir *et al.*, 2007; Yuan *et al.*, 2007; van Dyk *et al.*, 2009; Williams *et al.*, 2011; Semik-Gurgul *et al.*, 2018).

Although BPV is thought to be spread mostly through horizontal transmission, several studies have demonstrated the presence of BPV DNA in whole blood of infected cattle (Campo *et al.*, 1994; Campo, 2002a; Roperto *et al.*, 2008; Silva *et al.*, 2013; Melo *et al.*, 2015), horses (Brandt *et al.*, 2008; Nasir and Brandt, 2013; Sykora and Brandt, 2017), and in both affected and unaffected zebra (van Dyk *et al.*, 2009), which indicate the possibility of vertical transmission of the virus via the bloodstream. These findings may also indicate that specific blood cells may serve as host cells for BPV DNA, and thereby contribute to virus latency. This is supported by the findings of BPV DNA in the blood of both sarcoid-affected and sarcoid-unaffected zebra, even in parks where sarcoids had never been reported (Brandt *et al.*, 2008).

1.1.6 Global and Local Prevalence and Importance of BPV:

Bovine PVs are highly prevalent and present worldwide, with over 60% of cattle bearing lesions at any one time in the UK (Campo, 1997), and similar numbers in Brazil (Araldi *et al.*, 2017), Italy (Savini *et al.*, 2016), and Germany (Araldi *et al.*, 2017). While these numbers are probably an underestimation, given the asymptomatic nature of many BPV infections, they do give an indication of the high prevalence and the broad distribution of the BPV virus, and similar or higher numbers are expected in regions where management is less stringent, such as in developing countries. Diseases caused by BPVs may have a significant impact on the animals affected, and infection of the teats, facial, or genital areas can severely impair their feeding, eyesight, breathing, and breeding abilities (Daudt *et al.*, 2018). The warts often become large and uncomfortable, and animals may scratch against surfaces to relieve discomfort, breaking the

wart open and exposing a wound to the environment, making the animal susceptible to secondary bacterial infection and infestation by insects and parasites. It is not uncommon for larger warts to be infested with maggots, and the animals are often plagued by large numbers of flies and other insects, leading to the economic depreciation of animals, and the deterioration of the appearance of the animal and of the animal leather (K. Nel, personal communication). While BPV infections are endemic in both dairy and beef cattle breeding, the importance of warts generally depends on the purpose of the cattle or animal (Araldi *et al.*, 2017). For show animals presenting warts, the impacts may be extensive, as these animals are often banned from shows and competitions, or are likely to receive a low grade (Carter *et al.,* 2005; Radostits *et al.,* 2007). Affected animals sold as breeding stock are also unlikely to be bought and introduced to an uninfected herd. This is especially true if the warts occur in the genital area, where it may interfere with the virility and fecundity of the animal. Warts located in the genital areas of breeding bulls and cows may be torn or broken during the mating process, and could be transmitted to the mating partner (Radostits *et al.*, 2007). For dairy cattle, which generally live between 4-5 years, warts on their teats may cause discomfort and may interfere with milking, especially if the warts lead to mastitis which can cause a decrease in milk volume or quality. Cows with teat warts may be resistant to allowing calves to nurse, resulting in reduced growth rates in the calves, and an increased incidence of mastitis. These animals are generally culled, which leads to significant economic losses (Rushen and de Passillé, 2013).

1.1.7 Economic and Agricultural Impacts

Animal diseases have direct costs, such as those affecting the animal populations and agriculture; and indirect costs, such as treatments and control programmes, impacts on human health, and the effects on trade, tourism, and other revenues (Topp *et al.*, 2016). The role of the livestock sector as a contributor to food and nutritional security, and as a source of livelihood for approximately 1 billion people worldwide, highlights the need for the sustainable maintenance of this sector. In low-to-middle-income countries (LMIC), the livestock industry may contribute over 33% to their agricultural gross domestic product (GDP), and is often one of the fastest growing sectors in agriculture (Meissner *et al.*, 2014; Pérez Aguirreburualde *et al.*, 2016). In South

Africa, the beef industry accounts for R1.67 billion of the GDP, and 95% of the meat comes from large feedlots. South Africa's "national herd", which consists of 35 breeds of cattle, including 9 indigenous ones, amounts to approximately 14.2 million heads of cattle (Abstract of Agricultural Statistics, 2018).

While ever-expanding, the livestock sector worldwide is facing many challenges, with population growth, urbanisation, and increasing income per capita driving a rising demand for livestock products. With a continual decrease in the availability of agricultural land preventing the horizontal expansion of current modes of production, more pressure is being put on the sector to increase resource efficiency and higher output per animal. Advances in animal health through biotechnological innovations are predicted to increase the productive efficiency of the sector more than any other technology, and vaccines among these have proven to be one of the most cost-effective strategies to be pursued (Thornton, 2010; Pérez Aguirreburualde *et al.*, 2016). This is especially the case for administration to prize bulls and other stock animals, which are used for breeding for many years and are very expensive.

1.1.8 Equine Industry:

Equine sarcoids constitute a significant veterinary problem because of their common occurrence, resistance to therapy, and their tendency to degenerate to a more severe state following ineffective treatment (Brandt, 2016). These factors are compounded by the worldwide presence of these viruses, the number of hosts capable of being infected and serving as potential sources for viral transmission, and the various means of transmission utilised by BPV, as discussed previously. In spite of the severe health and welfare impacts of sarcoids on affected horses and other equine species, little information is available regarding the innate and adaptive immune responses to BPV1/2 infections, or of the mechanisms underlying the ability of the virus to escape immune surveillance, which includes the establishment of a permanent infection and the development of persistent sarcoids (Campo and Roden, 2010; Hainisch *et al.*, 2012).

South Africa is home to a variety of equids, with a population of 300,000 domestic equids (horses, mules, and donkeys) and 50,000 zebras of three different species (European Commission Audit, 2013). With the horseracing industry alone contributing R2.71 billion ($226 million) annually to the GDP (Ngalonkulu, 2018), and a thoroughbred racehorse costing an average of R300,000 ($25,000), and a further R50,000 ($4,000) to R60,000 ($5,000) a year to maintain a horse on a stud farm, the equine industry is of high significance in South Africa. Globally, the equine industry has an enormous significance, with a total global value of $300 billion, and creating and sustaining over 1.6 million full-time jobs, according to the Equine Business Association (https://www.equinebusinessassociation.com/equine-industry-statistics/). The development of BPV vaccines are therefore of great importance to this industry, and may have significant market value, as the global equine healthcare market is valued at approximately $600 million in 2017, yet is expected to increase to over $750 million by 2023, according to a report by Zion Market Research (https://www.zionmarketresearch.com/report/equine-healthcare-market).

1.1.9 Tourism and Wildlife Conservation:

Several species of wild animals are also afflicted by BPV: in South Africa, BPV has been detected in sable antelope (BPV1), giraffes (BPV1 and 2), Cape mountain zebra (BPV1 and/or 2), and African buffalo (Williams *et al.*, 2011). These warts and lesions caused by BPV may spread over large areas of the animals' bodies, making them unsightly for tourists and ruining their skin, which is often sold by locals or game parks. These afflictions may also become debilitating, resulting in the euthanasia of affected animals. High-value game, especially breeding stock, cost vast amounts of money (see Table 1.1), and vaccination against high-risk BPV types 1 and 2 could prevent large economic losses.

Table 1.1. Examples of the costs of game animals in South Africa

Animal	Price*
African Buffalo Bull	R2,500,000 ($173,000)
Giraffes	R20,000 ($1,380)
Zebra	R6,000 ($415)
Eland	R45,000 ($3,100)
Sable Antelope	R250,000 ($17,300)

The prices indicated in the table are the highest ones listed at the time, yet the prices vary enormously depending on the health, fitness, and other characteristics, as well as the season and supply-and-demand dynamics. Prices* were obtained from www.wildlifetrading.co.za [Accessed 01.07.2018].

Cape mountain zebras, shown in Figure 1.6, are classified as endangered on the International Union for the Conservation of Nature and Natural Resources (IUCN) Red List of 2006 (https://www.iucnredlist.org/), and are one of the world's rarest mammals (van Dyk *et al.*, 2009). These animals are protected in South African game parks, where they can exist within their natural environment, in small, isolated populations. These zebras are susceptible to sarcoid lesions, such as those associated with BPV1 and BPV2 (van Dyk *et al.*, 2009). The first cases of sarcoid lesions were reported in Cape mountain zebras from the Gariep Dam Nature Reserve, in June of 1995 (Nel *et al.*, 2006), and in 1998 in the Bontebok National Park. A number of cases of zebra afflicted with sarcoid lesions have since been reported (Marais *et al.*, 2007; van Dyk *et al.*, 2009; Williams *et al.*, 2011), and in at least one case an animal was euthanised due to the severity of these lesions. In 2002, the incidence of sarcoid lesions within Cape mountain zebra populations was 53% at the Bontebok National Park, and 24.7% at the Gariep Dam Nature Reserve (Nel *et al.*, 2006; van Dyk *et al.*, 2009). South African Cape Mountain zebras are highly inbred, descending from only 30 individuals from 3 populations, and show specific heterozygote deficiency and small genetic diversity (Sasidharan, 2006; Marais *et al.*, 2007). These factors could account for their high susceptibility to sarcoid lesions.

Figure 1.6. Cape mountain zebra afflicted with massive facial, submandibular, and abdominal sarcoids. **Figure 1.6.A** and .**C** (Roy Bengis; http://awp.eduwikis.co.za/index.php?title=Papillomavirus), and **Figure 1.6.B** (van Dyk *et al.*, 2009).

In a study by van Dyk *et al.* (2009), 12 sarcoid tumours were obtained from Cape mountain zebras from the Gariep Dam Nature Reserve, Bontebok National Park, and the Mountain Zebra National Park in the Eastern Cape, and analysed. Similar histological changes such as dermal proliferation of spindle-shaped fibroblast forming whorls, epidermal hyperplasia, hyperkeratosis and rete peg formation, which are typical of sarcoid, were observed in all the tumours (Martens *et al.*, 2000). Analysis of these tumours revealed that 58% were associated with BPV1 infection, 33% with BPV2 and 9% (1 tumour) had both BPV1 and 2 DNA present. Both BPV1 and BPV2, occurring either as single and mixed infections, were also detected in the skin and/or the blood of both sarcoid-afflicted and healthy zebras in the regions affected by sarcoids, as well as in the blood of zebras in regions where no sarcoids have yet been observed, where the infection was only singular. Most of the infections in both affected and unaffected parks were caused by BPV1.

1.1.10 BPV as a model for HPV (and vice versa)

There are over 170 types of PVs affecting humans, and it is estimated that 99% of cervical cancers and 5% of all human cancers are caused by HPVs, which highlights the importance of developing a cheap, broad-based vaccine against multiple of the most prevalent and high-risk HPV types (Kwak *et al.*, 2011; Chabeda *et al.*, 2018). Three HPV vaccines, two produced in yeast and one in insect cells, have been shown to be effective for up to 9.4 years. However, these only protect against 2 high-risk types (16 and 18; Cervarix, GlaxoSmithKline), 4 or 9 different types (Merck's

Gardasil and Gardasil-9), with some cross-protection against certain non-target types (Brotherton, 2017). Their type-restricted prophylactic efficacy, lack of therapeutic efficacy, and high costs restrict the widespread global application of these vaccines, and the HPV-related cancer burden remains high, especially in developing countries (Chabeda *et al.*, 2018).

Animal neoplasms have been crucial to the study of human oncogenic processes, such as elucidating the molecular mechanisms associated with carcinogenesis, highlighting the importance of comparative oncology, and aiding in the development of novel therapeutics (Munday, 2014; Christensen *et al.*, 2017). This is due to the largely high species- and tissue-specificity of papillomaviruses, which has required virologists to use BPV and other animal papillomaviruses as models for the study of HPV infection, and its interaction with the host and with environmental co-factors (Campo and Roden, 2010). While the advent of stable human cell cultures and sophisticated culture techniques has decreased the need for animal PVs to a large degree, animals still serve as useful *in vivo* models for HPV disease and vaccine studies, especially for determining host responses, and recent insights into BPV biology have opened new fields of discussion about coinfection, cross-species infection, and transmission of these viruses (Campo, 2002a; Christensen *et al.*, 2017). In turn, developments in HPV research may also provide important insights for the study of animal PVs and the development of vaccines against these.

1.1.11 Treatment of BPV Infections

1.1.11.1 Papillomas of cattle

Papillomatosis in cattle is most commonly a mild, self-limiting disease, for which neither prevention nor treatment is usually essential (Araldi *et al.*, 2014). Cutaneous warts commonly occur in younger animals (less than 2 years of age), and usually regress spontaneously within 6-18 months, as the immune system recognises and overcomes the disease. Immunity after a natural infection usually appears after 3-4 weeks, and persists for a minimum of 2 years, though papillomatosis occasionally recurs, probably due to a loss of immunity (Merck Veterinary Manual, 9th Edition). Rarely, epidemics in young cattle may occur, in which the affected individuals or

whole herds are so debilitated that culling is required. Severe disease may occur when papillomatosis affects the teats or udders and leads to mastitis. This is of particular concern in the case of milking cows, suckling calves, and breeding animals. A number of treatments have been tested for such cases, but there is a lack of evidence and unanimity regarding the efficacy of these treatments (Finlay, 2011). Warts are sometimes removed surgically, followed by cryogenic treatment with liquid nitrogen, and healing occurs relatively rapidly, with few cases of warts recurring. The Merck Veterinary Manual states that surgical removal of warts may be performed if the warts are "sufficiently objectionable", although they suggest only doing so once warts are close to their maximum size or regressing, so as to prevent recurrence or stimulation of growth. Immunotherapy has also been attempted, with immune potentiators such as interleukins or BCG (Bacillus Calmette-Guerin) tested in pilot studies and indicating some proof of efficacy (Carter and Wise, 2005). One common treatment is crushing of the warts to liberate and expose the viral antigens to the immune system, increasing the immune response, or inducing an inflammatory response in the area. Warts often regress after such exposure, and the animal is generally less susceptible afterwards (Pence, 2005; Thomas 2013). Autologous vaccines prepared from formalin-inactivated wart material, which also work on this principle, are also sometimes applied therapeutically, although prevention of BPV infection is often more successful and practical than treatment after the occurrence of infections (Radostits *et al*., 2007).

1.1.11.2 Sarcoids of horses and other equids

Both surgical and non-surgical methods for the treatment of equine sarcoids exist, as reviewed in Taylor and Haldorson (2013). These have variable success rates and none of the current techniques are fully successful, and sarcoids frequently recur after therapy (Lunardi *et al.*, 2013; Melkamu, 2018). Sarcoids in zebra have successfully been treated by surgical intervention and the subsequent administration of fluorouracil (Lange, 2004). Autologous vaccines have also been successfully used to treat sarcoid infected animals. These, as with autologous vaccines administered to cattle, usually consist of a cell-free supernatant fluid, prepared from formalin-inactivated, finely minced sarcoid tumours. A vaccine prepared from zebras affected by both BPV1 and 2, as opposed to a different vaccine prepared from tumour of zebra only infected with

BPV1, seemed to convey greater immunity to the animals (van Dyk *et al.*, 2009; Williams *et al.*, 2011).

1.1.12 Prevention of BPV Infections: BPV Vaccines and Vaccine Candidates

Various interventions are used to combat disease in animals, with vaccination being one of the most widely used and effective strategies (Ruiz *et al.*, 2015). While vaccination generally provides protection against viral pathogens, these may also contribute to the reduced use of antibiotics by lowering the incidence of secondary bacterial infections (Glass-Kaastra *et al.*, 2013; Topp *et al.*, 2016). Global sales of animal health products in 2013 were $23 billion, yet only $5 billion corresponded to veterinary vaccines, and vaccines and immunotherapeutics are available for only a limited number of animal diseases (Dolcera, 2014; Health for Animals). For veterinary vaccines to be applied widely and effectively, they need to be cheap, easy to administer, and, ideally, confer long-lasting protection. There are currently no widely available and affordable commercial vaccines for the prevention or treatment of BPV infections in cattle, horses, and other susceptible animals. The ubiquity and economic damages caused by diseases from BPV highlight the need for such a vaccine, especially in developing countries where meat production is a rapidly growing sector, and these economic losses are hardest felt, especially by small-scale and subsistence farmers. Because of the infectious nature of BPV, infected animals are usually banned from shows and exhibitions. However, not all animals infected with BPV will produce warts, and virus may be transmitted from asymptomatic to susceptible animals. It is therefore also important for disease control and management purposes that vaccines are DIVA/SIVA (Differentiation/Segregation of Infected from Vaccinated Animals) compliant, and capable of distinguishing between vaccinated and infected animals.

The development of vaccines against PVs has an extensive history, yet because of the high degree similarity in the genomic architecture of PVs, principles established in the studies of one set of PVs can often be applied generally to other species of PVs. Much of the early PV research was performed on BPV, cottontail rabbit PV (CRPV), and canine oral PV (COPV) animal models, which

have provided key insights into PV-induced diseases and have greatly aided in the development of both animal PV and HPV vaccines (Kirnbauer *et al.*, 1996; Ruiz *et al.*, 2015). Several classes of vaccines exist, each with their own set of advantages, disadvantages, and applications, and these are broadly categorised into two main categories: prophylactic and therapeutic vaccines. These classes of vaccines, and examples of the PV vaccines that fall within them are discussed below and in Chapter 3.

1.1.12.1 Prophylactic vaccines

Prophylactic (or preventative) vaccines, are vaccines that prevent viral infection or arrest the establishment of disease. This is usually achieved through exposing the immune system to structural proteins of the virus, and inducing a humoral immune response that leads to the production of neutralising antibodies (NAbs), which target and bind to conformational epitopes on the virus structure and prevent viral entry into the cell (Rosales and Rosales, 2017). This process involves both the innate and adaptive (humoral) arms of the immune system, and an example of the immune response to an HPV infection is illustrated in Figure 1.7, and discussed below. Despite their life cycle heterogeneity, key life cycle events and mechanisms are likely to be regulated in a similar manner, although the timing of such events vary widely (Peh *et al.*, 2002). Papillomaviral antigens, such as the HPV virus, enter the body, either as native viruses in a natural infection, or as part of an immunisation. This microtrauma triggers an inflammatory response, attracting innate immune cells such as neutrophils, macrophages, and lymphocytes, which can detect non-specific viral molecules such dsDNA. These cells recognise these particles as foreign, and produce inflammatory cytokines such as interleukins (IL) and interferons (IFN), which then activate natural killer (NK) cells. Viral proteins, when produced later, and taken up by antigen-presenting cells (APCs) such as Langerhans or dendritic cells (DCs), which process these proteins and present them as small peptides on the cell membrane, together with major histocompatibility complex (MHC) molecules (Doorbar, 2005; Rosales and Rosales, 2017). In BPV, the E5 late protein inhibits expression of the MHC, which is one of the mechanisms by which the BPV evades the host's immune response (Bocaneti *et al.*, 2016). These are detected by lymphocytes (T-cells), which initiate the adaptive immune response. Once activated, CD4+ helper

cells can differentiate into one of 3 phenotypes (Th1, Th2, or Treg/Th3), depending on the type of cytokines they produce. These can either help to activate B-cells for the production of virus-specific antibodies, or can assist CD8+ T-cells to differentiate into cytotoxic T-lymphocytes (CTLs) which secrete granzyme and perforin proteolytic enzymes, and are the cells most capable of terminating PV-infected cells. The adaptive, and ensuing cellular immune response, is the most effective means of controlling PV infections, as demonstrated by the fact that most PV infections are naturally eliminated by immunocompetent hosts. This is further illustrated by the breaking open the papilloma lesions to expose the virus to the immune system (self-hemotherapy) and stimulate an immune response also facilitates the rapid regression of lesions (Kirnbauer *et al.*, 1996; Turk *et al.*, 2005; Rosales and Rosales, 2017).

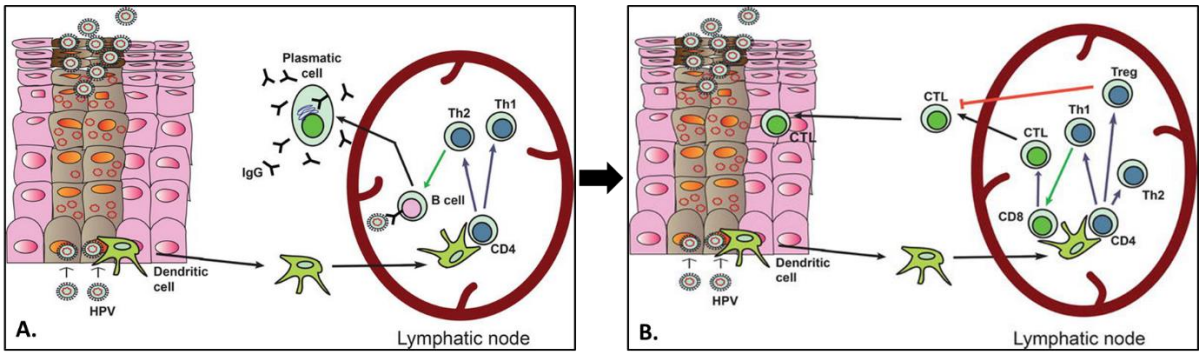

Figure 1.7. Immune response to PV infection

Image modified with permission from Rosales and Rosales (2017) depicts the humoral (**A**.), and cellular (**B**.) immune response to HPV. In the humoral response (**Figure 1.7.A**.), HPV antigens from infected cells are captured by dendritic cells (DCs), which then migrate to lymph nodes and present processed antigen to CD4+ T-cells. The T-cells subsequently differentiate into T-helper cells, Th1 or Th2, depending on the type of cytokines they produce. B-cells, which recognise the viral antigens, differentiate into antibody (IgG)-secreting plasma cells, with assistance from the Th2 cells. In the cellular response (**Figure 1.7.B**.), DCs which have taken up HPV antigens and migrated to lymph nodes present processed viral antigens to CD8+ T-cells, as MHC I molecules, and to Th1 or Th2 cells as MHC II molecules. Th1 cells help CD8+ T-cells to differentiate into cytotoxic T-cells (CTLs), which migrate back to destroy virus-infected epithelial cells. CD4+ cells may also differentiate into regulatory T-cells (Tregs), that inhibit the cytotoxic activity of the CTLs.

The immune response of cattle to BPV infection is remarkably poor, which is probably due to the fact that the viral life cycle is restricted to the epithelial cells, and does not come into contact

with the immune system, yet T- and B-cell responses to viral L1 and E7 antigens have been observed in later stages of the disease (Campo, 2002a; Brandt, 2016). Kirnbauer *et al.* (1996) found that while vaccinating calves with L1 VLPs was only effective at preventing disease, tumour regression of vaccinated animals appeared to occur more rapidly than animals not vaccinated. This principle has been applied by many farmers who treat papillomas through self-homeopathy by crushing the wart to expose the virus to the immune system (Turk *et al.*, 2005; Sreeparvathy *et al.*, 2011). This supports the theory that the exposure of the BPV to the immune system induces an immune response, and spontaneous regression of papillomas induced by BPV4 infections have been associated with high densities of activated lymphocytes, and particularly CD4+.

Current prevention methods for BPV often rely on autologous vaccines, whole-virus vaccines produced from inactivated wart material from other afflicted animals in the surrounds, which are useful for inducing a strong, type-specific response against challenge with the same virus (Turk *et al.*, 2005; Sreeparvathy *et al.*, 2011). These vaccines offer certain benefits, and are likely to protect against specific types or strains of virus common to the area, yet despite their relative success in preventing BPV-related diseases, autologous vaccines also have various limitations. One such limitation is the requirement of basic molecular biology and veterinary skills needed to produce and administer these vaccines. Autologous vaccines have the additional risk of reversion or recombination of the virus, which may result in disease outbreak. It is also often not known against which strains the vaccine protects, and differences in vaccines may be observed. Another downside is that autologous vaccines require large amounts of wart material (at least 200-300 grams) (Thomas, 2013). Some research also suggests that, depending on the amount of time since the initial infection, the degree of infection, and the health status of the animal, vaccination might worsen the infection – another reason why a prophylactic approach is preferable (Radostits *et al.*, 2007). Another limitation of autologous vaccines is their non-compliance of these vaccines with DIVA/SIVA vaccine requirements, which reduces the ability to monitor for outbreaks and to determine the detection of new infections. This is because DIVA is based on the detection of antibodies to non-structural proteins. As autologous vaccines contain the entire contents of the

virus, they would also not be DIVA compliant, yet vaccines based only on the structural proteins of the virus would be (Lee *et al.*, 2012). Subunit vaccines, which are composed of a fragment/fragments of a pathogen (usually expressed in cell culture systems) and trigger an immune response resulting in acquired immunity, may offer a useful alternative.

Prophylactic vaccines against PVs are primarily based on the structural proteins, L1 and L2, and several studies on BPV and other animal PV models have demonstrated that both L1 and L2 can independently elicit a protective antibody response in immunised animals, and are highly effective at preventing PV infection and disease (Araldi *et al.*, 2017; Harnacker *et al.*, 2017; Schellenbacher *et al.*, 2017). A number of subunit vaccine candidates have been produced against important BPV types, and have been shown to prevent warts and tumours in uninfected animals, as reviewed in Campo and Roden (2010), and more recently in Araldi *et al.* (2017). These vaccines are mainly based on virus-like particles (VLPs), and candidate vaccines have already been developed for BPV1, 2, and 4 (Modolo *et al.*, 2017; Ugochukwu *et al.*, 2018). VLPs are protein assemblages which mimic the structure and conformation of native virions, and are usually antigenically indistinguishable from their infectious native counterparts. These molecules are formed by multiple copies of one or more of the capsid proteins of viruses, and generally self-assemble when these are expressed in recombinant expression systems. As VLPs lack viral genetic material, risks associated with viral replication, insertion, reversion, recombination, or reassortment events are eliminated (Grgacic and Anderson, 2006; Crisci *et al.*, 2012; Liu *et al.*, 2012). These vaccines combine the advantages of whole-virus vaccines and recombinant subunit vaccines by maintaining key features of both, offering such advantages and features such as: 1) a particulate and multivalent nature; 2) a uniform and well-defined geometry with repetitive and ordered surface structures; 3) a preservation of native antigenic conformations; 4) high safety features, as these are non-replicative, non-pathogenic, and non-infectious; 5) a high stability, which is greater than most soluble antigens in extreme environments; 6) vector properties for the presentation of antigens and ligands, or the delivery of drugs and genetic elements to cells; 7) and an ability to Differentiate Infected from Vaccinated Animals (DIVA), making them DIVA-compliant (Crisci *et al.*, 2013). Pseudovirions (PsVs) are another class of synthetic viruses similar

to VLPs, but these contain additional genetic material deliberately encapsidated within the VLP-shell. These particles can be used for the delivery of third generation DNA vaccines, or to facilitate uploading foreign genetic material or other therapeutic agents into specific cells (Lund *et al.*, 2010; Ma *et al.*, 2011). PV PsVs, including BPV and HPV PsVs have already been successfully produced in mammalian cells (Buck *et al.*, 2003), and our research group recently demonstrated the first successful production of HPV PsVs in plants (Lamprecht *et al.*, 2016).

The majority of the candidate VLP-based BPV vaccines are produced in yeast, insect, and mammalian cell-cultures, which are associated with relatively high production costs owing to the costly facilities, expensive media, and high biosafety requirements associated with these systems. This makes them unsuitable as veterinary vaccines, especially if the goal is to vaccinate whole herds at a time, and limits their adoption in developing countries (Pogue *et al.*, 2002; Daniell *et al.*, 2009). While bacterial systems may offer a potential low-cost alternative for the production of antigens, these hosts lack the eukaryotic post-translational machinery often required for the correct assembly of animal vaccine antigens into structures such as capsomeres and VLPs (Li et al., 2001; Yuan et al., 2001). Additionally, these systems are prone to contamination by microorganisms, endotoxins, or pyrogens, therefore requiring stringent purification and monitoring of antigens produced in these systems (Tiwari *et al.*, 2009; Dadar *et al.*, 2018). Because of the aforementioned challenges and shortcomings, plant expression systems have increasingly been used for the production of foreign antigens for vaccine production (Brillault *et al.*, 2017; Wong-Arce *et al.*, 2017; Gonzalez-Castro *et al.*, 2018).

1.1.13 Plant Expression Systems

Biopharmaceuticals, or biologics, are commercially valuable proteins with applications in medicine, research, and industry, and comprise the fastest-growing sector of pharmaceutical industry (Karg and Kallio, 2009). Traditionally animal, bacterial, and yeast production systems have been used to produce recombinant proteins. However, these systems have various limitations, and plants are increasingly being used as alternative production system for

recombinant proteins (Rybicki, 2010; Marsian and Lomonossoff, 2016). Low production costs, due to the relatively simple and cheap growth requirements of plants, and the ease of up-scaling, are two of the main advantages offered by plant expression systems. Additionally, plants also perform the necessary post-translational modifications to produce functional proteins, which includes N- and O-glycosylation, phosphorylation and disulphide bridge formation. Plants also offer a much-reduced risk of contamination with human or animal pathogens (Karg and Kallio, 2009; Rybicki, 2010). Examples of recombinant proteins produced in plants include enzymes, hormones, monoclonal antibodies, and antigens for the development of vaccines and antibodies (Sharma and Sharma, 2009; Yao *et al.*, 2015).

Modification of plants for the production of recombinant proteins has traditionally relied on the generation of stable, transgenic lines, a procedure which is both costly and time-consuming. However, transient transformation, which uses the inherent ability of *Agrobacterium tumefaciens* (*Agrobacterium*) to transfer a designated segment of its DNA (T-DNA) to the nucleus of a plant cell as an episome, is a rapid, scalable, and relatively simple method of transforming plant tissues and producing recombinant proteins within a short period of time (Thuenemann *et al.*, 2013a; Sainsbury and Lomonossoff, 2014). During this process, the T-complex- a complex of the bacterial T-DNA derived from the Ti-plasmid, and virulence gene products- of *Agrobacterium* is transferred to the plant cells. DNA situated between left and right borders of 25 bp direct repeats, which delimit the single-stranded T-DNA, is transferred to the cell nucleus, where illegitimate recombination to its integration into the with the plant chromosome. However, many of the T-DNA copies that enter the nucleus are not integrated and remain episomal: these are still transcribed, leading to their transient expression. Because this expression is not influenced by positional effects and copy number may be high, it can generally produce far higher protein yields than can stable transformation (Maclean *et al.*, 2007). The transient transformation approach generally employs the use of binary vector systems in *Agrobacterium*, in which the T-DNA is separate (on a different vector/plasmid) from the *trans*-acting virulence proteins that perform the transfer of DNA to the host cell (Gelvin, 2003; Chen *et al.*, 2013). This makes it possible to generate and manipulate a diverse range of vector plasmids through molecular and

synthetic biology techniques. Furthermore, this feature allows for the inactivation of the *Agrobacterium's* native tumour-inducing genes, thereby restricting modification to the non-reproductive tissue. As the germ lines of the target plants are not modified, the plants are deemed environmentally benign – an important advantage over traditional genetically modified plants (GMPs), which face massive bureaucratic, financial, and social challenges over fears of their environmental impacts (Wilken and Nikolov, 2012; Sainsbury and Lomonossoff, 2014).

The injection or infiltration of recombinant *Agrobacterium* cultures containing binary vectors with heterologous genes into plant tissue, and mainly into the interstitial spaces of leaves, enables direct contact between multiple bacteria and the individual plant cells. This allows for the efficient transformation of large areas of plant tissue, and high levels of protein expression to be achieved in a whole plant in comparison with stable nuclear integration (Leuzinger *et al.*, 2013; Mardanova *et al.*, 2017). These advances have significantly improved our ability to alter and exploit the machinery of plants for our productive gains, and have created possibilities for several applications, such as macromolecule-complex production, and the modification and examination of metabolic pathways, allowing for the delivery of several genes into a single plant cell, as well as their efficient expression within in this cell over a period of just a few days. These advantages have made transient expression systems the preferred approach for plant-based applications, and these methods are increasingly being used both in research, and for the production of commercially relevant products (Sainsbury and Lomonossoff, 2014).

Host plants for expression are selected based on their total protein content, yield of biomass per area, and ease of transformation. Tobacco (*Nicotiana benthamiana* or *N. tabacum* species) has long been the host most commonly used for the production of recombinant proteins (Tremblay *et al.*, 2010; Hefferon, 2017). This is due to the fact that it is well-studied, robust, has a high biomass, and can be infiltrated with *Agrobacterium* with relative ease and without considerable damage to the tissue. Tobacco has a high transformation efficiency due to its desert origins and, thus, relatively low exposure to plant pathogens. This has likely led to the loss or lack of

development of strong host defences against such pathogens, from which plant expression vectors are largely derived. *Nicotiana benthamiana* plants have proven capable of high-level transient expression of antigens, which are then purified and used to formulate injectable vaccines, although other plants are also capable of producing high yields of recombinant proteins. Several companies are currently conducting clinical trials of candidate vaccines produced in plants, including plant-derived Influenza A H5/N1 (pandemic flu) and seasonal flu strain VLPs, which have already undergone Phase I and Phase II clinical trials. The quadrivalent plant-made seasonal flu vaccine made by Medicago Inc. is expected to be the first plant-made vaccine to be marketed (http://www.medicago.com/en/pipeline/, Accessed: 10.01.2019). Other plant-made pharmaceuticals include the plant-expressed anti-HIV Env IgG, 2G12, which has undergone phase I clinical testing, and is intended for topical application to prevent the transmission of HIV infections (Vamvaka *et al.*, 2016); and ZMapp for the treatment of *Ebolavirus* infections, for which treatments of humans with ZMapp proved the product to be well-tolerated, and for which the mortality rate in the treated group appeared to be 40% lower than in the nontreated participants, although sample size was too small for these findings to be of statistical significance (Lomonossoff and D'Aoust, 2016).

1.1. Project Aims and Objectives:

The main aim of this study was to express virus-like particles (VLPs) and pseudovirions (PsVs) derived from bovine papillomavirus type 1 in *N. benthamiana* plants, and to demonstrate their immunogenicity (VLPs) and gene transfer capabilities in cell culture (PsVs). This was done in the pursuit of eventually producing cheap, safe, and efficacious prophylactic (and potentially therapeutic) BPV1 vaccine candidates, as there are currently no such vaccines on the market. Although other researchers have expressed BPV1 L1 VLPs in plants, to date there are no examples in the literature where BPV PsVs have been produced in plant expression systems. A second aim of this study was, therefore, to expand on research into the expression and purification of plant-produced PV proteins, as well as their research and clinical applications.

The three main objectives of this study were:

1. To express BPV1 L1 and L2 in tobacco plants, and to extract, purify, and analyse BPV1 L1 and L1/L2 VLPs.

   The first objective of this study was to express BPV1 L1 and L2 proteins in *N. benthamiana*, in order to determine optimal expression conditions and, as BPV1 L1 VLPs have previously been expressed in *N. benthamiana* plants (Love *et al.*, 2012), to expand on previous research by producing L1/L2 VLPs through co-infiltrating L1 and L2 constructs.

2. To produce BPV PsVs in *N. benthamiana*, analyse these for infectivity using a SEAP assay, and to test for neutralisation by neutralising antibodies in PBNA.

   Following the successful production of both putative BPV1 L1/L2 VLPs, the second objective was to produce BPV1 PsVs in plants, and to pseudo-infect mammalian cells with these particles. This would involve co-infiltration of *N. benthamiana* plants with plasmids expressing the two structural proteins as well as a self-replicating vector capable of making genome-sized circular dsDNAs with a mammalian expression cassette containing a reporter gene.

3. To optimise VLP and PsV expression and purification, and to explore cheaper and more efficient methods for the expression, purification, and analysis of VLPs and PsVs.

   The third objective was to increase the yields of VLPs and PsVs obtained, and to explore methods for the production, purification, and analysis of these particles which would be less costly, more time-efficient, or produce a better product. Several methods of extraction and purification were explored in order to optimise yields of PsVs.

2 Chapter 2: Expression Optimisation and Production of BPV1 VLPs in Plants

2.1 Introduction

2.1.1 Plant Expression Systems for the Production of Recombinant Proteins

Plants offer several features which make them attractive alternatives to cell-based systems, which include their sustainability, ease of cultivation, rapid scalability, low cost and relatively simple growth requirements (Marsian and Lomonossoff, 2016; Sohrab *et al.*, 2017; Wong-Arce *et al.*, 2017). This allows plant production systems to be implemented nearly anywhere, without the requirement of expensive facilities and equipment. It has been estimated that plant systems could reduce the actual production costs of vaccines by 31%, including cost of materials and all downstream costs (Rybicki, 2009; Rybicki, 2010). This, in turn, allows for the low upstream production costs of large amounts of recombinant proteins, as well as the ability to rapidly scale up production in response to increasing demands, or in rapid-response scenarios such as disease outbreaks and bioterror attacks (Chichester *et al.*, 2009; Rybicki, 2010). Plants also contain eukaryotic protein modification machinery, which allows for subcellular targeting for the expression of recombinant proteins, as well as post-translation modifications and correct folding (Fischer *et al.*, 2015; Lomonossoff and D'Aoust, 2016). Because plants do not harbour animal pathogens, proteins produced in these systems are also generally free of contamination by bacterial toxins, animal viruses, and prions (Fischer *et al.*, 2012; Thuenemann *et al.*, 2013b).

Various plant hosts have successfully been used to express human and animal vaccine antigens, including various PV proteins, such as BPV1 L1 (Love *et al.*, 2012) and HPV16 L1, L2, and various early genes (Pineo *et al.*, 2013; Lamprecht *et al.*, 2016; Chabeda *et al.*, 2018; Salyaev *et al.*, 2018). Those tested in animal trials have been proven both safe and efficacious, and as production and purification methods improve, plant-made pharmaceuticals have already started to compete

with many of the current therapeutic proteins and antibodies produced using conventional expression systems, many of which are outdated and insufficient for current demands (Lamprecht *et al.*, 2016; Dennis *et al.*, 2018; Rybicki, 2018).

Transient expression levels depend on various variables, and may be improved by consideration of factors such as choice of host plant, expression conditions and parameters, features of the gene(s) of interest, and elements included in the expression vectors. These vectors can sometimes even be modified to enable differential expression of their encoded genes (Sainsbury and Lomonossoff, 2014). Vectors and expression cassette elements used for stable transformation of plants are often derived from plant pathogens, due to their prevailing abilities to overcome host defences and subvert gene expression. Examples of such elements include promoters, such as the commonly used Cauliflower mosaic virus (CaMV) 35S promoter, translational enhancer elements, and silencing suppressors (which reduce post-translational silencing through mRNA stabilisation), all of which have a substantial impact on the yields of protein obtainable. Other evolutionary developments in vector technology include the transition from replicating viral vectors, to high yielding non-replicating vectors and deconstructed viral vectors, such as those based on Tobacco mosaic virus (TMV), Cowpea mosaic virus (CPMV), and Bean yellow dwarf virus (BeYDV) (Pogue *et al.*, 2002; Sainsbury *et al.*, 2009; Regnard *et al.*, 2010; Sainsbury *et al.*, 2010; Hefferon, 2012; Sainsbury and Lomonossoff, 2014). This permitted the massive reduction of components required for replication and translation, reducing restrictions on insert sizes, and enabling the co-expression of multiple proteins. This is of particular importance in intricate biological applications, such as the production of complex macromolecules. Macromolecule complexes usually consist of multiple copies of one or more polypeptides, which may be required in different amounts or ratios. One class of such molecules, which is of significant importance due to their potential use in vaccines and nanotechnology, are complexes known as virus-like particles (VLPs) (Marsian and Lomonossoff, 2016; Edgue *et al.*, 2017).

In this Chapter, I describe the cloning of BPV1 L1 and L2 genes into plant expression vectors, transformation of these into *Agrobacterium tumefaciens*, and syringe-infiltration into *N. benthamiana* plants. Optimisation of expression included testing of different *Agrobacterial* concentrations for infiltration, and the analysis of protein expression levels over a seven-day period, to establish conditions for VLP production.

2.2 Materials and Methods:

2.2.1 Construct Design and Generation of Recombinant *Agrobacterium*

2.2.1.1 Gene design and synthesis

Native gene sequences for BPV1 L1 (1488 bp) and L2 (1410 bp) major and minor capsid proteins were obtained from the PaVE (Papillomavirus Episteme: https://pave.niaid.nih.gov/ BPV1 Genbank ID: X02346) website. The sequences were manually modified in CLCbio Workbench 6.2 (Qiagen) by adding restriction enzyme (RE) cut sites to the 5' and 3' ends for subcloning into plant expression vectors: pTRAc, pTRAkc-rbcs1-cTP (pTRAkc-cTP) (provided by Prof Rainer Fischer, Fraunhofer Institute for Molecular Biology and Applied Ecology, Germany), and pRIC3.0 (Regnard et al., 2010). Codon-optimisation for *Nicotiana benthamiana* (*N. benthamiana*) and gene synthesis were performed by GenScript (USA), and the L1 and L2 genes were provided in the pUC57 plasmid vector. All references to L1 and L2 in this study refer to BPV1 L1 and L2, unless otherwise specified.

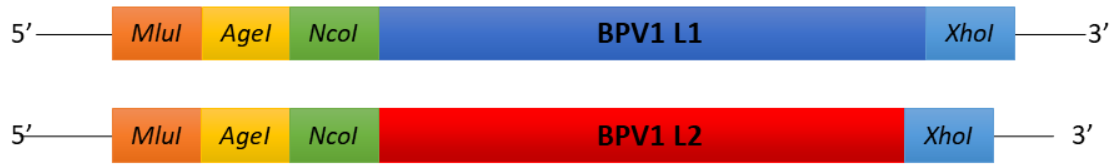

Figure 2.1. Schematic representation of the BPV capsid protein genes, L1 and L2, and their restriction enzyme recognition sites.

2.2.1.2 Transformation of *E. coli* and plasmid extraction

The pUC57-L1 and -L2 plasmids obtained from GenScript were transformed into chemically competent DH5-α *E. coli* cells (E. cloni®, Lucigen) via the heat-shock transformation method described in Sambrook *et al.* (2019). The transformation mixture was plated onto Luria-Bertani (LB) agar [1.0% tryptone, 0.5% yeast extract, 1.0% NaCl, 1.5% agar, pH 7.0] plates containing 100 mg/ mL ampicillin (LBamp), and incubated overnight at 37°C.

2.2.1.3 Confirmation and selection of positive clones by colony PCR screening

To select for positive bacterial clones, colonies from the overnight plates were screened using colony PCR. For the reaction, the KAPA Taq ReadyMix with dye (Roche) was used, as per the manufacturer's instructions. Forward and reverse primers (Table 2.1) were used at a final concentration of 0.4 µM per primer. All colony PCR reactions in this study were performed using these reagents and method, with vector-specific primers flanking the multiple cloning site into which the L1 and L2 genes were cloned, unless otherwise specified. PCR cycling conditions are shown in Table 2.2.

Table 2.1. Primer sequences and annealing temperatures

Primer name & orientation		Primer 5' → 3' sequence	PCR Ta	Function
pUC57 M13	Fwd	CGCCAGGGTTTTCCCAGTCACGAC	53°C	Colony PCR of pUC57 parent vectors
	Rev	AGCGGATAACAATTTCACACAGGA		
pTRAc	Fwd	CATTTCATTTGGAGAGGACACG	48°C	Colony PCR and sequencing of pTRAc, pTRAkc-rbcs1-cTP, and pRIC3.0 constructs
	Rev	GAACTACTCACACATTATTCTGG		
16-1642	Fwd	gtggacgcgttaggtgcATGGCGTTGTGG	71°C	Add *Mlu*I and protease cleavage sequence to 5' end of L1
16-1643	Rev	gcatgtagcagcgacgCTCGAGCTATTTCT		
16-1644	Fwd	gtggacgcgttaggtgcATGAGTGCTAGGA	68°C	Add *Mlu*I and protease cleavage sequence to 5' end of L2
16-1645	Rev	cgagatCTCGAGTCAAGCGTGTTTCCTCTT		
pJET	Fwd	CGACTCACTATAGGGAGAGCGGC	60°C	Colony PCR of pJET constructs
	Rev	AAGAACATCGATTTTCCATGGCAG		

Table 2.2. PCR conditions used throughout this study

Cycle step	Temperature	Time	Cycles
Initial Denaturation	95°C	5 minutes	1
Denaturation Annealing Extension	95°C Primer specific annealing temp (Ta): Table 2.1 72°C	30 seconds 30 seconds 1 minute	30
Final Extension	72°C	2 minutes	1
Hold	4°C	∞	1

PCR products were separated and visualised on 0.8% TBE agarose gels. Gel imaging was performed using short-wave (254 nm) UV light (Syngene Gene Genius Bioimaging System). PCR positive clones were inoculated into LB media with antibiotics and incubated at 37°C with agitation (120 rpm) for 12-20h. Recombinant *E. coli* containing plant expression vectors pTRAc, pTRAkc-rbcs1-cTP, and pRIC3.0 were grown in LB containing appropriate antibiotics, under the same conditions. Plasmid DNA extraction was performed on all the plasmids using the QIAprep® Spin Miniprep kit (Qiagen) according to the manufacturer's instructions, and DNA concentrations were measured by NanoDrop™ (ThermoFisher Scientific).

2.2.1.4 Cloning of L1 and L2 Genes into Plant Expression Vectors

The L1 and L2 genes were each excised from the parent vectors, and subcloned separately into the 4 different plant expression vectors. The plant expression vectors used were: i.) **pTRAc**, a cytoplasmic expression vector; **pTRAkc-rbcs1-cTP (pTRAkc-cTP)**, a chloroplast targeting expression vector (both provided by Prof. Rainer Fischer, Fraunhofer Institute for Molecular Biology and Applied Ecology, Germany); and **pRIC3.0**, a geminivirus-derived self-replicating viral vector (Regnard *et al.*, 2010).

The pTRAc, pTRAkc-cTP, and pRIC3 vectors each contain: p35SS, a CaMV 35S promoter which contains a duplicated transcriptional enhancer; a CHS (chalcone synthase) 5' untranslated region; pA35S, a CaMV 35S polyadenylation signal for foreign gene expression; ColE1ori, an *E. coli* origin of replication; RK2ori, an *Agrobacterium* origin of replication; *bla*, an ampicillin/carbenicillin resistance gene; and LB/RB, the left and right borders for T-DNA integration. The pTRAc vector also contains SAR, tobacco Rb7 scaffold attachment regions which flank the expression cassette, while the pTRAkc-rbcs1-cTP vector contains *npt II*, a kanamycin-resistant gene; Pnos/pAnos, a promoter or polyadenylation signal of the nopaline synthase gene; and a rbcs1-cTP, *Solanum tuberosum* chloroplast-transit peptide sequence of the RuBisCO (Ribulose-1,5-bisphosphate carboxylase/oxygenase) small-subunit gene rbcS1 (Maclean *et al.*, 2007). The pRIC3.0 vector contains: LIR, a BeYDV long intergenic region; SIR, a BeYDV short intergenic region; and Rep/RepA, a BeYDV rep gene (Regnard *et al.*, 2010).

2.2.1.5 Preparation of L1 and L2 for pTRAkc-rbcs1-cTP cloning and expression

To facilitate cloning of the L1 and L2 genes into pTRAkc-rbcs1-cTP, gene specific primers (16-1642 → 16-1645: Table 2.1) were designed to add a peptide cleavage recognition sequence and an *Mlu*I RE site to the 5' ends of the L1 and L2 genes.

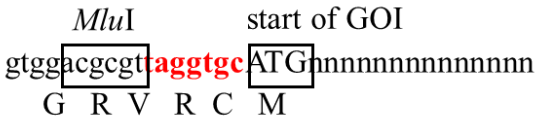

Figure 2.2. Peptide cleavage sequence required for post-translational cleavage of pTRAkc-rbcs1-cTP proteins

The nucleotide sequence (red) between the *Mlu*I site and the start of the gene of interest (GOI) is required for the post-translational cleavage of the chloroplast targeting sequence upstream of the *Mlu*I site, from the target protein. This sequence was omitted from the synthesised BPV1 L1 and L2 genes, and had to be added by PCR for cloning into the pTRAkc-rbcs1-cTP plant expression vector.

The primers were tested *in silico,* using the CLC Genomics Workbench (Qiagen), for their potential to yield the correct product, and synthesised by the DNA Synthesis Unit (MCB, UCT). PCR was performed with KAPA Taq ReadyMix using 50ng each of pUC57-L1 and pUC57-L2 as

template DNA. PCR amplification conditions are specified in Tables 2.1 and 2.2. The PCR products were confirmed on a 1% agarose gel, followed by ligation into the blunt-ended and dephosphorylated pJET vector, using the the CloneJET PCR Cloning Kit (#K1231, ThermoFisher Scientific), as per the manufacturer's instructions. The ligation reaction was transformed into competent *E. coli* (E. cloni®, Lucigen). Positive colonies were confirmed by PCR using pJET specific primers, as well as by RE digestion. The RE digestions and visualisations were performed as previously described.

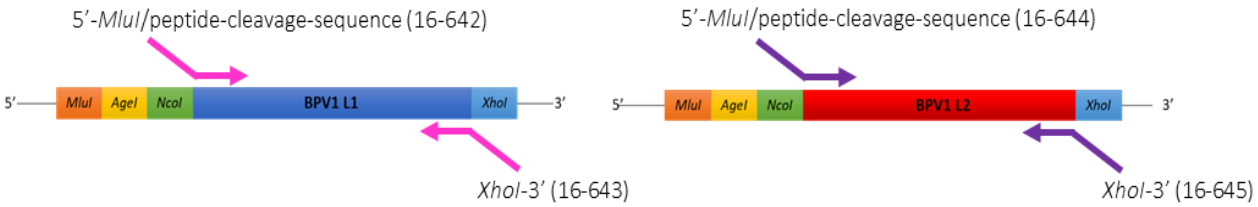

Figure 2.3. PCR addition of 5'-*MluI* site and peptide cleavage sequence.

Figure 2.3. illustrates the primer binding sites and extension directions for the addition of the 5'-*MluI* and peptide cleavage sequence, thereby replacing the other 5' RE sites. The same is shown for the 3'-*Xho*I sites for both L1 and L2.

2.2.1.6 Creation of recombinant clones by ligation

The purified DNA vector and insert fragments were ligated at a 1:3, vector: insert ratio. The fragments were ligated at 37°C for 2h using T4 DNA Ligase (ThermoFisher Scientific). Chemically competent DH5-α *E. coli* cells (E. cloni®, Lucigen) were transformed with the ligation reaction mixtures, and plated onto LB agar plates containing (100 µg/mL) Ampicillin (LB_A). These were incubated overnight at 37°C. Recombinant clones were selected and grown as before, and their DNA isolated and used to transform *Agrobacterium*.

Table 2.3. Vector and construct properties

Vector	Insert	Construct Name	Construct Size (kbp)	RE Sites Vector (5'/3')	RE Sites Insert (5'/3')	Subcellular Target	Antibiotic Resistance
Plant Expression Vector/s							
pTRAc	L1	pTRAc-L1	7.64	*Afl*III/*Xho*I	*Nco*I/*Xho*I	Cytoplasm	Ampicillin (*E. coli*) Carbenicillin (*Agro*)
	L2	pTRAc-L2	7.56	*Afl*III/*Xho*I	*BspH*I/*Xho*I		
pTRAkc-rbcs1-cTP	L1	pTRAkc-cTP-L1	9.22	*Mlu*I/XhoI	*Mlu*I/XhoI	Chloroplast	
	L2	pTRAkc-cTP-L2	9.15	*Mlu*I/XhoI	*Mlu*I/XhoI		
pRIC3.0	L1	pRIC3-L1	7.38	*Afl*III/*Xho*I	*Nco*I/*Xho*I	Cytoplasm	
	L2	pRIC3-L2	7.3	*Afl*III/*Xho*I	*BspH*I/*Xho*I		
Intermediate Vector/s							
pJET1.2	L1	pJET-L1	4.48	Blunt	PCR blunt	-	Ampicillin (*E. coli*)
	L2	pJET-L2	4.37	Blunt	PCR blunt	-	
pUC57	BPV1 L1	pUC57-BL1	4.22	-	-	-	
				-	-	-	
	BPV1 L2	pUC57-BL2	4.14	-	-	-	
				-	-	-	

2.2.1.7 Transformation of *Agrobacterium tumefaciens*

Agrobacterium tumefaciens (*Agrobacterium*) GV3101::pMP90RK were made electrocompetent using the method described by Shen and Forde (1989). These were then transformed with the plant expression constructs, by pipetting 100 µL competent *Agrobacterium* cells into a pre-cooled cuvette with a 1mm gap, adding 200-400 ng of plasmid DNA, and cooling on ice for 5 min. Electroporation was carried out at 1.8 kV, 25 µF, and 200 Ω, and a capacitance reading of ~1.4 was obtained. The cells were supplemented with 900 µL of LB media, and the mixture transferred to a microcentrifuge tube and incubated with agitation at 27°C for 2 h. Following the incubation step, the cells were spread plated onto LB agar plates containing antibiotics Rifampicin (50

µg/mL), Kanamycin (30 µg/mL) and Carbenicillin (50 µg/mL) (LB_{RCK}). The plates were incubated for 24-48 h at 27°C, until colonies were observed.

2.2.1.8 Confirmation of recombinant *Agrobacterium* constructs

Colony PCR was performed on the recombinant *Agrobacterium* colonies, as previously described. Recombinant clones were inoculated into 10 mL LB_{RCK} media containing 2mM $MgSO_4$. These cultures were grown for 24-36 h at 27°C with shaking (220 rpm). Glycerol stocks were prepared from the cultures, and recombinant clones were verified by sequencing of the plasmids using vector-specific primers, after back transformation into *E. coli*. Sequencing was performed by Macrogen Inc. (Netherlands), and the sequencing results were aligned with the native sequences and analysed using CLC Main Workbench 6 (Qiagen), to confirm sequence integrity.

2.2.2 Small-scale Expression Studies in *N. benthamiana*

2.2.2.1 *Agrobacterium*-mediated transient expression in *N. benthamiana*

To determine which *Agrobacterium* cell concentrations yielded the highest protein expression levels, 4-8-week-old *N. benthamiana* plants were infiltrated with recombinant *Agrobacterium* containing the pTRAc, pTRAkc-rbcs1-cTP, and pRIC3.0 L1 and L2 constructs. *Agrobacterium* containing empty vectors were used as negative controls. Overnight cultures were prepared by inoculation of glycerol stocks into 10 mL LB_{RCK} media containing $MgSO_4$ and supplemented with acetosyringone (20 µM). These were grown at 27°C for ~24h with agitation at 120 rpm. *Agrobacterium* suspensions were prepared at 3 cell densities (OD_{600}): 0.25, 0.5, and 1.0, using overnight cultures diluted in induction medium [10mM 2-morpholinoethanesulfonic acid (MES), 10 mM $MgCl_2$, 3% sucrose, and 200 µM acetosyringone, pH 5.6] (Maclean *et al.*, 2007). Diluted cultures were incubated at room temperature for 2h to allow the *vir* genes to be induced by the acetosyringone. The plants were lightly sprayed with water 2h before infiltration, to open the stomata and allow for easier introduction of the cell suspensions into the abaxial spaces of the leaves (M. Sack, personal communication). Three leaves each were infiltrated per construct and per OD, by pricking the leaves with a needle and injecting the cell suspensions into the underside

of the leaves, using a blunt-ended syringe. Approximately 5 mL of cell-suspension was injected per leaf.

2.2.2.2 Small scale protein extraction

The plants were grown at 22°C under 16h: 8h, light: dark cycles. On days 3, 5, and 7 post-infiltration (dpi), three leaf clippings (~0.15g) were harvested from each of the leaves (one per leaf) using a 2 mL microcentrifuge tube to cut and collect the clippings. A volume of 200 µL extraction buffer was added to the leaf clippings; for L1, 1x high salt phosphate buffered saline (HSPBS) [0.5 M sodium chloride (NaCl), 10 mM disodium hydrogen phosphate (Na_2HPO_4), 2.7 mM potassium chloride (KCl), 2 mM potassium dihydrogen phosphate (KH_2PO_4), pH 7.4] solution was used as an extraction buffer and for the extraction of L2, 8M urea was used. Both extraction buffers were supplemented with 1x Complete Mini EDTA-free Protease Inhibitor Cocktail (Roche). Samples were frozen at-80℃ for 10min, after which the leaf clippings were homogenised by bead-milling with two ¼-inch ceramic beads on the VortexGenie2 (Eppendorf) for approximately 1-2 min, until a homogenous green juice was obtained. The samples were clarified by centrifugation at 13,000 x *g* for 5 min, using a benchtop centrifuge. The supernatant was transferred to clean 1.5 mL microcentrifuge tubes and the total soluble protein (TSP) of the crude extracts determined for western blot analysis.

2.2.2.3 Protein Quantification and Analysis

2.2.2.3.1 Total Soluble Protein (TSP) determination

The TSP of L1 was determined using the *DC* Protein Assay (Bio-Rad), as per instructions by the manufacturer, and bovine serum albumin (BSA, Sigma-Aldrich) was used as protein standard for quantification. Absorbance values were determined at 750 nm using a Bio-Tek Powerwave XS Spectrophotometer.

2.2.2.3.2 Protein Separation by SDS-PAGE

The L1 and L2 protein extracts were prepared for 10 % SDS-PAGE by adding 5 x sample application buffer [94 mM Tris-Cl pH 7.5, 1.9 mM EDTA, 10% SDS, 50% glycerol, 4% β-mercaptoethanol (β-ME), and 5% w/v bromophenol blue] to a final concentration of 1 x, and denatured at 95℃ for 10 min. To analyse plant-produced proteins, equal amounts of TSP were denatured as described above. Proteins were loaded on 10% SDS polyacrylamide gels using equal TSP. The Colour Protein Standard, Broad Range (11-2545kDa) (#P7712S, NEB) was used as the molecular weight marker for all SDS-PAGE gels in this study. Proteins were separated by electrophoresis in a BioRad Tetra Cell System at 120 V for approximately 80min. Polyacrylamide (PA) gels were either Coomassie-stained or used for western blots.

2.2.2.3.3 Coomassie-stained Gel

For total protein detection, 10% SDS-PAGE gels were submerged in 1% Coomassie Brilliant Blue stain (Bio-Rad) prepared in dH_2O at 37 °C for 2 h, and destained overnight with destaining solution [45% methanol and 45% glacial acetic acid in distilled water].

2.2.2.3.4 Western Blot Analysis

For western blot analysis, the SDS-PAGE gels were placed on top of a sheet of Amersham™ Protran® nitrocellulose membrane (Merck) of the same size, and fitted between two sheets of blotting paper soaked in transfer buffer [25 mM Tris, 190 mM glycine, 20% methanol, pH~9.2]. The protein was transferred to the nitrocellulose membrane by blotting in the Trans-blot® Semi-dry Transfer Cell at 15 V for 1h15. The membranes were then placed in blocking buffer [5% non-fat dairy milk powder (NFDM), 0.1% Tween20, 1x PBS] for 30min, after which a primary antibody was added. For BPV L1 two primary antibodies were used within this study:

i. A commercially available mouse monoclonal anti-BPV1-L1 antibody [BPV-1/1H8 + CAMVIR] (abcam2417), further referred to as “Abcam antibody”. The Abcam-anti-BPV1 antibody was used at a concentration of 1:1000, with a goat anti-Mouse IgG

whole molecule-AP (Sigma-Aldrich) used as a secondary antibody, at a concentration of 1:5000 (https://www.abcam.com/hpv-antibody-bpv-11h8--camvir-ab2417.html).

ii. A rabbit anti-BPV1 (Dako: B0580, Carpinteria, CA) antibody, further referred to as "Dako antibody". The Dako antibody was used at a 1:1000 dilution, with a goat anti-Rabbit IgG whole molecules-AP (Sigma-Aldrich) used as secondary antibody, at a concentration of 1:5000 (Christensen *et al.*, 1990).

This was followed by incubation overnight at 4°C with agitation. The following day, the membranes were washed 4 x 15min with blocking buffer, after which the secondary antibody, was added, and the membranes were incubated at 37°C for 1h with agitation. Following 4 x 15min wash steps in 1 x PBS-T (blocking buffer without milk), the blots were developed with 5-bromo-4-chloro-3-indolyl-phosphate (BCIP) (Sigma-Aldrich) for 1h.

2.2.3 Evaluation of L2 expression

As no anti-BPV-L2 antibody was available commercially, and as research performed in our labs showed that HPV L2 levels too low to be observed on Coomassie-stained PA gels, two approaches were explored to determine whether L2 was successfully expressing in plants. The first approach was to perform a western blot using two different anti-HPV16 L2 antibodies to probe for BPV L2. One was L2-4B4, a mouse monoclonal antibody (Embers *et al.*, 2002), kindly provided by Neil Christensen, and the other, anti-hL2, was a rabbit polyclonal antibody, previously produced in our group against *E. coli* raised HPV16-L2 antibody. Both of these antibodies were used at a concentration of 1:500, and probed with either an anti-mouse (for L2-4B4), or an anti-rabbit (for anti-hL2) secondary antibody, both at a concentration of 1:5000. A second approach of co-infiltrating L1 and L2 to determine whether L2 expression would have an effect on L1 expression was also explored.

2.2.4 Large-scale expression of BPV1 L1 and L1/L2 VLPs in *N. benthamiana*

2.2.4.1 *Agrobacterium* infiltration of *N. benthamiana*

Agrobacterium starter cultures of the six pRIC3, pTRAc, and pTRAkc-rbcs1-cTP L1 and L2 constructs were prepared from glycerol stocks in 10 mL enriched induction medium (Maclean *et al.*, 2007) supplemented with appropriate antibiotics (LB_{RCK}), as well as 2mM $MgSO_4$, and 200 µM acetosyringone. The starter cultures were grown overnight at 28°C with shaking (220rpm), then transferred to a larger flask and volume of the same media (without rifampicin) for overnight (16-24h) growth. Culture suspensions were prepared for infiltration in induction medium, as previously described, at the optimal ODs as determined in section 2.2.2. The L1:L2 co-infiltration ratios used were based on the optimal ODs for L1 expression as established in Chapter 1, and those previously determined for HPV VLP production (A.R. van Zyl, personal communication)(van Zyl and Hitzeroth, 2016). *Agrobacterium* containing empty vectors were infiltrated alongside the L1 and L1/L2 constructs, as negative controls. These were infiltrated at ODs of 1.0, to establish whether any physiological effects on the plant were due to the expression of the L1 and L2 genes, or other factors related to agroinfiltration. For each construct or construct pair, 10-15 4-8-week old *N. benthamiana* plants were vacuum-infiltrated by submerging the plants in the bacterial suspension and applying a vacuum pressure of -100 kPa for ~20s before releasing the pressure. Plants were incubated for 5 days under 16h: 8h, light: dark cycles at 22°C.

2.2.4.2 Protein extraction and density gradient purification of VLPs

The extraction and purification strategy used was based on one established for HPV16 VLP extraction and purification, and a simplified workflow detailing the major steps of these experiments is shown in Figure 2.4 (A.R. van Zyl, personal communication). Whole leaves were harvested at 5 dpi, and kept frozen at -80°C till use. Crude extracts were prepared by homogenising the leaf material in 2x v/w extraction buffer (HSNaOAc) [0.1 M NaOAc/0.5 M NaCl, pH5.2, supplemented with protease inhibitor cocktail] using a T25 digital ULTRA-TURRAX® homogeniser (IKA). Homogenates were incubated at 4°C for 2h with shaking, then filtered through 4 layers of Miracloth (Calbiochem). Samples were further clarified by centrifugation at 10,000 x *g* (BeckmanT Coulter Avanti® J25TI centrifuge) at 4°C for 15min.

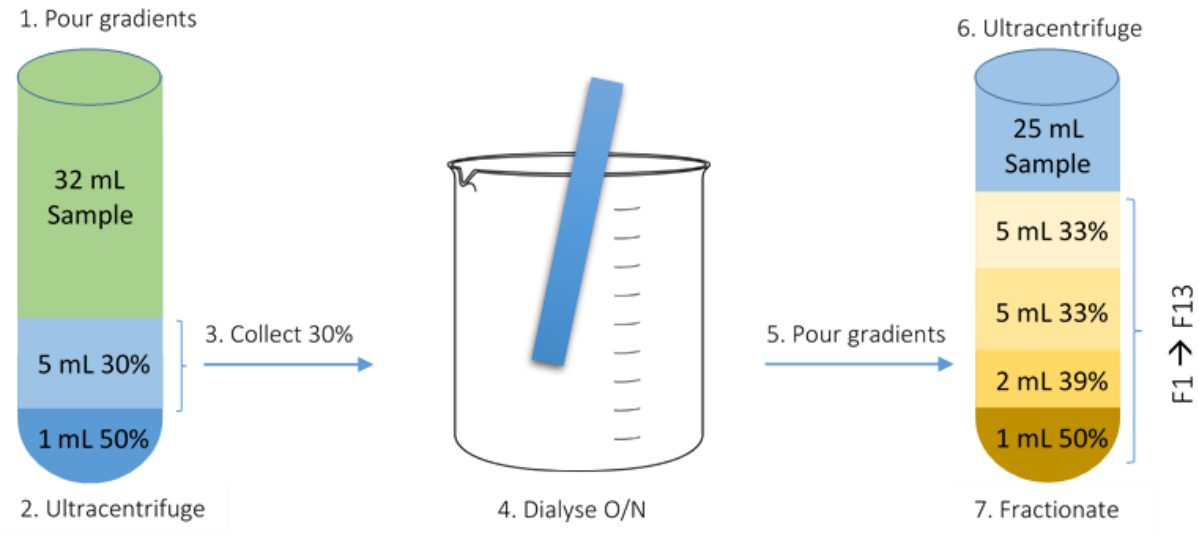

Figure 2.4. Schematic of large-scale protein purification process of BPV VLPs and PsVs.

Sucrose cushion gradients of 50% and 30% w/v sucrose were prepared with the NaOAc extraction buffer, and under-layered beneath the clarified sample (see Figure 2.4). The particles were partially purified onto the cushions by ultracentrifugation at 174,500 x *g* in a SW 32 Ti Rotor (Beckman) at 4°C for 1h15min. The 5 mL 30% cushions were collected and combined, and placed into dialysis tubing. The sample was dialysed overnight at 4°C in 60-100x v/v dialysis buffer (1x HSPBS, pH 7.4). Purification of VLPs was performed by isopycnic centrifugation on a discontinuous sucrose gradient. Gradients were prepared using 1 x HSPBS [1x PBS/ 0.5 M NaCl, pH 7.4] to establish solutions of 50% (1 mL), 39% (2 mL), 33% (5 mL), 27% (5 mL) w/v sucrose. These gradients were under-layered beneath the samples using a long syringe needle. High speed ultracentrifugation was performed at 174,500 x *g* in a SW 32 Ti Rotor (Beckman) at 15°C for 3h30min. The samples were manually fractionated from the bottom of the centrifuge tube, into 13 x 1 mL fractions. These were immediately used for analysis, and the remaining sample frozen at -80°C. Once successful VLP expression and purification was confirmed, large-scale PsV expression and purification was performed.

2.2.5 Protein analysis of purified BPV VLPs

2.2.5.1 Dot blot analysis

Following purification of VLPs, dot blot analyses were performed as a rapid means of detecting whether expression and purification was successful, and for establishing which fractions contained the highest protein yields for further analysis. A grid was drawn onto nitrocellulose membrane, and each square dotted with 4 µL of non-denatured sample. This was allowed to air dry, and the membrane was processed in the same manner as western blots, described in section 2.2.2.3.4.

2.2.5.2 Coomassie-stained PA gel and western blot analysis of protein expression

Samples were prepared for SDS-PAGE separation immediately following fractionation, and dyed with Coomassie blue stain to indicate whether any contaminating plant proteins were co-purified with the VLPs, and to determine protein yields. Western blot analysis was performed by the same procedure described in section 2.2.2.3.4., and was used to confirm the presence of L1 in the various fractions.

2.2.5.3 Particle visualisation and analysis

Transmission electron microscopy (TEM) was used to visualise the purified protein fractions with the highest yields, as established by dot blot analysis. For this, carbon-coated copper grids of mesh size 200 were glow discharged at 25 mA for 30s, using a Model 900 SmartSet Cold Stage Controller (Electron Microscopy Sciences), to make them hydrophilic. The grids were placed onto 20 µL samples of each of the selected fractions for 5min, after which they were washed twice with double-distilled water. The grids were then negatively stained for 1min with 2% w/v uranyl acetate and allowed to dry. The grids were viewed using a Technai 20 transmission electron microscope (FEI) equipped with a LaB6 emitter, operated at 200 kV.

2.3 Results:

2.3.1 Generation and Confirmation of Constructs for Plant Expression

2.3.1.1 Cloning L1 and L2 into pTRAkc-rbcs1-cTP

A 5' peptide cleavage sequence on the pTRAc-cTP vector, located between the *Mlu*I cloning site and the start-codon of the gene of interest (see Figure 2.2), is required for the post-translational cleavage of the protein of interest from the the chloroplast targeting peptide (cTP), which directs the target protein to the chloroplast. Failure to cleave the recombinant protein from the cTP may interfere with the post-translational folding of the protein, and may affect its functionality. When the L1 and L2 genes were synthesised, this sequence was omitted from the gene constructs. Prior to cloning of L1 and L2 into pTRAc-cTP, an *Mlu*I RE site, followed by the peptide cleavage sequence was therefore added to the 5' end of the genes by PCR. The blunt-ended PCR products of ~1.6 and ~1.5 kbp for L1 and L2 respectively, were confirmed by agarose gel electrophoresis (Figure 2.5.A). The PCR products were cloned into pJET and transformed into *E. coli*. Colonies were screened by colony PCR, using pJET primers provided in the pJET cloning kit (Figure 2.5).

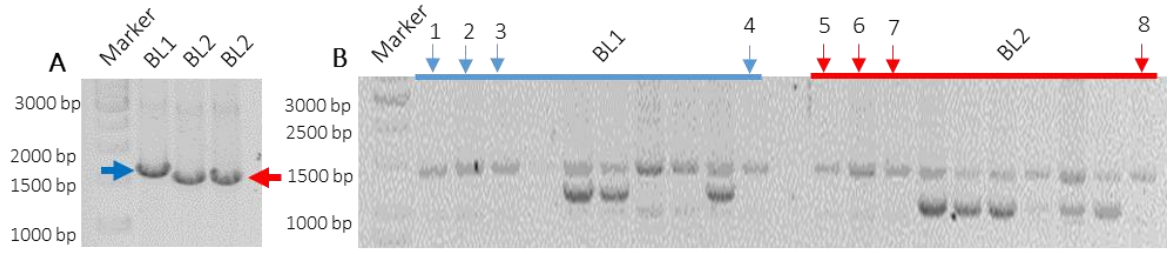

Figure 2.5. PCR addition of *Mlu*I and protein cleavage sequence to L1 and L2 for pTRAkc-rbcs1-cTP cloning.

Figure 2.5.A.) PCR product of MluI and peptide cleavage addition. The blue and red arrows at the ~1.6 and ~1.5 kbp bands indicate L1 and L2 genes with added sequences. **Figure 2.5.B.**) Colony PCR of pJET-BL1 and pJET-BL2 clones. Blue and red arrows indicate positive colonies selected for L1 (1-4) and L2 (5-6) respectively, as only the expected ~1.5/1.6 kbp bands are present in these lanes. Agarose gel electrophoresis was performed using 0.8% gels with EtBr (0.5ug/ml).

The pJET constructs were also digested with *Mlu*I/*Hind*III RE digestion for confirmation of positive constructs and correct cloning orientation. This step was required, as an additional *Xho*I RE site

was present on the pTRAc-cTP vector upstream of the insertion site. Thus, if RE digestion for *Mlu*I was incomplete, and only the *Xho*I sites on the vector and insert were cut, this would yield a fragment of the expected size of the gene of interest, in which both ends of the fragment would have *Xho*I sites. This would mean that the 5'-end would not have a compatible end with the *Mlu*I digested vector yet, and cloning would be unsuccessful. However, all colonies selected yielded the expected band sizes for correct directional cloning, i.e. 2735bp + 1765bp for pJET-L1, and 2670bp + 1704bp for pJET-L2.

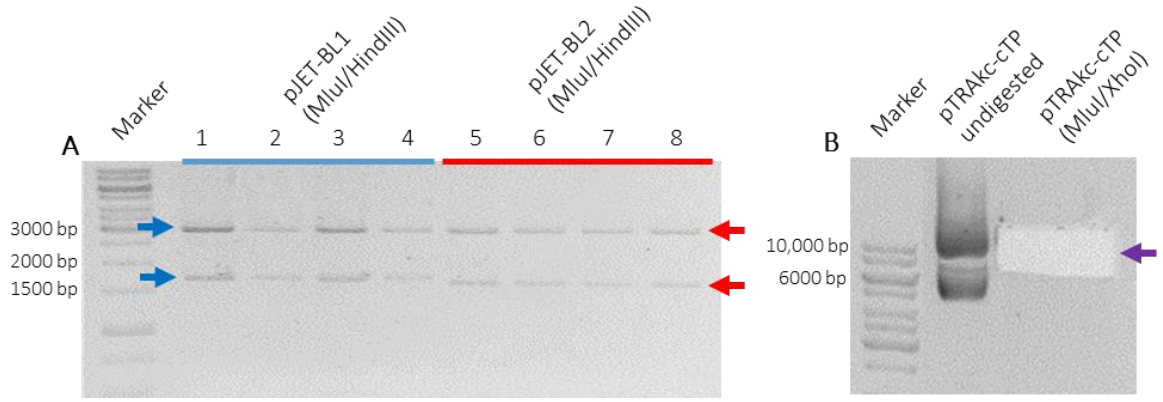

Figure 2.6. RE digestion of pJET and preparation for pTRAkc-rbcs1-cTP cloning.

Figure 2.6.A. shows agarose gel separated fragments of restriction digestion confirmation of positive colonies of pJET-L1 and pJET-L2. Expected band sizes for L1 (2735bp + 1765bp) and L2 (2670bp + 1704bp) are indicated by blue and red arrows respectively. **Figure 2.6.B**.) Agarose gel image of undigested pTRAkc-rbcs1-cTP (pTRAkc-cTP), and excision of pTRAkc-cTP vector linearised with *Mlu*I and *Xho*I (indicated by the purple arrow at ~7.8kbp. Agarose gel electrophoresis was performed using 0.8% gels with EtBr (0.5ug/ml).

Plasmid DNA of pJET-L1 and L2 was digested with *Mlu*I and *Xho*I, and the resulting DNA fragments separated by agarose gel electrophoresis (data not shown). Fragments for L1 (~1.6kbp) and L2 (~1.5kbp) were excised and purified from the gel, ligated with pTRAkc-rbcs1-cTP vector DNA prepared with *Mlu*I/*Xho*I RE digestion (Figure 2.6.B), and transformed into *E. coli*. Multiple colonies were observed after overnight incubation of the transformation mixture on LBamp plates, and screened by colony PCR, the results of which are shown in Figure 2.7.

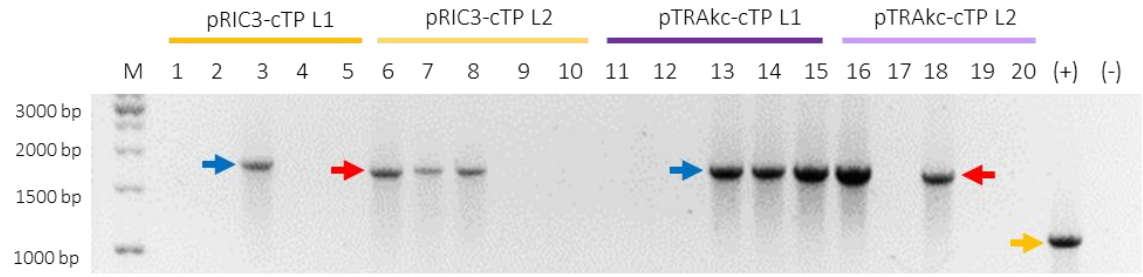

Figure 2.7. Colony PCR confirmation of pTRAkc-rbcs1-cTP (and pRIC3-rbcs1-cTP) constructs in *E. coli.*

The PCR products from the pTRAkc-rbcs1-cTP L1 and L2 constructs are indicated by the blue (~1.6 kbp) and red (~1.5 kbp) arrows respectively. The positive control was pTRAc-AHS-VP7 DNA (kindly provided by Sue Dennis), which yields a 1064 bp product (indicated by the yellow arrow). Agarose gel electrophoresis was performed using 0.8% gels containing EtBr (0.5µg/ml).

2.3.1.2 Cloning L1 and L2 into pTRAc and pRIC3

The L1 and L2 genes were excised from their pUC57 parent vector in which they were delivered, using the respective isoschizomers of *Afl*III (*Nco*I for L1, and *BspH*I for L2) and *Xho*I, and were each successfully cloned into plant expression vectors, pTRAc and pRIC3, and transformed into *E. coli.* Recombinant *E. coli* clones were detected by colony PCR (Figure 2.8), using vector specific primers (Table 2.1).

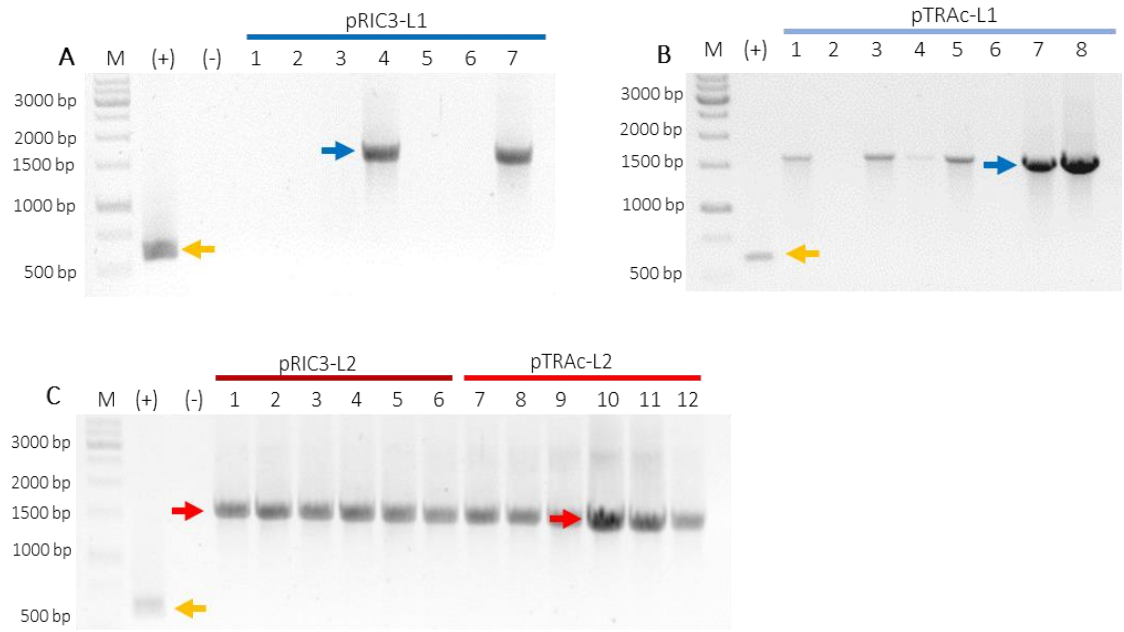

Figure 2.8. Colony PCR of *E. coli* transformed with L1 and L2 pTRAc and pRIC3 constructs.

Positive *E. coli* colonies of pRIC3-L1 and pTRAc-L1 are indicated by blue arrows (~1.6kbp) in **Figure 2.8.A**. and **B**., respectively, and positive colonies of pRIC3-L2 and pTRAc-L2 are indicated by red arrows (~1.5kbp) in **Figure 2.8.C.** The yellow arrows (~600bp) indicate the expected band size for the positive control, pRIC3-LALF-E7 (kindly provided by Renate Lamprecht). Agarose gel electrophoresis was performed using 0.8% gels containing EtBr (0.5µg/ml).

2.3.1.3 Verification of recombinant *Agrobacterium* clones

Recombinant constructs of pTRAc, pTRAkc-cTP, and pRIC3 L1 and L2 were electroporated into *Agrobacterium*. Positive colonies were detected by colony PCR (Figure 2.9) as indicated by the single band of ~1.6kbp for L1, and the slightly smaller ~1.5kbp band for L2 (data not shown for pTRAkc-cTP).

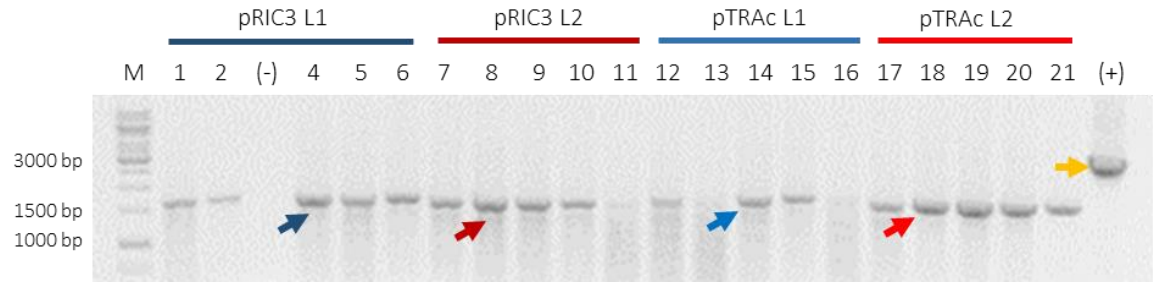

Figure 2.9. Colony PCR of *Agrobacterium* transformed with L1 and L2 pTRAc and pRIC3 constructs.

Positive colonies of *Agrobacterium* transformed with pRIC3-L1 and pTRAc-L1 are indicated by blue arrows (~1.6 kbp), and positive colonies of pRIC3-L2 and pTRAc-L2 are indicated by red arrows (~1.5 kbp). The yellow arrow indicates the expected band size (~2.9 kbp) for the positive control, the AHS-VP3 gene (kindly provided by Sue Dennis). Agarose gel electrophoresis was performed using 0.8% gels containing EtBr (0.5µg/ml).

The integrity of gene sequences was confirmed by sequencing with vector specific primers, from construct DNA obtained after back-transformation into *E. coli*. Sequence data were analysed with CLCBio (Qiagen) by creating a consensus sequence of the forward and reverse sequencing reactions, followed by an alignment with the original sequence data. Sequence analyses confirmed that genes were correct, as no mismatches were observed (data not shown).

2.3.2 Optimisation of L1 Expression in Tobacco Plants

To determine the highest expression conditions of L1 and L2, *N. benthamiana* plants were syringe-infiltrated with each of the constructs at different *Agrobacterium* concentrations, as defined by OD_{600} 0.25, 0.5, and 1.0, as an increase in the *Agrobacterium* concentration has been demonstrated to increase transgene expression (Wroblewski *et al.*, 2005). Cultures containing empty vectors of pTRAc, pTRAkc, and pRIC3 were infiltrated at an OD_{600} 1.0, to determine the effect of the expression vector presence on the plants. The plants were monitored over a 7-day period following infiltration, and protein harvested on days 3, 5, and 7 post-infiltration. The time-trials for pTRAc and pRIC3 were carried out twice, independently. The results of the first of two such independent repeats are shown in the figures below. The physiological effects observed in the repeat of the expression trial were similar to the first set of experiments, and therefore the

leaf samples displayed in Figure 2.10 below were deemed to be representative of the overall effects observed.

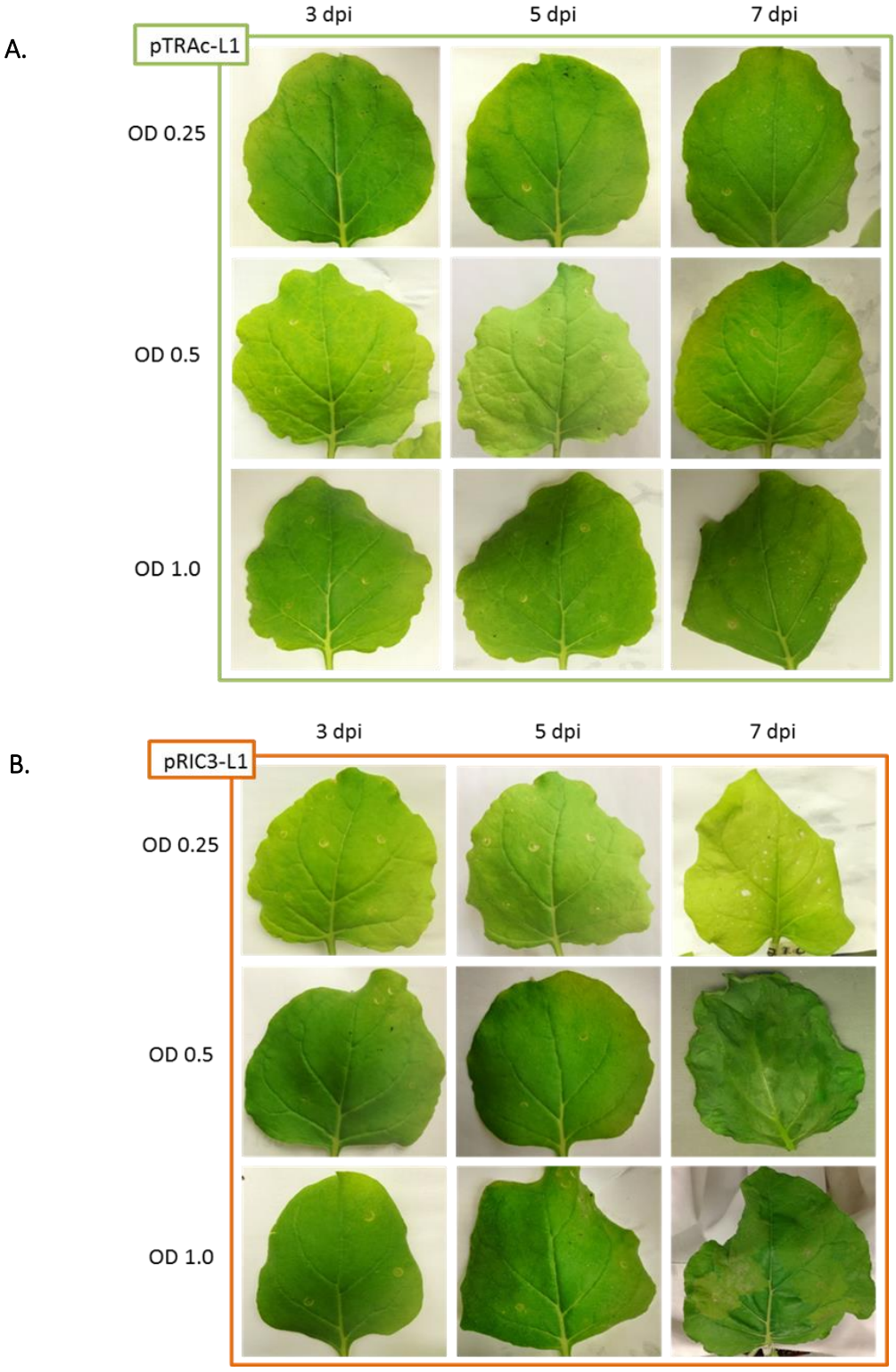

C.

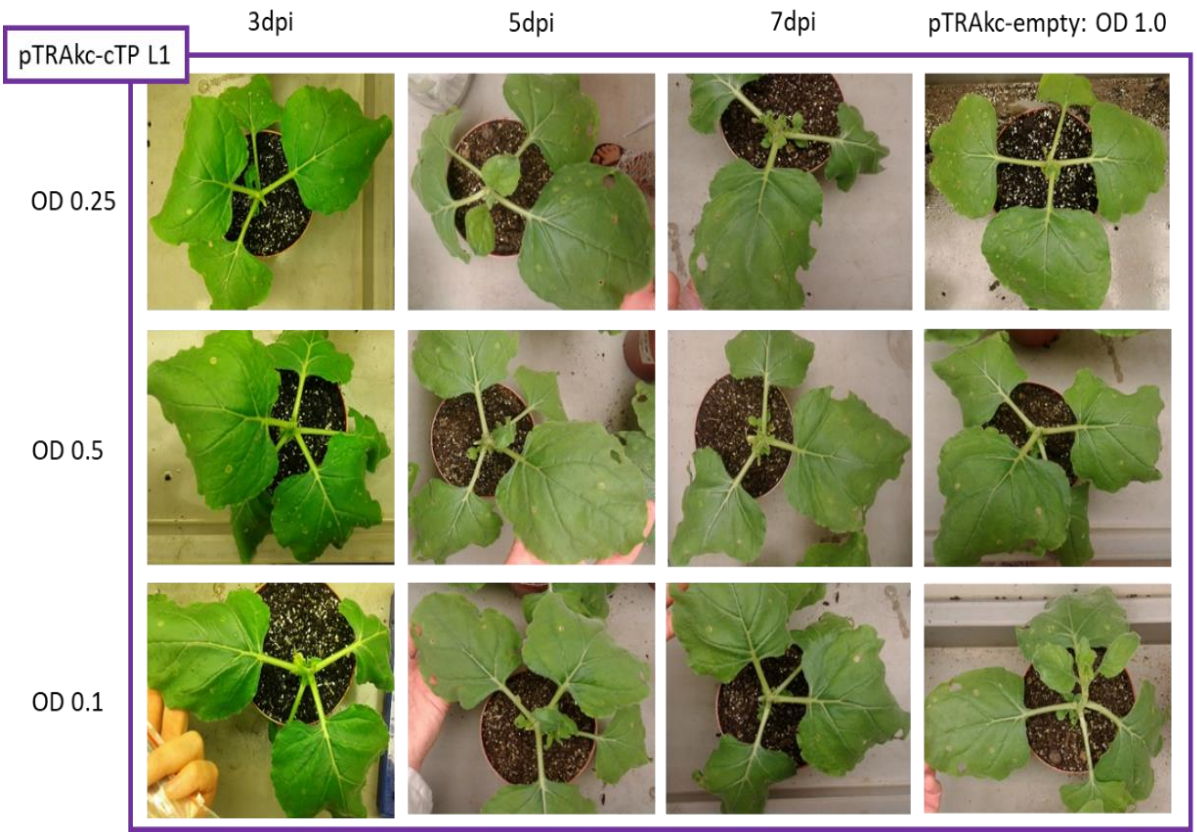

Figure 2.10. Physiological effects of pTRAc-L1, pRIC3-L1, and pTRAkc-rbcs1-cTP-L1 expression on syringe-infiltrated *N. benthamiana*.

Representative samples of leaves from tobacco leaves indicating changes in leaf physiology over time, post infiltration with recombinant *Agrobacterium* containing either A.) pTRAc-L1, B.) pRIC-L1, or C.) pTRAkc-rbcs1-cTP-L1 (pTRAkc-cTP-L1) constructs. Each of the cultures were infiltrated at OD_{600} values of 0.25, 0.5, and 1.0.

2.3.2.1.1 Expression yields

Expression of L1 and L2 in pRIC3, pTRAc, and pTRAkc-cTP was monitored over a 7-day period, with protein harvested at 3, 5, and 7dpi, separated by SDS-PAGE, and analysed on western blots and Coomassie-stained PA gels. Total soluble protein of the pRIC3 and pTRAc L1 infiltrated plants was determined in a Bradford assay against a BSA standard curve and corrected for background. The results of this assay are shown in Figure 2.11. To determine whether the TSP expression correlated with L1 expression, equal amounts of TSP were loaded onto SDS-PAGE gels and

separated for analysis by western blot (Figure 2.12) and Coomassie-stained PA gels (data not shown).

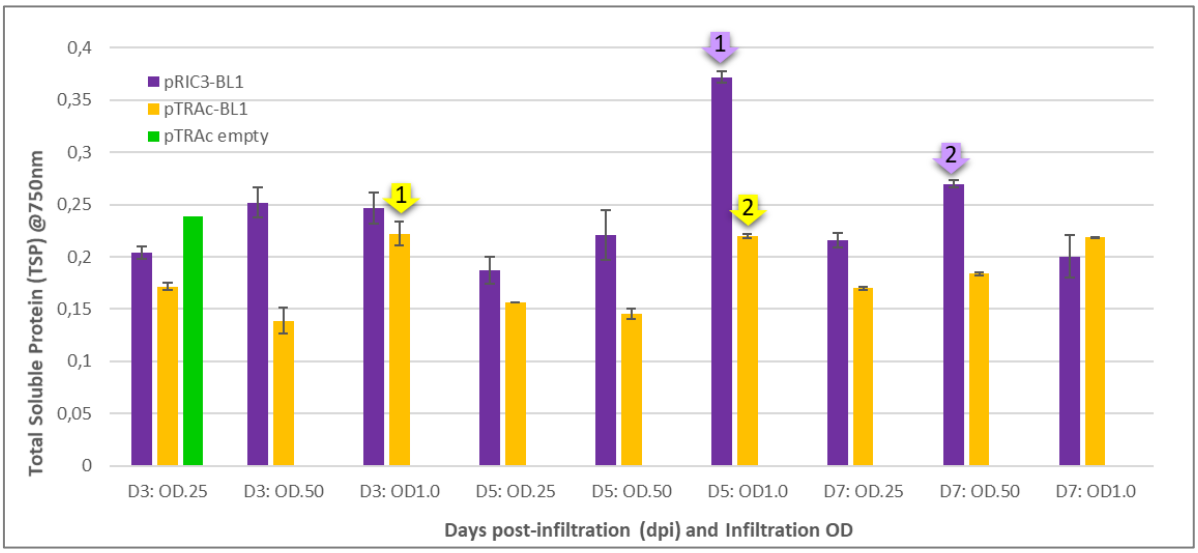

Figure 2.11. Bradford assay of plants infiltrated with pTRAc and pRIC3 L1 constructs

Total soluble protein from plant expression trials with plants infiltrated at different concentrations, as analysed against a BSA standard curve. The arrows indicate the highest and second highest TSP values for pRIC3 and pTRAc each.

Ten percent SDS-PAGE gels were loaded with equal volumes of protein, and the L1 protein probed with the anti-L1 Dako antibody. Western blot analysis (Figure 2.12) of the TSP indicated that L1 was expressed from day 3 onwards for all constructs, and at all OD_{600} values tested, as indicated by the faster migrating band observed at ~52kDa on the western blot Figure 2.12.

Some variation was observed between the results of the first and the second time-trials for pRIC3, with L1 yields highest for the first time-trial at OD 0.25 between 5-7dpi, followed by OD 0.5 between 3-5dpi, and OD 0.5 between 3-5dpi for the second time-trial. Plants had started showing signs of chlorosis by 7dpi for both OD 0.5 and more severe symptoms at OD 1.0. It was therefore decided that both ODs 0.25 and 0.5 would be examined for large-scale infiltrations/VLP production. In the second set of time trials plants infiltrated with pRIC3-L1 at all ODs had started showing signs of necrosis by 7dpi. As this only occurred in one batch, this effect was probably

due to poor plant health compounded by infiltration and expression stress. Taking into account plant physiology and protein levels, a 5dpi harvest time was selected for future studies.

Protein harvested from pTRAc-L1 in both expression time trials indicated that the highest levels of L1 expression occurred at an OD value of 1.0, and that accumulation was relatively consistent throughout the week, with a slight decrease by 7dpi for the second iteration. An OD of 1.0 and harvest time of 5dpi was selected as a median between the results of the different iterations.

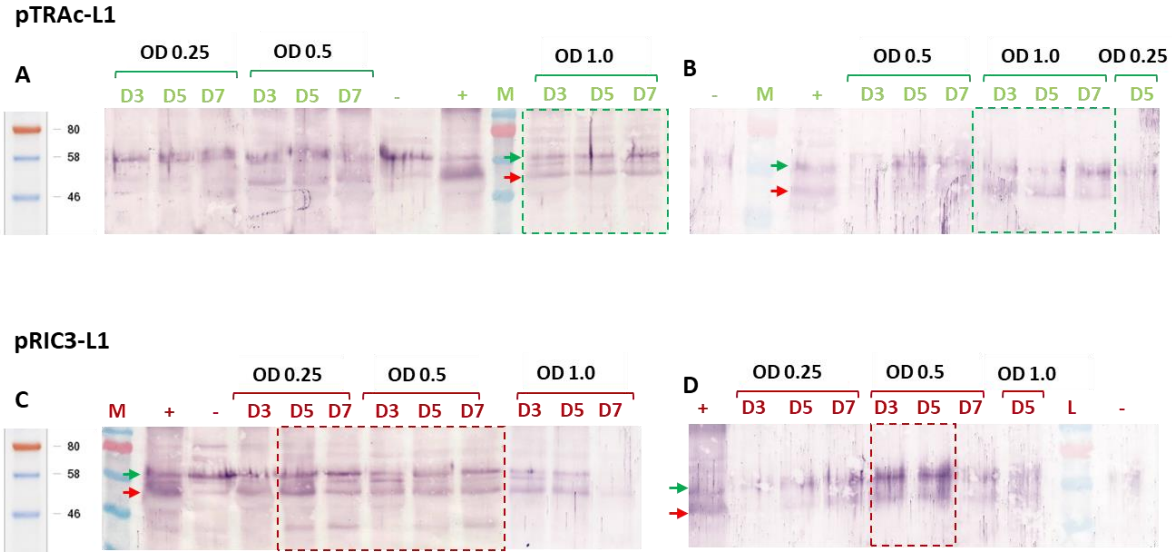

Figure 2.12. Western blots of L1 expression trial and repetition in *N. benthamiana* using pTRAc and pRIC3 plant expression vectors.

Detection of protein expression trials with plants infiltrated with pRIC3-L1 is shown in Figure 2.12.A. & B.) and pTRAc-L1 (C. & D.). The L1 protein was probed with Dako anti-L1 antibody (1:1000) and anti-rabbit IgG alkaline phosphatase-conjugated secondary antibody (1:5000). Labels: M = molecular marker (kDa); D3, D5, D7 = days post infiltration (dpi); green arrows = ~58 kDa protein; blue arrows = ~52 kDa protein; (-) = negative control, plants infiltrated with empty vector; (+) = positive control, for A + C: purified HPV16-L1, for B + D: BPV L1 crude.

Time trials of pTRAkc-cTP L1 expression revealed that the highest levels of L1 expression was obtained at OD 0.5, with expression levels remaining relatively consistent throughout the week (data not shown). Large-scale expression with pTRAkc-cTP for VLP production was performed at OD 0.5, and plants were harvested 5dpi. While these findings did not correlate with those of the

Bradford assay, such differences are expected, as the TSP does not necessarily indicate the levels of target protein expression, which will form only a small portion of the TSP (Maclean *et al.*, 2007).

2.3.3 Antibody detection of BPV proteins

Two different anti-BPV1 antibodies were used to determine expression of L1 in this study. One was a commercially available mouse monoclonal antibody Anti-HPV antibody [BPV-1/1H8 + CAMVIR] produced by Abcam, and referred to as the "Abcam antibody" throughout this study. The BPV1 component (1H8) of this broad-spectrum HPV antibody was produced against SDS-disrupted BPV1 virions and used to identify the product of the L1 ORF of BPV1, and IH8 was found to be reactive with purified major capsid protein, L1. The CAMVIR-1 antibody, was produced against the L1 protein of HPV16, using a recombinant vaccinia virus to express the L1 protein as a target for screening. This antibody reacted with a 56kDa protein in cells infected with the L1-vaccinia virus, and the protein was present in HPV16. The antibody was tested with ELISA and with an immunofluorescent technique and detected HPV-1, 6, 11, 16, 18, and 31 in formalin-fixed paraffin-embedded biopsy specimens. This antibody was the only commercially available anti-BPV1 L1 antibody, and had successfully been used in a study by Love *et al.* (2012) to detect plant-expressed BPV1 L1. The other antibody used was produced by Dako, and is referred to as the "Dako antibody" throughout this study. This unfractionated rabbit antiserum was prepared against BPV1 virions which had been chemically disrupted to expose cryptic determinants prior to their use as immunogens, and was reported to be reactive with papillomavirus genus-specific (common) structural antigens regardless of host species.

The BPV L1 protein has an expected size of ~55 kDa (Kirnbauer *et al.*, 1992), yet bands of ~52 kDa and ~58 kDa were observed in western blots of crude L1 samples, as well as an unexpected ~58 kDa band in the negative control, infiltrated with empty vector. To determine whether these inconsistencies were due to non-specific binding of the specific antibody used, and to compare the different antibodies for their specificity and ability to detect L1, two sets of western blots

were performed using crude L1 samples (Figure 2.13). For both sets of westerns, crude L1 samples of different concentrations were analysed alongside a negative control of empty vector, and a positive control of either crude HPV16 L1, or crude BPV L1. The one set of westerns was probed with either anti-Gardasil (which contains an anti-HPV16-L1 component), or Abcam. These blots were processed as described previously, although the blot probed with anti-Gardasil was developed overnight as nothing had appeared in the BPV L1 lanes after an hour.

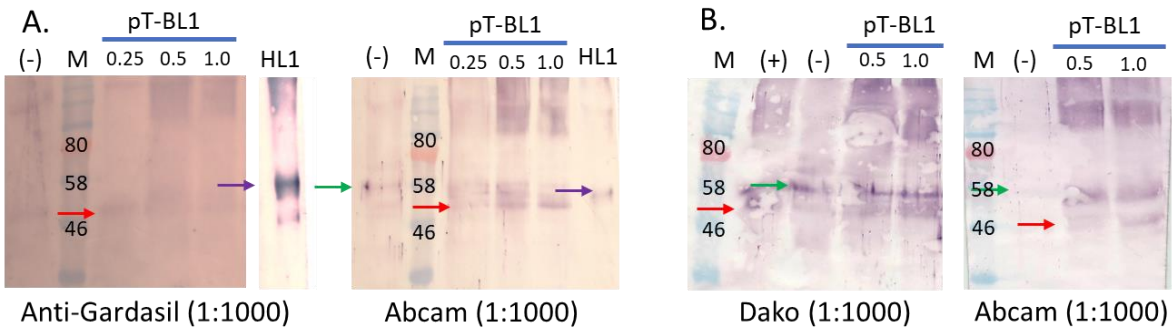

Figure 2.13. Antibody comparison for detection of BPV L1

Western blot analysis of BPV1 L1 obtained from plants infiltrated at different *Agrobacterium* concentrations of pTRAc-L1, from which protein was harvested at 3pi. These blots were probed with different antibodies. Western blot set A compared anti-Gardasil, an anti-HPV cocktail antibody which includes an anti-HPV16 component, with Abcam, an antibody capable of detecting both BPV1 L1 and HPV16 L1. Set B compared the anti-BPV1-L1 antibodies, Dako and Abcam. All antibodies were applied at 1:1000 dilution. Red arrows indicate L1, and green arrows indicate plant protein. Labels: M = molecular marker (kDa); (-) = negative control, plants infiltrated with empty vector; HL1 = purified HPV16 L1; (+) crude BPV L1.

Little difference was observed between the blots probed with the BPV antibodies, Dako and Abcam, with the same bands as previously seen present in the BPV L1 and negative samples, and the only slight difference in the higher background levels and band intensity in the Dako vs. the Abcam antibodies. The disparity between the position of the band observed for HPV16 and BPVL1 observed indicates that it is not the antibody affecting the BPV L1 position, and it is unclear why the band observed for BPV L1 appears lower than the HPV16 L1, which is detected at the expected position. While the Dako was an old antibody, it was still functional and comparable

with the Abcam antibody (Figure 2.13) and as there was a larger amount of this antibody available this antibody was primarily used throughout the study.

2.3.4 Evaluation of L2 expression

Constructs of L1 and L2 for both pTRAc and pRIC3 were syringe infiltrated at OD_{600} concentrations as follows: pTRAc-L1 and pRIC3-L1 were infiltrated at OD_{600} = OD0.5. This was kept the same for individual infiltrations and co-infiltrations. The pTRAc-L2 and pRIC3-L2 constructs were diluted to OD_{600} = 0.25, alongside the pTRAc-L1 and pRIC3-L1 constructs, to give a final co-infiltration OD_{600} of 0.75. Plant leaf clippings were sampled 5dpi, and protein extractions performed. The samples were denatured as previously described, and evaluated by western blot and Coomassie-stained PA gel, the results of which are shown in Figure 2.14.

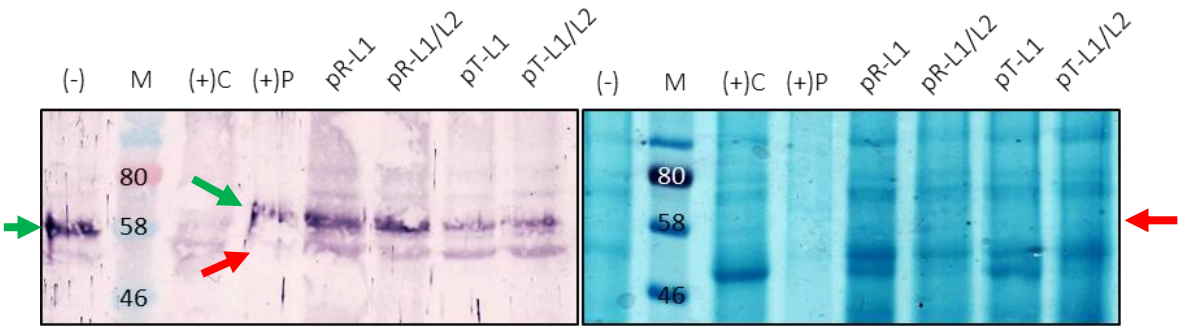

Figure 2.14. Western blot and Coomassie-stained PA gel analysis of co-infiltration of L1 and L2.

Detection of protein expression of plants individually and co-infiltrated with pRIC3 and pTRAc L1 and L2. For the western blot image on the left, the L1 protein was probed with Dako antibody (1:1000) and anti-rabbit IgG alkaline phosphatase-conjugated secondary antibody (1:5000). The same samples were analysed by Coomassie-stained PA gel (image on the right). Labels: M = molecular marker (kDa); (-) = negative control, plants infiltrated with empty vector; (+) = positive control, (P) = purified BPV-L1, (C) = BPV L1 crude.

Western blot analysis of L1 and L1/L2 co-infiltrated plants yielded similar results to what was observed in the expression time-trials, with a band of 58 kDa observed in the crude negative sample, and two bands of ~58 kDa and ~52 kDa in the L1 samples. The bands observed in the Coomassie-stained PA gel were, however, somewhat different to those observed in the western

blot. The ~58 kDa band observed in the positive and negative samples of the western blot, was not observable in the Coomassie-stained PA gel, and an additional band was observed in the Coomassie-stained PA gel for L1-only infiltrated samples at ~48 kDa, just below the ~52 kDa band also observed in the western blot. This additional band was only observed in the L1 samples, which had strong bands at both ~48 kDa and ~52 kDa, while fainter ~52 kDa bands were observed in the L1/L2 co-expressed samples, and no ~50 kDa bands observable. A ~48 kDa band was the only strong band present in the BPV L1 crude positive Coomassie-stained PA gel, for which the western blot had only very faint bands. For clarity on the disparity between the results obtained for HPV L1 and BPVL1, and between the Coomassie-stained PA gels and western blots of BPV L1, mass spectrometry was performed on the bands observed in the Coomassie-stained PA gels.

2.3.5 Mass Spectrometry

To determine whether the bands of ~48 kDa observed in the Coomassie-stained PA gels were L1-only, L1 as well as plant proteins, or only plant protein, crude plant extracts were separated on SDS-PAGE gels, then stained with Coomassie dye. Bands of ~48 kDa were excised and sent for liquid chromatography-mass spectrometry (LC-MS) analysis at the Centre for Proteomic and Genomic Research (CPGR, Cape Town, South Africa). Analyses were performed by in-gel trypsin digestion of the polypeptides, as described by (Shevchenko *et al.*, 2007). The peptide solution was analysed using a Q Exactive™ Hybrid Quadrupole-Orbitrap Mass Spectrometer (ThermoFisher Scientific, USA), coupled to a Dionex Ultimate 3000 nano-HPLC system (ThermoFisher Scientific, USA). Comparison of the sample spectra with sequences obtained from the UniProt Swissprot protein database was performed using Byonic Software (Protein Metrics USA). Samples were analysed against profiles from *Nicotiana* spp. and BPV proteomes. Crude extracts, as opposed to purified protein, were used, in order to obtain a band with sufficient protein present for detection and analysis, and for a greater inclusion of the various components observed throughout the study.

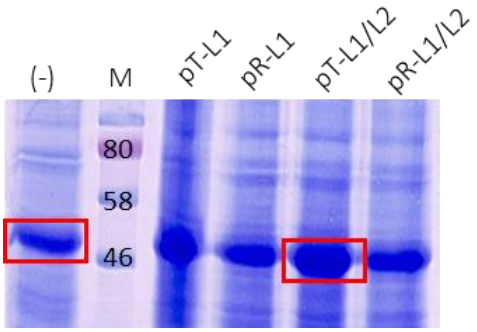

Figure 2.15. Protein bands submitted for mass spectrometry analysis

The identities of the ~48kDa protein species observed on the Coomassie-stained PA gel of both L1 and uninfiltrated (negative) plant samples were independently determined by mass spectrometry. Coomassie-stained PA gel fragments sent for liquid chromatography-mass spectrometry (LC-MS) analysis. The samples were of crude plant extracts, and the two bands selected were the (-) band, a pTRAc empty plant infiltrated sample, and pT-L1/L2, from a plant co-infiltrated with pTRAc-L1 and pTRAc-L2.

Results of this analysis are shown in Appendix A (Figure 1) and revealed that the highest detected (highest ranked) proteins in both the L1 and plant negative samples were proteins of *N. benthamiana.* These included phosphoglycerate kinase, a transferase that catalyses ATP production from ADP, and glycolate oxidase, which is located in the peroxisome, and is involved in the oxidative photorespiratory cycle, assisting in the photosynthetic CO_2 assimilation in C3 plants (Zelitch *et al.*, 2009). Only *N. benthamiana* proteins were detected in the negative sample, but in the L1-sample, BPV1 L1 was detected as well, and ranked 9th overall, with a coverage of 6.67%, indicated against the native protein sequence in Figure 2.16 below.

Figure 2.16. Protein rankings and fragments of BPV1 L1 identified by mass spectrometry

Three sets of amino acid sequences were identified by mass spectrometry analysis of the ~52 kDa band observed in western blots of crude and purified samples of L1-infiltrated plants, and in the Coomassie-stained PA gels of both L1- and uninfiltrated plants.

2.3.6 Large-scale purification of putative BPV1 L1 and L1/L2 VLPs in *N. benthamiana*

Large-scale expression of L1 and L1/L2 were performed using the conditions listed in Table 2.4 below, as established by the expression time trials.

Table 2.4. OD600 values of *Agrobacterium* per construct used for VLP expression

	L1 only	L1:L2	Empty vector
pRIC3	0.25 and 0.5	0.25: 0.5	1.0
pTRAc	1.0	0.5: 0.5	1.0
pTRAkc-cTP	0.5	-	1.0

Papillomavirus L1 and L1/L2 VLPs expressed in plants have successfully been purified by both CsCl (caesium chloride) and sucrose gradient ultracentrifugation in previous studies (Zahin *et al.*, 2016), as well as iodixanol (Love *et al.*, 2012), and sucrose and iodixanol were used in this study for the isopycnic centrifugation purifications of the L1 and L1/L2 VLPs. Plant material was harvested 5dpi from symptom-free plants, and homogenised in HSNaOAc. Purifications were

performed on frozen plant material and the fractions obtained analysed. The results of these purifications are shown below.

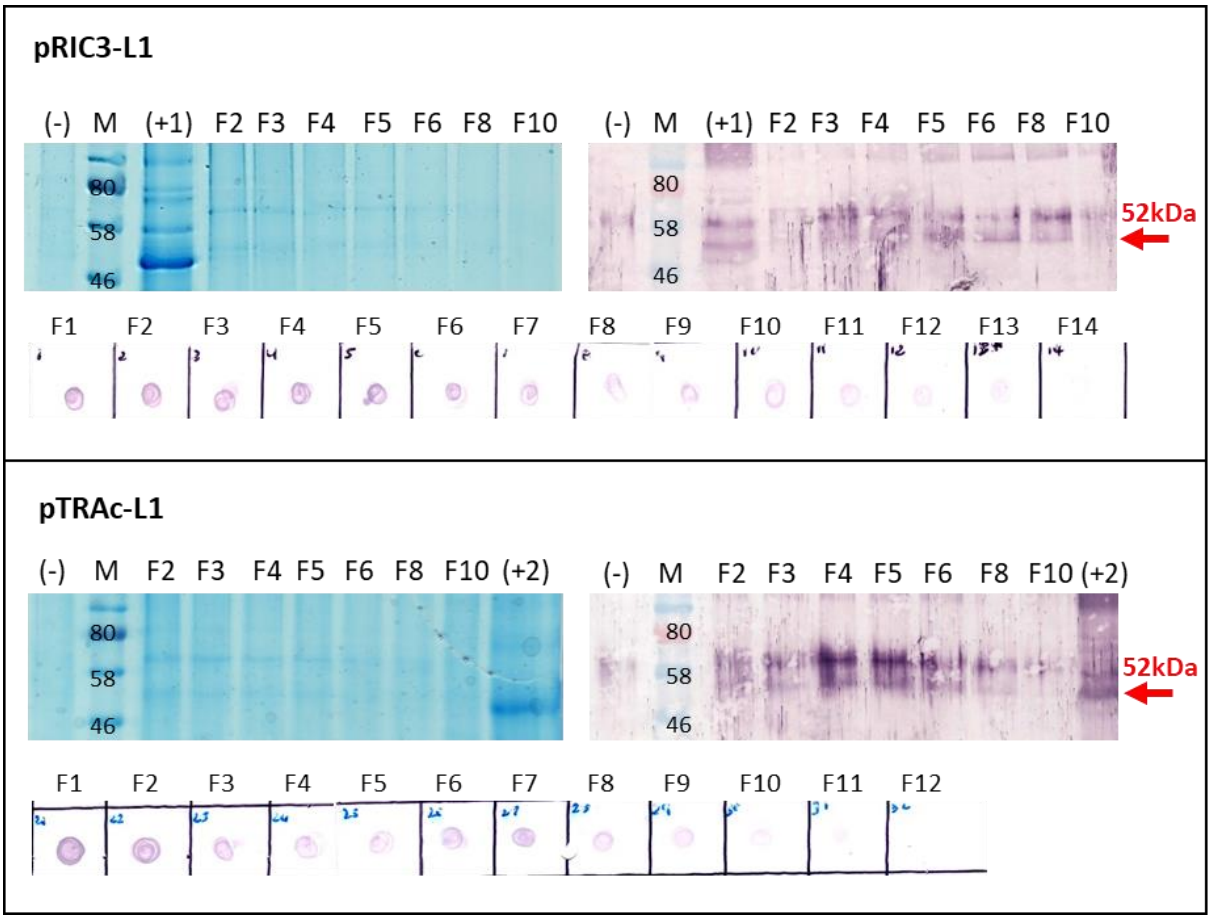

Figure 2.17. Protein analysis of large-scale purified plant-expressed BPV1 L1

Dot blot, western blot, and Coomassie-stained PA gels of large-scale expression and purification of pRIC3-L1 and pTRAc-L1 constructs. Dot and western blots were probed with Dako anti-BPV1-L1 (1:1000). Abbreviations: M = protein marker in kDa; (-) = negative control, purified pTRAc empty F6; (+1) = crude pRIC3 L1, OD 0.25, 3dpi; (+2) = crude pRIC3 L1, OD 0.25, 5dpi.

Protein analysis by western blot, dot blot, and Coomassie-stained PA gel, all revealed the successful expression and purification of L1. TEM analysis was performed on the fractions with the highest signal and these images are shown in Figure 2.18. Magnification was performed at 40,000x, unless otherwise specified.

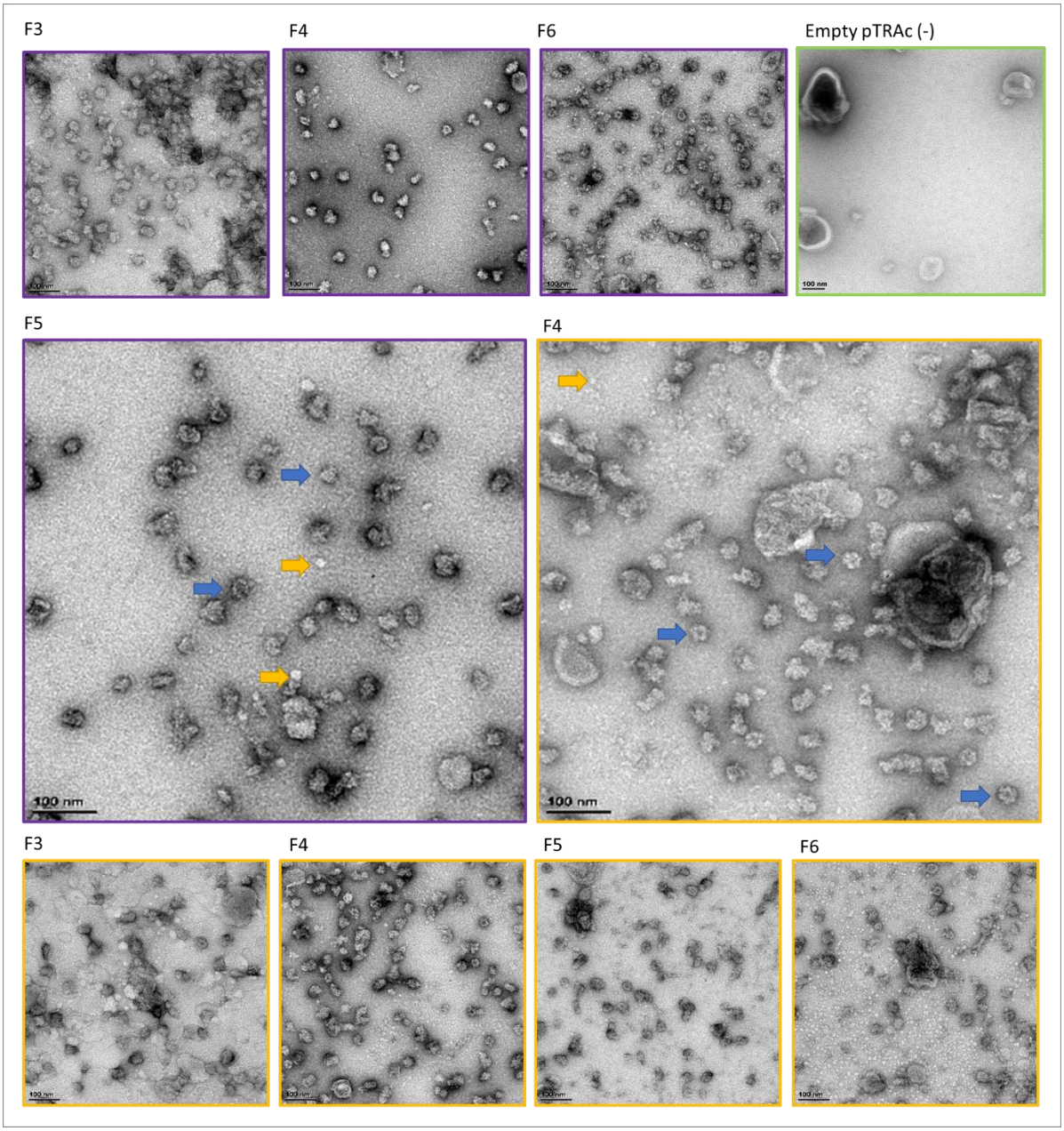

Figure 2.18. Transmission electron micrographs of pRIC3 and pTRAc BPV1 L1 VLPs produced in plants

TEM images of protein purified from large-scale pRIC3-L1 (purple), pTRAc-L1 (yellow), and pTRAc-empty (green) infiltrated plants, harvested 5dpi. Particles were negatively stained with uranyl acetate and visualised under TEM. Capsomeres (~10nm) are indicated by yellow arrows, and T=1 VLPs (20-30nm) are indicated by blue arrows. The scale bar is 100 nm for all images. Magnification was performed at 40,000 x.

TEM analysis of pRIC3 and pTRAc expressed L1 showed the presence of structures (blue arrows), resembling the characteristic doughnut-like, plant-produced T=1 L1 VLPs of ~30nm in size, obtained by Love *et al.* (2012). These structures also correspond with the T=1 VLPs observed in plant-produced HPV16 L1, expressed by Matic *et al.* (2012), and it was thus inferred that these were BPV1 L1 VLPs. Assembly intermediates such as capsomeres (pentameres) of ~10nm (yellow arrows) were also detected in the samples. These results indicate that when the L1 protein is expressed in plants, it maintains its ability to assemble into higher, virus-like structures, and that its integrity is maintained throughout the purification process. No VLP-like structures were observed in the pTRAc empty control.

A comparison of pRIC3 and pTRAc expressed L1 (Figure 2.18) showed little observable difference in the size and number of particles obtained, although those produced by pTRAc L1 expression appeared to be slightly more structured. Purifications of pTRAkc-cTP L1 were also analysed by TEM (see Figure 2.19). Discrete particles were observed in these samples, yet these particles were greatly varied in size and structure, and were dissimilar to the particles expressed with pTRAc and pRIC3. Highly structured spherical balls with diameters ranging from 20 to over 100nm were observed in various fractions surveyed, and while they had some structural similarities to those expected for PV VLPs, appeared to be anomalies. Loosely structured particles in the 20-30nm size range were also observed in these samples, which corresponded to the fractions in which the highest signal was detected in the dot blot (Figure 2.19), and were probably loose VLP assemblages. However, protein yields, as indicated by dot blot, and the number and quality of particles obtained by pTRAkc-cTP L1 expression were lower than those obtained by pRIC3 and pTRAc L1. As these structures did not resemble the native virus, in either its formative or assembled state, and as chloroplast targeting of proteins could not be used for PsV assembly, the use of the pTRAkc-cTP vector for VLP expression was discontinued.

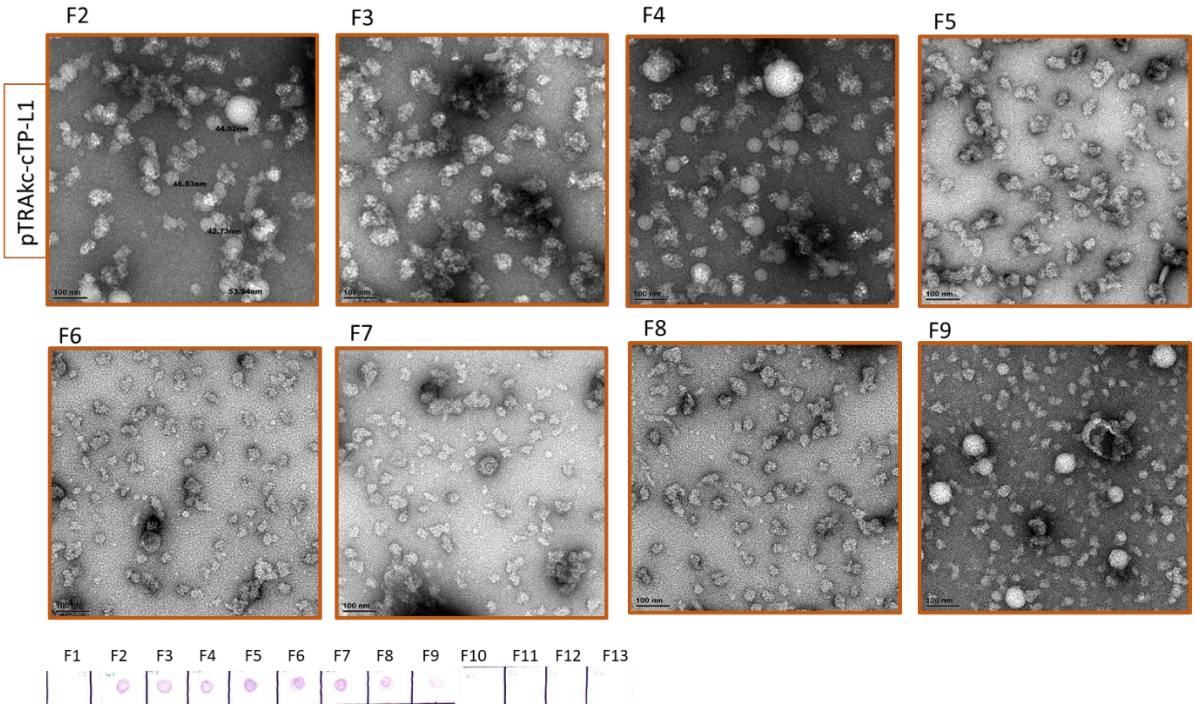

Figure 2.19. Electron micrographs and dot blot analysis of pTRAkc-rbcs1-cTP L1 purified protein fractions

TEM images of sucrose-purified fractions of pTRAkc-cTP L1 expressed in plants, with the corresponding dot blot probed with Dako antibody (1:1000). The scale bar is 100 nm for all images. F= fraction.

Purified co-expressed L1/L2 proteins were also analysed by dot blot, and visualised by TEM to examine the nature of the recombinant protein and to determine whether self-assembly into higher structures had occurred. Results of these purifications are shown in Appendix A, Figure 2. While similar structures were observed in the co-expression studies, there were far fewer VLPs present than in the L1-only samples. Since it has been shown that pentamers self-assemble into VLPs in a concentration dependent manner (Casini *et al.*, 2004), and a decrease in L1 expression would therefore likely result in fewer VLPs forming, this finding may be explained by what has previously been observed for HPV16 L1 expression in our lab, where co-expression with L2 resulted in decreased L1 expression (A.R. van Zyl, personal communication).

2.4 Discussion

The structural proteins of PVs, L1 and L2, can spontaneously co-assemble into VLPs, and do so in a protein-dependent manner (Kirnbauer *et al.*, 1996; Casini *et al.*, 2004). Heterologous protein expression can be dramatically increased through the use of different host plants, gene modifications, and protein targeting, yet the production of transgenic plants through stable gene integration is a complicated process and requires a lot of time. Transient expression of heterologous proteins via agroinfiltration of whole plants has been shown to be a rapid and efficient alternative for protein expression, allowing the investigation of various constructs to be rapidly assessed (Fischer *et al.*, 2015). Several studies have demonstrated that the use of plant expression vectors with different properties may significantly affect the yields of recombinant protein obtained by transient expression (Casini *et al.*, 2004; Shah *et al.*, 2013; Wang and Roden, 2013; Sainsbury and Lomonossoff, 2014; Hefferon, 2017). To investigate the conditions conducive to the highest L1 and L2 expression levels, three binary *Agrobacterium* plant expression vectors were tested: pRIC3, pTRAc, and pTRAc-rbcs1-cTP. These conditions were then applied to large-scale expression of L1 and L1/L2, for the production of VLPs.

Amino acids are encoded by numerous synonymous codons, which are not used with the same frequency. This unequal use of synonymous codons to encode amino acids, known as codon bias, is different for every organism and is known to influence protein expression. Differences between the source and recipient species' codon-usage and RNA regulatory mechanisms may contribute to the often low and unpredictable expression of transgenes (Jackson *et al.*, 2014). In a study by Love *et al.* (2012), in which BPV1 L1 was successfully expressed in *N. benthamiana*, they found that plant codon-optimisation of L1 yielded higher levels of expression than its native counterpart. Therefore, in order to more closely match the L1 and L2 genes of BPV to those of the tobacco expression system, these genes were modified from their native sequences through *N. benthamiana* codon-use-optimisation.

Analysis of L1 expression levels was performed by Bradford assay, Coomassie-stained PA gels, and western blots, and L1 was successfully detected in all of these approaches. While a few disparities were between the expected and observed results, it is clear from analyses in this study, as well as comparisons with previous studies, that crude *N. benthamiana*-produced BPV1 L1 protein appears to migrate to ~52 kDa. There are several potential factors that may affect L1 migration, and therefore the band positions observed in the Coomassie-stained PA gel and western blot, including the close association and co-migration of L1 with RuBisCO and other plant proteins. This may explain why attempts to remove RuBisCO in our lab often result in unintended losses of HPV16 L1 (A.R. van Zyl, personal communication). Potential approaches to overcoming this issue may include the denaturation of the crude extracts to dissociate L1 and RuBisCO. This would, however, linearise L1, and would require its refolding/renaturation and reassembly to form VLP and PsV particles. The reassembly of disrupted BPV1 virions into BPV VLPs has already successfully demonstrated by Paintsil *et al.* (1998), lending viability to this approach.

Mass spectrometry identification was performed on the ~48 kDa bands observable in both the crude L1 and negative samples in Coomassie-stained PA gels (Figure 2.15). As RuBisCO can contribute up to 50% to the soluble leaf proteins in C3 plants, it was hypothesised that the prominent band observed in these samples was the large RuBisCO subunit (expected at ~55 kDa (Ma *et al.*, 2009)), and potentially L1 as well, as the two proteins have a similar expected size. Mass spectrometry analysis of the crude samples of L1-infiltrated plants revealed that the BPV1 L1 protein was detected at a relatively low intensity (1/10th of the average reading) and a low coverage of ~7%, whereas other plant proteins were detected more strongly (see Appendix A, Figure 1, and section 2.3.5). it could also be the case that the band selected only included a portion of the L1 protein, as western blot results indicate that L1 migrates to ~52 kDa, which is slightly higher than the band selected for mass spectrometry. Analysis of purified BPV1 L1 indicates that L1 is strongly detected by western blot, but only weakly detectable by Coomassie-stained PA gel, as can be seen Figure 2.14. The identities of the plant proteins detected strongly in both the negative and the L1 samples largely included enzymes and proteins involved in photosynthesis, with RuBisCO 11th below L1, and 16th in the negative sample. However, mass

spectrometry is not inherently quantitative without a calibration curve of target protein (Urban, 2016), and these results should not be interpreted as such, yet they do provide two important pieces of information: a.) that L1 is present at approximately the same position as the ~48 kDa position band observed in the Coomassie-stained PA gel, and b.) that RuBisCO, among other plant proteins, is also present at the ~48 kDa position. This is further supported by findings of previous studies in our lab, in which the large RuBisCO subunit at was detected in both Coomassie-stained PA gels and western blots at 48 kDa. This supports the theory that RuBisCO and L1 co-migrate and that their interaction may explain the disparity between the expected and observed sizes.

Studies in our lab have shown that plant-produced HPV L2 is not generally expressed at high enough levels to observe in Coomassie-stained PA gels after gradient purification, and since there was no commercially available BPV L2 antibody, and as the HPV L2 antibodies were not able to detect BPV L2, there was no direct way to detect or measure L2 expression. However, in expression studies of HPV16 L1 performed in our lab, it has been observed that plant-based co-expression of L2 has been shown to decrease expression levels of L1. A co-infiltration of BPV L1 and L2 was therefore performed to determine the effect of L2 expression on the levels of L1, and thereby indirectly indicate whether L2 was expressing. The results of L1-only and L1/L2 expression observed in the western blot were largely similar, yet observable differences between the expression levels were seen in the corresponding Coomassie-stained PA gels, as indicated by the lower band intensity observed in the co-infiltrated samples in comparison with those infiltrated with L1 alone (Figure 2.14). This indicates that some decrease in overall plant protein expression had occurred, and suggests that L2 was being expressed, and that these plasmids could be used for the production of L1/L2 VLPs and PsVs. However, the only way to definitively determine whether L2 was expressing would be either through the use of an anti-L2 antibody, or through the production of BPV PsVs, as both L1 and L2 are required for the formation of infectious PsVs for both HPV and BPV (Roden *et al.*, 2001; Buck *et al.*, 2003; Lamprecht *et al.*, 2016). As optimal conditions for L2 expression could not be determined, conditions established in previous studies in our lab on the expression of HPV16 PsVs were used for BPV PsV production, and are detailed in the following chapter.

The targeting of proteins to certain cellular components for post-translational modification and isolation has been shown to increase the yields of recombinant protein (Maclean *et al.*, 2007). Expression levels of L1 were highest when localized to the cytoplasm, such as when using pTRAc and pRIC3, and were higher than L1 targeted to the chloroplast for pTRAkc-cTP. However, the pTRAkc-cTP vector has previously been shown to increase yields of recombinant PV protein expression (Maclean *et al.*, 2007; Yanez *et al.*, 2018), and as the time trial for pTRAkc-cTP was only performed once due to time constraints, additional repetitions should be performed for a more robust analysis. Based on expression time trials, the optimal L1 expression conditions for each vector were established as follows: pRIC3 produced the highest yields of L1 at an *Agrobacterium* OD of 0.25 and 0.5, followed by pTRAc at an OD 1.0, and pTRAkc-cTP at an OD of 0.5. Overall, protein expression of L1 was highest at days 3 to 5 post-infiltration for all the vectors, and as the leaves were still healthy at this point with minimal chlorosis observed, a harvesting time of 5dpi was selected for large-scale expression and VLP production.

In a previous study of BPV L1 expression in insect cells, it was demonstrated that L1 first self-assembles into pentamers, which then combine and form higher order T=1 or T=7 VLPs, which are composed of 12 or 72 pentamers respectively. It was also found that both types of VLPs and their pentameric subunits were highly immunogenic, capable of conferring protection to future challenge with the BPV types from which they were derived, and were thus recognized as suitable prophylactic vaccines (Kirnbauer *et al.*, 1992). In this study, purification of large-scale L1 and L1/L2 expression was performed using a protocol established for HPV purification of plant-expressed proteins (Maclean *et al.*, 2007; Pineo *et al.*, 2013). Purifications of both pTRAc and pRIC3 constructs yielded 20-30nm T=1 particles resembling those obtained in a study Love *et al.* (2012), in which L1 VLPs were produced in plants and were shown to be highly immunogenic and capable of eliciting a strong and highly specific immune response in rabbits. Although no animal studies were performed on the VLPs produced in this study, based on their similarity to those of Love *et al.* (2012), it is likely that these would elicit a similar response.

2.5 Conclusions and Future Work

Both the cloning of L1 and L2 major and minor capsid proteins into 3 different plant expression vectors and their subsequent transformation into *Agrobacterium* was successfully achieved, and these cultures were used to establish favourable expression conditions for the accumulation of L1 and L2 protein. All constructs of L1 successfully expressed recombinant protein in small-scale expression studies, and optimal conditions for large-scale L1 expression was established. These conditions were used to express L1 and L1/L2 VLPs.

In this study, L1 and L2 genes were codon-optimised for *N. benthamiana*, as plant codon-optimisation had previously been shown to improve expression of BPV1 L1 in plants (Love *et al.*, 2012). However, studies in our lab have demonstrated that human codon-optimisation of HPV16 L1 resulted in the highest levels of protein accumulation in comparison with plant-codon optimised and native L1 sequences (Maclean *et al.*, 2007). Therefore human, or potentially bovine codon-optimisation might be explored in future studies. Furthermore, although multiple factors such as the relative abundance of iso-accepting transfer RNAs, gene expression level, gene length, gene conversion, messenger RNA structure, and DNA base composition have been suggested to affect codon usage, it is believed that the most significant contributor to codon bias difference between different organisms is GC-content (or guanine-cytosine content) (Li *et al.*, 2015). A GC-content of ~50-60% has previously been shown in our lab to increase the L1 expression of HPV (Maclean *et al.*, 2007). The plant codon-optimised BPV1 L1 and L2 genes used in this study have GC contents of ~43% and ~48% respectively, and increasing these to 55%-60% might also improve expression levels, and should be explored in future studies.

Particles of L1 and putative L1/L2 VLPs, as well as assembly intermediates, were obtained by expression with pTRAc and pRIC3, and confirmed the ability of these vectors to express proteins at levels sufficient for the production of VLPs. These findings indicate that methods established for HPV protein expression and purification can be used for BPV protein production. Based on

these findings, strategies for HPV PsV production were used as a baseline for the production of BPV PsVs, explored in the following chapter.

As probing of L2 was not possible, it is unclear whether the co-infiltration of L1 and L2 yielded L1/L2 VLPs, yet the successful expression of L1 VLPs formed in this study reaffirms the findings by Love *et al.* (2012) and studies on other PV expression in plants, and sets the platform for the novel production of BPV PsVs in plants. Previous studies in our lab have shown that PsVs are unable to form/encapsidated a pseudogenome without the presence of both L1 and L2, therefore the successful formation of PsVs in the following chapter confirms the first successful expression of BPV L1/L2 VLPs in plants.

3 Chapter 3: Expression and Optimisation of Plant-Produced PsVs

3.1 Introduction

VLP-based vaccines exploit the ability of the PV coat proteins to associate and self-assemble into particles which are physically and immunogenically similar to native virions. Accumulated L1 is capable of self-assembling into higher structures such as capsomeres and VLPs, and can do so both individually or through the co-integration of L2. In a recent study, BPV1 L1 proteins were transiently expressed in tobacco and purified, and were found to have self-assembled into VLPs. These assemblages elicited a strong and highly specific immune response in rabbits, demonstrating the first example of a BPV candidate vaccine produced in plants (Love *et al.*, 2012). Immunisations with PV VLPs in both humans and animals have proven to provide efficient protection against PV infections (Noad and Roy, 2003; Grgacic and Anderson, 2006; Fuenmayor *et al.*, 2017; Mohsen *et al.*, 2017). Early studies have shown that BPV-1 L1 VLPs and BPV-4 L2 multimeric vaccines constitute safe and highly immunogenic vaccine candidates in horses and bovines, respectively (Shafti-Keramat *et al.*, 2009; Hainisch *et al.*, 2012). More recently, the administration of BPV1 L1 VLPs to horses also demonstrated the safety and high immunogenicity of these particles as vaccine candidates (Hainisch *et al.*, 2017), and similar findings were observed in cattle immunised with BPV4 L1 and L1/L2 VLPs produced in insect cells (Kirnbauer *et al.*, 1996), and multimeric BPV4 L2 vaccines (Jagu *et al.*, 2011).

Because L1 is the immunodominant protein in the viral capsid structure, L1 VLP vaccination elicits far higher titres of NAbs than other viral proteins, and it has been the main focus of PV vaccinology studies (Jiang *et al.*, 2016). L1-based vaccines are highly specific, and their effects only cover the viral type included in the vaccine, with the rare exception of BPV1 and 2, which are closely related serotypes and are capable of cross-neutralisation of one another (Shafti-

Keramat *et al.*, 2009). However, anti-L2 antibodies have also been shown to neutralise a range of different HPV types (Pastrana 2005), and an L2-based vaccine might be effective in overcoming the type-specificity of L1 vaccines (Karanam). Furthermore, L2 has been shown to exhibit therapeutic effects. A study by Jarrett *et al.* (1990) showed that when calves were prophylactically and therapeutically vaccinated with BPV2 L1- and L2-beta-galactosidase fusion proteins, the L2 fusion protein was found to be highly effective in promoting tumour rejection, regardless of whether it was administered before or after the challenge, whereas the L1 vaccine prevented BPV2-induced tumour formation only if administered prior to the challenge.

Several animal studies have demonstrated the ability of full-length proteins and polypeptides derived from L2 to protect naïve animals from viral challenge, including that of CRPV and BPV1 and-4, yet very low titres of NAbs were obtained (Jagu *et al.*, 2011). This is due to the fact that the L2 minor capsid protein is subdominant, occurring in lower levels than L1, and is dispersed across the capsid surface to promote B-cell receptor cross-linking and activation. L2 is also largely concealed within the capsid structure of the virion, except during infections (Buck *et al.*, 2008). The weak immunogenicity of L2 is also due to an inability to multimerise and assemble into VLPs, a major shortcoming when aiming for a long-term, preferably life-long, protection. Therefore, L2-based vaccine studies have largely focused on enhancing immunogenicity through strategies such as capsid display, selection of cross-reactive epitopes, fusion with toll-like receptor (TLR) ligands, adjuvant selection, and fusion with early PV-genes, thereby incorporating the therapeutic activity of these elements (Jiang *et al.*, 2016). It was also discovered that the majority of the protective epitopes recognised by NAbs were present in the N-terminus of L2, which is also highly conserved between PV types, making this region an attractive choice for the production of a broadly cross-protective prophylactic vaccine (Kirnbauer *et al.*, 1996; Jiang *et al.*, 2016; Schellenbacher *et al.*, 2017). For these reasons, the incorporation of L2 into a BPV vaccine is of great utility, and this approach was explored in this study.

3.1.1 Therapeutic vaccines

One of the main limitations of current prophylactic vaccines based on structural proteins, is that they do not elicit a cell-mediated response (Bocaneti *et al.*, 2016). DNA vaccines are a relatively recent technology which utilises antigen-encoding DNA plasmids, that are directly administered to elicit both humoral and cellular immune responses. Promoters or enhancers are included on plasmids which promote antigen-specific T-cell immunity yet, unlike subunit vaccines, DNA vaccines do not produce NAbs (Gurunathan *et al.*, 2000). This allows for repeated vaccination, which is useful, as DNA vaccines have been found to have low transformation efficiency in vivo and are poorly immunogenic (Hitzeroth *et al.*, 2009; Peng *et al.*, 2010). Once PVs integrate into the host's genome in late malignancies, the late genes L1 and L2 are lost, and NAbs targeting these proteins, such as those produced through vaccination, are no longer effective against the infected cells (Cheng *et al.*, 2018). To treat and eliminate established infections, early genes which constitutively express in both infected and cancerous cells are targeted by therapeutic vaccines, which induce T-cell-mediated immune responses. These vaccines have been tested in a number of clinical studies, and have been shown to be safe, although to avoid risks associated with the integration of DNA plasmids into the host, such as those of HPV vaccines, genes with oncogenic properties such as E6 and E7 were modified to lack transformation properties (Hung *et al.*, 2007; Lin *et al.*, 2010). Due to their DNA nature, these vaccines are safer, more stable, easier to transport and store, and are capable of inducing a broader range of immune responses than conventional vaccines (Gurunathan *et al.*, 2000). However, DNA has a limited ability to spread or amplify between cells in vivo and does not hold intrinsic specificity for targeting antigen-presenting cells (APCs) (Cheng *et al.*, 2018).

PsVs have emerged as a new class of vaccines which can improve naked DNA vaccine delivery *in vivo*. Through the packaging of plasmid DNA in a protein structure, these vaccines stimulate both the humoral and cellular immune responses, while serving as vectors for nucleic acid gene delivery into various cell types and tissues (Cheng *et al.*, 2018; Hancock *et al.*, 2018). These particles therefore have numerous potential applications, including virion characterisation, *in*

vitro and *in vivo* testing for Nab titres in vaccine testing, and medical applications such as gene therapy and vaccinology (Ma *et al.*, 2011).

PV PsVs package plasmid DNA into L1 and L2 capsid proteins, which stabilises and protects the DNA from nucleases, and delivers the encapsidated DNA into infected cells in an efficient and targeted manner (Cerqueira and Schiller, 2017). The process by which PV PsVs assemble is illustrated in Figure 3.1. In HPV16, PsVs have already been demonstrated to have anti-tumour activity, in their delivery of specific genes to tumour cells in mice, and delivery of the ovalalbumin (OVA) antigen generated the high numbers of OVA-specific CD8+ T-cells in comparison with other DNA delivery methods (Peng *et al.*, 2010). As PV PsVs contain the genes of interest not occurring in the native PV viral genome, these do not replicate, and are thus safer than live viral vectors.

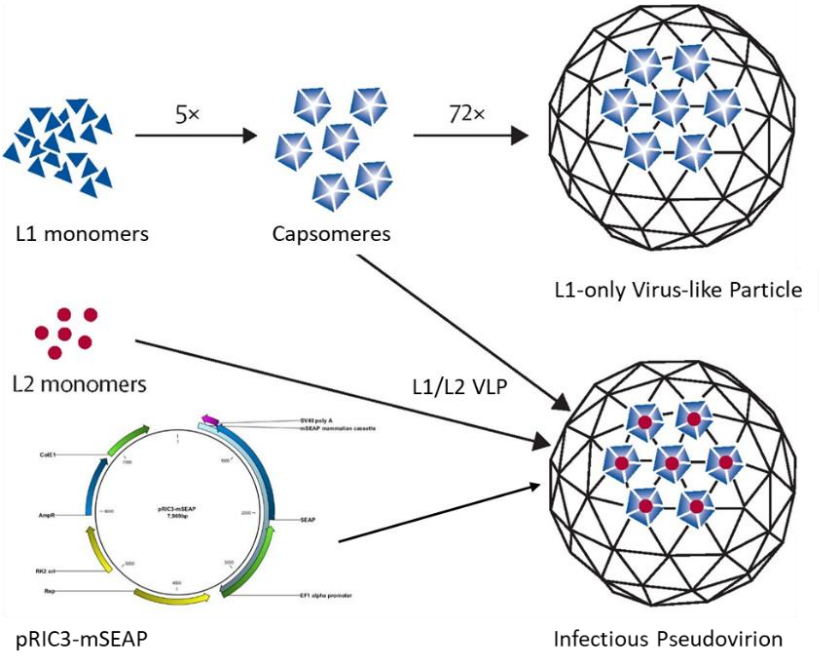

Figure 3.1. Assembly of L1 and L2 monomers into VLPs or PsVs

Assembly procedure of Bovine papillomavirus L1 and L2 proteins into VLPs and PsVs. L1 = BPV major capsid protein, L2= BPV minor capsid protein, x=times. Image modified from Schiller and Müller (2015).

Furthermore, PsVs have been shown to act as adjuvants, facilitating the activation and maturation of APCs, such as DCs (Shi *et al.*, 2001; Peng *et al.*, 2010). Since NAbs are generally not

cross-reactive and target specific PV types, the broad spectrum of PV types within each species may be exploited for the repeated application of different PV PsVs, without the concern for pre-existing immunity. This presents a promising means for the safe delivery of genes for applications such as personalised medicine and gene therapy (Cerqueira and Schiller, 2017). Besides the range of clinical applications that PsVs may be used for, they are also of great research value, especially for vaccine testing in pseudovirion-based neutralisation assays (PBNAs).

Serological testing is an essential part of epidemiological studies and vaccine development, where it is used to determine the efficacy of the vaccine through the detection of virus-specific antibodies. Several assays for measuring antibodies have been developed, the gold standard of which is the PBNA, because it is an independently conducted, unbiased means of assessing the presence of protective antibodies induced by a specific prophylactic vaccine. A PBNA detects all antibodies capable of neutralising and preventing infection by pseudovirions, and which are thus potentially capable of providing protection against a virus. PBNAs have been extensively used in studies on HPV, BPV, and other PVs, and this method is a well-established assessment of both antibody and PsV evaluation (Zhao *et al.*, 2014). One example of this, is the

In this chapter, an optimised strategy for the expression in and purification of BPV PsVs in *N. benthamiana* is described. This construct, referred to as pRIC3-mSEAP was co-infiltrated with BPV1 L1 and L2 to produce plant-produced BPV1 PsVs. Putative PsVs were purified, and analysed by TEM and serological assays, after which they were applied to mammalian cells to determine whether pseudoinfection would occur, and finally tested in PBNAs with various different antibodies to establish whether these particles would be useful for vaccine production and analysis.

3.2 Materials and Methods:

3.2.1 Transient expression of BPV1 PsVs in *N. benthamiana*

Pseudovirion expression of BPV1 was based on methods established for HPV16 PsV production (Lamprecht *et al.*, 2016). The pseudogenome, pRIC3-mSEAP, used in both this and the aforementioned study, was the self-replicating plant expression vector, pRIC3, which was modified to include a mammalian expression cassette encoding for secreted embryonic alkaline phosphatase (SEAP). The autonomous replication of this construct would yield replicons of 4.8 kb, which is within the 8 kb size limit capable of being packaged by PV capsid proteins (Maclean *et al.*, 2007; Lamprecht *et al.*, 2016).

For large scale expression of PsVs, starter cultures of recombinant *Agrobacterium* containing pTRAc-L1, pTRAc-L2 and the pRIC3-mSEAP reporter-gene construct (kindly provided by Megan Hendrikse) were prepared from glycerol stocks, as described in section 3.1.1. Cultures were scaled up for vacuum infiltration, with the final overnight culture free of rifampicin. The cell concentrations (OD_{600} values) used for co-infiltration of pTRAc-L1, pTRAc-L2, and pRIC3-mSEAP are indicated in Table 3.1, and were initially optimised for the expression of HPV16 PsVs. Infiltrated plants were incubated under 16h: 8h, light: dark cycles at 22°C. Biomass was harvested at 4dpi and frozen at-80℃. Purification of PsVs was performed using the same method described in 2.2.4.2 for VLP purification, purified protein fractions were analysed by the methods described for VLPs in section 2.2.5.

Table 3.1. OD600 values of Agrobacterium per construct used for PsV expression

	pTRAc-L1	pTRAc-L2	pRIC3-mSEAP	Total
OD_{600}	0.25	0.05	0.70	= 1.0

3.2.2 Optimisation of PsVs Expression and Purification:

After initial successful expression of VLPs and PsVs were achieved, several methods related to expression and purification of putative VLPs/PsVs were explored to increase overall expression

levels and particle yields. Pseudovirions were mainly used for this purpose, due to their ability to be quantified by SEAP assay, and for their ability to produce a greater number and diversity of particles. Methods explored are categorised as either expression optimisation or purification optimisation, and are listed chronologically in the order in which they were performed. Certain of the optimisation techniques were adopted once their results were known, and thus further optimisation studies were performed using a modified/optimised method. For clarity, a flow chart demonstrating the order and adoption of purification techniques is shown in Figure 3.2, and specific modifications to the standard protocol are specified in the relevant sections below. Head-to-head comparisons were established using the same batches of PsV-infiltrated plant material (harvested at 4dpi) per set, unless otherwise specified. The results of these purifications were analysed by a combination of one or more of the following: dot blots, western blots and Coomassie-stained gels, TEM, and SEAP assays.

Purification Optimisation

3.2.2.1 Purification Optimisation: Fresh vs. Frozen Plant Material

The protocol established in our labs for HPV purification uses frozen plant material for purification of VLPs and PsVs, with no losses in the quality or quantity of yields observed in comparison to fresh plant material. To determine whether freezing and thawing of plant material would have a detrimental effect on the BPV particles obtained, plant material from a single batch of PsV-infiltrated plant material was compared for these two variables. One half of the batch was immediately processed following the standard protocol described in section 2.2.4.2., and the other half of the plant material was frozen at -80℃ for 14 days, before processing by the same method. All further experiments were performed using plant material that had been stored at -80℃.

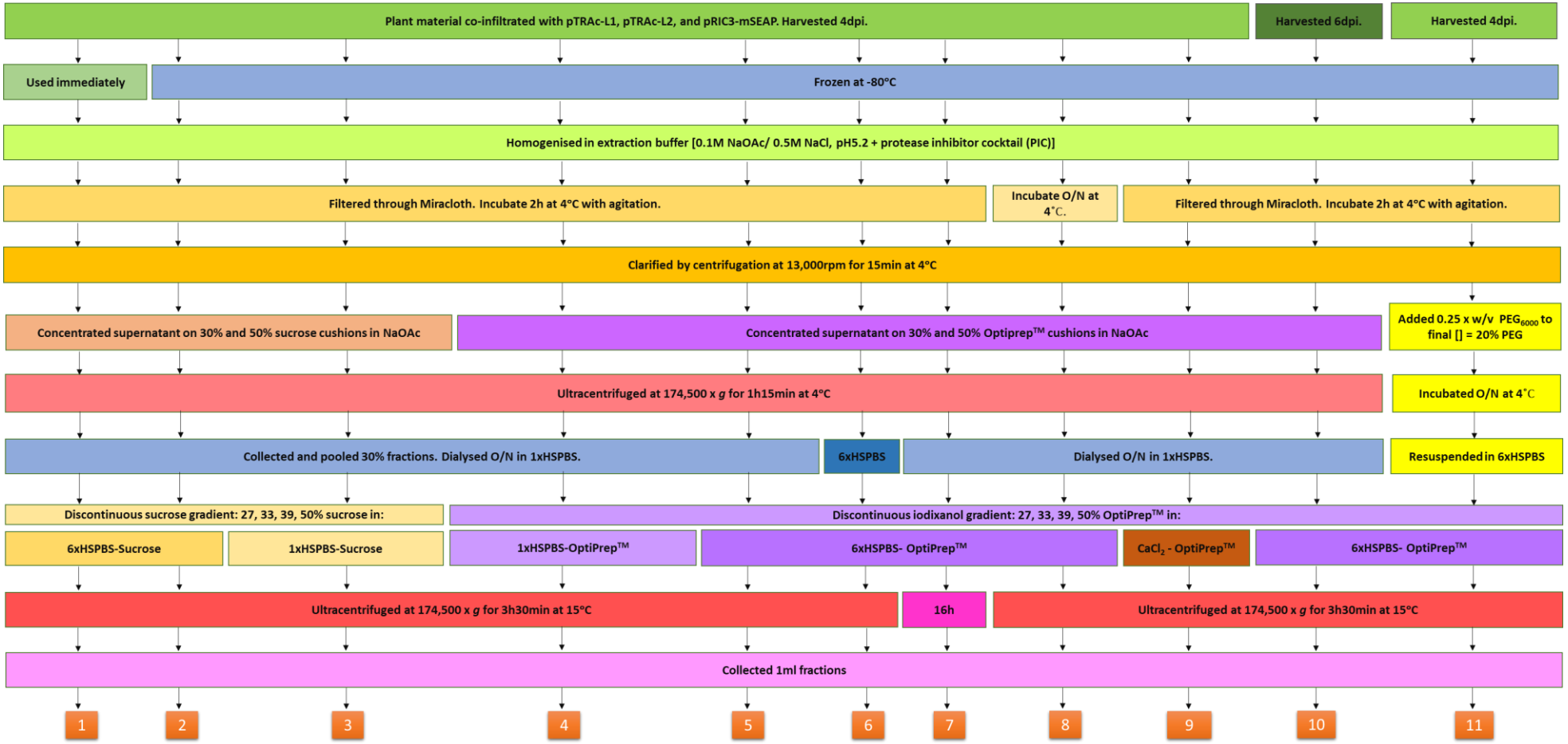

Figure 3.2. Flow chart of purification strategies of transiently expressed PsVs.

Numbers 1-11 indicate the different purification methods that were explored for PsV purification purposes. While following the same basic strategy, the rows of arrows indicate separate, independent purifications, with variations on the standard purification method, represented by #4.

3.2.2.2 Purification Optimisation: Iodixanol vs. Sucrose Gradients

OptiPrep™ Density Gradient Medium (Merck) is a sterile endotoxin-free iodixanol medium which can be applied directly to cells. It is regularly used for the purification of VLPs and PsVs, and has been established in our lab as a suitable medium for the purification of plant-produced HPV VLPs and PsVs, and is also the medium of choice for the purification of VLPs/PsVs from mammalian cells (Buck *et al.*, 2003). To determine whether there was an observable difference in the quantity and quality of the particles obtained when purifying with either iodixanol or sucrose gradients, crude extracts from the same batch of PsV-infiltrated plants were cushioned on, and separated using the same concentration (%) steps of either iodixanol or sucrose gradients. Crude plant extract was underlaid with cushions of 30% and 50% iodixanol, then subjected to ultracentrifugation, after which the 30% steps were collected and dialysed overnight in 1xHSPBS, as per the standard protocol. Purification of particles from the dialysed sample was performed using a discontinuous iodixanol gradient, in which the gradients were prepared with 1xHSPBS. This set of experiments was later repeated using 6xHSPBS for preparation of the discontinuous iodixanol gradients. As greater separation was achieved with iodixanol, all further experiments were performed using iodixanol gradients.

3.2.2.3 Purification Optimisation: 1xHSPBS vs. 6xHSPBS Buffer

Preliminary results of BPV PsV purification indicated that higher salt concentrations in the final density gradient may have a positive influence on the number and quality of particles obtained. To determine whether a 1x or 6x concentration of the HSPBS buffer used in the overnight dialysis buffer and/or final density gradient affected the yields and quality of samples, two sets of experiments were performed.

For the first experiment, the effects of using 1xHSPBS or 6xHSPBS to dilute the OptiPrep for the iodixanol gradients of the final density gradient were explored. Partially-purified PsV samples were prepared by overnight dialysis of the 30% iodixanol cushion in 1xHSPBS. One half of the sample volume was underlaid with 1xHSPBS-iodixanol gradients, and the other half underlaid with 6xHSPBS-iodixanol gradients. The samples were further processed as per the protocol.

For the second set of experiments, the effects of overnight dialysis in a high salt buffer was explored. The 30% iodixanol sample was divided, with one half dialysed overnight in 1xHSPBS and the other half dialysed overnight in 6xHSPBS. Both sets of samples were separated by discontinuous gradients prepared with 6xHSPBS-iodixanol gradients. All further experiments were performed with overnight dialysis in 1xHSPBS, and the final density gradients prepared with 6xHSPBS-iodixanol.

3.2.2.4 Purification Optimisation: Extended centrifugation

From the purification processes tried thus far, particles of different sizes were obtained in some of the fractions, yet it was of particular interest to be able to analyse particles of different sizes separately in order to analyse their properties, and specifically to determine whether the different sizes corresponded to either VLPs or PsVs. Isopycnic density gradient centrifugation separates particles based on their densities, and while it is possible that particles of different sizes might have similar densities, it could also be that the centrifugation time of 3h30min (3.5h) was not sufficient to allow particles to migrate to their true densities. Thus, in order to try further separate and concentrate the particles by their densities by allowing a longer migration time, the final density gradient ultracentrifugation was performed extended to 16h. This experiment was carried out at the same time, and with the same plants as those in sections 3.2.2.3 and 3.2.2.6.

3.2.2.5 Purification Optimisation: Extended maturation

The production of PsVs in mammalian cells requires an overnight maturation step (Buck *et al.*, 2003), which indicates that the protein assemblages may benefit from additional time in which to form more stable structures, and studies on the production of plant-produced African horse sickness (AHS) VLPs in our lab found that overnight incubation of crude extract produced higher levels of VLPs (Sue Dennis, personal communication). To determine whether an extended incubation period of the crude extract would yield higher number of particles, an overnight incubation was performed on the crude extract of PsVs. The rest of the procedure was performed as per the standard protocol.

3.2.2.6 Purification Optimisation: $CaCl_2$ buffer

In addition to modifications on the standard protocol, two separate techniques/buffers were explored for purification purposes. These were the use of a $CaCl_2$ (calcium chloride) buffer, discussed below, as well as purification using PEG (polyethylene glycol) precipitation (discussed in section 3.2.2.7). A $CaCl_2$ buffer had been used in a study by Paintsil *et al.* (1998), in which they demonstrated that calcium was essential for the reassembly of disrupted BPV virions. A modified version of this buffer was used for the overnight dialysis and density gradient ultracentrifugation of partially purified PsVs. The $CaCl_2$ dialysis buffer, in which the 30% cushion sample (obtained by the standard procedure) was dialysed overnight at 4℃ in a 100x v/v ratio, consisted of 150mM NaCl, 25mM $CaCl_2$, 0.01% Triton X-100, 100mM Tris-acetate, balanced to a pH of 5.0 with acetic acid. The same buffer, to which DMSO was added to a final concentration of 10%, was used for the preparation of iodixanol gradients. This was subjected to density gradient ultracentrifugation as per the standard protocol.

3.2.2.7 Purification Optimisation: PEG precipitation

Precipitation of particles by PEG has been shown to be a rapid, cheap, and efficient method to precipitate plant viruses and recombinant protein produced in plants, and has been shown to be an effective tool in eliminating RuBisCO from plant protein samples, and enhancing detection of low abundance proteins (Xi *et al.*, 2006). This approach was tested to separate the BPV particles from the RuBisCO and other plant proteins.

Plant material was homogenised and clarified as per the standard protocol, then poured into a 500mL Schott bottle, and 0.25x v/v 20% PEG/1M NaCl was added to a final concentration of 4% PEG, 0.2M NaCl. This mixture was incubated at 4℃ for 2h with stirring. The suspension was then centrifuged at 10,000 x *g,* and the pellet resuspended in 25 mL 6xHSPBS. This suspension was loaded onto a 6xHSPBS-iodixanol gradient, and further processed as per the standard protocol.

Expression Optimisation

Once the best purification techniques were established, the focus of this study shifted to improving expression levels of BPV PsVs.

3.2.2.8 Expression Optimisation: 200 vs. 500 µM acetosyringone

A recent study by Norkunas *et al.* (2018) found that the use of 500 µM acetosyringone, amongst other chemical additives such as 5 µM lipoic acid and 0.002% of a surfactant, Pluronic F-68, significantly increased recombinant gene expression. The current protocol employed in our research unit and used throughout this study uses 200 µM acetosyringone for *vir* gene induction. To determine whether increasing the acetosyringone levels could increase expression of the target genes, *Agrobacterium* suspensions for PsV expression in plants were prepared as described in section 2.2.4.1. *Agrobacterium* cultures of pTRAc-L1, pTRAc-L2, and pRIC3-mSEAP plasmids were combined in the OD ratio 0.25: 0.05: 0.75, and diluted with infiltration media. This suspension was split, and half supplemented with 200 µM acetosyringone, and the other half with 500 µM acetosyringone. The suspension was incubated at room temperature for 2h to allow the acetosyringone to act on the *vir* genes. These suspensions were used to infiltrate 10-15 plants each, and the plants were harvested 4dpi and maintained at -80℃ until processed.

3.2.2.9 Expression Optimisation: Heat shock

In the same study mentioned in the previous section (Norkunas *et al.*, 2018), it was also discovered that a simple heat-shocking of whole plants 2 days post infiltration, increased transgene expression by up to fivefold. To test whether such a heat shock procedure would increase the expression of BPV PsVs, 10-15 whole plants infiltrated with Agrobacterium suspensions prepared as per the standard protocol, were incubated for 30min in a 37℃ incubator at 2 days post infiltration. These were harvested at 4dpi, processed, and compared with plants that had not undergone heat shock treatment.

3.2.2.10 Expression Optimisation: Extended incubation of PsVs *in planta*

Production of PV VLPs and PsVs in mammalian cells includes a maturation period for the accumulated capsid proteins to self-assemble into higher structures (Buck *et al.*, 2003). From this principle, an additional *in planta* maturation period to allow accumulated protein to assemble into PsVs and VLPs was explored. A batch of plants infiltrated by the standard PsV protocol were harvested either 4 days or 6 days post-infiltration, and processed as per the optimised strategy. These purifications were compared for particle formation and yield, by dot blot and TEM analysis.

3.2.3 Quantification and analysis of PsV expression and activity

3.2.3.1 Growth and maintenance of HEK293TT cell culture

HEK293TT cells were used for all mammalian cell culture experiments. Cells were cultured in complete Dulbeco's Modified Eagle Medium (cDMEM) with 1% GlutaMAX (Life Technologies), supplemented with 10% Fetal Bovine Serum (Hyclone™ FBS, Separations), 1% non-essential amino acids (Gibco), Penicillin-Streptomycin (100 units/mL penicillin, 100 µg/mL streptomycin) (Sigma Aldrich) and 250 µg/mL Hygromycin B (Roche). Cells were incubated at 37°C in 5% CO_2 and 95% humidity. Cells were passaged when they reached 90% density, with a seeding density of 10% (approximately $1x10^5$ cells/ml).

3.2.3.2 SEAP Assay for PsV pseudoinfection of mammalian cells

In order to perform vaccine testing on BPV1 PsVs, it is necessary to demonstrate both their ability to pseudoinfect mammalian cells, as well as the prevention of such an infection through the use of BPV1 NAbs. To quantify the relative abundance of PsVs in the different fractions, and to determine whether these could be used for a pseudovirion-neutralisation assay (PBNA), mammalian cells were pseudoinfected with plant-produced PsVs. HEK293TT cells were trypsinated, resuspended in cDMEM, and counted in a counting chamber. Cells were aliquoted in a Corning® Costar®24-well plate (Merck) at $1.5x10^5$ cells/well, and incubated overnight at 37°C and 5% CO_2. PsV fractions were diluted 1:10 in cDMEM, and added to the cells in triplicate at 500 µL/well. The cells were further incubated for an additional 72h, after which SEAP activity was

assayed using the Great EscAPe SEAP Chemiluminescence Kit (Clontech Laboratories, Inc.), as per the manufacturer's instructions, although the protocol was slightly modified to change the volumes of the dilution and substrate buffer to 0.6 volumes of the stated instructions. Briefly, 45 µL buffer from the kit was added to the wells of a white porvair 96-well plate (Porvair Sciences), and 15 µL of each sample added to a well. The plate was covered with plastic film and foil, and incubated at 65℃ for 30min, cooled for 1min at 4℃, and 60 µL of SEAP substrate was added to each well. The plate was incubated at room temperature for 30-60 min, after which the SEAP signal was read using a GloMax® 20/20 Luminometer (Promega). All samples were assayed in triplicate, and standard deviation was calculated for all samples.

3.2.3.3 Particle Distribution Script analysis of particles

A custom Python script (https://github.com/CorrieGunter/particle_counter), designed and kindly provided by Ryan Sweke, was used for estimating and compiling an approximate distribution plot of the different sized particles [VLPs, PsVs and UFOs (unidentified floating objects)] based on their radii. The script assumes that the particles are roughly circular in shape, and irregular particles are often not detected, although parameters such as sensitivity and radius parameters detected can be modified. It also assumes that the TEM contrast is reasonably consistent across the image. This script is run through Jupyter Notebook, in a Python 3.5 environment, and requires numpy, matplotlib, and opencv3 packages to be installed.

3.2.3.4 Agarose gel visualisation of PsVs

There are several methods currently available for the detection and quantification of PsVs, but these are often expensive and require a long period of time for their analysis. However, previous studies have shown that it is possible to detect both DNA and protein using agarose gels for analysis, and recently studies have used this method for the analysis of VLPs (Saunders and Lomonossoff, 2015; Belval *et al.*, 2016). A combination of protein and DNA detection by agarose gel analysis was explored as a rapid and cheap alternative approach for the analysis of PsVs, VLPs, and native virion samples.

A 1% (w/v) agarose-TBE gel was used for the gel electrophoresis and visualisation of BPV1 PsVs. Samples of different fractions of purified BPV1 PsVs (*#170612*), and fraction 9 of purified pTRAc empty, used as a negative control, were prepared as displayed in Table 3.2. For both PsVs and negative control, 30 µL of sample were transferred to a microcentrifuge tube. Samples 17-32 were denatured at 65°C for 10 min, and to samples 1-8 and 17-24, 5 µg/mL EtBr was added. All samples were mixed with 6 µL 6xOrange Loading Dye before loading into the gel. The samples were electrophoresed at 100V for 1h30min, and gel imaging was performed using short-wave (254 nm) ultraviolet (UV) light (Syngene Gene Genius Bioimaging System).

Table 3.2. BPV PsVs analysis by agarose gel electrophoresis

Fractions	F5	F6	F7	F8	F9	F10	F11	-ve
1. EtBr	1	2	3	4	5	6	7	8
2. No EtBr	9	10	11	12	13	14	15	16
3. Denatured + EtBr	17	18	19	20	21	22	23	24
4. Denatured no EtBr	25	26	27	28	29	30	31	32

A second 1% (w/v) agarose slide gel was prepared with 0.1 M Tris-Maleate buffer (0.05M Tris + 0.05M Maleate, pH 6.5), supplemented with 10 µg/mL EtBr (Rybicki, 1979). Fifty microliter samples of purified plant produced BPV1 PsVs, Brome mosaic virus (BMV) virions (kindly provided by Prof Ed Rybicki), and a control of purified empty pTRAc were each supplemented with 12.5 µL 5 x sample loading dye [50% glycerol, 0.5M Tris, bromophenol blue, pH 6.8], and loaded onto the gel. The particles were migrated at 50V (~250A) in Tris-Maleate buffer for 80min, and visualised under UV light, as described above. After UV visualisation the gel was stained with Coomassie dye for 5 min, followed by a 1h destain period in water.

3.2.3.5 Lunch-box pre-absorption of antibody

In order to remove antibodies or degraded antibody fragments which bind non-specifically to plant proteins, the Dako antibody was pre-absorbed against a nitrocellulose membrane treated with a filtered, crude homogenate of uninfiltrated plant extract. Six grams of plant material was

homogenised in extraction buffer, and filtered through a double-layer of Miracloth. This was poured onto a 3 cm^2 block of nitrocellulose membrane, and incubated for 1h at 37°C with shaking. The nitrocellulose was washed 3 x 15min in blocking buffer. Dako antibody, prepared to 1:500 in 15 mL blocking buffer, was poured onto the membrane, and incubated for 2h at 37°C with shaking. The membrane was discarded, and the antibody solution was used for western blot analysis of BPV PsVs.

3.2.4 Pseudovirion neutralisation studies and antibody comparison

3.2.4.1 ELISA antibody test

An indirect ELISA was performed on plant-made VLPs to determine the binding capacity of different antibodies to be used in the PBNA. The antibodies tested were the polyclonal antibodies (PAbs) used thus far in this study, as well as a set of monoclonal antibodies (MAbs), kindly provided by Neil Christensen. These included BPV1 antibodies B1:A1, B1:B3, B1:E2, B1:E3, as well as an HPV antibody, H16:J4, which recognises a linear neutralising epitope on HPV16. An additional anti-PV of unknown origin was also used. As it was unclear in which animal the PV antibody had been isolated from, this antibody was tested with both an anti-mouse and an anti-rabbit secondary antibody, and against both BPV and HPV particles. The reactions performed are listed in Table 3.3 below.

Table 3.3. Antibody ELISA

		Antigen	Primary antibody	Dilution	Secondary antibody
1		BPV1 L1 VLPs	B1:A1	1:1000	anti-mouse
2		BPV1 L1 VLPs	B1:B3	1:1000	anti-mouse
3		BPV1 L1 VLPs	B1:E2	1:1000	anti-mouse
4		BPV1 L1 VLPs	B1:E3	1:1000	anti-mouse
5		BPV1 L1 VLPs	H16:J4	1:1000	anti-mouse
6		BPV1 L1 VLPs	Dako	1:1000	anti-mouse
7		BPV1 L1 VLPs	Abcam	1:1000	anti-rabbit
8		HPV16 L1 VLPs	PV	1:1000	anti-mouse
9		BPV1 L1 VLPs	PV	1:1000	anti-mouse
10		HPV16 L1 VLPs	PV	1:1000	anti-rabbit
11		BPV1 L1 VLPs	PV	1:1000	anti-rabbit
	Controls:				
12	Positive	HPV16 L1 VLPs	H16:J4	1:1000	anti-mouse
13		HPV16 L1 VLPs	Gardasil	1:2000	anti-rabbit
14	Negative	HPV16 L1 VLPs	None	N/A	anti-mouse
15		BPV1 L1 VLPs	None	N/A	anti-mouse
16		Buffer	None	N/A	anti-mouse

Briefly, wells of a 96-well Nunc Polysorp assay plate (ThermoFisher, Scientific) were coated with 100 µL of 1:10 dilutions of antigen in coating buffer [10mM Tris, pH 8.5], and the plate incubated overnight at 4℃. Plates were blocked with 300 µL blocking buffer [1xTBS, pH 7.5 + 5% NFDM (non-fat dairy milk)] for 2h at room temperature and subsequently washed 4 x with wash buffer [1xTBS + 0.05% Tween-20 (TST), pH 7.5]. One hundred microlitres of the respective primary antibodies diluted in blocking buffer was added to the wells, and the plate incubated for 2h at room temperature. After incubation the plate was washed 4 x with wash buffer, after which 100 µL of secondary antibody diluted in blocking buffer was added to each well, and the plate incubated for 1h at 37℃. The plate was washed 4x in a final wash buffer [1xTBS, pH 9.0], and 200 µL of SIGMAFAST™ p-Nitrophenyl phosphate substrate solution (Sigma #N2770) was added and the plate incubated for 30min in the dark. Absorbance values at 405nm were determined and analysed.

3.2.4.2 Pseudovirion-based neutralisation assay (PBNA)

To demonstrate that they are an effective biological tool for use in PBNA and vaccine testing, plant-produced PsVs were tested in an *in vitro* neutralisation assay for their responses to various antibodies. For this assay, HEK293TT cells were prepared at $1.5x10^5$ cells/well in a 24-well plate, as described for SEAP assay (see section 3.2.3.2), and incubated overnight at 37°C and 5% CO_2. The following day, PsVs were diluted to a 1:13 concentration in DMEM without antibiotics and serum, and prepared with the antibodies tested in the ELISA in the previous section (section 3.2.4.1). Fraction 9 of the PsVs produced in section 3.2.1, which had an average SEAP reading of ~$1,3x10^6$ RLUs was used. The antibodies were all used at a 1:500 dilution, and were incubated with the PsVs for 1h at 4℃ before infecting being applied to the cells. Controls included a cell-only negative control, which provides a baseline reading for the cell supernatant, and a PsVs-only positive control, which demonstrates 0% neutralisation. It has been postulated that cellular components of mammalian cells, which would be present during natural infections of PVs, might contribute to the virus' ability to infect new host cells (Cerqueira *et al.*, 2015). A reaction in which cell lysate was added to the PsVs was therefore also included. The lysate was obtained through freeze-thaw cycling of cells, and clarification by brief centrifugation. The lysate was applied to the PsVs at a dilution of 1:5 in cDMEM. All of the reactions were performed in duplicate. The cells were incubated for a further 72h, and SEAP reporter gene expression measured as previously described (see section 3.2.3.2). This experiment was performed twice, with PsVs obtained from the same plant extraction, but purified on separate gradients.

3.3 Results:

3.3.1 Purification of PsVs

As per the protocol established for HPV16 PsV production in plants, BPV1 PsV-infiltrated plants were harvested at 4dpi, at which time no signs of chlorosis were present. The first set of PsV extractions were performed as per the standard protocol (strategy #5, see Figure 3.2), using frozen plant material. As iodixanol is routinely used for HPV purifications in our lab, and iodixanol-purified samples can be added directly to mammalian cells, the final density gradients were prepared using OptiPrep (iodixanol), and a 6xHSPBS buffer was used to prepare the fractions.

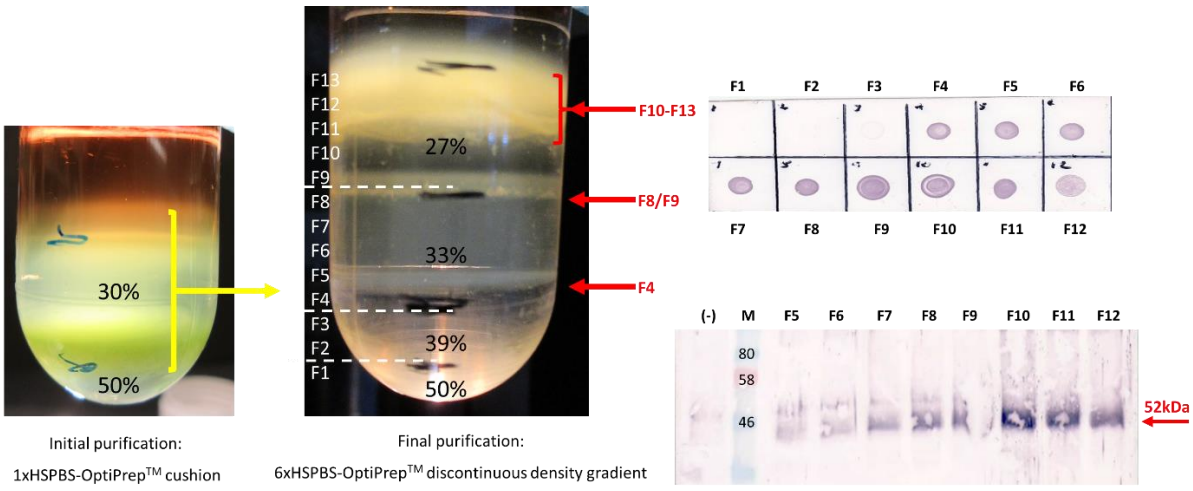

Figure 3.3. Images of density gradients for PsV purifications and corresponding immunoblots

The image on the left shows the cushion gradient with the yellow arrow indicating the 30% fraction that was pooled and further processed on the discontinuous gradient. The red arrows indicate the opaque bands observed, and their corresponding fractions, the dot blot and western blot analyses of which are also shown. (-) = F6 of purified pTRAc-empty infiltrated plants. M = marker (kDa). F = fraction.

Samples were extracted in HSNaOAc and initially partially purified on 30% and 50% iodixanol cushions, after which the 30% cushions collected and pooled for further purification. Visual inspection of the final density gradient revealed 3 distinct opaque bands, which appear to correspond with the fractions in which L1 was detected on the dot blot and western blots, suggesting that these bands are L1 protein.

Dot and western blot analysis revealed that L1 was present in all fractions from F4 (33%) on, and most strongly in the F8-F12 (33%-27%) region, indicating that particles of different densities were present across the gradient. However, only faint L1 bands were visible on Coomassie-stained PA gels (data not shown), indicating low overall yields of protein. To confirm that the Dako and Abcam antibodies react to purified proteins in the same manner, western blots of the same samples were probed separately against these two antibodies. Western blot analysis revealed that the results of the antibodies were almost identical, and the Dako antibody was used in further analyses of purified L1 protein. As an additional band was still observed in both the positive and negative purified protein samples, the Dako antibody was pre-absorbed against plant extract captured on nitrocellulose membrane and used for the western blot. Little difference was observed in blots probed with the pre-absorbed vs. normal antibody, and the pre-absorption of Dako antibody was unsuccessful in preventing the detection of non-L1 proteins. However, this may be due to the fact that the plant proteins in the crude homogenate were non-denatured, whereas the antibodies probe linearised proteins in western blot analyses. This is further supported by the fact that both the Dako and Abcam antibodies detect a plant-specific protein in the western blots of both BPV and HPV L1 expressed in plants, they do not seem to detect this plant protein in dot blots of empty-vector infiltrated plants (data not shown), which indicates their binding to a linear epitope that probably bears some similarity to the L1 epitope recognised by the antibodies.

3.3.1.1 TEM analysis of PsVs

TEM analysis was performed on the fractions with the strongest signal in order to analyse whether particles were successfully assembled. The results of these, and other PsV TEM analyses, are shown in Figure 3.4 on the following page. Electron micrograph imaging confirmed the presence of particles of ranging from 20-60nm in F6 and higher. It is possible that the signal detected in F4 and F5 were due to the formation of L1 aggregates, which had migrated into the denser fractions but are not recognisable as VLPs due to their lack of structure.

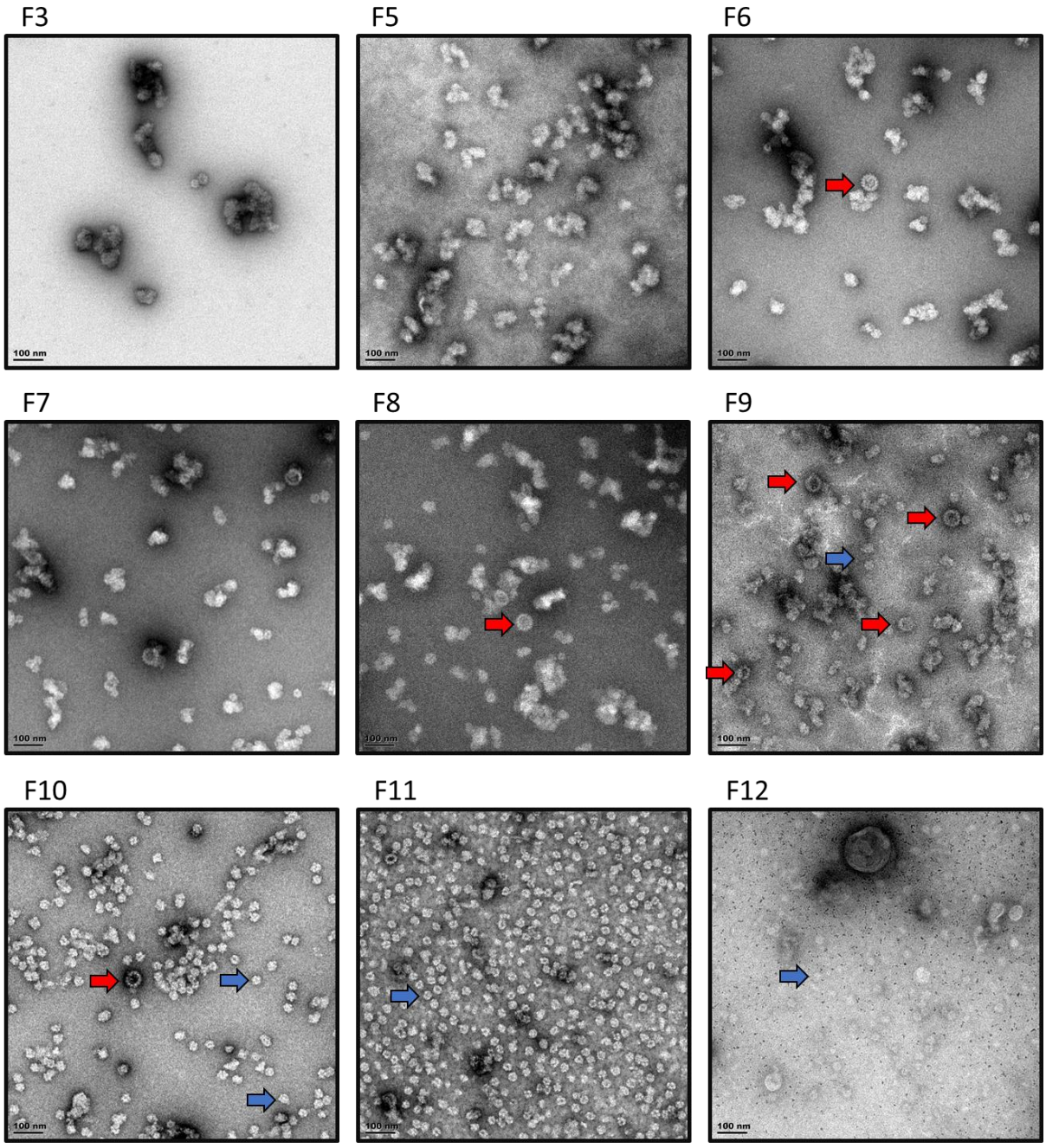

Figure 3.4. TEM images of BPV1 PsV fractions obtained by purification strategy #5

Electron micrographs of PsV fractions (F) 3-12. Particles were negatively stained with uranyl acetate and visualised under TEM. BPV1 T=7 particles (~40-60nm) are indicated by red arrows, and T=1 VLPs (20-30nm) indicated by blue arrows. The scale bar is 100 nm for all images.

TEM analysis revealed the presence of larger, ~40-60nm particles (shown by red arrows), which closely resemble the T=7 structure of native BPV virions. These particles were mostly present in F6-F10 (33% - 27%). Multiple particles resembling the T=1 VLPs observed in the L1 and L1/L2 infiltrations were also observed, mostly in the higher (less dense: 27%) fractions, F9-F12. As the larger particles were not present in any of the L1 L1/L2 VLP purifications, it was postulated that the T=7 particles were PsVs, and that the T=1 particles were VLPs. Selected TEM images were subjected to further analysis with a particle distribution script (PDS). Results of these analyses are shown in Table 3.4 and Figure 3.5 and Figure 3.6.

Table 3.4. Particle sizes and distribution from purified plant-made PsVs

	Mean particle radius (nm)	Mean particle diameter (nm)	Median particle radius (nm)	Median particle diameter (nm)	Gradient density (%)	Number of particles	Number of particles (1/5th)
F5	19,2	38,4	18,9	37,9	33	44	9
F6	18,3	36,5	17,6	35,1	33	35	7
F7	18,2	36,5	17,5	35,0	33	46	9
F8	19,5	39,0	18,6	37,3	33	51	10
F9	18,9	37,7	17,9	35,8	27	73	15
F10	14,4	28,8	13,3	26,6	27	166	33
F11	11,8	23,6	11,7	23,3	27	425	85
F12	10,7	21,4	10,8	21,5	27	54	11

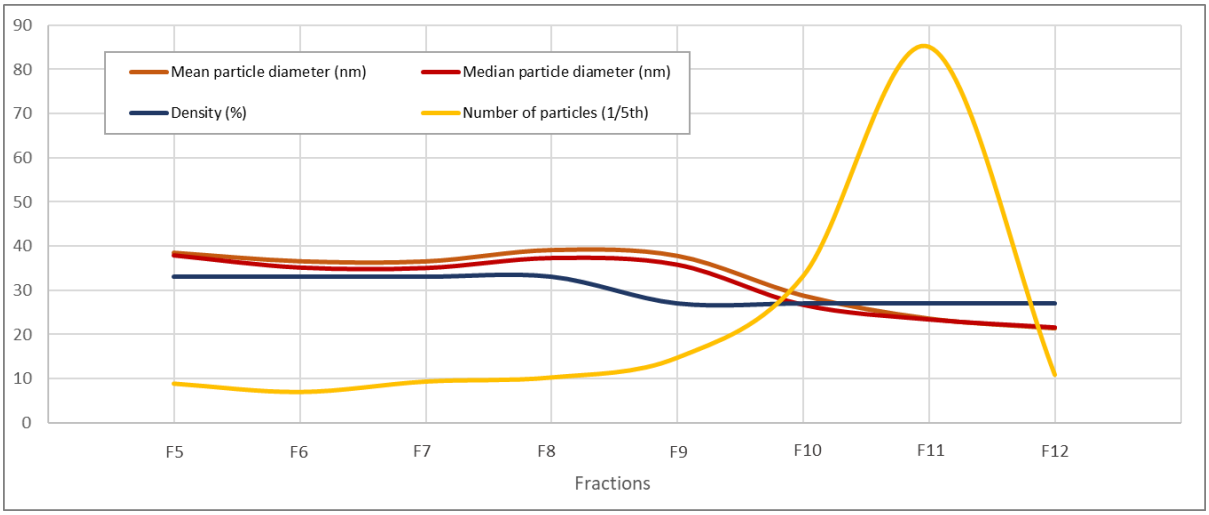

Figure 3.5. Line graph of particle analysis

The graph illustrates the distribution of particle size and number with decreasing density. Note: in order to visualise the number of particles on the same graph as the particle size and medium density, 1/5th of the total particle number was plotted.

The values shown in Table 3.4 and plotted on the graph in Figure 3.5 were derived from the average values obtained by PDS analysis of 3-5 electron micrographs of each fraction.

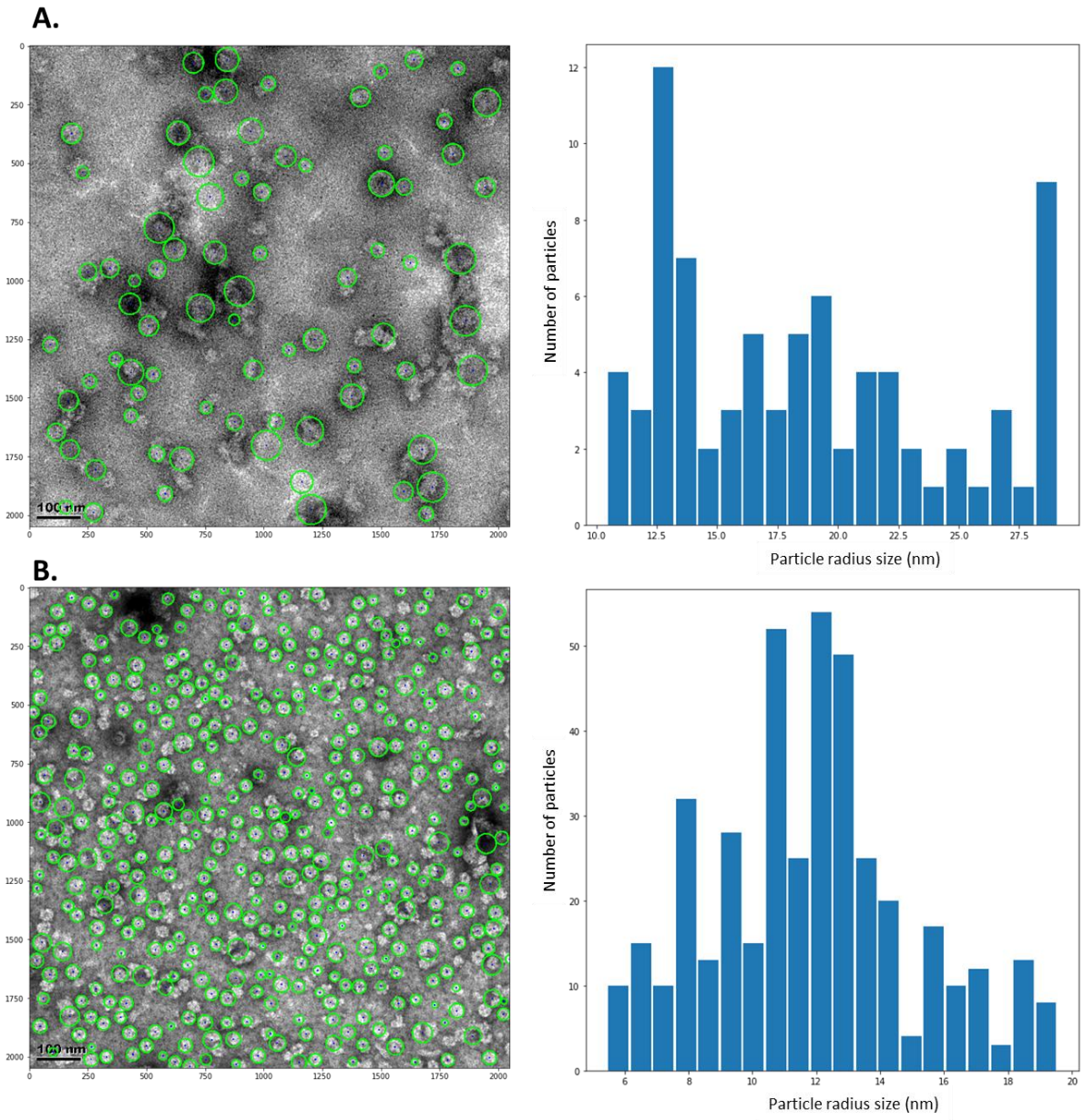

Figure 3.6. Electron micrographs and size distribution plots of BPV1 PsVs produced in plants

Figure 3.6.A. shows the TEM image and corresponding distribution plot of fraction 9, in which T=7 particles and T=1 VLPs are both present, and **Figure 3.6.B.** shows that of F11, in which the smaller T=1 VLPs predominate, and in which few T=7 particles are observed. The bar graphs indicate the particle size distribution, in which the non-overlapping particles (circled in green) are plotted. Particles sizes are given in radius (r). The scale bar is 100 nm for all images. Magnification was performed at 40,000x.

Fraction 6 was the first fraction in which the T=7 particles were observed by TEM, and these particles were observed in F7-F11, peaking at F9, shown in Figure 3.6.A., from which point their presence began to diminish, and high numbers of T=1 particles began to appear. The L1-containing fractions were then analysed by SEAP assay to determine whether PsVs were present in the samples and capable of infecting the cells.

3.3.1.2 SEAP Assay of PsVs

Mammalian cells were pseudoinfected with purified plant-produced PsVs, to determine the applicability of these PsVs for use in PBNAs, and SEAP reporter gene activity was assayed 72h post-infection.

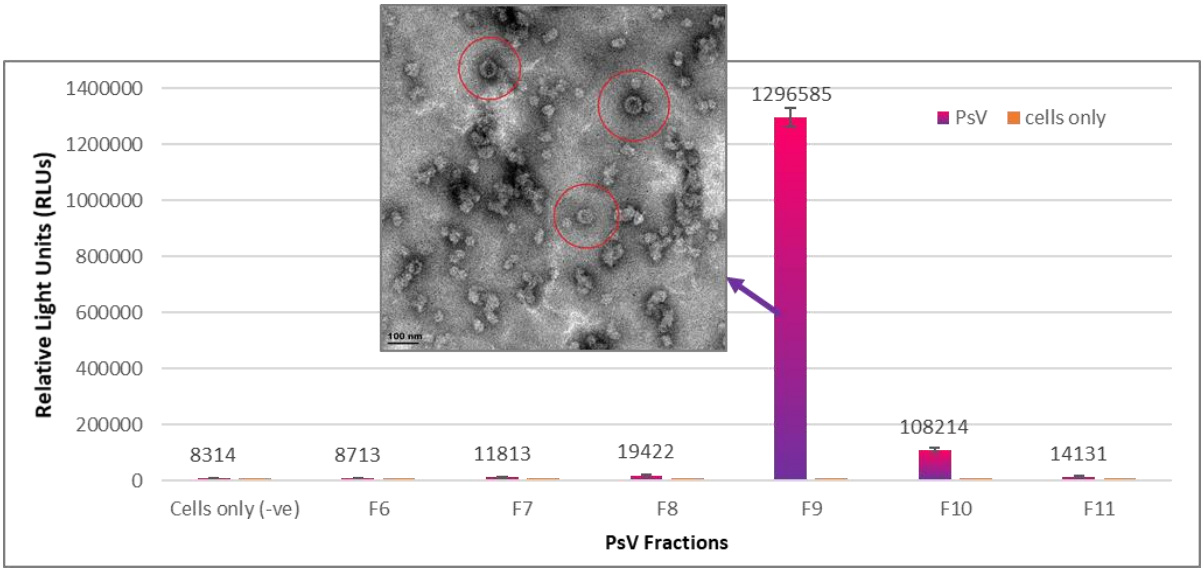

Figure 3.7. SEAP Assay of BPV1 PsVs

Reporter gene SEAP expression as indicated by relative light units (RLUs), shown in pink on the bar graph. The cells only negative control is displayed next to the reading of each fraction.

Results from the SEAP assay (Figure 3.7) showed that the pRIC3-mSEAP reporter gene plasmid was successfully transfected into HEK293TT cells, and was capable of expressing SEAP within these cells. The highest expression was obtained in F9, at ~1,3x10^6 RLUs, and F10, which had a reading 12-fold lower than that of F9, yet still 13-fold higher than that of the cell-only

background. This indicates that the majority of PsVs migrated to between F9 and F10, the lower fractions of the 27% density medium. The results from the SEAP assay, taken together with the TEM and immunoblot analyses, strongly suggest that the T=7 particles most frequently observed in F9, which corresponds with the highest SEAP reading, are indeed PsVs.

3.3.2 Optimisation studies

Once the expression, formation, and infectivity of PsVs was established, optimisation techniques were performed to increase the particle and protein yields. The results from these purification and expression optimisations are briefly discussed below, and summarised in Table 3.5. TEM images of the purifications are shown in Appendix A, unless otherwise specified. Coomassie-stained PA gel analyses of the highest yielding PsV purifications continued to show only faint L1 bands, and are not shown. Alternative quantification by TEM analysis, Bradford assay, SEAP assay, and different staining techniques were explored, and are discussed below.

Purification Optimisation

3.3.2.1 Purification Optimisation: Stability of BPV PsVs particles with freeze-thawing

To ascertain whether the PsV particles were stable with freezing, plant expression and purification of PsVs was performed using a batch of plant material of which half was purified directly and the other half frozen at-80°C for a week. A small increase in yields of both particles and protein levels was observed when using the frozen leaf material, as seen by TEM and western blot analysis (results not shown). This increase may be due to the fact that the freeze-thawing helps to disrupt the plant cells, releasing greater amounts of protein during the extraction process. Based on the study by Love *et al.* (2012) and studies on HPV VLPs/PsVs in our lab in which frozen material is routinely used, freezing seems to have no observable impact on the yields or integrity of PV particles, and all further extractions and purifications of VLPs and PsVs were performed on frozen material.

3.3.2.2 Purification Optimisation: Iodixanol vs. sucrose gradients

PsVs were purified on either sucrose or iodixanol gradients, prepared with NaOAc. When PsVs were concentrated on sucrose cushions, large numbers of particles, particularly T=7 particles, were observed in the 50% sucrose cushion, which is not collected and used for further processing in the current protocol, as well as in a small pellet that had formed at the bottom of the tube (see Figure 3.8). No particles were present in the 50% iodixanol cushion, nor was a pellet present. The OptiPrep (iodixanol) medium was thus used to prepare all further cushion gradients for PsV purifications. No L1 protein was detected in the remaining samples above the 30% cushions of either iodixanol or sucrose, which indicates that centrifugation conditions are sufficient for their migration into the 30% cushion.

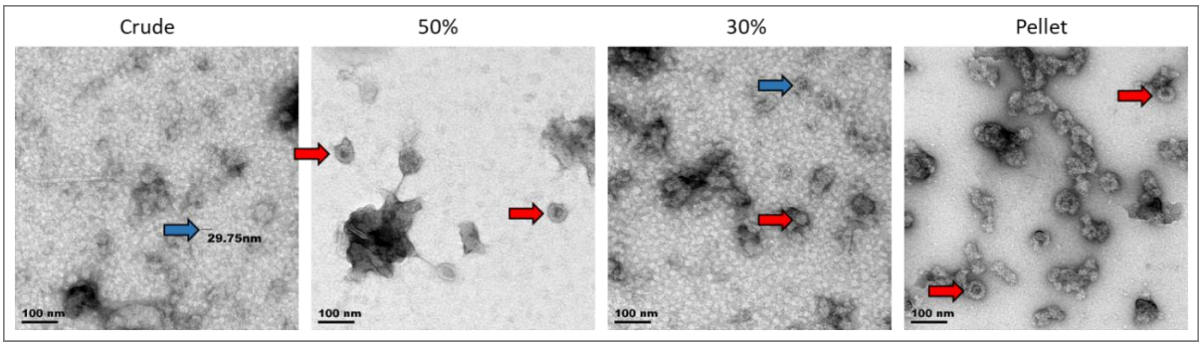

Figure 3.8. TEM analysis of crude sample and sucrose cushions

Electron micrograph images of the crude plant extract, 50% sucrose cushion, 30% sucrose cushion, and the pellet underneath the 50% cushion. Arrows of representative particles viewed in the electron micrographs are shown, with blue arrows indicating T=1 VLPs, and red arrows indicating T=7 PsVs.

A comparison of TEM images of samples in which iodixanol vs. sucrose preparations were used for the final isopycnic purification gradients, revealed that the iodixanol purified samples seemed to yield slightly greater numbers of more-structured particles, with fewer artefacts observed than in some sucrose preparations, in which crystals and large, spherical objects could be seen (see Appendix A, Figure 3, F7 and F9). As other studies on mammalian and plant-made PV VLPs and PsVs routinely use iodixanol for purification, and as the particles obtained could potentially be used for animal studies for which the sterile iodixanol medium would be ideal, this medium was selected for all further purification strategies.

3.3.2.3 Purification Optimisation: 1xHSPBS vs. 6xHSPBS buffer comparison

The first set of experiments compared the effects of the buffer concentration on the separation of the particles on discontinuous gradients. These experiments were performed with both iodixanol and sucrose gradients prepared with either 1xHSPBS or 6xHSPBS buffer, and were performed in parallel using the same set of plant material. The sucrose gradient comparison was done in order to determine protein yields using a Bradford assay, as iodinated media strongly absorbs UV and has been shown in our lab to interfere with readings, and sucrose preparations should therefore yield more accurate results. The results of this assay are shown in Figure 3.9., and discussed below.

1xHSPBS vs. 6xHSPBS-sucrose purifications

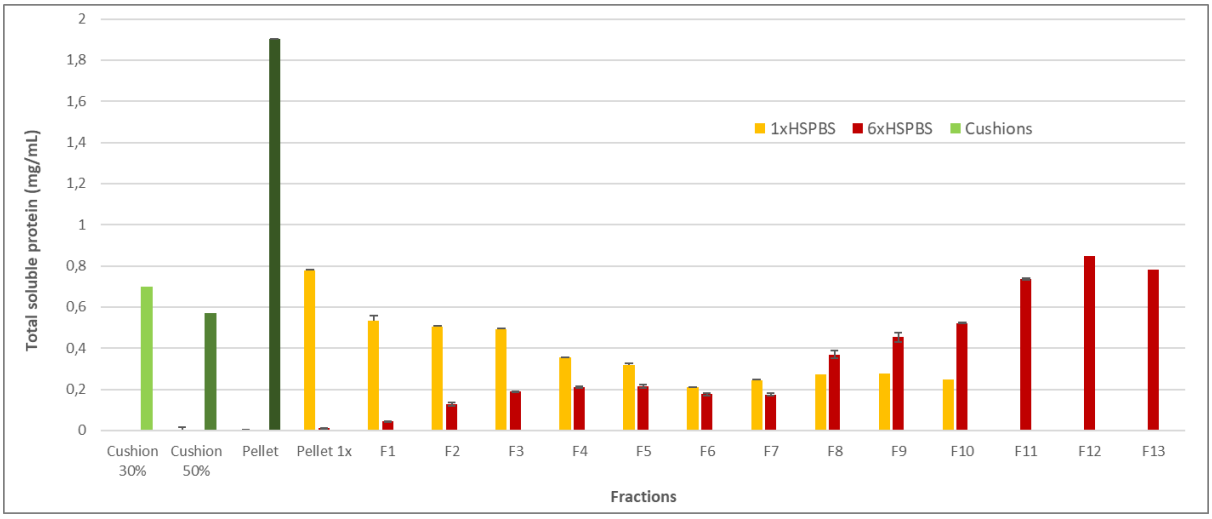

Figure 3.9. Bradford assay of 1xHSPBS vs. 6xHSPBS sucrose purified PsVs

Figure shows the bar graph of the total soluble protein (mg/mL) of each of the fractions of 1x or 6xHSPBS sucrose purified PsVs, as derived from a Bradford assay. The values were corrected against a 6xHSPBS-50% sucrose control, to account for any effects the HSPBS or sucrose might have on the readings.

Findings from the Bradford assay support what was found in section 3.3.2.2, showing that large amounts of protein, including particles, are pelleted and/or contained within the 50% sucrose cushion, which is not generally collected. The protein yields of the 1x and 6x series as analysed in the Bradford assay are obtained from the 30% cushion, which is collected, pooled, dialysed,

and further concentrated and separated by density gradient centrifugation. Proteins from the 1xHSPBS preparations aggregated in the lower fractions, and for the 6xHSPBS preparations protein was present in the higher fractions, resulting from the difference in density due to the increased salt concentration. Overall the protein yields for the 6xHSPBS appeared to be roughly the same as 1xHSPBS, which is expected, as these gradients were prepared from the same sample. There was no visible pellet in the 6x tubes after centrifugation, yet a small, slightly green pellet had formed in the bottom of the 1x tubes, in which a significant amount of TSP was detected, as shown by Bradford assay (Figure 3.9), including what appeared to be a significant number of BPV particles, as seen by TEM analysis (Figure 3.8).

1xHSPBS vs. 6xHSPBS-iodixanol purifications

Gradient and dot blot analysis from 1xHSPBS or 6xHSPBS-iodixanol purifications performed in parallel, revealed that the protein yields of these were approximately the same in these purifications, although the protein distribution of the 6x preparation appeared to be one fraction higher than that of the 1x samples. This can be seen by the appearance of protein in the dot blot at F=7 vs. F=8 in the 1x vs. 6x dot blot (Figure 3.10), and in the position of the white band which corresponds to the highest dot blot signal, as well as the highest number of PsVs (Figure 3.11). No pellet was present after centrifugation in either of these tubes, reaffirming that the sucrose gradient is less dense than that of iodixanol.

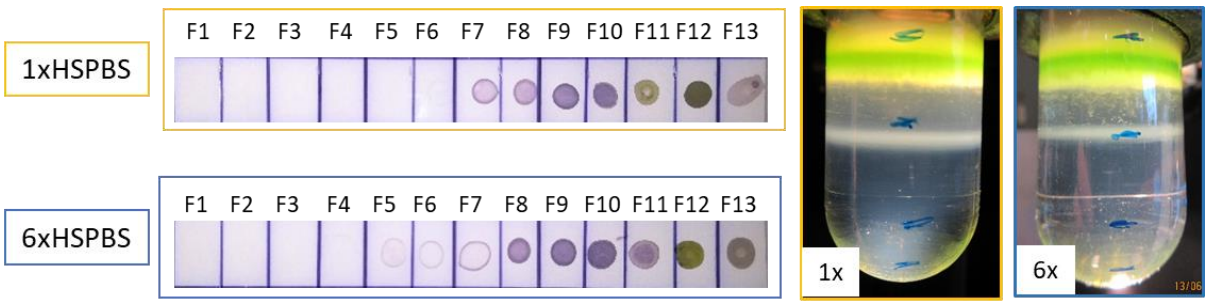

Figure 3.10. Dot blot and gradient images of PsVs purified on iodixanol gradients prepared with 1x or 6xHSPBS.
Dot blots were probed with Dako (1:1000).

To determine whether the quantity and quality of the particles were affected by the difference in HSPBS concentration, and to examine in which fractions the PsVs concentrated for each, TEM and SEAP assay were performed on the 1x and 6x fractions prepared with iodixanol. The results from TEM analysis are shown in Appendix A, Figure 4, and the SEAP assay was performed on the fractions with the dot blot signal. The positive control was F9 from PsVs prepared in 3.2.2.2, (Figure 3.4), for which a reading of ~1,3x10^6 RLUs was obtained (Figure 3.7).

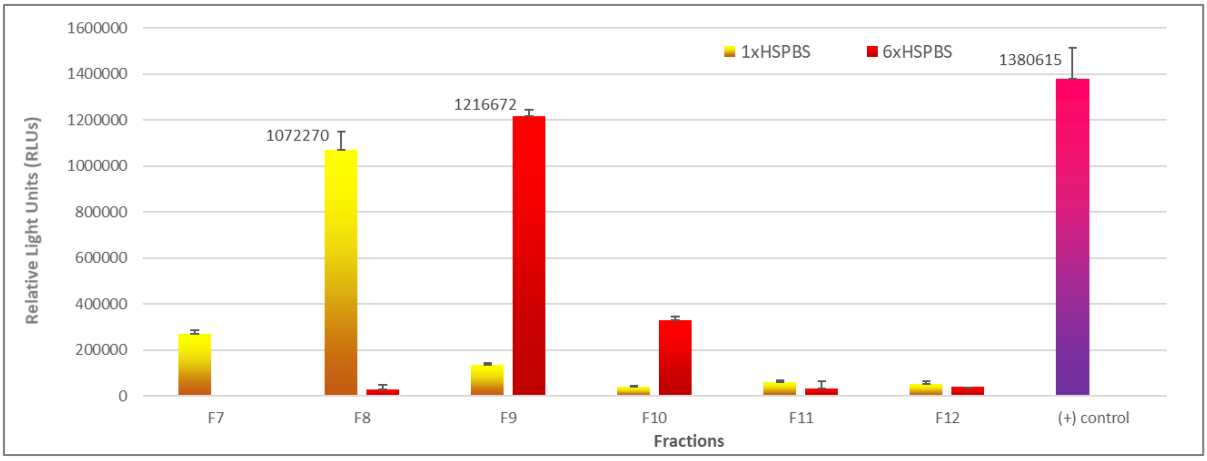

Figure 3.11. SEAP assay of 1xHSPBS vs. 6xHSPBS PsVs

SEAP assay of 1xHSPBS (F7-F12) and 6xHSPBS-Iodixanol (F8-F12) purified fractions. The (+) positive control was F9 from the previous SEAP assay.

The SEAP assay revealed that the distribution and the total RLU values obtained were similar after purification of PsVs in the 1x and 6x buffer preparations, however PsVs did not migrate to the denser layers of the gradients in the 6x buffer It was also found that the PsVs were mostly concentrated in F9 and F10 (27% iodixanol), which were the fractions in which the highest number of T=7 particles observable, and which is also consistent with what was previously found for the first PsV extraction in 6xHSPBS-Iodixanol. The SEAP readings obtained from this purification were slightly lower than those in the positive control, which further supports the theory that the T=7 particles are PsVs, as slightly fewer of these particles were observed in the TEM images of this purification than that of the positive control (Appendix A, Figure 4).

1xHSPBS vs. 6xHSPBS overnight dialysis

As purifications of PsVs on gradients with 6xHSPBS yielded favourable results, a further analysis was performed to determine whether dialysing the samples in the high concentration buffer could prevent loss of protein and produce higher quality particles. For this, PsVs were prepared after overnight dialysis in 1xHSPBS or 6xHSPBS, then separated on a 6xHSPBS-iodixanol gradient. TEM analysis (Figure 3.12), revealed that dialysis in 6xHSPBS resulted in the purification of far fewer particles compared to 1xHSPBS, this method was not adopted for future purifications.

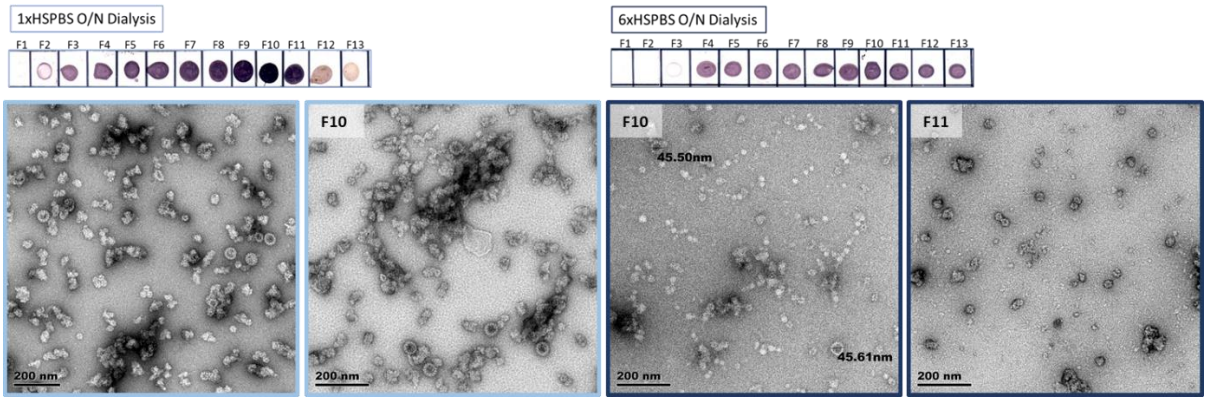

Figure 3.12. TEM and dot blot comparison of overnight dialysis of BPV1 PsVs in 1xHSPBS vs. 6xHSPBS

Dot blot analysis of partially purified PsVs dialysed overnight (O/N) in either 1x or 6x HSPBS, then separated on discontinuous 6xHSPBS-iodixanol gradients. Dot blots were probed with Dako anti-BPV antibody (1:1000).

3.3.2.4 Purification Optimisation: Centrifugation-time analysis

Isopycnic density-based centrifugation did not fully separate the particles based on their size, as can be seen in the TEM imagery (for example, Figure 3.4, F9 and F10), yet it was unclear whether this was due to the different densities of the particles or insufficient separation time. To allow for a longer sedimentation time, which might result in greater particle separation and concentration into their respective densities, an overnight centrifugation was performed on PsV extracts that had been concentrated on a 30% iodixanol cushion and dialysed overnight in 1xHSPBS. These were separated by 16h ultra-centrifugation on discontinuous iodixanol gradients, prepared with either 1x or 6xHSPBS.

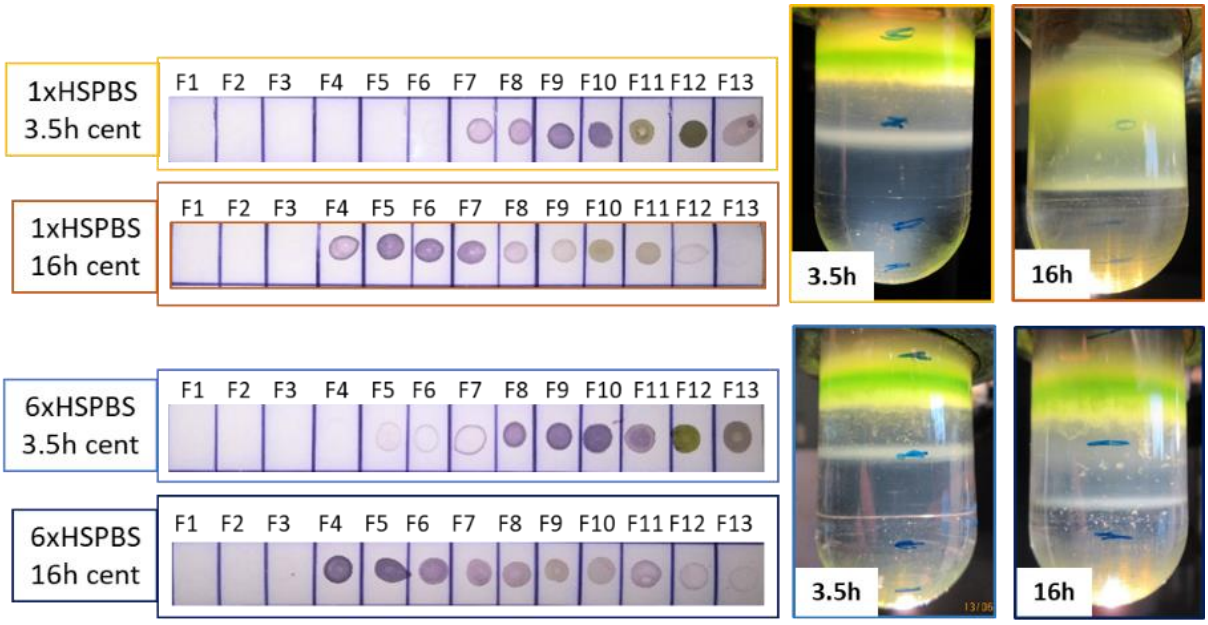

Figure 3.13. Comparison of BPV1 PsVs purified at different centrifugation times and buffers

Dot blot and gradient comparison of extended centrifugation with standard centrifugations (from section 3.3.2.3), performed in 1xHSPBS- or 6xHSPBS-iodixanol gradients.

Dot blot analysis and gradient comparisons (Figure 3.13) show that the extended centrifugation concentrates the proteins further down the density gradient, and although T=1 and T=7 particles were not fully separated, TEM analysis (Appendix A, Figure 5) indicated that the different structures seemed to be separated more fully based on their sizes, especially in the separation of particles from assembly intermediates such as capsomeres. The differently-sized particles also appeared to be more concentrated within certain fractions.

A SEAP assay of the sets of particles purified by overnight centrifugation was performed alongside PsVs purified from the same set of plants using the standard 3.5h centrifugation times (Figure 3.14). Results from the assay revealed that although there were no observable losses of protein on the dot blots and TEM, the number of PsVs had diminished as reflected by the lower SEAP readings of the overnight purifications in comparison with both sets of standard centrifugation purifications.

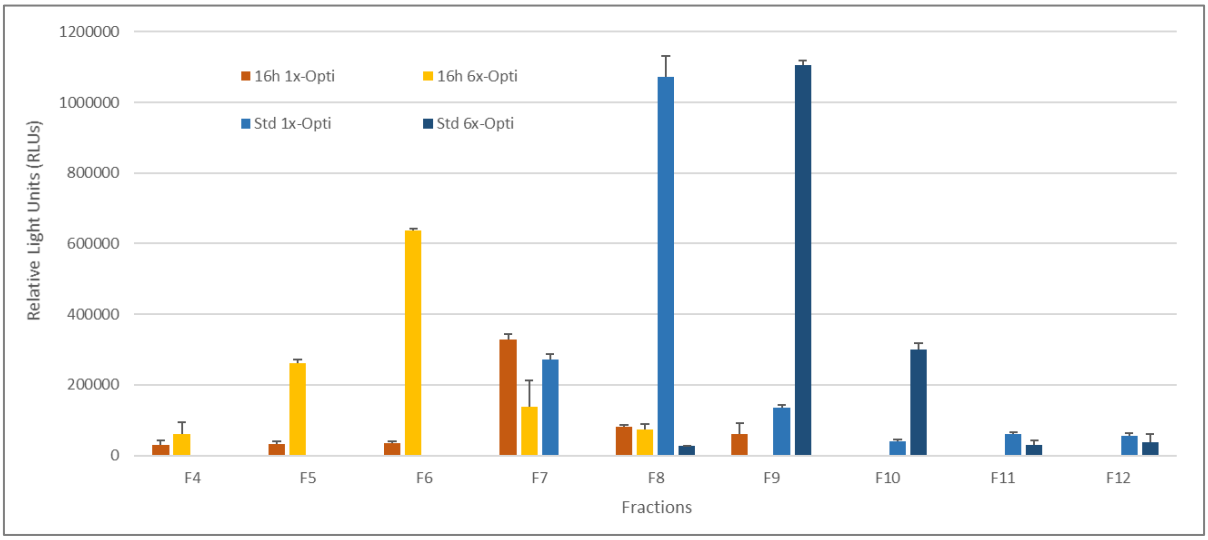

Figure 3.14. SEAP assay of BPV1 PsVs purified by standard or extended centrifugation times

SEAP assay of PsVs centrifuged at 16h in 1xHSPBS-OptiPrep (F4-F9: yellow) or 6xHSPBS-OptiPrep (F4-F8: orange). Purifications from standard 3.5h centrifugations, 1xHSPBS-OptiPrep (F7-F12: light blue) and 6xHSPBS-OptiPrep (F8-F12: dark blue), were included as positive controls and for comparisons.

3.3.2.5 Purification Optimisation: Extended maturation of plant extract

Based on the successful maturation of AHS VLPs by extended incubation of crude plant extract, as well as the maturation step required for the production of PV VLPs and PsVs in mammalian tissue culture (Buck *et al.*, 2003), an overnight incubation was performed on clarified crude PsV extract, to provide the L1 and L2 proteins more time to associate with each other and to encapsidate the reporter plasmid DNA and assemble into structured particles. Following incubation, the sample was processed via the modified protocol in which clarified plant extractions were separated on a 6x-HSPBS iodixanol density gradient. An opaque band above the 27% iodixanol step of the discontinuous gradient was observed, and was collected and analysed in addition to the fractions collected from the gradient.

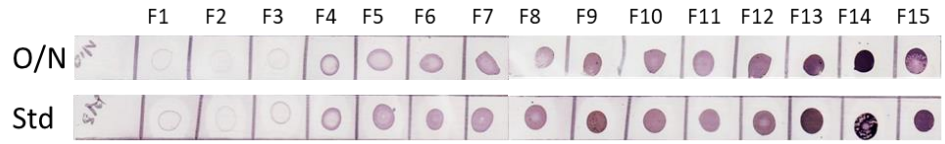

Figure 3.15. Dot blot of overnight maturation of crude BPV1 PsV extract

Dot blots were probed with Dako anti-BPV antibody (1:500). Abbreviations: O/N = overnight centrifugation (16h), Std = standard centrifugation times (3.5h)

Dot blot analysis (Figure 3.15) did not reveal any obvious protein losses after overnight maturation of the sample in comparison with a sample processed by the standard protocol, yet it did show that high levels of L1 was detected in fractions F13-F15. TEM analysis of F8 – F15 (results not shown) revealed that neither the standard (control) nor the overnight incubation yielded particles of the quality observed in previous experiments. Thus, the lack of particles was not due the processing technique, and results from this experiment were inconclusive, yet it appeared as though fewer assemblages were present in the matured samples. The majority of the L1 protein appeared to aggregate in the upper fractions, in which structures resembling ~10nm capsomeres, and loosely structured spheres of ~30nm which might represent VLPs, were observed. This indicates that although protein expression had occurred, assembly of the L1 proteins into higher structures had not taken place.

3.3.2.6 Purification Optimisation: $CaCl_2$ buffer

The use of a $CaCl_2$ buffer based on the one used by the Paintsil *et al.* (1998) study was explored in this study. Plant material containing PsVs was processed as per the standard protocol, and 30% iodixanol cushions pooled and dialysed overnight in the $CaCl_2$ buffer. The sample was then separated on a discontinuous iodixanol gradient prepared with the $CaCl_2$ buffer. Resulting gradients and dot blots (Figure 3.16) revealed that protein losses has occurred, and TEM analysis (data not shown) showed that no distinct particles were obtained. This method was thus not further pursued.

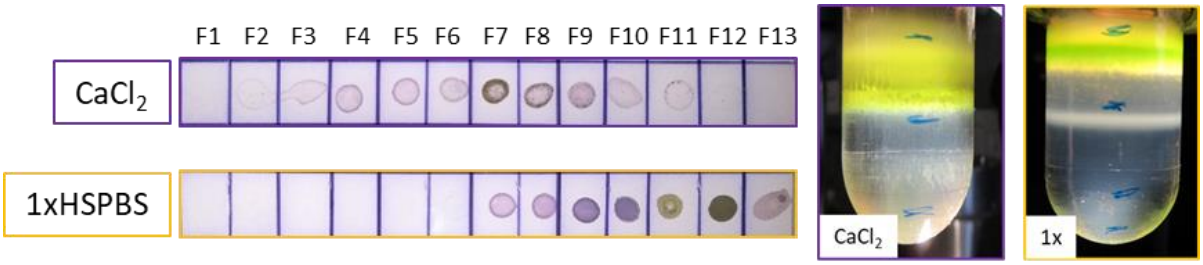

Figure 3.16. Dot blot and gradient of $CaCl_2$ buffer purification of BPV1 PsVs

3.3.2.7 Purification Optimisation: PEG precipitation

PEG precipitation is a commonly used method to concentrate and capture proteins during the initial stages of a purification process (Sim *et al.*, 2012), yet the precipitation of BPV VLPs and PsVs by PEG precipitation had limited success, as indicated by protein yield losses in the dot blot (Figure 3.17), and a lack of distinct particles in TEM analysis (data not shown), and was not further pursued.

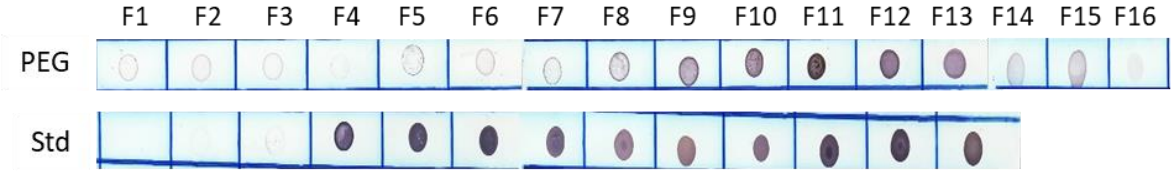

Figure 3.17. Dot blot of PEG precipitated BPV1 PsVs

Expression Optimisation

Expression optimisation approaches such as increasing acetosyringone concentrations, applying a heat-shock treatment, and extended *in planta* maturation were next explored. Dot blot and western blot analyses of PsVs obtained from these studies, as well as images of the final density gradients are shown in Figure 3.18 below, and the individual results briefly discussed. TEM analyses of the various fractions are shown in Appendix A (Figure 5), and a representative image for each technique of the fraction with the highest number of T=7 particles is displayed in Figure 3.19.

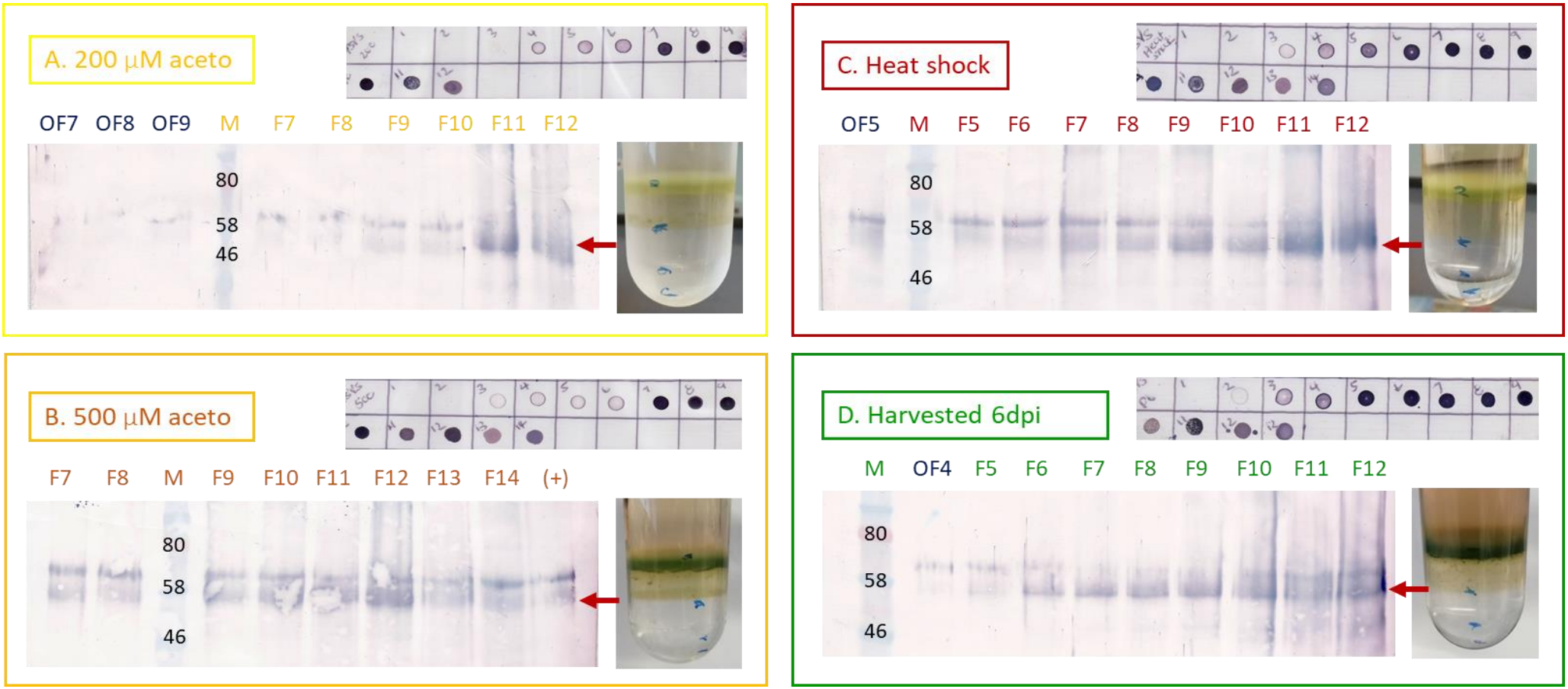

Figure 3.18. Results from expression optimisation studies 3.2.4.9- 3.2.4.5 for production of BPV1 PsVs

Dot blot, western blot, and density gradient images of BPV1 PsVs expressed in the same set of plants under different conditions. The red arrow indicates the L1 protein at ~55kDa. **Figure 3.18.A.** shows PsVs expressed by the standard protocol using 200 µM acetosyringone (aceto) to induce *Agrobacterial* cultures. **Figure 3.18.B.** shows PsVs with *Agrobacterium* induced with increased (500 µM) aceto. **Figure 3.18.C.** shows PsVs expressed by the standard protocol, but subjected to heat shock treatment 2dpi, and **Figure 3.18.D.** PsVs from plants harvested 6dpi, as opposed to 4dpi as per the standard protocol. OF4-9 = PsVs from ON incubation, F4-F9. Blots were probed with Dako anti-BPV antibody (1:1000) and developed for 1h.

Increasing the concentration of acetosyringone added to the final *Agrobacterium* suspensions from the standard 200 µM to 500 µM, significantly increased the yields of protein and particles produced, as shown in western blot (Figure 3.18.A. and B.) and TEM analysis (Appendix A, Figure 5.B.,and Figure 3.19.A and B.) of the standard vs. experimental purifications. Western blots (Figure 3.18.A. and C.) also showed that an exposure of PsV-infiltrated plants to a 30min 37℃ heat shock treatment on 2dpi appeared to increase protein yields significantly, and also produced greater numbers of T=7 particles, as observed by TEM analysis (Appendix A, Figure 5.C and Figure 3.19. A and C).

While PV L1 VLPs have been shown self-assemble in a protein dependent manner (Casini *et al.*, 2004), the integration of L2 into pentamers which then assemble into higher order structures such as small T=1 L1/L2 VLPs and T=7 VLPs and PsVs, in which DNA is also encapsidated, may require additional time, since high levels of protein accumulation may result in a bottleneck effect. Therefore, high levels of protein accumulation may not necessarily correlate with the highest numbers of higher order structures/particles obtained, as was seen in PsVs studied in section 3.3.2.5. To determine whether a longer incubation period might result in greater particle formation, PsV-infiltrated plants were harvested either on the standard 4dpi, or 6dpi. Plants harvested 6dpi yielded far greater numbers of structured, T=7 PsVs, (Figure 3.19.A vs. D, and Appendix A, Figure 5.D), and a stronger signal was also detected in western blot analysis of 6dpi harvested plants (Figure 3.18.A. vs. D).

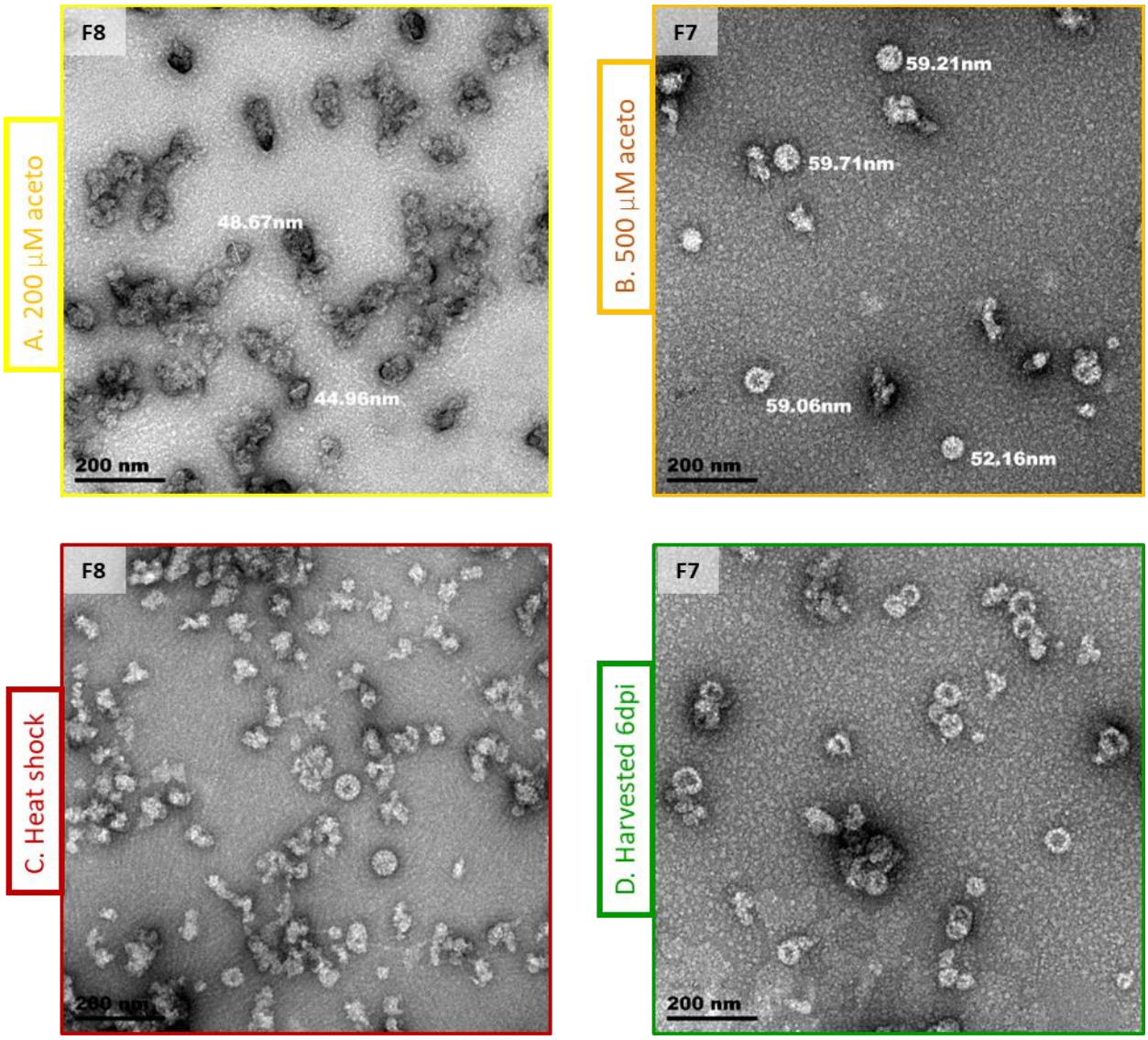

Figure 3.19. TEM images of BPV1 PsV expression optimisation studies

Representative transmission electron micrographs of fractions with the highest 40-60nm T=7 particles per purification from expression optimisation studies are shown in **Figure 3.19.A-D.** Magnification was performed at 35,000x, and the size bar is indicated in each of the images. Particle diameters are also indicated next to certain particles.

Table 3.5. Comparison of expression and purification optimisation strategies

Strategies compared	Variable tested	VLPs/PsVs obtained	Comments	Strategy adoption
1 vs. 2	Frozen plant material	More	Slight increase in yields of proteins and particles, and because it is more convenient to process frozen material, this method was adopted.	Yes
3 vs. 4	Iodixanol gradients	More	Higher yields due to fewer losses of protein through pelleting, and fewer artefacts in samples. Iodixanol is more sterile media than sucrose, which is important for vaccination.	Yes
4 vs. 5	6xHSPBS gradient	Same	Particles more concentrated and confined within fractions, and possibly more stable.	Yes
2 vs. 3 & 5 vs. 6	6xHSPBS dialysis	Fewer	Protein and particle yield losses.	No
5 vs. 7	Extended centrifugation	Fewer	Extended centrifugation concentrated the particles somewhat, and separated particles from assembly intermediates, yet did not fully separate T=1 and T=7 particles from each other. Possible pelleting of T=7 particles.	No
5 vs. 8	Extended maturation	Inconclusive	No obvious protein yield losses yet no particles observed in experiment nor control, and experiment should be repeated	No
5 vs. 9	$CaCl_2$ buffer	Fewer	No structured particles were present and protein yield losses observed.	No
5 vs. 11	PEG precipitation	Fewer	Protein yield losses and fewer distinguishable particles observed.	No
Exp 1	Increased acetosyringone	More	Significantly higher number of T=7 particles observed than in control, less loose aggregates	Yes
Exp 2	Heat shock	More	Somewhat higher number of T=7 particles observed than in control, less loose aggregates	Yes
5 vs. 10	In planta maturation	More	Far higher number of T=7 particles observed than in control, less loose aggregates	Yes

3.3.3 Quantification and analysis of PsV expression and activity

3.3.3.1 Antibody testing by indirect ELISA

To determine the binding capacity of the antibodies to be used in the PBNA, an indirect ELISA was performed on BPV1 VLPs from F11 of the first PsV extraction, which were probed with a variety of MAbs and PAbs antibodies available in our lab. A sample of HPV16 VLPs (kindly provided by Albertha van Zyl) was also included as a positive control.

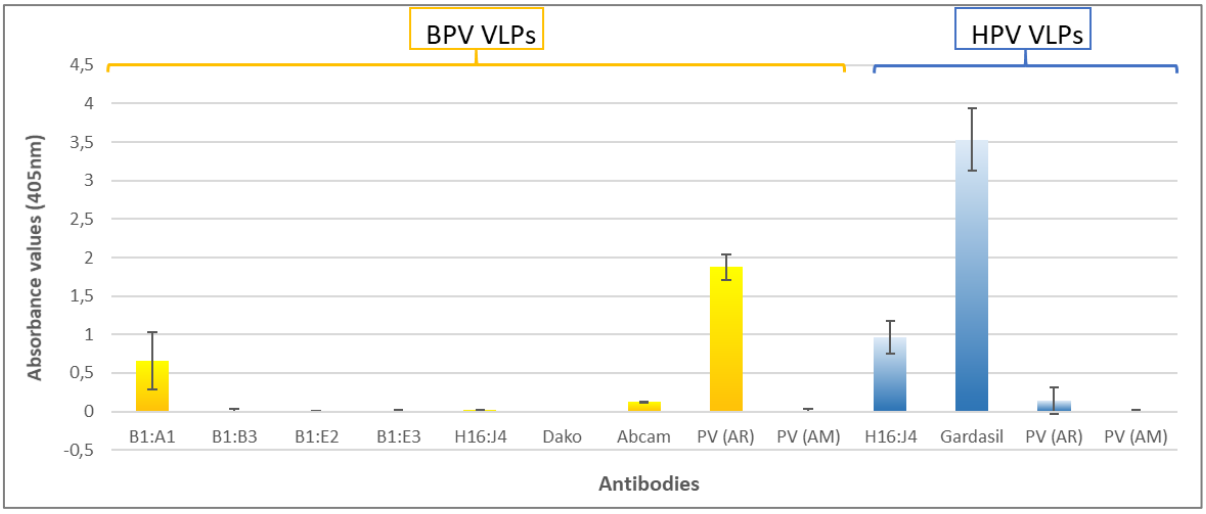

Figure 3.20. ELISA readings of BPV1 and HPV16 L1 VLPs probed with different antibodies

Values obtained from an indirect ELISA of BPV1 and HPV16 VLPs, probed with various anti-BPV, anti-HPV, or anti-PV antibodies. These values were corrected for background against a buffer-only control. (AR) = anti-rabbit secondary. (AM) = anti-mouse secondary.

The negative controls of BPV and HPV VLPs not probed yielded negligible readings, as did samples probed with B1:B3, B1:E2, H16:J4 and Dako for BPV. The HPV VLP control reacted with H16:J4 and, to a lesser extent, PV, but reacted strongly with anti-Gardasil. BPV VLPs reacted most strongly with the PV antibody, followed by the B1:A1 and Abcam antibodies, and from these results, it appears that the PV antibody was produced in rabbits. As HPV VLPs had a much smaller response to the PV antibody, it is also likely that this antibody was produced against BPV L1, or a PV whose L1 shares more similarity with BPV than HPV. Both the Abcam and Dako anti-BPV1 L1 antibodies had low readings, and the Dako reading was similar to that of the buffer control. This might be due to the fact that this antibody was created against chemically disrupted proteins,

and thus recognises a linearised epitope and may not bind as efficiently to the conformational epitope on the VLP structures. To determine whether the results of the ELISA correlate with those of a PBNA, and whether an ELISA-based approach could potentially be used as an alternative to PBNAs, the same set of antibodies was applied to PsVs, and their effects measured by PBNA.

3.3.3.2 Pseudovirion neutralisation studies and antibody comparison

In previous studies in our lab, incubation of plant-made HPV16 PsVs with different antibodies resulted in their partial/full neutralisation, as indicated by an abrogation in the SEAP reporter gene signal (Lamprecht *et al.*, 2016). In this study, a PBNA was performed with plant-made BPV1 PsVs, which were incubated with various antibodies to determine their neutralisation effects at different dilutions. These effects were measured indirectly via SEAP assays, as shown in the graphs in Figure 3.21.A and C. Percentage neutralisation is indicated in the corresponding graphs, Figure 3.21.B and D. This experiment was carried out twice, at antibody dilutions 1:500 and 1:200, using the F9 fraction of the first batches of PsVs purified, which had previously been proven capable of pseudoinfection of mammalian cells and expression of high levels of SEAP (see Figure 3.7). Successful neutralisation of the PsVs by the antibodies was demonstrated by a reduction of 50% or greater in the relative light reading.

In the first PBNA, antibodies were applied to PsVs at dilutions of 1:500. The PsVs used originally had a SEAP reading of ~1,3x10^6 RLUs, yet in the PBNA, the PsV-only control had a baseline reading of ~93x10^3 RLUs, a 14-fold reduction of the original reading. This is probably due to the fact that the PsVs had undergone 3 freeze-thaw cycles for their use in other SEAP assays, and had to be diluted to 1:13 to test for all the antigens, as opposed to the 1:10 dilution for the SEAP assay. The PsVs used in the second PBNA were prepared from the same plant extract to those used in the SEAP assay in 3.3.1.2., but had been purified on a different gradient and maintained at-80℃ for several months.

The B1:A1 antibody was the only completely neutralising antibody in both PBNAs, with a 100% reduction achieved at a 1:500 as well as 1:200 dilutions. The Abcam antibody was partially neutralising at 1:500, showing a 43% decrease in the reading, and fully neutralising at 1:200, showing a 61% reduction. The PV, H16:J4, and B1:E2 showed a 20%, 8%, and 5% reduction at 1:200, which doubled for PV to 41% reduction in the second PBNA, yet decreased to 5% for H16:J4, though this difference is too small to be of significance. Interestingly, the Dako and Gardasil antibodies appeared to increase PsV activity in the first PBNA, yet both were partially neutralising at dilutions of 1:200, showing reductions of 37% and 39% respectively. Similar effects were seen with the B1:B3, B1:E2, and B1:E3, where increases or reductions were observed, depending on the antibody dilution. However, the standard deviation in the readings was quite high, and these increases are not statistically significant, yet it might be the case that conformational changes induced by antibodies binding to PsVs may enhance their ability to pseudoinfect the cells. Furthermore, the cell lysate, which had been thought might increase the pseudoinfection, demonstrated a significant reduction of 32% in the first PBNA, and 19% in the second, indicating that cellular factors might, instead, have an inhibiting effect on the pseudoviruses.

As the PsVs used in the second PBNA, in which antibody dilutions of 1:200 were used, had higher SEAP reading and a lower background (cell-only negative) to signal (PsVs-only positive) ratio than the first PBNA, the neutralisation effects were better observed and of greater statistical significance in the second PBNA, and these results were regarded as the more accurate. Overall the B1:A1, Abcam, PV, Dako, and anti-Gardasil were identified as completely, fully, or partially neutralising antibodies, that may be used in future BPV PBNAs.

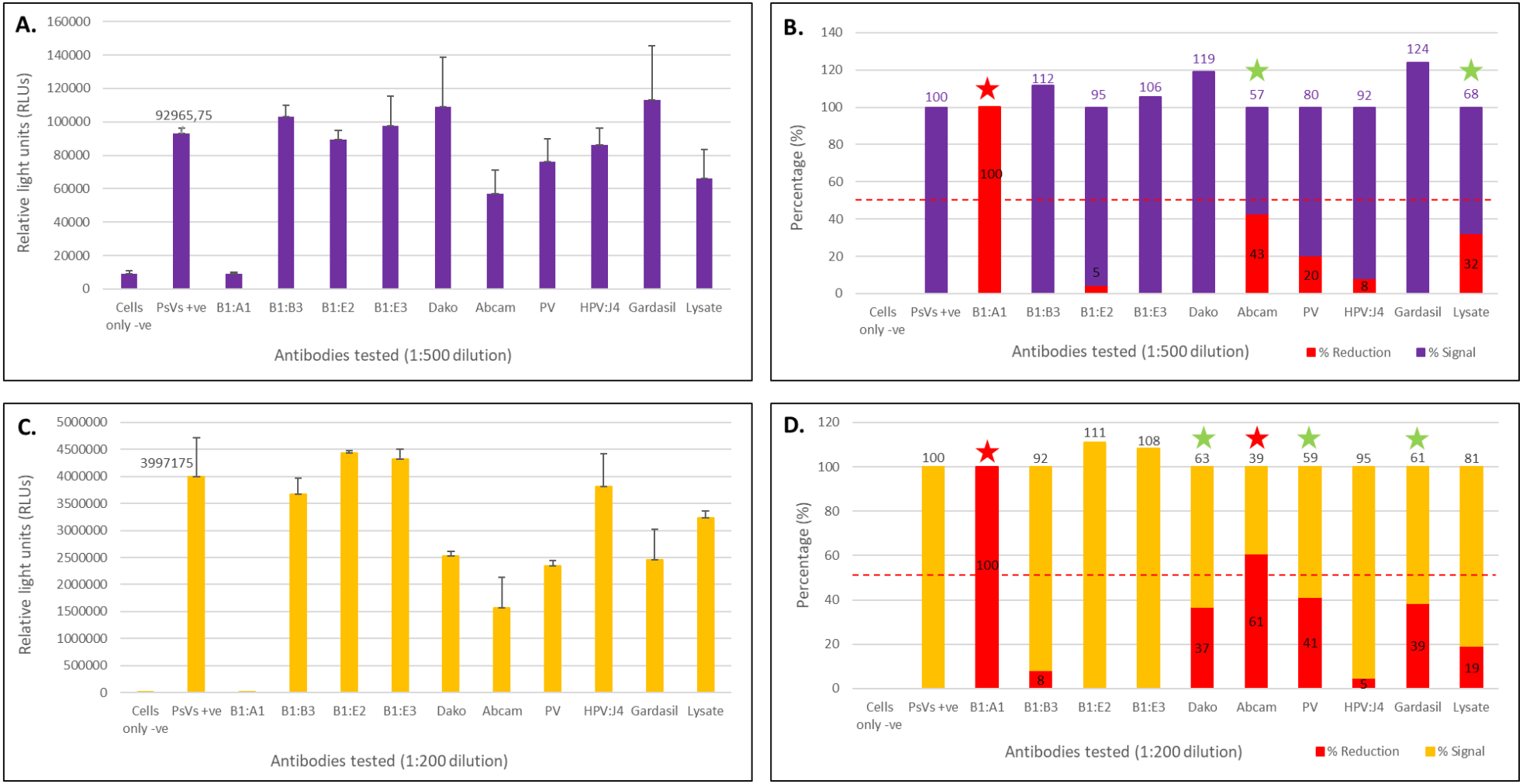

Figure 3.21. Pseudovirion-based neutralisation assay of BPV1 PsVs

Figure 3.21.A. and C. show the SEAP readings of PsVs incubated with the listed antibodies at 1:500 and 1:200 dilutions respectively. Figure 3.21.B. and D. indicate their relative reduction to signal in percentages. A reduction of >50% indicates full neutralisation (indicated by red stars), and partial neutralisation of >30% is indicated by green stars.

3.3.3.3 Agarose gel analysis of PsVs

To determine if an agarose gel stained with EtBr could be used to rapidly visualise and distinguish VLPs from PsVs, samples containing T=1 VLPs and T=7 PsVs were either pre-stained or electrophoresed directly on an agarose gel stained with EtBr. No bands were observed on the first gel, which was similar in thickness to one used to visualise PCR products, so a second, thinner gel containing 10 µg/mL EtBr was prepared on a glass slide. Bromo mosaic virus (BMV) virions were used as a positive control, and purified PsV fractions were analysed alongside a purified negative plant control, which had been infiltrated with empty vector.

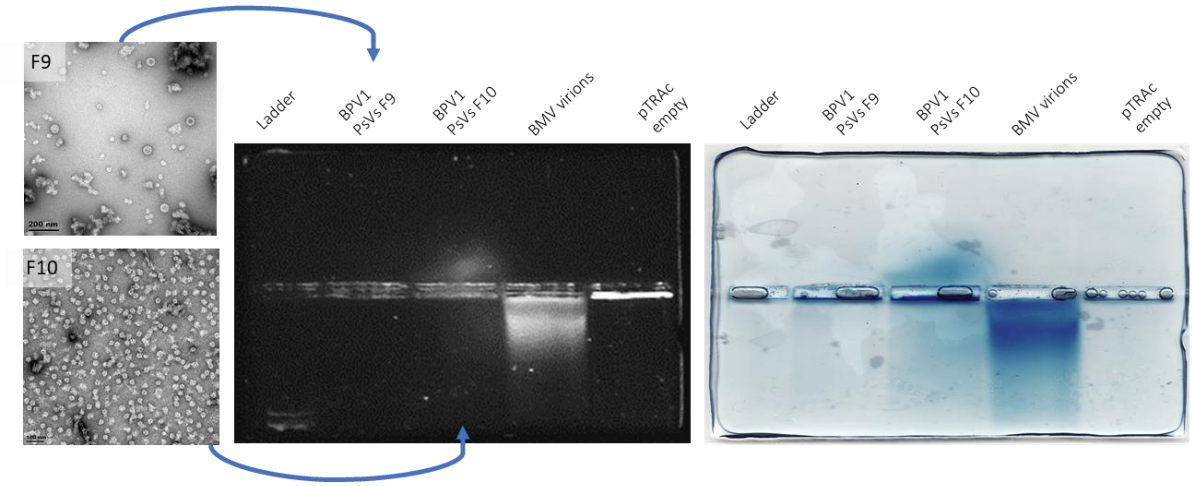

Figure 3.22. Agarose slide gel analysis of BPV1 PsVs and BMV virions

Gel electrophoresis separation of BPV1 PsVs and BMV virions on a 1% 1M Tris-Maleate-EtBr agarose slide gel. The two images are of the same gel, first visualised under UV light, following which it was stained with Coomassie dye.

The slide gel (Figure 3.22) observed under UV light indicated a light signal of DNA present in both the BMV and one of the PsV samples. A strong band of DNA appears to be present in the well of the empty vector negative sample, although given that no/very little migration occurred in this sample, this may simply be an artefact caused by the UV light. Protein staining revealed that the bands/light patches observed under UV light correlated strongly with protein detected by Coomassie staining. The gel further shows that the migration profile of the BPV PsVs were different to that of the BMV particles. These differences are probably due to differences in net charge, density, and the mass of various particles (Belval *et al.*, 2016). Differences in the net

charge, which would be influenced by both the charge on the capsid proteins as well as the encapsidated DNA, might explain why the PsVs appeared mostly to migrate upwards (towards the negative charge), but protein was also observed migrating towards the positive charge, for which no/only a faint corresponding light reading was detected by UV, potentially indicating VLPs.

3.4 Discussion

The production of NAbs against specific foreign antigens by the humoral immune system is the most important factor in the prevention of infection by PVs. These antibodies target immunodominant epitopes, and vaccine antigens are therefore selected on the basis of their immunogenicity (Kirnbauer *et al.*, 1992; Kirnbauer *et al.*, 1996). For PVs, these antigens are generally L1 VLPs, although low-titre antibodies against L2 have also been shown to neutralise PsVs *in vitro* (Roden *et al.*, 2000). Various studies have explored the use of different plants for the production of PV vaccines (Maclean *et al.*, 2007), and recently BPV1 L1 was produced in *N. benthamiana* at sufficient quantities to induce a strong immune response when rabbits were immunised with the purified VLP extracts (Love *et al.*, 2012). The co-expression of L1 and L2 to form L1/L2 VLPs in plants was putatively established in the previous chapter, and in this chapter the further encapsidation of a reporter gene plasmid into the L1/L2 structures for the formation of BPV1 PsVs was explored.

3.4.1 *In planta* production of BPV1 PsVs

The standard method of PsV production through the use of mammalian HEK293TT cell culture, although recognised as a robust and effective means for produced high-titres of PsVs containing a SEAP reporter plasmid, is also a highly expensive and time-consuming method (Buck *et al.*, 2003). Recently, however, HPV16 PsVs were produced in our lab (Lamprecht *et al.*, 2016), demonstrating the ability of plant-made DNA expression vectors to be used in mammalian cells, and thus that DNA vaccines may be encapsidated *in planta.* The expression and purification conditions established in these studies were used for the initial BPV1 PsV production in this study, and then later optimised to improve yields. Thus, for BPV1 PsV production, plants were infiltrated with pTRAc-L1, pTRAc-L2, and pRIC3-mSEAP, and harvested 4dpi. The plant material was stored at -80℃ for 4 months before purifications were performed. The first set of purifications were performed as per the HPV-PsV strategy, except that 6xHSPBS was used in preparation of the final iodixanol density gradients.

Examination of these purifications by TEM revealed the presence of both high numbers of T=1 particles such as those observed in VLP production, and also several T=7 particles which resembled those of the native BPV virions (Figure 3.4). Similar findings have been shown in previous studies, in which particles of the same size range were obtained for both BPV and HPV expression (Love *et al.*, 2012; Matic *et al.*, 2012). These findings also correlate with what was previously observed for HPV16 L1 expression in our labs (Pineo *et al.*, 2013; Chabeda *et al.*, 2018), supporting the theory that there is a high degree of similarity between papillomaviral species. As the larger, T=7 particles had not yet been observed in the production of L1 or L1/L2 VLPs in either this or previous studies, it was proposed that these particles represented BPV PsVs. This hypothesis was further supported by the findings of a SEAP assay, performed by pseudoinfection of mammalian HEK293TT cells with the purified fractions. In this assay, the highest levels of SEAP expression were detected in the fraction (F9), which corresponded with TEM images containing the largest number of T=7 particles. SEAP assay analysis also affirmed that the T=1 particles observed in large numbers in the upper fractions of the gradient were not PsVs, but small VLPs.

Two, separate attempts were also made to produce BPV1 VLPs and PsVs through the transfection of HEK293TT cells using the method established by (Buck *et al.*, 2003), yet low proteins yields were obtained and very few particles observed by TEM, and this work was not included in this report. Although the limited success of this method was likely due to overconfluent cells, or, potentially, a mycoplasma infection, this highlights one of the shortcomings of cell culture systems- the delicate set of conditions required for the maintenance and successful production of protein in these systems. In contrast, only one set of plants failed to produce PsVs and VLPs, which highlights the versatility and robustness of the plant expression of particles, in spite of their high batch-to-batch variation. Despite the large number of particles in TEM imagery and high SEAP readings, only very faint protein bands were detected on Coomassie-stained PA gels, indicating that low yields of protein were expressed. Such low levels would probably not be viable for animal studies, and thus optimisation strategies to enhance protein expression and purification were explored.

3.4.2 Optimisation of PsV purifications: optimisation of density gradient centrifugation

OptiPrep™ is a sterile and endotoxin-free, iso-osmotic, and isotonic iodixanol density gradient medium with a density of 1.32 g/mL. It is suitable for animal and tissue cell culture studies, and allows for the rapid sedimentation and separation of viruses through discontinuous or continuous gradient, while reducing destabilisation of proteins (Axis-Shield PoC AS, 2016). As the ultimate goal of the PsV purifications was to administer these to animals, for which iodixanol is the preferred choice of medium, iodixanol was compared to sucrose medium for density gradient purification of BPV PsVs. High-salt PBS buffer concentrations were also compared in the preparation of both iodixanol and sucrose gradients.

No visible pellet was present in the iodixanol cushion gradients, yet one was observed in the bottom of the double sucrose cushion tube. Analysis of the pellet and the 50% sucrose cushion revealed the presence of relatively high numbers of T=7 particles, alongside other aggregates. No particles were present in the 50% cushion of the iodixanol gradient, and as the migration of PsVs and other particles into and through the 50% sucrose cushion would result in yield losses if only the 30% fractions are collected, or in a dilution of the PsVs if the 50% cushions were included, Optiprep (iodixanol) was selected for preparation of subsequent 50% cushions. Previous comparisons of iodixanol and sucrose on HPV PsVs and VLPs performed in our lab have also shown iodixanol to be successful and favourable for such purifications (Maclean *et al.*, 2007; Chabeda *et al.*, 2018).

From the overall results, the use of high salt (HS) concentrations in the buffer appeared to help maintain the integrity of VLPs and PsVs during the purification process, as demonstrated by PsVs purified in either sucrose or iodixanol gradients prepared with 6xHSPBS, in comparison to those prepared with 1xHSPBS (Appendix A, Figures 3, 4, and 6). However, an overnight dialysis with a 6xHSPBS resulted in large protein losses and a reduction in particles (Figure 3.12), which indicates that the HS buffer is beneficial only in combination with iodixanol.

Calcium chloride buffer

Calcium is essential for the assembly process of several different viruses, including simian virus 40 (SV40) and mouse polyomavirus, in which the reassembly of disrupted particles occurred following the addition of exogenous calcium, and it is also thought to play a role in virus stability (Michelangeli *et al.*, 1995). Paintsil *et al.* (1998) showed that a calcium-supplemented reassembly buffer (pH 5.0) was capable of reassembling BPV particles that had been chemically disrupted using EGTA (ethylene glycol-bis (β-aminoethyl ether) -*N,N,N',N'*-tetraacetic acid) and DTT (dithiothreitol). They found that these particles did not reassemble into capsids when Ca^{+} was omitted from the buffer, indicating the necessity of the cation for reassembly. Furthermore, they also found that the presence of Ca^{+} in the EGTA/DTT disruption buffer prevented the disruption of BPV, suggesting that Ca^{+} also stabilises the viral structure.

While the use of a $CaCl_2$ buffer was not successful in increasing the yields of BPV particles, and in fact fewer particles were obtained, it has been demonstrated that Ca^{+} ions appear to stabilise the viral structure (Paintsil *et al.*, 1998). The addition of Ca^{+} ions in the final gradient buffer may thus aid in the stability and assembly of BPV particles, and should be explored in future work. Paintsil *et al.* (1998) also tested a pH range and found that pH 5.0 – 6.5 was optimal for reassembly of BPV particles. However, the pH of the HSPBS buffer used in this study has a pH of 7.4, and future research may therefore also include determining the optimal pH for the final gradient buffer for BPV particle purification.

Extended centrifugation for greater particle separation

It is of both research and practical importance to have particles with similar sizes and properties, such as the T=1 VLPs and T=7 PsVs, separated and concentrated within a limited number of fractions. The standard protocol separates particles on a discontinuous gradient by isopycnic centrifugation, which is based on the density of the particles (van Zyl and Hitzeroth, 2016). Although this method has been largely successful in concentrating the PsVs within a narrow range fractions, as seen by SEAP assay analyses, the presence of both small and large particles

within the same fraction could be a result of these particles having the same density, or may be due to insufficient separation by centrifugation. To ensure that the separation time was sufficient, an overnight centrifugation on a discontinuous iodixanol density gradient was performed on PsV extracts. Based on TEM analysis, the T=1 VLPs and T=7 PsVs appeared to be concentrated within fewer fractions, which may be of some utility for immunisation studies in which smaller volumes of more concentrated protein is useful, especially for smaller animals. However, SEAP assay analysis of the overnight purified fractions compared with those with a 3.5h centrifugation times showed a large reduction in the overall SEAP readings, indicating a significant loss of PsVs. It is possible that the prolonged centrifugation time led to the pelleting of PsVs, although no obvious pellet was observed or analysed, or that the extended centrifugal time, and thus the overall force applied was greater, leading to shearing or disruption of the particles.

3.4.3 Optimisation of PsV expression

Once an improved purification technique was established, some expression optimisation techniques were explored. Results from expression studies were analysed by dot blot, western blot, and TEM analysis, yet, as the mammalian cell culture in our lab was unusable at the time, due to a mycoplasma contamination of the cells, no SEAP assays could be performed to confirm whether, or to what degree, an increase in PsVs had occurred.

A brief heat shock treatment of whole plants at 2 dpi, or the induction of *Agrobacterium* cultures with acetosyringone concentrations of 500 µM prior to infiltration were two of the methods shown to be successful in increasing transient expression of GUS protein in *N. benthamiana* in a study by Norkunas *et al.* (2018). Both of these techniques were applied in the production of BP1 PsVs, and appeared to increase both the number of particles and the protein yields obtained from these purifications (Figure 3.18 and Figure 3.19). The same study also explored various other techniques, including the addition of chemical additives such as lipoic acid, ascorbic acid,

and PVP to *Agrobacterium* suspensions, as well as other approaches which should be explored in future work.

While studies on HPV16 PsV expression in plants indicated that protein accumulation was highest at 4dpi (Lamprecht *et al.*, 2016), at which point plant material was also harvested in this study, studies on AHS in our lab, and PV VLP/PsV production in mammalian tissue culture have shown that a maturation period enhances the formation of VLPs and PsVs (Buck *et al.*, 2003; Dennis *et al.*, 2018). Plants infiltrated for BPV PsV production were thus incubated for an additional 2dpi, allowing for an extended period of time for *in planta* expression, assembly, and maturation of particles. This approach was highly successful, and significantly higher numbers of particles and stronger protein signals on western blots were observed in these purifications than those of plants harvested 4dpi.

Future work should explore a combination of these approaches, and large-scale expression studies should examine particle formation and PsV activity, in addition to protein yields, which have been the main point of focus previously. Furthermore, SEAP assays and TEM analyses should be performed on the purified fractions, which have been maintained at -80℃, to further assess the results obtained in this study, and to examine the particle stability.

3.4.4 Detection and Quantification of BPV1 PsVs and VLPs

Transmission electron microscopy of PsVs

Transmission electron microscopy images analysed by the particle size distribution script show that the highest number of small T=1 VLPs were observed in the higher (i.e. lower density) fractions of the density gradients, and that other slightly larger T=1 VLPs were observed in the lower (higher density) fractions, and also distributed throughout the gradient. Similar findings have also been observed in HPV16 VLPs expressed in plants, in which VLPs of between 30-65 nm in diameter were obtained and mostly contained within the lower half of the density gradient,

with another batch/peak in the upper fractions (Maclean *et al.*, 2007). The same study also found that particles localised in the cytoplasm were generally smaller (40-52 nm) than those targeted to the chloroplast, and that while the chloroplast-targeted VLPs had sedimentation coefficients comparable to insect-cell derived VLPs, the VLPs localised to the cytoplasm had a lower sedimentation coefficient. This indicates that particles of different sizes may have different properties, and that these are determined by the cellular environment in which they are formed. However, all the particles in this study would have been formed in the same/similar environments, and if it is the case that all T=1 particles are formed from the same number of capsomeres, larger particles would be expected to be less dense than small ones (as their mass per volume ratio would be lower). It is therefore possible that the smaller VLPs are assembly intermediates or consist of only L1 protein, as opposed to L1/L2 counterparts in the lower fractions. It is not known whether the T=1 particles present in the fractions with high SEAP readings may have successfully encapsidated the reporter gene replicon, but if they have not, this might explain their lower mass and lower density. There is also a possibility that these particles may associate with, but not encapsidate the pseudogenome, which may also affect their sedimentation. TEM analyses also showed that the number of particles observed seemed to correspond with the signal on the western and dot blot, and a SEAP assay was performed on fractions in which particles were observed.

Agarose gel analysis of PsVs

Current methods for the detection of PsVs, such as rolling-circle amplification and assays for the detection of expressed reporter protein are expensive and time-consuming (Zhao *et al.*, 2014; Lamprecht *et al.*, 2016). A cheap and rapid alternative for determining whether target DNA is encapsidated in, or associated with the expressed proteins might be found in a simple agarose gel analysis of PsV samples. Recently Belval *et al.* (2016) demonstrated that it was possible to visually examine particles such as VLPs for nucleic acid content and protein by agarose gel electrophoresis. Such a gel electrophoresis has also been performed on native BMV viral particles by Rybicki (1979), and these two methods were combined for the analysis of purified plant-produced BPV1 PsVs. From the results, shown in Figure 3.22, it appears that this method was

relatively successful and that it could be used to detect encapsidated DNA, allowing for the rapid preliminary detection of PsVs.

Direct analysis of protein yields

In spite of large numbers of particles observed in the TEM images of PsV purifications, and high readings of SEAP expression compared with those of plant-produced HPV PsVs produced in our lab (Lamprecht *et al.*, 2016), only faint bands of protein were observed on Coomassie-stained PA gels, and quantification of protein yields via this method was unsuccessful. Without a quantified BPV standard, L1 quantification by ELISA was also not possible, and a Bradford assay was performed on sucrose-purified PsV fractions to determine the TSP of PsV purifications (see Figure 2.11). Although iodixanol was established as the medium of choice for PsV purifications, this medium is known to scatter light in an unpredictable manner, and cannot be used for absorbance readings. For this reason, sucrose-purified PsV fractions, obtained in section 3.2.2.2, were used for analysis. As no additional bands were observed on Coomassie-stained PA gels (data not shown), it is assumed that most of the plant proteins are removed by the purification and the TSP calculations largely indicate yields of recombinant protein. Estimates from the Bradford assay found between 120mg/kg – 160mg/kg of TSP, most of which is therefore probably L1. However, large amounts of protein had been lost through pelleting during early steps in the purification, and these results only provide an indication of the true yields obtained.

Purifications of large-scale L1-only infiltrated plants showed faint bands visible on the Coomassie-stained PA gel, yet few of those analysing PsVs did. This indicates that higher L1 expression occurs when L1 is expressed alone. This is not surprising, as L1-only infiltrated plants were infiltrated at *Agrobacterium* ODs optimal for L1 expression, i.e. OD 0.5 for pRIC3, and OD 1.0 for pTRAc. Plant biomass for these was also harvested 5dpi, allowing for higher levels of protein accumulation. Furthermore, less competition between the homologous protein expression could also have played a role. It is, however, interesting that the PsV-infiltrated plants produced far greater number of particles than either L1 or L1/L2 infiltrated plants, indicating that the presence of the

pRIC3-mSEAP reporter gene plasmid might facilitate particle formation, as discussed later. Studies of other proteins expressed in our labs have had similar difficulties with achieving protein staining and quantification in Coomassie-stained PA gels, yet other quantification techniques such as gold-staining have proven successful for these. While both silver- and gold-staining were explored in this study, these techniques were only applied once and neither proved successful for the samples analysed (data not shown). These methods were not repeated due to time constraints, yet may be explored in future work.

Indirect analysis of protein yields

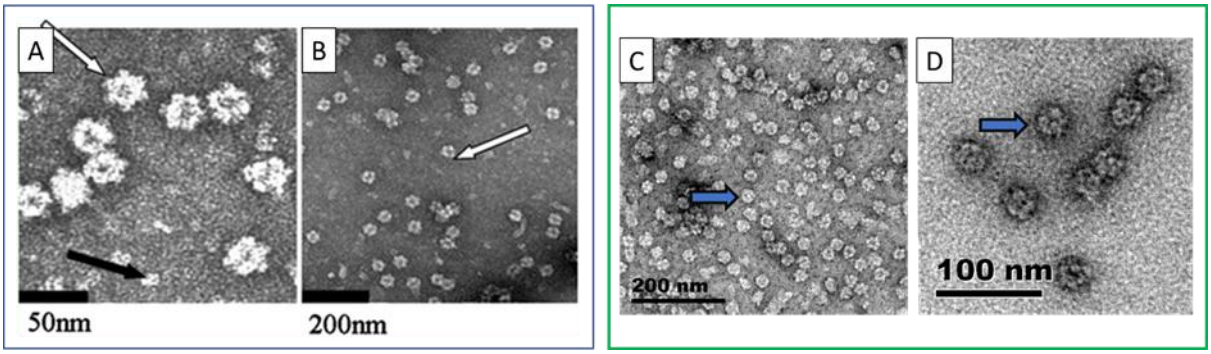

Figure 3.23. Comparison of plant-made BPV1 VLPs with those from literature

Figure 3.23.A and **B**. are electron micrographs of BPV1 L1 VLPs expressed in plants using a pEAQ plant expression vector, from the study by Love *et al.* (2012). Images **C.** and **D.** are VLPs expressed in this study, obtained by co-infiltration of pTRAc-L1, pTRAc-L2, and pRIC3-mSEAP. The size bars are indicated at the bottom of each of the images.

To indirectly analyse VLP yields, electron micrographs of the T=1 VLPs produced by Love *et al.* (2012) were compared by TEM to the T=1 particles obtained in this study (Figure 3.23). As more abundant particles were obtained through BPV1 PsV production methods in this study, fractions containing T=1 particles from PsV purifications were used for this comparison. In the Love *et al*. (2012) study, researchers had obtained high yields (183 mg/kg fresh weight leaf tissue) of relatively pure L1 VLPs, and the administration of this protein in rabbits was shown to elicit a strong and highly specific immune response. While their study does not state whether a dilution

was performed prior to TEM imagery, nor in how many fractions/what volumes these particles were observed, a comparison of TEM images in Figure 3.23.B. and C., indicates that a higher abundance of VLPs was obtained in this study than that of Love *et al.* (2012). It is therefore also possible that the overall protein yields obtained in this study would be as high or higher than the 183mg/kg achieved in this previous study.

3.4.5 Testing the immunogenic potential of BPV1 VLPs and PsVs

The use of PBNAs in serological testing of vaccines has been well-established, yet these assays are expensive and labour-intensive and ELISAs have been explored as an alternative method for quantification of antibodies against viral antigens, as these are cheaper and more rapid (Zhao *et al.*, 2014). To demonstrate this, direct ELISAs were performed on HPV L1 VLPs, with the values obtained from these assays reflecting the binding of all the IgG antibodies bound to the L1 VLP antigens, which were fixed to a solid surface. This method is independent of neutralising activity, yet studies have shown that neutralisation and antibody titres for VLP ELISAs are highly correlated in their measurements of vaccine-induced anti-HPV responses, and ELISAs have often been used as a surrogate for PBNAs (Zhao *et al.*, 2014).

Usually PBNAs are used to determine the neutralising potential of sera, thereby determining whether an antigen is capable of eliciting a strong immune response and, thus, whether it is useful as a candidate vaccine. In this study, PBNAs were used to determine the immunogenic potential of plant-made PsVs against different BPV1 MAbs (B1:A1, B1:B3, B1:E2, B1:E3), HPV16 MAb (H16:J4), PAbs (Gardasil, Dako), an oligoclonal Ab (Abcam), and a PV antibody of unknown nature. Furthermore, cell lysate was also incubated with PsVs prior to infection of mammalian cells, to determine whether cellular components would aid or detriment pseudoinfection of the cells. The PBNA was performed twice on PsVs obtained from the same plant sample, but maintained at different conditions. In the first PBNA, antibody dilutions of 1:500 were used, for which only B1:A1 showed a reduction in the light readings of greater than 50%, and the Abcam was shown to be partially neutralising at 43% reduction (Figure 3.21.A and C). When antibody

dilutions were increased to 1:200, both of these antibodies were neutralising, and the Dako, PV, and Gardasil antibodies partially neutralising (Figure 3.21.B and D). It was observed that the cell lysate reduced the light readings. This might be because components of the cell lysate, such as intrinsic anti-viral cellular restriction factors, may inhibit viral/pseudoviral cell entry (Porter *et al.*, 2017), or because cellular components affect cell health, causing cells incubated with lysate to die or to express poorly (Cerqueira *et al.*, 2015; Cerqueira *et al.*, 2017).

Overall, the B1:A1 antibody was the only completely neutralising antibody, showing a 100% reduction at both antibody concentrations. In the future, a titration series might be performed to determine at what concentration this antibody is no longer neutralising. The Abcam, Dako, PV, and Gardasil antibodies proved to be partially or fully neutralising at higher antibody concentrations, indicating that these bind to some, but not as many epitopes on the PsV structure as does the B1:A1 antibody. This is expected, as both the Abcam and Dako antibodies were produced against chemically disrupted BPV1 virions, in which conformational epitopes were likely lost. The Gardasil antibody was prepared against the Gardasil vaccine, which contains HPV6,-11,-16, and-18 VLPs, and as these are from a different PV species, would only share some epitopes with BPV1. The origin and preparation of the PV antibody is unknown, so either of the aforementioned scenarios could explain why it is partially, but not fully neutralising.

The data from the PBNA correlate somewhat to those obtained in the ELISA, in which the B1:A1 and Abcam antibodies showed some binding capacity to the T=1/VLP-dominated fractions. Interestingly, the results for the PV antibody showed a high binding capacity relative to the BPV-specific antibodies. This indicates that the small VLPs may have more of certain epitopes prevalent in PVs, or may allow for more effective binding of certain antibodies. It is also conceivable that the T=1 VLPs might be capable of eliciting a greater antibody response than their T=7 PsV/VLP counterparts, due to the increased surface area provided by many, small vs. fewer, large particles. The smaller nature might also make it easier for these particles to be taken up and processed by APCs such as DCs, stimulating a more rapid and stronger immune response

(Grgacic and Anderson, 2006). However, to determine whether this is the case, it would be useful to test the immune response of equal amounts of protein of the T=1 vs. T=7 particles, administered to animals, and the separation of these particles would be useful. The absorbance values obtained for the HPV VLPs tested with HPV antibodies were higher overall than those obtained for the BPV samples, which might indicate that the HPV VLPs are more immunogenic, or it may be due to a higher amount of VLPs used in the assay, as the protein quantities of the samples were not known and thus not matched.

3.4.6 Analysis of PsV formation and stability

The ability to replicate and spread genetic material is the main evolutionary driving force of viruses. To achieve this, infectious virions need to be produced in order to infect cells and replicate their genomes for repackaging into new virions. This process of assembly and packaging are thus highly regulated. Assembly of the viral capsid is achieved through the integration of a limited number of viral proteins present within a cell, as well as the encapsidation of the viral genome. One of the challenges DNA viruses face, is the selective packaging of the viral DNA in the presence of large amount of cellular DNA. An understanding of the mechanisms by which viruses assemble is important for the development of pharmacological agents that might inhibit the process, and thus disrupt viral replication and transmission (Cerqueira *et al.*, 2017). Furthermore, these mechanisms could be appropriated for the development of gene delivery approaches, such as the use of viral vectors to package specific nucleic acid sequences and deliver these to target cells, and PsVs have already been proved useful as antigens in vaccines, delivery molecules for DNA and other antigens, and as agents in vaccine testing through PBNAs (Buck *et al.*, 2008; Kines *et al.*, 2015; Schiller and Müller, 2015; Cerqueira and Schiller, 2017; Cerqueira *et al.*, 2017; Bayer *et al.*, 2018).

In a previous study on HPV16 PsVs, the highest SEAP readings obtained were ~135,000 RLUs (Lamprecht *et al.*, 2016), which were obtained for PsVs used at the same dilution as the BPV PsVs in this study, in which 10-fold higher SEAP readings were obtained. This suggests that either

higher numbers of PsVs produced in planta than HPV, or that pseudoinfection by BPV PsVs is more efficient. The fact that relatively high numbers of particles were observed and that high levels of SEAP expression was obtained by pseudoinfection with the PsVs, yet no or only faint bands corresponding with L1 were visible in Coomassie-stained PA gels of PsVs, suggests that although low overall yields of protein expression were obtained, that the packaging of pRIC3-mSEAP into L1+L2 VLPs is highly efficient. This might be due to inclusion of L2, which has a strong hydrophobic domain in its C-terminus which has been shown to bind to L1, and that in BPV, L2 binds to L1 prior to capsid assembly, which triggers the assembly process (Finnen *et al.*, 2003).

In a study examining the expression and assembly papillomavirus vectors (i.e. PsVs) in mammalian cell culture, Buck *et al.* (2003) found that the production efficiency of PsVs was greatly influenced by the size of the plasmid to be packaged. They found that BPV1 vector yields were higher when packaging plasmids of 6kbp than those closer in size to the 7.9kbp PV genome, although packaging of plasmids up to 10kbp was observed. This suggests that intracellular assembly of papillomaviral structural proteins around heterologous reporter plasmids is reasonably promiscuous, and that a size discrimination mechanism may be the primary driver for vector formation. The pRIC3-mSEAP plasmid used throughout this study was ~8kbp, and had a resulting replicon of 4.8kbp (Lamprecht *et al.*, 2016). It is clear from TEM and SEAP analyses that although high yields of PsVs are produced, there are even higher numbers of small, non-infectious VLPs formed. This suggests that either these structures form preferentially, which would explain why small T=1 VLPs, and not T=7 VLPs are observed during VLP production, or that packaging of DNA into the L1/L2 structures is performed at a lower rate.

In this study, PsVs were purified from the same sample by two separate but parallel final gradient centrifugation steps. One set of these was used in the SEAP assay, and the second maintained at -80℃ for over 10 months, at which point it was used in the PBNA. The PsVs used in the PBNA gave a SEAP reading of $4x10^6$ RLUs, a 3-fold higher reading than those obtained from the parallel batch of PsVs explored in the SEAP assay. However, there are various factors that might influence the

readings obtained in these assays and which may explain the disparity. While the cells for both the initial SEAP assay and PBNA were seeded at the same number, the cell health affects adherence to the plate and, thus, the cell density, meaning that more cells may have been available for pseudoinfection and expression. Healthier cells are also expected to express higher yields of proteins. Experimental error is always a factor, yet in the case of plant-made PsVs, repeatability is also somewhat difficult due to the large batch-to-batch variability in plant expression of proteins. There is a possibility that the particles matured throughout the process, and formed more stable and infectious PsVs, although this would have to be tested experimentally (Buck *et al.*, 2003; Peng *et al.*, 2010).

Fraction 9 (F9) of the first set of PsVs extracted was used throughout this study in a number of SEAP assays. The SEAP readings remained relatively consistent for the first 3 freeze-thaw cycles, after which a decline in the readings was observed, and in the future aliquots of the purified fractions might be made to prevent freeze-thawing. However, this was not a controlled experiment, and merely observation from different assays in which the same sample was used. Future work might therefore also include stability experiments at different temperatures, as this information would be important for vaccine production and cold-chain management. Overall, however, it is clear that the PsVs are very stable at -80℃ for extended periods of time (at least 10 months), and that the particles appear to maintain their structure and function through a number of freeze-thaw cycles. This stability might be explained by the high osmotic pressure of the 6xHSPBS buffer, or the iodixanol medium, which is known to stabilise proteins. It might also be that as infectious agents of the skin, the viral structure of BPVs are very stable, as native virions would often be exposed to the environment for extended periods of time during their dissemination through wart material (Campo and Roden, 2010).

3.5 Conclusions and Future Work

In this chapter I set out to expand on the previous research performed in our group, in which HPV PsVs were produced in *N. benthamiana* plants and shown to work in PBNAs. Using methods established for HPV PsV production, I showed that BPV1 PsVs could successfully be produced in *N. benthamiana*, and that these could be purified in large numbers using the same principles. Various additional techniques for expression and purification optimisation were also explored, and my findings suggest that the following optimised protocol should be applied for the production of high levels of BPV1 PsVs and VLPs in *N. benthamiana*:

Agrobacterium cultures should be prepared as per the standard protocol, although a final incubation of ~1-2h with 500 µM acetosyringone should be performed prior to infiltrations of *N. benthamiana* plants. These plants should be incubated as per usual, with a heat shock treatment of 30min at 37℃ 2dpi inbetween. The plants should be harvested at 6dpi, and stored at -80℃. Purifications should be performed in NaOAc, as for HPV, and concentrated on a double iodixanol cushion. The 30% cushions should be collected and pooled, and dialysed overnight in 1xHSPBS, as for HPV. The dialysed sample should be separated on a discontinuous gradient (27%- 50%) prepared with iodixanol diluted with 6xHSPBS, and fractions stored at -80℃.

Application of putative BPV1 PsVs to mammalian cells demonstrated that these particles were capable of infecting mammalian cells and transferring their encapsidated reporter gene into these cells, in which the SEAP reporter gene was expressed. Furthermore, I showed that the pre-incubation of NAbs with the PsVs prevented, or neutralised their ability to infect mammalian cells, which demonstrates their immunogenic potential as possible vaccine candidates. These findings correlate with literature showing that the underlying mechanisms of PV species are generally similar, and support the notion that technologies developed for specific PV species might be applicable to PVs more broadly.

Additional avenues that might be explored in future work to increase PsV production include:

- Increasing the size of the pRIC3-mSEAP replicon to ~6kbp, which might result in a higher packaging rate and greater PsV production as suggested by findings from (Buck *et al.*, 2003), or exploring the use of different replicon sizes.
- Examining the different properties of the T=1 and T=7 particles, which would require their separation. Established methods for size-based particle separation, such as rate-zonal centrifugation, nanofiltration, or chromatography, might be explored to further separate these particles.
- Inclusion of GFP or other reporter genes to observe and quantify individually infected cells.
- *In planta* expression of the codon-optimised L2 gene from Zhou *et al.* (1999), and the modified L1 gene included in the Buck *et al.* (2003) pSheLL plasmid, both of which expressed high levels of protein in mammalian cells.
- Repetition of the approaches that were inconclusive, as these could perhaps be expanded or altered to provide favourable results.

4 Chapter 4: Discussion and Conclusions

4.1 General Discussion

Bovine papillomaviruses are viruses of considerable veterinary and research importance, but BPV1 and 2 especially, due to their ability to cross species-boundaries and to provide cross-protection against one another (Campo and Roden, 2010). These two BPV types are also among the most prevalent, and lead to veterinary diseases such as papillomatosis of cattle and equine sarcoids of horses and both wild and domestic ungulates, for which there is no effective treatment (Bocaneti *et al.*, 2016; Araldi *et al.*, 2017). BPVs are globally endemic, which highlights the need for an effective prophylactic vaccine that can be administered widely and early, before infection occurs. While various VLP-based candidate vaccines against BPV have been produced and shown to confer long-lasting and efficient protection against BPV challenge, there is currently no widespread, commercially available BPV vaccine, largely due to the costs associated with the cell-based production platforms required for their production (Love *et al.*, 2012; Bocaneti *et al.*, 2016). However, plant-expression platforms could potentially mitigate the associated production costs of VLP-based vaccines whilst maintaining the integrity of the antigens through post-translational modifications, and several studies have demonstrated the proof of efficacy for plant-produced PV vaccines (Love *et al.*, 2012; Dennis *et al.*, 2018; Gonzalez-Castro *et al.*, 2018; Rybicki, 2018; Yanez *et al.*, 2018). This study explored the possibility of producing a cost-effective prophylactic, and potentially therapeutic vaccine against BPV, through the production of BPV1 VLPs and PsVs in plant expression systems.

The first, preliminary aim of this study was to express BPV1 L1 and L2 in *N. benthamiana*, and to determine optimal conditions for the production of L1 and L1/L2 VLPs. For this, 3 binary plant expression vectors with different properties and cellular targeting of the proteins were explored. Cloning was only successful, and protein expression of L1 was analysed in small-scale expression studies of these. While all 3 vectors expressed L1, only pRIC3 and pTRAc yielded small, 20-30nm

T=1 VLPs, such as those observed in other studies of BPV1 L1 expression in plants (Love *et al.*, 2012). These two vectors also expressed higher yields of L1 than pTRAkc-cTP. While pRIC3 yielded the most protein, it appeared that pTRAc produced slightly better VLPs. As no antibody was available against L2, expression of this protein was later confirmed indirectly through the production of PsVs, which require L2 to encapsidate the reporter gene plasmid. In an effort to produce L1 and L2 antibodies without the need for animal immunisations, phage display and biopanning were explored as a means of finding L1 and L2 binders. However, these methods yielded no positive results, likely due to aberrant helper phage, and were not further pursued nor discussed in this study.

Once it was established that VLPs could be expressed *in planta*, the second and main aim of the study – the production of BPV1 PsVs in plants – was explored. To achieve this, expression and purification methods established for the plant production of HPV16 PsVs were initially used. pTRAc-L1 and-L2 plasmids were co-expressed in plants, along with a self-replicating reporter plasmid encoding for SEAP. Purifications from these experiments revealed that in addition to numerous small VLPs and capsomeres contained largely in the upper fractions of the 27% gradient, T=7 particles of 50-60nm had formed (Buck *et al.*, 2003). The T=7 particles were similar in structure to those of the native virus and PsVs produced in mammalian expression systems, and infection of mammalian cells with these fractions later revealed these particles to be PsVs. This was deduced as high levels of SEAP protein expression were observed in the fractions containing the largest number of the T=7 particles, but not in the fractions in which the multitude of small VLPs dominated. These data showed that plant-expressed BPV L1/L2 VLPs had successfully encapsidated the reporter plasmid and were capable of were capable of delivering DNA into mammalian cells, thereby indirectly proving that L2 had successfully been expressed.

To determine the immunogenic potential of these small and large particles, an ELISA and PBNA were performed. An indirect ELISA was first performed with VLP fractions, as these contained the highest number of particles. The VLPs were probed with different primary BPV and PV MAbs

and PAbs. A positive control of HPV16 VLPs probed with Gardasil, PV, and MAb H16:J4 was also included. The ELISA revealed that the PV antibody had a strong binding with the BPV1 VLP structures, as did the MAb B1:A1, and that the oligoclonal Abcam also showed some binding. A PBNA was next performed by applying the antibodies tested in the ELISA to PsVs, and measuring the neutralising abilities of the antibodies through a reduction (of at least 50%) in SEAP expression. The B1:A1 monoclonal antibody was found to completely neutralise PsV activity at dilution of 1:200 and 1:500, and the Abcam antibody was neutralising at 1:200. The PV, Dako, and Gardasil antibodies were partially neutralising only at the lower dilution (1:200). These findings affirm the presence of antigenic epitopes capable of eliciting an appropriate immune response present on the PsV/VLP structures, and demonstrate that these particles are useful as components in PBNAs.

Protein expression levels of PsVs were analysed by Bradford assay, as protein bands were too faint to be quantified on Coomassie stained gels. Bradford assay analysis indicated that >120 mg/kg TSP was purified from the plants. However, this value might include some plant proteins still present, and as losses of L1 protein had also been observed early in this analysis, this figure only gives an indication of the protein yields obtained after purification on a density gradient. However, TEM images of VLPs obtained in this study, compared with those obtained by Love *et al.* (2012), the only other study demonstrating expression of BPV VLPs proteins in plant, indicated higher numbers of particles obtained in this study, and thus that protein yields higher than the 183 mg/kg fresh weight they obtained may have been achieved in this study.

As the largest number of particles (both T=1 VLPs and T=7 PsVs) were formed when PsVs were expressed, compared to VLPs, it therefore makes sense to further pursue this method for the production of a BPV1 vaccine in plants. Furthermore, Grgacic and Anderson (2006) showed that VLPs in the range of ~40nm, which is between the ~30nm T=1 VLPs and ~50nm T=7 PsVs, were ideal for uptake by DCs. Thus, a mixed population of particles might make an ideal candidate vaccine, presenting a mixture of epitopes and sizes which may elicit different immune reactions.

Although Thönes *et al.* (2008) showed that capsomeres were at least 20-fold less immunogenic than T=7 VLPs, Schädlich *et al.* (2009) found that small T=1 VLPs elicited humoral immune responses similar to those of the T=7 particles. To enhance the yields of particles obtained in PsV expression, several expression and purification methods were explored. The expression optimisation methods of heat shock treatment 2dpi, increasing acetosyringone induction concentrations to 500 µM, and harvesting at a 6dpi to allow for *in planta* particle assembly and maturation all yielded positive results, with greater protein and particle yields observed. Of the purification techniques, using iodixanol as opposed to sucrose in both cushion and density gradients, and preparing the density gradients with 6x concentration of high salt buffer as opposed to the standard 1x buffer yielded the best results. A combination of these methods has not yet been tested, and should be explored in future work.

4.2 Conclusions and Future Work

This study is the first report of plant-made BPV PsVs encapsidating a self-replicating reporter gene. In this study, I demonstrated that these PsVs are capable of infecting mammalian cells and expressing the SEAP reporter gene efficiently. I also showed that the PsVs could be neutralised by co-incubation with specific antibodies, indirectly demonstrating their immunogenic potential as vaccines. Furthermore, I explored several procedures to improve purification and expression, and demonstrated that a number of these techniques produced higher yields of protein and PsVs and, if applied in combination, could potentially lead to even greater yields of PsVs. For plants to be a viable production platform of recombinant proteins, it is necessary to achieve higher protein yields, thus continuous optimisation is important. There are several aspects of this study that may be further explored in future studies, including:

- Vaccine testing in animals, preferably in cattle or horses so that host-specific responses can be determined, and so that these studies can be followed by dose-escalation trials. Studies in our and other labs have already proved the safety of plant-produced PV vaccines *in vivo.*

- Investigations to improve expression of the L1 and L2 capsid proteins through increased GC-content, codon-optimisation (e.g. human or bovine), codon modifications, the use of different plant expression vectors, the use of silencing suppressors, the addition of chemical additives, cellular targeting, etc.

- The lack of an L2 antibody was of some hindrance in this study, as it was not possible to optimise L2 expression and thus PsV expression conditions. Furthermore, I was not able to fully determine whether *T*=1 VLPs were L1-only or L1/L2 VLPs. It would thus be of benefit to future research to produce such an antibody. While not discussed in this thesis, the BPV1 L1 and L2 genes were successfully cloned into the pProEX bacterial expression vector, and transformed into both and DH5α and BL21 (DE3) *E. coli.* These genes were expressed for the production of antigen to eventually produce antibodies in rabbits. Expression of insoluble protein was detected by probing for the His-tag introduced by the pProEX plasmid, and was low for both genes and in both of the bacterial strains. This is likely due to the fact that the genes were codon-optimised for *N. benthamiana*, and not for bacterial expression. However, as PsVs had been successfully produced at this point, confirming L2 expression, this was not further pursued, yet could be further explored in future work, using L1 and L2 genes codon-optimised for *E. coli*.

- The optimal size of encapsidated DNA may be explored to further optimise production of PsVs and VLPs in plants, and large-scale expression studies should assess both the protein yields and particle formation for optimisation.

- Expansion of PsVs to include other reporter gene plasmids for further research purposes: PsVs containing reporter genes encoding a protein with some visual marker, such as fluorescent protein GFP, could be observed within infected cells. This would allow for the monitoring of infection and quantification of infected cells, and thus, infective particles.

- Expansion of PsVs to include therapeutic genes for clinical purposes: In BPV, E5 is the major oncoprotein, and plays a pivotal role in the formation of papillomas. The constitutive expression of E5 in the basal layer and throughout the disease, downregulates the MHC I expression, and reduces the MHC I-mediated antigen presentation to CD8+ T-cells, making it the ideal target for a therapeutic BPV vaccine (Bocaneti *et al.*, 2016; Araldi *et al.*, 2017). Although BPV is not the most important of cattle diseases, but as it is exposed to the environment, the BPV capsid structure may be more stable than other viruses, and could be used to and can be used to deliver DNA vaccines of other important viral and bacterial pathogens as multivalent vaccines.

- Separation and individual assessment of the T=1 and T=7 particles, and immunisation studies with these particles to determine their applicability as candidate prophylactic and potentially therapeutic vaccines. Once PsVs have been established as viable candidate vaccines, the encapsidation of therapeutic elements and DNA vaccines may be explored, for the production of dual prophylactic and therapeutic vaccine candidates.

PVs are generally host-specific, which has complicated the development of HPV vaccines, for which the demonstration of protective efficacy is required for human clinical trials (Rybicki, 2009). Animal PVs, such as BPV, have long been used to elucidate the PV mechanisms, and vaccines produced against these can be applied to live animal models and used to test/demonstrate the immunogenicity and safety of vaccines. This study has demonstrated that techniques established for the production of HPV work for BPV, and it is therefore reasonable to assume that the reverse may be true, and also that these principles may be expanded for other PVs. Thus, this project has demonstrated that BPV is valuable as an animal model for the development and analysis of HPV vaccines. This study has also expanded on the research into the expression of PV proteins and vaccines in tobacco, and was a step towards the generation of a plant-produced BPV vaccine.

⯭ *"It's still magic, even if you know how it's done." - Terry Pratchett* ⯭

References:

Araldi, R.P., Assaf, S.M.R., Carvalho, R.F., Carvalho, M., Souza, J.M., Magnelli, R.F., Modolo, D.G., Roperto, F.P., Stocco, R.C. and Becak, W. (2017) Papillomaviruses: a systematic review. *Genet Mol Biol* **40**, 1-21.

Araldi, R.P., Giovanni, D.N., Melo, T.C., Diniz, N., Mazzuchelli-de-Souza, J., Sant'Ana, T.A., Carvalho, R.F., Becak, W. and Stocco, R.C. (2014) Bovine papillomavirus isolation by ultracentrifugation. *J Virol Methods* **208**, 119-124.

Araldi, R.P., Melo, T.C., Neves, A.C., Spadacci-Morena, D.D., Magnelli, R.F., Modolo, D.G., de-Sa-Junior, P.L., Mazucchelli-de-Souza, J., Carvalho, R.F., Becak, W. and Stocco, R.C. (2015) Hyperproliferative action of bovine papillomavirus: genetic and histopathological aspects. *Genet Mol Res* **14**, 12942-12954.

Ashrafi, G.H., Piuko, K., Burden, F., Yuan, Z., Gault, E.A., Muller, M., Trawford, A., Reid, S.W., Nasir, L. and Campo, M.S. (2008) Vaccination of sarcoid-bearing donkeys with chimeric virus-like particles of bovine papillomavirus type 1. *J Gen Virol* **89**, 148-157.

Bauermann, F.V., Joshi, L.R., Mohr, K.A., Kutish, G.F., Meier, P., Chase, C., Christopher-Hennings, J. and Diel, D.G. (2017) A novel bovine papillomavirus type in the genus Dyokappapapillomavirus. *Arch Virol* **162**, 3225-3228.

Bayer, L., Gümpel, J., Hause, G., Müller, M. and Grunwald, T. (2018) Non-human papillomaviruses for gene delivery in vitro and in vivo. *PLOS ONE* **13**, e0198996.

Belval, L., Hemmer, C., Sauter, C., Reinbold, C., Fauny, J.-D., Berthold, F., Ackerer, L., Schmitt-Keichinger, C., Lemaire, O., Demangeat, G. and Ritzenthaler, C. (2016) *Display of whole proteins on inner and outer surfaces of Grapevine fanleaf virus-like particles*.

Bernard, H.U., Burk, R.D., Chen, Z., van Doorslaer, K., zur Hausen, H. and de Villiers, E.M. (2010) Classification of papillomaviruses (PVs) based on 189 PV types and proposal of taxonomic amendments. *Virology* **401**, 70-79.

Biryukov, J., Meyers, C. and Banks, L. (2018) Superinfection Exclusion between Two High-Risk Human Papillomavirus Types during a Coinfection. *Journal of Virology* **92**.

Bocaneti, F., Altamura, G., Corteggio, A., Velescu, E., Roperto, F. and Borzacchiello, G. (2016) Bovine Papillomavirus: New Insights into an Old Disease. *Transbound Emerg Dis* **63**, 14-23.

Bogaert, L., Martens, A., De Baere, C. and Gasthuys, F. (2005) Detection of bovine papillomavirus DNA on the normal skin and in the habitual surroundings of horses with and without equine sarcoids. *Res Vet Sci* **79**, 253-258.

Bogaert, L., Martens, A., Kast, W.M., Van Marck, E. and De Cock, H. (2010) Bovine papillomavirus DNA can be detected in keratinocytes of equine sarcoid tumors. *Vet Microbiol* **146**, 269-275.

Bogaert, L., Martens, A., Van Poucke, M., Ducatelle, R., De Cock, H., Dewulf, J., De Baere, C., Peelman, L. and Gasthuys, F. (2008) High prevalence of bovine papillomaviral DNA in the normal skin of equine sarcoid-affected and healthy horses. *Vet Microbiol* **129**, 58-68.

Borzacchiello, G., Iovane, G., Marcante, M.L., Poggiali, F., Roperto, F., Roperto, S. and Venuti, A. (2003) Presence of bovine papillomavirus type 2 DNA and expression of the viral oncoprotein E5 in naturally occurring urinary bladder tumours in cows. *J Gen Virol* **84**, 2921-2926.

Borzacchiello, G. and Roperto, F. (2008) Bovine papillomaviruses, papillomas and cancer in cattle. *Vet Res* **39**, 45.

Borzacchiello, G., Russo, V., Gentile, F., Roperto, F., Venuti, A., Nitsch, L., Campo, M.S. and Roperto, S. (2006) Bovine papillomavirus E5 oncoprotein binds to the activated form of the platelet-derived growth factor beta receptor in naturally occurring bovine urinary bladder tumours. *Oncogene* **25**, 1251-1260.

Brandt, S. (2016) Immune response to bovine papillomavirus type 1 in equine sarcoid. *Vet J* **216**, 107-108.

Brandt, S., Haralambus, R., Shafti-Keramat, S., Steinborn, R., Stanek, C. and Kirnbauer, R. (2008) A subset of equine sarcoids harbours BPV-1 DNA in a complex with L1 major capsid protein. *Virology* **375**, 433-441.

Brillault, L., Jutras, P.V., Dashti, N., Thuenemann, E.C., Morgan, G., Lomonossoff, G.P., Landsberg, M.J. and Sainsbury, F. (2017) Engineering Recombinant Virus-like Nanoparticles from Plants for Cellular Delivery. *ACS Nano* **11**, 3476-3484.

Brotherton, J.M.L. (2017) Confirming cross-protection of bivalent HPV vaccine. *The Lancet Infectious Diseases* **17**, 1227-1228.

Buck, C.B., Cheng, N., Thompson, C.D., Lowy, D.R., Steven, A.C., Schiller, J.T. and Trus, B.L. (2008) Arrangement of L2 within the papillomavirus capsid. *J Virol* **82**, 5190-5197.

Buck, C.B., Day, P.M. and Trus, B.L. (2013) The papillomavirus major capsid protein L1. *Virology* **445**, 169-174.

Buck, C.B., Pastrana, D.V., Lowy, D.R. and Schiller, J.T. (2003) Efficient Intracellular Assembly of Papillomaviral Vectors. *Journal of Virology* **78**, 751-757.

Campo, M.S. (1997) Bovine papillomavirus and cancer. *The Veterinary Journal* **154**, 175-188.

Campo, M.S. (2002a) Animal models of papillomavirus pathogenesis. *Virus Research*

Campo, M.S. (2002b) Animal models of papillomavirus pathogenesis. *Virus Research* **89**, 249-261.

Campo, M.S., Jarrett, W.F.H., Barron, R., O'Neil, B.W. and Smith, K.T. (1992) Association of Bovine Papillomavirus Type 2 and Bracken Fern with Bladder Cancer in Cattle. *Cancer Research* **52**, 6898-6904.

Campo, M.S., Jarrett, W.F.H., O'Neil, W. and Barron, R.J. (1994) Latent papillomavirus infection in cattle. *Research in Veterinary Science* **56**, 151-157.

Campo, M.S. and Roden, R.B. (2010) Papillomavirus prophylactic vaccines: established successes, new approaches. *J Virol* **84**, 1214-1220.

Carr, E.A., Theon, A.P., Madewell, B.R., Griffey, S.M. and Hitchcock, M.E. (2001) *Bovine papillomavirus DNA in neoplastic and non-neoplastic tissues obtained from horses with and without sarcoids in the Western United States*.

Carvalho, R.F., Sakata, S.T., Giovanni, D.N., Mori, E., Brandao, P.E., Richtzenhain, L.J., Pozzi, C.R., Arcaro, J.R., Miranda, M.S., Mazzuchelli-de-Souza, J., Melo, T.C., Comenale, G., Assaf, S.L., Becak, W. and Stocco, R.C. (2013) Bovine papillomavirus in Brazil: detection of coinfection of unusual types by a PCR-RFLP method. *Biomed Res Int* **2013**, 270898.

Casini, G.L., Graham, D., Heine, D., Garcea, R.L. and Wu, D.T. (2004) In vitro papillomavirus capsid assembly analyzed by light scattering. *Virology* **325**, 320-327.

Cerqueira, C., Samperio Ventayol, P., Vogeley, C. and Schelhaas, M. (2015) Kallikrein-8 Proteolytically Processes Human Papillomaviruses in the Extracellular Space To Facilitate Entry into Host Cells. *Journal of virology* **89**, 7038-7052.

Cerqueira, C. and Schiller, J.T. (2017) Papillomavirus assembly: An overview and perspectives. *Virus Res* **231**, 103-107.

Cerqueira, C., Thompson, C.D., Day, P.M., Pang, Y.S., Lowy, D.R. and Schiller, J.T. (2017) Efficient Production of Papillomavirus Gene Delivery Vectors in Defined In Vitro Reactions. *Mol Ther Methods Clin Dev* **5**, 165-179.

Chabeda, A., Yanez, R.J.R., Lamprecht, R., Meyers, A.E., Rybicki, E.P. and Hitzeroth, II (2018) Therapeutic vaccines for high-risk HPV-associated diseases. *Papillomavirus Res* **5**, 46-58.

Chambers, G., Ellsmore, V.A., O'Brien, P.M., Reid, S.W., Love, S., Campo, M.S. and Nasir, L. (2003) Association of bovine papillomavirus with the equine sarcoid. *J Gen Virol* **84**, 1055-1062.

Chen, E.Y., Howley, P.M., Levinson, A.D. and Seeburg, P.H. (1982) The primary structure and genetic organization of the bovine papillomavirus type 1 genome. *Nature* **299**, 529-534.

Chen, Q., Lai, H., Hurtado, J., Stahnke, J., Leuzinger, K. and Dent, M. (2013) Agroinfiltration as an Effective and Scalable Strategy of Gene Delivery for Production of Pharmaceutical Proteins. *Adv Tech Biol Med* **1**.

Chen, X.S., Garcea, R.L., Goldberg, I., Casini, G. and Harrison, S.C. (2000) Structure of Small Virus-like Particles Assembled from the L1 Protein of Human Papillomavirus 16. *Molecular Cell* **5**, 557-567.

Cheng, M.A., Farmer, E., Huang, C., Lin, J., Hung, C.F. and Wu, T.C. (2018) Therapeutic DNA Vaccines for Human Papillomavirus and Associated Diseases. *Hum Gene Ther* **29**, 971-996.

Chichester, J.A., Haaheim, L.R. and Yusibov, V. (2009) Using plant cells as influenza vaccine substrates. *Expert Review of Vaccines* **8**, 493-498.

Christensen, N., Kreider, J., Cladel, N., Patrick, S. and Welsh, P. (1990) Monoclonal antibody-mediated neutralization of infectious human papillomavirus type 11. *Journal of Virology* **64**, 5678-5681.

Christensen, N.D., Budgeon, L.R., Cladel, N.M. and Hu, J. (2017) Recent advances in preclinical model systems for papillomaviruses. *Virus Res* **231**, 108-118.

Ciuffo, G. (1907) Innesto positivo con filtrato di verruca volgare. *Giorn Ital Mal Venereol* **48**, 12-17.

Crisci, E., Barcena, J. and Montoya, M. (2012) Virus-like particles: the new frontier of vaccines for animal viral infections. *Vet Immunol Immunopathol* **148**, 211-225.

Crisci, E., Bárcena, J. and Montoya, M. (2013) Virus-like particle-based vaccines for animal viral infections. *Inmunología* **32**, 102-116.

da Silva, F.R., Cibulski, S.P., Daudt, C., Weber, M.N., Guimaraes, L.L., Streck, A.F., Mayer, F.Q., Roehe, P.M. and Canal, C.W. (2016) Novel Bovine Papillomavirus Type Discovered by Rolling-Circle Amplification Coupled with Next-Generation Sequencing. *PLoS One* **11**, e0162345.

Dadar, M., Chakraborty, S., Dhama, K., Prasad, M., Khandia, R., Hassan, S., Munjal, A., Tiwari, R., Karthik, K., Kumar, D., Iqbal, H.M.N. and Chaicumpa, W. (2018) Advances in Designing and

Developing Vaccines, Drugs and Therapeutic Approaches to Counter Human Papilloma Virus. *Frontiers in Immunology* **9**.

Dagalp, S.B., Dogan, F., Farzani, T.A., Salar, S. and Bastan, A. (2017) The genetic diversity of bovine papillomaviruses (BPV) from different papillomatosis cases in dairy cows in Turkey. *Arch Virol* **162**, 1507-1518.

Daniell, H., Singh, N.D., Mason, H. and Streatfield, S.J. (2009) Plant-made vaccine antigens and biopharmaceuticals. *Trends Plant Sci* **14**, 669-679.

Daudt, C., da Silva, F.R., Streck, A.F., Weber, M.N., Mayer, F.Q., Cibulski, S.P. and Canal, C.W. (2016) How many papillomavirus species can go undetected in papilloma lesions? *Sci Rep* **6**, 36480.

Daudt, C., Da Silva, F.R.C., Lunardi, M., Alves, C., Weber, M.N., Cibulski, S.P., Alfieri, A.F., Alfieri, A.A. and Canal, C.W. (2018) Papillomaviruses in ruminants: An update. *Transbound Emerg Dis* **65**, 1381-1395.

de Villiers, E.M., Fauquet, C., Broker, T.R., Bernard, H.U. and zur Hausen, H. (2004) Classification of papillomaviruses. *Virology* **324**, 17-27.

Dennis, S.J., O'Kennedy, M.M., Rutkowska, D., Tsekoa, T., Lourens, C.W., Hitzeroth, II, Meyers, A.E. and Rybicki, E.P. (2018) Safety and immunogenicity of plant-produced African horse sickness virus-like particles in horses. *Vet Res* **49**, 105.

DiMaio, D. and Petti, L.M. (2013) The E5 proteins. *Virology* **445**, 99-114.

Doorbar, J. (2005) The papillomavirus life cycle. *J Clin Virol* **32 Suppl 1**, S7-15.

Doorbar, J. (2013) The E4 protein; structure, function and patterns of expression. *Virology* **445**, 80-98.

Edgue, G., Twyman, R.M., Beiss, V., Fischer, R. and Sack, M. (2017) Antibodies from plants for bionanomaterials. *Wiley Interdiscip Rev Nanomed Nanobiotechnol* **9**.

Embers, M.E., Budgeon, L.R., Pickel, M. and Christensen, N.D. (2002) Protective immunity to rabbit oral and cutaneous papillomaviruses by immunization with short peptides of L2, the minor capsid protein. *Journal of virology* **76**, 9798-9805.

Finlay, M., Yuan, Z., Burden, F., Trawford, A., Morgan, I.M., Campo, M.S. and Nasir, L. (2009) The detection of Bovine Papillomavirus type 1 DNA in flies. *Virus Res* **144**, 315-317.

Finnen, R.L., Erickson, K.D., Chen, X.S. and Garcea, R.L. (2003) Interactions between Papillomavirus L1 and L2 Capsid Proteins. *Journal of Virology* **77**, 4818-4826.

Fischer, R., Schillberg, S., Hellwig, S., Twyman, R.M. and Drossard, J. (2012) GMP issues for recombinant plant-derived pharmaceutical proteins. *Biotechnol Adv* **30**, 434-439.

Fischer, R., Vasilev, N., Twyman, R.M. and Schillberg, S. (2015) High-value products from plants: the challenges of process optimization. *Curr Opin Biotechnol* **32**, 156-162.

Fuenmayor, J., Godia, F. and Cervera, L. (2017) Production of virus-like particles for vaccines. *N Biotechnol* **39**, 174-180.

Gaynor, A.M., Zhu, K.W., Dela Cruz, F.N., Jr., Affolter, V.K. and Pesavento, P.A. (2016) Localization of Bovine Papillomavirus Nucleic Acid in Equine Sarcoids. *Vet Pathol* **53**, 567-573.

Gelvin, S.B. (2003) Agrobacterium-Mediated Plant Transformation: the Biology behind the "Gene-Jockeying" Tool. *Microbiology and Molecular Biology Reviews* **67**, 16-37.

Glass-Kaastra, S.K., Pearl, D.L., Reid-Smith, R.J., McEwen, B., McEwen, S.A., Amezcua, R. and Friendship, R.M. (2013) Describing antimicrobial use and reported treatment efficacy in

Ontario swine using the Ontario swine veterinary-based Surveillance program. *BMC Veterinary Research* **9**, 238.

Gonzalez-Castro, R., Acero Galindo, G., Garcia Salcedo, Y., Uribe Campero, L., Vazquez Perez, V., Carrillo-Tripp, M., Gevorkian, G. and Gomez Lim, M.A. (2018) Plant-based chimeric HPV-virus-like particles bearing amyloid-beta epitopes elicit antibodies able to recognize amyloid plaques in APP-tg mouse and Alzheimer's disease brains. *Inflammopharmacology* **26**, 817-827.

Grgacic, E.V. and Anderson, D.A. (2006) Virus-like particles: passport to immune recognition. *Methods* **40**, 60-65.

Gurunathan, S., Klinman, D.M. and Seder, R.A. (2000) DNA Vaccines: Immunology, Application, and Optimization. *Annual Review of Immunology* **18**, 927-974.

Hainisch, E.K., Abel-Reichwald, H., Shafti-Keramat, S., Pratscher, B., Corteggio, A., Borzacchiello, G., Wetzig, M., Jindra, C., Tichy, A., Kirnbauer, R. and Brandt, S. (2017) Potential of a BPV1 L1 VLP vaccine to prevent BPV1- or BPV2-induced pseudo-sarcoid formation and safety and immunogenicity of EcPV2 L1 VLPs in horse. *Journal of General Virology* **98**, 230-241.

Hainisch, E.K., Brandt, S., Shafti-Keramat, S., Van den Hoven, R. and Kirnbauer, R. (2012) Safety and immunogenicity of BPV-1 L1 virus-like particles in a dose-escalation vaccination trial in horses. *Equine Vet J* **44**, 107-111.

Hancock, G., Hellner, K. and Dorrell, L. (2018) Therapeutic HPV vaccines. *Best Pract Res Clin Obstet Gynaecol* **47**, 59-72.

Harnacker, J., Hainisch, E.K., Shafti-Keramat, S., Kirnbauer, R. and Brandt, S. (2017) Type-specific L1 virus-like particle-mediated protection of horses from experimental bovine papillomavirus 1-induced pseudo-sarcoid formation is long-lasting. *J Gen Virol* **98**, 1329-1333.

Hartl, B., Hainisch, E.K., Shafti-Keramat, S., Kirnbauer, R., Corteggio, A., Borzacchiello, G., Tober, R., Kainzbauer, C., Pratscher, B. and Brandt, S. (2011) Inoculation of young horses with bovine papillomavirus type 1 virions leads to early infection of PBMCs prior to pseudo-sarcoid formation. *J Gen Virol* **92**, 2437-2445.

Haspeslagh, M., Vlaminck, L. and Martens, A. (2018) The possible role of Stomoxys calcitrans in equine sarcoid transmission. *Vet J* **231**, 8-12.

Hatama, S. (2012) Cutaneous Papillomatosis in Cattle. *Journal of Disaster Research* **7**, 319-323.

Hefferon, K. (2017) Plant Virus Expression Vectors: A Powerhouse for Global Health. *Biomedicines* **5**.

Hefferon, K.L. (2012) Plant virus expression vectors set the stage as production platforms for biopharmaceutical proteins. *Virology* **433**, 1-6.

Hitzeroth, I.I., Passmore, J.-A.S., Shephard, E., Stewart, D., Müller, M., Williamson, A.-L., Rybicki, E.P. and Kast, W.M. (2009) Immunogenicity of an HPV-16 L2 DNA vaccine. *Vaccine* **27**, 6432-6434.

Hung, C.-F., Monie, A., Alvarez, R.D. and Wu, T.C. (2007) DNA vaccines for cervical cancer: from bench to bedside. *Experimental &Amp; Molecular Medicine* **39**, 679.

Jackson, M.A., Sternes, P.R., Mudge, S.R., Graham, M.W. and Birch, R.G. (2014) Design rules for efficient transgene expression in plants. *Plant Biotechnol J* **12**, 925-933.

Jagu, S., Malandro, N., Kwak, K., Yuan, H., Schlegel, R., Palmer, K.E., Huh, W.K., Campo, M.S. and Roden, R.B. (2011) A multimeric L2 vaccine for prevention of animal papillomavirus infections. *Virology* **420**, 43-50.

Jarrett, W.F., O'Neil, B.W., Gaukroger, J.M., Smith, K.T., Laird, H.M. and Campo, M.S. (1990) Studies on vaccination against papillomaviruses: the immunity after infection and vaccination with bovine papillomaviruses of different types. *The Veterinary record* **126**, 473-475.

Jelinek, F. and Tachezy, R. (2005) Cutaneous papillomatosis in cattle. *J Comp Pathol* **132**, 70-81.

Jiang, R.T., Schellenbacher, C., Chackerian, B. and Roden, R.B. (2016) Progress and prospects for L2-based human papillomavirus vaccines. *Expert Rev Vaccines* **15**, 853-862.

Karamanou, M., Agapitos, E., Kousoulis, A. and Androutsos, G. (2010) From the humble wart to HPV: a fascinating story throughout centuries. *Oncology Reviews* **4**, 133-135.

Karanam, B., Jagu, S., Huh, W.K. and Roden, R.B. (2009) Developing vaccines against minor capsid antigen L2 to prevent papillomavirus infection. *Immunol Cell Biol* **87**, 287-299.

Karg, S.R. and Kallio, P.T. (2009) The production of biopharmaceuticals in plant systems. *Biotechnol Adv* **27**, 879-894.

Kines, R.C., Zarnitsyn, V., Johnson, T.R., Pang, Y.Y., Corbett, K.S., Nicewonger, J.D., Gangopadhyay, A., Chen, M., Liu, J., Prausnitz, M.R., Schiller, J.T. and Graham, B.S. (2015) Vaccination with human papillomavirus pseudovirus-encapsidated plasmids targeted to skin using microneedles. *PLoS One* **10**, e0120797.

Kirnbauer, R., Booy, F., Cheng, N., Lowy, D. and Schiller, J. (1992) Papillomavirus L1 major capsid protein self-assembles into virus-like particles that are highly immunogenic. *Proceedings of the National Academy of Sciences* **89**, 12180-12184.

Kirnbauer, R., Chandrachud, L.M., O'Neil, B.W., Wagner, E.R., Grindlay, G.J., Armstrong, A., McGarvie, G.M., Schiller, J.T., Lowy, D.R. and Campo, M.S. (1996) Virus-like Particles of Bovine Papillomavirus Type 4 in Prophylactic and Therapeutic Immunization. *Virology* **219**, 37-44.

Koch, C., Ramsauer, A.S., Drogemuller, M., Ackermann, M., Gerber, V. and Tobler, K. (2018) Genomic comparison of bovine papillomavirus 1 isolates from bovine, equine and asinine lesional tissue samples. *Virus Res* **244**, 6-12.

Kwak, K., Yemelyanova, A. and Roden, R.B. (2011) Prevention of cancer by prophylactic human papillomavirus vaccines. *Curr Opin Immunol* **23**, 244-251.

Lamprecht, R.L., Kennedy, P., Huddy, S.M., Bethke, S., Hendrikse, M., Hitzeroth, II and Rybicki, E.P. (2016) Production of Human papillomavirus pseudovirions in plants and their use in pseudovirion-based neutralisation assays in mammalian cells. *Sci Rep* **6**, 20431.

Lee, N.H., Lee, J.A., Park, S.Y., Song, C.S., Choi, I.S. and Lee, J.B. (2012) A review of vaccine development and research for industry animals in Korea. *Clin Exp Vaccine Res* **1**, 18-34.

Leuzinger, K., Dent, M., Hurtado, J., Stahnke, J., Lai, H., Zhou, X. and Chen, Q. (2013) Efficient agroinfiltration of plants for high-level transient expression of recombinant proteins. *J Vis Exp*.

Li, J., Zhou, J., Wu, Y., Yang, S. and Tian, D. (2015) GC-Content of Synonymous Codons Profoundly Influences Amino Acid Usage. *G3 (Bethesda)* **5**, 2027-2036.

Lima, E.G., Lira, R.C., Jesus, A.L., Dhalia, R. and Freitas, A.C. (2014) Development of a DNA-based vaccine strategy against bovine papillomavirus infection, involving the E5 or L2 gene. *Genet Mol Res* **13**, 1121-1126.

Lin, K., Roosinovich, E., Ma, B., Hung, C.F. and Wu, T.C. (2010) Therapeutic HPV DNA vaccines. *Immunol Res* **47**, 86-112.

Liu, F., Ge, S., Li, L., Wu, X., Liu, Z. and Wang, Z. (2012) Virus-like particles: potential veterinary vaccine immunogens. *Res Vet Sci* **93**, 553-559.

Lohr, C.V., Juan-Salles, C., Rosas-Rosas, A., Paras Garcia, A., Garner, M.M. and Teifke, J.P. (2005) Sarcoids in captive zebras (Equus burchellii): association with bovine papillomavirus type 1 infection. *J Zoo Wildl Med* **36**, 74-81.

Lomonossoff, G.P. and D'Aoust, M.-A. (2016) Plant-produced biopharmaceuticals: A case of technical developments driving clinical deployment. *Science* **353**, 1237-1240.

Love, A.J., Chapman, S.N., Matic, S., Noris, E., Lomonossoff, G.P. and Taliansky, M. (2012) In planta production of a candidate vaccine against bovine papillomavirus type 1. *Planta* **236**, 1305-1313.

Lunardi, M., de Alcantara, B.K., Otonel, R.A., Rodrigues, W.B., Alfieri, A.F. and Alfieri, A.A. (2013) Bovine papillomavirus type 13 DNA in equine sarcoids. *J Clin Microbiol* **51**, 2167-2171.

Lunardi, M., de Camargo Tozato, C., Alfieri, A.F., de Alcantara, B.K., Vilas-Boas, L.A., Otonel, R.A., Headley, S.A. and Alfieri, A.A. (2016) Genetic diversity of bovine papillomavirus types, including two putative new types, in teat warts from dairy cattle herds. *Arch Virol* **161**, 1569-1577.

Lund, P.E., Hunt, R.C., Gottesman, M.M. and Kimchi-Sarfaty, C. (2010) Pseudovirions as vehicles for the delivery of siRNA. *Pharm Res* **27**, 400-420.

Ma, B., Roden, R.B., Hung, C.F. and Wu, T.C. (2011) HPV pseudovirions as DNA delivery vehicles. *Ther Deliv* **2**, 427-430.

Ma, Z., Cooper, C., Kim, H.-J., Janick-Buckner, D. and Ledbetter, M.L. (2009) A Study of Rubisco through Western Blotting and Tissue Printing Techniques. *CBE—Life Sciences Education* **8**, 140-146.

Maclean, J., Koekemoer, M., Olivier, A.J., Stewart, D., Hitzeroth, II, Rademacher, T., Fischer, R., Williamson, A.L. and Rybicki, E.P. (2007) Optimization of human papillomavirus type 16 (HPV-16) L1 expression in plants: comparison of the suitability of different HPV-16 L1 gene variants and different cell-compartment localization. *J Gen Virol* **88**, 1460-1469.

Marais, H.J., Nel, P., Bertschinger, H.J., Schoeman, J.P. and Zimmerman, D. (2007) Prevalence and body distribution of sarcoids in South African Cape mountain zebra (Equus zebra zebra). *2007* **78**, 4.

Mardanova, E.S., Blokhina, E.A., Tsybalova, L.M., Peyret, H., Lomonossoff, G.P. and Ravin, N.V. (2017) Efficient Transient Expression of Recombinant Proteins in Plants by the Novel pEff Vector Based on the Genome of Potato Virus X. *Front Plant Sci* **8**, 247.

Marsian, J. and Lomonossoff, G.P. (2016) Molecular pharming- VLPs made in plants. *Curr Opin Biotechnol* **37**, 201-206.

Martens, A., Moor, A.D.E., Demeulemeester, J. and Ducatelle, R. (2000) Histopathological characteristics of five clinical types of equine sarcoid. *Research in Veterinary Science* **69**, 295-300.

Matic, S., Masenga, V., Poli, A., Rinaldi, R., Milne, R.G., Vecchiati, M. and Noris, E. (2012) Comparative analysis of recombinant Human Papillomavirus 8 L1 production in plants by a variety of expression systems and purification methods. *Plant Biotechnol J* **10**, 410-421.

Mazzuchelli-de-Souza, J., de Carvalho, R.F., Modolo, D.G., Thompson, C.E., Araldi, R.P. and Stocco, R.C. (2018) First detection of bovine papillomavirus type 2 in cutaneous wart lesions from ovines. *Transbound Emerg Dis* **65**, 939-943.

Meissner, H.H., Scholtz, M.M. and Palmer, A.R. (2014) Sustainability of the South African Livestock Sector towards 2050 Part 1: Worth and impact of the sector. *South African Journal of Animal Science* **43**.

Melkamu, S. (2018) *A Review on Equine Sarcoid: Current Techniques Employed in Sciences for Diagnosis, Prevention and Control*.

Melo, T.C., Araldi, R.P., Pessoa, N.S., de-Sa-Junior, P.L., Carvalho, R.F., Becak, W. and Stocco, R.C. (2015) Bos taurus papillomavirus activity in peripheral blood mononuclear cells: demonstrating a productive infection. *Genet Mol Res* **14**, 16712-16727.

Michelangeli, F., Liprandi, F., E Chemello, M., Ciarlet, M. and C Ruiz, M. (1995) *Selective depletion of stored calcium by thapsigargin blocks rotavirus maturation but not the cytopathic effect*.

Modis, Y., Trus, B.L. and Harrison, S.C. (2002) Atomic model of the papillomavirus capsid. *The EMBO journal* **21**, 4754-4762.

Modolo, D.G., Araldi, R.P., Mazzuchelli-de-Souza, J., Pereira, A., Pimenta, D.C., Zanphorlin, L.M., Becak, W., Menossi, M., de Cassia Stocco, R. and de Carvalho, R.F. (2017) Integrated analysis of recombinant BPV-1 L1 protein for the production of a bovine papillomavirus VLP vaccine. *Vaccine* **35**, 1590-1593.

Mohsen, M.O., Zha, L., Cabral-Miranda, G. and Bachmann, M.F. (2017) Major findings and recent advances in virus-like particle (VLP)-based vaccines. *Semin Immunol* **34**, 123-132.

Monke, D.R., Tank, J.L., Good, A.E. and Lahmers, E.A. (2018) 10- Diseases Specific to or Common in Dairy Bulls. In: *Rebhun's Diseases of Dairy Cattle (Third Edition)* (Peek, S.F. and Divers, T.J. eds), pp. 508-525. Elsevier.

Moroni, P., Nydam, D.V., Ospina, P.A., Scillieri-Smith, J.C., Virkler, P.D., Watters, R.D., Welcome, F.L., Zurakowski, M.J., Ducharme, N.G. and Yeager, A.E. (2018) 8- Diseases of the Teats and Udder. In: *Rebhun's Diseases of Dairy Cattle (Third Edition)* (Peek, S.F. and Divers, T.J. eds), pp. 389-465. Elsevier.

Munday, J.S. (2014) Bovine and human papillomaviruses: a comparative review. *Vet Pathol* **51**, 1063-1075.

Nasir, L. and Brandt, S. (2013) Papillomavirus associated diseases of the horse. *Vet Microbiol* **167**, 159-167.

Nasir, L., Gault, E., Morgan, I.M., Chambers, G., Ellsmore, V. and Campo, M.S. (2007) Identification and functional analysis of sequence variants in the long control region and the E2 open reading frame of bovine papillomavirus type 1 isolated from equine sarcoids. *Virology* **364**, 355-361.

Nel, P.J., Bertschinger, H., Williams, J. and Thompson, P.N. (2006) Descriptive study of an outbreak of equine sarcoid in a population of Cape mountain zebra (Equus zebra zebra) in the Gariep Nature Reserve. *2006* **77**, 7.

Noad, R. and Roy, P. (2003) Virus-like particles as immunogens. *Trends in Microbiology* **11**, 438-444.

Norkunas, K., Harding, R., Dale, J. and Dugdale, B. (2018) *Improving agroinfiltration-based transient gene expression in Nicotiana benthamiana*.

O'Brien, P.M. and Saveria Campo, M. (2002) Evasion of host immunity directed by papillomavirus-encoded proteins. *Virus Research* **88**, 103-117.

Paintsil, J., Muller, M., Picken, M., Gissmann, L. and Zhou, J. (1998) Calcium is required in reassembly of bovine papillomavirus in vitro. *J Gen Virol* **79 (Pt 5)**, 1133-1141.

Palanivel, K.M., Surendar, A.P. and Kanimozhi, P. (2017) Sero Biochemical Profile of Crossbred Calves Naturally Infected By Bovine Papilloma Virus. *International Journal of Current Microbiology and Applied Sciences* **6**, 366-371.

Peh, W.L., Middleton, K., Christensen, N., Nicholls, P., Egawa, K., Sotlar, K., Brandsma, J., Percival, A., Lewis, J., Liu, W.J. and Doorbar, J. (2002) Life Cycle Heterogeneity in Animal Models of Human Papillomavirus-Associated Disease. *Journal of Virology* **76**, 10401-10416.

Peng, S., Monie, A., Kang, T.H., Hung, C.F., Roden, R. and Wu, T.C. (2010) Efficient delivery of DNA vaccines using human papillomavirus pseudovirions. *Gene therapy* **17**, 1453-1464.

Pérez Aguirreburualde, M.S., Petruccelli, S., Bravo Almonacid, F. and Wigdorovitz, A. (2016) Plant-Based Vaccine for Livestock: Key Points to Unleash Platform Translation in Developing Countries. *Current Molecular Biology Reports* **2**, 171-179.

Pesavento, P.A., Agnew, D., Keel, M.K. and Woolard, K.D. (2018) Cancer in wildlife: patterns of emergence. *Nat Rev Cancer* **18**, 646-661.

Pineo, C.B., Hitzeroth, II and Rybicki, E.P. (2013) Immunogenic assessment of plant-produced human papillomavirus type 16 L1/L2 chimaeras. *Plant Biotechnol J* **11**, 964-975.

Pogue, G.P., Lindbo, J.A., Garger, S.J. and Fitzmaurice, W.P. (2002) Making an ally from an enemy: plant virology and the new agriculture. *Annu Rev Phytopathol* **40**, 45-74.

Porter, S.S., Stepp, W.H., Stamos, J.D. and McBride, A.A. (2017) Host cell restriction factors that limit transcription and replication of human papillomavirus. *Virus Res* **231**, 10-20.

Radostits, M.O., Blood, C.D. and Done, H.S. (2007) *Veterinary Medicine: A Textbook of the Diseases of Cattle, Sheep, Pigs, Goats and Horses*.

Rector, A. and Van Ranst, M. (2013) Animal papillomaviruses. *Virology* **445**, 213-223.

Regnard, G.L., Halley-Stott, R.P., Tanzer, F.L., Hitzeroth, II and Rybicki, E.P. (2010) High level protein expression in plants through the use of a novel autonomously replicating geminivirus shuttle vector. *Plant Biotechnol J* **8**, 38-46.

Roden, R.B., Day, P.M., Bronzo, B.K., Yutzy, W.H.t., Yang, Y., Lowy, D.R. and Schiller, J.T. (2001) Positively charged termini of the L2 minor capsid protein are necessary for papillomavirus infection. *J Virol* **75**, 10493-10497.

Roden, R.B., Yutzy, W.H.t., Fallon, R., Inglis, S., Lowy, D.R. and Schiller, J.T. (2000) Minor capsid protein of human genital papillomaviruses contains subdominant, cross-neutralizing epitopes. *Virology* **270**, 254-257.

Roperto, S., Brun, R., Paolini, F., Urraro, C., Russo, V., Borzacchiello, G., Pagnini, U., Raso, C., Rizzo, C., Roperto, F. and Venuti, A. (2008) Detection of bovine papillomavirus type 2 in the peripheral blood of cattle with urinary bladder tumours: possible biological role. *J Gen Virol* **89**, 3027-3033.

Roperto, S., Munday, J.S., Corrado, F., Goria, M. and Roperto, F. (2016a) Detection of bovine papillomavirus type 14 DNA sequences in urinary bladder tumors in cattle. *Vet Microbiol* **190**, 1-4.

Roperto, S., Russo, V., Corrado, F., De Falco, F., Munday, J.S. and Roperto, F. (2018) Oral fibropapillomatosis and epidermal hyperplasia of the lip in newborn lambs associated with bovine Deltapapillomavirus. *Sci Rep* **8**, 13310.

Roperto, S., Russo, V., Leonardi, L., Martano, M., Corrado, F., Riccardi, M.G. and Roperto, F. (2016b) Bovine Papillomavirus Type 13 Expression in the Urothelial Bladder Tumours of Cattle. *Transbound Emerg Dis* **63**, 628-634.

Roperto, S., Russo, V., Ozkul, A., Sepici-Dincel, A., Maiolino, P., Borzacchiello, G., Marcus, I., Esposito, I., Riccardi, M.G. and Roperto, F. (2013) Bovine papillomavirus type 2 infects the urinary bladder of water buffalo (Bubalus bubalis) and plays a crucial role in bubaline urothelial carcinogenesis. *J Gen Virol* **94**, 403-408.

Rosales, C. and Rosales, R. (2017) Prophylactic and Therapeutic Vaccines against Human Papillomavirus Infections.

Ruiz, V., Mozgovoj, M.V., Dus Santos, M.J. and Wigdorovitz, A. (2015) Plant-produced viral bovine vaccines: what happened during the last 10 years? *Plant Biotechnol J* **13**, 1071-1077.

Rybicki, E. (2018) History and Promise of Plant-Made Vaccines for Animals. In: *Prospects of Plant-Based Vaccines in Veterinary Medicine* pp. 1-22.

Rybicki, E.P. (2009) Plant-produced vaccines: promise and reality. *Drug Discov Today* **14**, 16-24.

Rybicki, E.P. (2010) Plant-made vaccines for humans and animals. *Plant Biotechnol J* **8**, 620-637.

Sainsbury, F., Canizares, M.C. and Lomonossoff, G.P. (2010) Cowpea mosaic virus: the plant virus-based biotechnology workhorse. *Annu Rev Phytopathol* **48**, 437-455.

Sainsbury, F. and Lomonossoff, G.P. (2014) Transient expressions of synthetic biology in plants. *Curr Opin Plant Biol* **19**, 1-7.

Sainsbury, F., Thuenemann, E.C. and Lomonossoff, G.P. (2009) pEAQ: versatile expression vectors for easy and quick transient expression of heterologous proteins in plants. *Plant Biotechnol J* **7**, 682-693.

Salazar, K.L., Zhou, H.S., Xu, J., Peterson, L.E., Schwartz, M.R., Mody, D.R. and Ge, Y. (2015) Multiple Human Papilloma Virus Infections and Their Impact on the Development of High-Risk Cervical Lesions. *Acta Cytologica* **59**, 391-398.

Salyaev, R.K., Rekoslavskaya, N.I. and Stolbikov, A.S. (2018) Synthesis of Proteins Encoded by the Early Genes E2, E6, and E7 of Papillomavirus of Type 16 in the Plant Expression System. *Dokl Biochem Biophys* **482**, 271-274.

Sambrook, J., Maniatis, T. and F Fritsch, E. (2019) *Molecular cloning : a laboratory manual / J. Sambrook, E.F. Fritsch, T. Maniatis*.

Sasidharan, S.P. (2006) Sarcoid tumours in Cape mountain zebra (Equus zebra zebra) populations in South Africa: a review of associated epidemiology, virology and genetics. *Transactions of the Royal Society of South Africa* **61**, 11-18.

Saunders, K. and Lomonossoff, G.P. (2015) The Generation of Turnip Crinkle Virus-Like Particles in Plants by the Transient Expression of Wild-Type and Modified Forms of Its Coat Protein. *Front Plant Sci* **6**, 1138.

Savini, F., Mancini, S., Gallina, L., Donati, G., Casa, G., Peli, A. and Scagliarini, A. (2016) Bovine papillomatosis: First detection of bovine papillomavirus types 6, 7, 8, 10 and 12 in Italian cattle herds. *Vet J* **210**, 82-84.

Schädlich, L., Senger, T., Gerlach, B., Mücke, N., Klein, C., Bravo, I.G., Müller, M. and Gissmann, L. (2009) Analysis of modified human papillomavirus type 16 L1 capsomeres: the ability to

assemble into larger particles correlates with higher immunogenicity. *Journal of virology* 83, 7690-7705.

Schellenbacher, C., Roden, R.B.S. and Kirnbauer, R. (2017) Developments in L2-based human papillomavirus (HPV) vaccines. *Virus Res* 231, 166-175.

Schiller, J.T. and Müller, M. (2015) Next generation prophylactic human papillomavirus vaccines. *The Lancet Oncology* 16, e217-e225.

Semik-Gurgul, E., Ząbek, T., Fornal, A., Gurgul, A., Pawlina-Tyszko, K., Klukowska-Rötzler, J. and Bugno-Poniewierska, M. (2018) Analysis of the methylation status of CpG sites within cancer-related genes in equine sarcoids. *Annals of Animal Science* 0.

Shafti-Keramat, S., Schellenbacher, C., Handisurya, A., Christensen, N., Reininger, B., Brandt, S. and Kirnbauer, R. (2009) Bovine papillomavirus type 1 (BPV1) and BPV2 are closely related serotypes. *Virology* 393, 1-6.

Shah, K.H., Almaghrabi, B. and Bohlmann, H. (2013) Comparison of Expression Vectors for Transient Expression of Recombinant Proteins in Plants. *Plant Mol Biol Report* 31, 1529-1538.

Sharma, A.K. and Sharma, M.K. (2009) Plants as bioreactors: Recent developments and emerging opportunities. *Biotechnol Adv* 27, 811-832.

Shevchenko, A., Tomas, H., Havli, J., Olsen, J.V. and Mann, M. (2007) In-gel digestion for mass spectrometric characterization of proteins and proteomes. *Nature Protocols* 1, 2856.

Shi, W., Liu, J., Huang, Y. and Qiao, L. (2001) Papillomavirus pseudovirus: a novel vaccine to induce mucosal and systemic cytotoxic T-lymphocyte responses. *Journal of virology* 75, 10139-10148.

Silva, M.A., De Albuquerque, B.M., Pontes, N.E., Coutinho, L.C., Leitao, M.C., Reis, M.C., Castro, R.S. and Freitas, A.C. (2013) Detection and expression of bovine papillomavirus in blood of healthy and papillomatosis-affected cattle. *Genet Mol Res* 12, 3150-3156.

Silvestre, O., Borzacchiello, G., Nava, D., Iovane, G., Russo, V., Vecchio, D., D'Ausilio, F., Gault, E.A., Campo, M.S. and Paciello, O. (2009) Bovine papillomavirus type 1 DNA and E5 oncoprotein expression in water buffalo fibropapillomas. *Vet Pathol* 46, 636-641.

Sim, S.-L., He, T., Tscheliessnig, A., Mueller, M., Tan, R.B.H. and Jungbauer, A. (2012) Protein precipitation by polyethylene glycol: A generalized model based on hydrodynamic radius. *Journal of Biotechnology* 157, 315-319.

Sohrab, S.S., Suhail, M., Kamal, M.A., Husen, A. and Azhar, E.I. (2017) Recent Development and Future Prospects of Plant-Based Vaccines. *Curr Drug Metab* 18, 831-841.

Sreeparvathy, M., Harish, C. and Anuraj, K. (2011) Autogenous vaccination as a treatment method for bovine papillomatosis. *J. Livestock Sci* 2, 38-40.

Sundström, K., Ploner, A., Arnheim-Dahlstrom, L., Eloranta, S., Palmgren, J., Adami, H.O., Ylitalo Helm, N., Sparen, P. and Dillner, J. (2015) Interactions Between High- and Low-Risk HPV Types Reduce the Risk of Squamous Cervical Cancer. *J Natl Cancer Inst* 107.

Sykora, S. and Brandt, S. (2017) Papillomavirus infection and squamous cell carcinoma in horses. *Vet J* 223, 48-54.

Taylor, S. and Haldorson, G. (2013) A review of equine sarcoid. *Equine Veterinary Education* 25, 210-216.

Thönes, N., Herreiner, A., Schädlich, L., Piuko, K. and Müller, M. (2008) A direct comparison of human papillomavirus type 16 L1 particles reveals a lower immunogenicity of

capsomeres than viruslike particles with respect to the induced antibody response. *Journal of virology* **82**, 5472-5485.

Thornton, P.K. (2010) Livestock production: recent trends, future prospects. *Philosophical transactions of the Royal Society of London. Series B, Biological sciences* **365**, 2853-2867.

Thuenemann, E., Lenzi, P., Love, A., Taliansky, M., Becares, M., Zuniga, S., Enjuanes, L., Zahmanova, G., Minkov, I., Matic, S., Noris, E., Meyers, A., Hattingh, A., Rybicki, E., Kiselev, O., Ravin, N., Eldarov, M., Skryabin, K. and Lomonossoff, G. (2013a) The Use of Transient Expression Systems for the Rapid Production of Virus-like Particles in Plants. *Current Pharmaceutical Design* **19**, 5564-5573.

Thuenemann, E.C., Meyers, A.E., Verwey, J., Rybicki, E.P. and Lomonossoff, G.P. (2013b) A method for rapid production of heteromultimeric protein complexes in plants: assembly of protective bluetongue virus-like particles. *Plant Biotechnol J* **11**, 839-846.

Tiwari, S., Verma, P.C., Singh, P.K. and Tuli, R. (2009) Plants as bioreactors for the production of vaccine antigens. *Biotechnology Advances* **27**, 449-467.

Tomaic, V. (2016) Functional Roles of E6 and E7 Oncoproteins in HPV-Induced Malignancies at Diverse Anatomical Sites. *Cancers (Basel)* **8**.

Tomita, Y., Ogawa, T., Jin, Z. and Shirasawa, H. (2007) Genus specific features of bovine papillomavirus E6, E7, E5 and E8 proteins. *Virus Res* **124**, 231-236.

Topp, E., Irwin, R., McAllister, T., Lessard, M., Joensuu, J.J., Kolotilin, I., Conrad, U., Stoger, E., Mor, T., Warzecha, H., Hall, J.C., McLean, M.D., Cox, E., Devriendt, B., Potter, A., Depicker, A., Virdi, V., Holbrook, L., Doshi, K., Dussault, M., Friendship, R., Yarosh, O., Yoo, H.S., MacDonald, J. and Menassa, R. (2016) The case for plant-made veterinary immunotherapeutics. *Biotechnol Adv* **34**, 597-604.

Tremblay, R., Wang, D., Jevnikar, A.M. and Ma, S. (2010) Tobacco, a highly efficient green bioreactor for production of therapeutic proteins. *Biotechnol Adv* **28**, 214-221.

Trewby, H., Ayele, G., Borzacchiello, G., Brandt, S., Campo, M.S., Del Fava, C., Marais, J., Leonardi, L., Vanselow, B., Biek, R. and Nasir, L. (2014) Analysis of the long control region of bovine papillomavirus type 1 associated with sarcoids in equine hosts indicates multiple cross-species transmission events and phylogeographical structure. *J Gen Virol* **95**, 2748-2756.

Turk, N., Zupancic, Z., Staresina, V., Kovac, S., Babic, T., Kreszinger, M., Curic, S., Barbic, L. and Milas, Z. (2005) Severe bovine papillomatosis: detection of bovine papillomavirus in tumour tissue and efficacy of treatment using autogenous vaccine and parammunity inducer. *Veterinarski arhiv* **75**, 391.

Ugochukwu, I.C.I., Aneke, C.I., Idoko, I.S., Sani, N.A., Amoche, A.J., Mshiela, W.P., Ede, R.E., Ibrahim, N.D.G., Njoku, C.I.O. and Sackey, A.K.B. (2018) Bovine papilloma: aetiology, pathology, immunology, disease status, diagnosis, control, prevention and treatment: a review. *Comparative Clinical Pathology*.

Urban, P.L. (2016) Quantitative mass spectrometry: an overview. *Philos Trans A Math Phys Eng Sci* **374**.

Vamvaka, E., Twyman, R.M., Murad, A.M., Melnik, S., Teh, A.Y.-H., Arcalis, E., Altmann, F., Stoger, E., Rech, E., Ma, J.K.C., Christou, P. and Capell, T. (2016) Rice endosperm produces an underglycosylated and potent form of the HIV-neutralizing monoclonal antibody 2G12. *Plant Biotechnology Journal* **14**, 97-108.

Van Doorslaer, K. (2013) Evolution of the papillomaviridae. *Virology* **445**, 11-20.

van Dyk, E., Oosthuizen, M.C., Bosman, A.M., Nel, P.J., Zimmerman, D. and Venter, E.H. (2009) Detection of bovine papillomavirus DNA in sarcoid-affected and healthy free-roaming zebra (Equus zebra) populations in South Africa. *J Virol Methods* **158**, 141-151.

van Zyl, A.R. and Hitzeroth, I.I. (2016) Purification of Virus-Like Particles (VLPs) from Plants. In: *Vaccine Design: Methods and Protocols, Volume 2: Vaccines for Veterinary Diseases* (Thomas, S. ed) pp. 569-579. New York, NY: Springer New York.

Wang, J.W. and Roden, R.B. (2013) L2, the minor capsid protein of papillomavirus. *Virology* **445**, 175-186.

Wilken, L.R. and Nikolov, Z.L. (2012) Recovery and purification of plant-made recombinant proteins. *Biotechnol Adv* **30**, 419-433.

Williams, J.H., Dyk, E.v., Nel, P.J., Lane, E., Wilpe, E.V., Bengis, R.G., Klerk-Lorist, L.-M.d. and Heerden, J.v. (2011) Pathology and immunohistochemistry of papillomavirus-associated cutaneous lesions in Cape mountain zebra, giraffe, sable antelope and African buffalo in South Africa. *Journal of the South African Veterinary Association* **82**, 97-106.

Wilson, A.D., Armstrong, E.L., Gofton, R.G., Mason, J., De Toit, N. and Day, M.J. (2013) Characterisation of early and late bovine papillomavirus protein expression in equine sarcoids. *Vet Microbiol* **162**, 369-380.

Wolf, M., Garcea, R.L., Grigorieff, N. and Harrison, S.C. (2010) Subunit interactions in bovine papillomavirus. *Proc Natl Acad Sci U S A* **107**, 6298-6303.

Wong-Arce, A., Gonzalez-Ortega, O. and Rosales-Mendoza, S. (2017) Plant-Made Vaccines in the Fight Against Cancer. *Trends Biotechnol* **35**, 241-256.

Wroblewski, T., Tomczak, A. and Michelmore, R. (2005) Optimization of Agrobacterium-mediated transient assays of gene expression in lettuce, tomato and Arabidopsis. *Plant Biotechnology Journal* **3**, 259-273.

Xi, J., Wang, X., Li, S., Zhou, X., Yue, L., Fan, J. and Hao, D. (2006) Polyethylene glycol fractionation improved detection of low-abundant proteins by two-dimensional electrophoresis analysis of plant proteome. *Phytochemistry* **67**, 2341-2348.

Yanez, R.J.R., Lamprecht, R., Granadillo, M., Torrens, I., Arcalis, E., Stoger, E., Rybicki, E.P. and Hitzeroth, II (2018) LALF32-51-E7, a HPV-16 therapeutic vaccine candidate, forms protein body-like structures when expressed in Nicotiana benthamiana leaves. *Plant Biotechnol J* **16**, 628-637.

Yao, J., Weng, Y., Dickey, A. and Wang, K.Y. (2015) Plants as Factories for Human Pharmaceuticals: Applications and Challenges. *Int J Mol Sci* **16**, 28549-28565.

Yuan, Z., Gallagher, A., Gault, E.A., Campo, M.S. and Nasir, L. (2007) Bovine papillomavirus infection in equine sarcoids and in bovine bladder cancers. *Vet J* **174**, 599-604.

Yuan, Z.Q., Bennett, L., Campo, M.S. and Nasir, L. (2010) Bovine papillomavirus type 1 E2 and E7 proteins down-regulate Toll Like Receptor 4 (TLR4) expression in equine fibroblasts. *Virus Res* **149**, 124-127.

Zahin, M., Joh, J., Khanal, S., Husk, A., Mason, H., Warzecha, H., Ghim, S.J., Miller, D.M., Matoba, N. and Jenson, A.B. (2016) Scalable Production of HPV16 L1 Protein and VLPs from Tobacco Leaves. *PLoS One* **11**, e0160995.

Zelitch, I., Schultes, N.P., Peterson, R.B., Brown, P. and Brutnell, T.P. (2009) High Glycolate Oxidase Activity Is Required for Survival of Maize in Normal Air. *Plant Physiology* **149**, 195-204.

Zhao, H., Lin, Z.-J., Huang, S.-J., Li, J., Liu, X.-H., Guo, M., Zhang, J., Xia, N.-S., Pan, H.-R., Wu, T. and Li, C.-G. (2014) Correlation between ELISA and pseudovirion-based neutralisation assay for detecting antibodies against human papillomavirus acquired by natural infection or by vaccination. *Human Vaccines & Immunotherapeutics* **10**, 740-746.

Zhou, J., Liu, W.J., Peng, S.W., Sun, X.Y. and Frazer, I. (1999) Papillomavirus capsid protein expression level depends on the match between codon usage and tRNA availability. *Journal of virology* **73**, 4972-4982.

Websites and Other References:

- Axis-Shield PoC AS (2016) Optiprep—product description. In: http://www.axis-shield-density-gradient-media.com/230571%20OptiPrep.pdf . [Accessed 3 November, 2018].
- Endecott, R. (2014). Warts in Cattle: Cause and Cure. Montana State University. [Online] Available at: http://www.thecattlesite.com/articles/3999/warts-in-cattle-cause-and-cure/. [Accessed: 22 October, 2018].
- Equine Healthcare Market by Product (Drugs, Vaccines and Supplemental Feed Additives) by Disease (West Nile Virus, Equine Rabies, Equine Influenza, Equine Herpes Virus, Potomac Horse Fever and Others), by Distribution Channel (Veterinary Hospitals and Clinics, Retail Pharmacies and Drug Stores and Others): Global Industry Perspective, Comprehensive Analysis and Forecast, 2017 - 2023. [Online]. Available at: https://www.zionmarketresearch.com/report/equine-healthcare-market. [Accessed: 20 November, 2018].
- Morter, R.L.(2016) Cattle Warts: Bovine Papillomatosis. Animal Health, Purdue University. [Online] Available at: https://www.extension.purdue.edu/extmedia/VY/VY-58.html. [Accessed: 4 December, 2018].
- Ngalonkulu, M (2018) The South African Horse Industry: A Potential Billion Rand Market. [Online] available at: https://www.forbesafrica.com/economy/2018/04/10/south-african-horse-industry-potential-billion-rand-market/ . [Accessed: 3 October, 2019].
- Pence, M. (2015) Cattle Warts – and show cattle. University of Georgia, College of Veterinary Medicine.

- Rushen and de Passillé (2013) The importance of improving cow longevity. Cow Longevity Proceedings. [Online] Available at: http://www.milkproduction.com/Library/Editorial-articles/Cow-Longevity-Conference-2013---proceedings/. [Accessed: 2 November, 2018].
- Rybicki, E.P. (1979) The serology of Bromoviruses. MSc. University of Cape Town.
- Thomas, H.S. (2013) Skin Problems in Young Cattle: Warts and Ringworm. [Online] Available at: https://www.tsln.com/news/cattle-health/skin-problems-in-young-cattle-warts-and-ringworm/. [Accessed: 23 October, 2018].
- The Equine Industry: A Global Perspective. Equine Business Association. [Online] Available at: https://www.equinebusinessassociation.com/equine-industry-statistics/. [Accessed: 24 November, 2018].

Appendix A:

A.

Protein Rank	Description	|Log Prob|	Best |Log Prob|	Best score	Total Intensity
1	|E1AXT8|E1AXT8_NICBE Glycolate oxidase OS=Nicotiana benthamiana GN=GOX PE=2 SV=1	42,69	6,41	392,40	75779457,
2	|E5LLE7|E5LLE7_NICBE Phosphoglycerate kinase OS=Nicotiana benthamiana PE=2 SV=1	31,01	6,43	430,30	12142751,
3	|A0A0F7R5Z5|A0A0F7R5Z5_NICBE Adenosylhomocysteinase OS=Nicotiana benthamiana GN=NbSAHH1a PE=2 SV=1	28,25	6,33	461,30	42012698,
3	|I3QHX5|I3QHX5_NICBE Adenosylhomocysteinase OS=Nicotiana benthamiana PE=2 SV=1				
4	|Q6XX19|Q6XX19_NICBE Translation elongation factor 1 alpha (Fragment) OS=Nicotiana benthamiana PE=2 SV=1	24,48	6,42	510,40	405380664,
5	|A0A0A8IBT8|A0A0A8IBT8_NICBE Glyceraldehyde-3-phosphate dehydrogenase OS=Nicotiana benthamiana GN=NbGAPDH-A PE=2 SV=1	22,93	6,21	379,80	25750556,
6	|A4D0K0|A4D0K0_NICBE Carbonic anhydrase (Fragment) OS=Nicotiana benthamiana PE=2 SV=1	18,94	6,33	445,20	37794118,
7	|C0LSK7|C0LSK7_NICBE Guanosine nucleotide diphosphate dissociation inhibitor OS=Nicotiana benthamiana GN=GDI PE=2 SV=1	14,07	4,95	362,70	16276037,
8	|C6FFS2|C6FFS2_NICBE Catalase OS=Nicotiana benthamiana GN=CAT1 PE=2 SV=1	11,15	6,25	330,40	6043461,
8	|K0IBB4|K0IBB4_NICBE Catalase (Fragment) OS=Nicotiana benthamiana PE=2 SV=1				
9	>sp|P03103|VL1_BPV1 Major capsid protein L1 OS=Bovine papillomavirus type 1 GN=L1 PE=1 SV=1	10,77	6,16	353,30	10661921,
10	|C9DFB9|C9DFB9_NICBE Heat shock protein 70-like protein (Fragment) OS=Nicotiana benthamiana GN=HSP70 PE=2 SV=1	10,54	6,73	296,10	583205,
10	|D4P5A4|D4P5A4_NICBE HSP70-like protein (Fragment) OS=Nicotiana benthamiana PE=2 SV=1				
11	|A0A0S4IJL0|A0A0S4IJL0_NICBE Ribulose bisphosphate carboxylase small chain OS=Nicotiana benthamiana GN=rbcS PE=2 SV=1	8,88	4,39	387,30	79953320,
12	|H9C954|H9C954_NICBE Actin (Fragment) OS=Nicotiana benthamiana GN=act PE=2 SV=1	8,54	3,83	184,10	5652647,
13	|A0A0F7JJ49|A0A0F7JJ49_NICBE Glyceraldehyde-3-phosphate dehydrogenase OS=Nicotiana benthamiana GN=GAPC3 PE=2 SV=1	8,22	3,47	218,60	447900,
14	|Q7XAF5|Q7XAF5_NICBE Phosphotransferase OS=Nicotiana benthamiana GN=HXK1 PE=2 SV=1	7,43	6,20	360,50	669329,
15	|A0A0S0N5Y9|A0A0S0N5Y9_NICBE Tubulin alpha chain OS=Nicotiana benthamiana GN=TUA6 PE=2 SV=1	6,55	3,43	207,00	4666540,
17	|A0A0F7R0S4|A0A0F7R0S4_NICBE Cystathionine gamma synthase OS=Nicotiana benthamiana GN=NbCGS1a PE=2 SV=1	6,00	5,89	252,70	6401087,
19	|A0A0H5AWB2|A0A0H5AWB2_NICBE Hydroxymethylglutaryl coenzyme A synthase OS=Nicotiana benthamiana GN=NbHMGS1a PE=2 SV=1	4,65	4,51	313,90	7449664,
21	|B7U9Z3|B7U9Z3_NICBE ER luminal-binding protein OS=Nicotiana benthamiana GN=BLP4 PE=2 SV=1	3,61	2,52	179,90	700883,

B.

Protein Rank	Description	|Log Prob|	Best |Log Prob|	Best score	Total Intensity
1	|E5LLE7|E5LLE7_NICBE Phosphoglycerate kinase OS=Nicotiana benthamiana PE=2 SV=1	51,41	7,25	413,40	16230002,2
2	|A0A0A8IBT8|A0A0A8IBT8_NICBE Glyceraldehyde-3-phosphate dehydrogenase OS=Nicotiana benthamiana GN=NbGAPDH-A PE=2 SV=1	42,12	7,51	377,30	41992513,6
3	|Q6XX19|Q6XX19_NICBE Translation elongation factor 1 alpha (Fragment) OS=Nicotiana benthamiana PE=2 SV=1	31,61	7,12	521,70	215658508,6
4	|A0A0F7R5Z5|A0A0F7R5Z5_NICBE Adenosylhomocysteinase OS=Nicotiana benthamiana GN=NbSAHH1a PE=2 SV=1	30,76	6,77	447,50	37779445,2
4	|I3QHX5|I3QHX5_NICBE Adenosylhomocysteinase OS=Nicotiana benthamiana PE=2 SV=1				
5	|A0A088F8F4|A0A088F8F4_NICBE Chloroplast ATP-dependent Clp protease chaperone protein OS=Nicotiana benthamiana GN=ClpC1B PE=2 SV=1	26,14	6,86	312,30	21949980,7
6	|E1AXT8|E1AXT8_NICBE Glycolate oxidase OS=Nicotiana benthamiana GN=GOX PE=2 SV=1	22,91	6,54	351,30	34546467,0
7	|B7U9Z3|B7U9Z3_NICBE ER luminal-binding protein OS=Nicotiana benthamiana GN=BLP4 PE=2 SV=1	18,94	7,22	328,40	5175487,2
8	|A0A0S0N5Y9|A0A0S0N5Y9_NICBE Tubulin alpha chain OS=Nicotiana benthamiana GN=TUA6 PE=2 SV=1	18,75	6,32	275,90	15661705,5
9	|C9DFB9|C9DFB9_NICBE Heat shock protein 70-like protein (Fragment) OS=Nicotiana benthamiana GN=HSP70 PE=2 SV=1	18,19	7,33	361,50	1015885,6
9	|D4P5A4|D4P5A4_NICBE HSP70-like protein (Fragment) OS=Nicotiana benthamiana PE=2 SV=1				
10	|C0LSK7|C0LSK7_NICBE Guanosine nucleotide diphosphate dissociation inhibitor OS=Nicotiana benthamiana GN=GDI PE=2 SV=1	17,77	7,20	287,10	32146184,3
11	|A0A0F7R0S4|A0A0F7R0S4_NICBE Cystathionine gamma synthase OS=Nicotiana benthamiana GN=NbCGS1a PE=2 SV=1	16,18	5,56	297,60	39701438,3
12	|H9C954|H9C954_NICBE Actin (Fragment) OS=Nicotiana benthamiana GN=act PE=2 SV=1	14,64	7,07	278,10	10412959,0
13	|A0A0F7JJ49|A0A0F7JJ49_NICBE Glyceraldehyde-3-phosphate dehydrogenase OS=Nicotiana benthamiana GN=GAPC3 PE=2 SV=1	14,33	7,33	288,00	5733772,9
14	|A4D0K0|A4D0K0_NICBE Carbonic anhydrase (Fragment) OS=Nicotiana benthamiana PE=2 SV=1	14,06	7,39	439,00	9341365,0
14	|A4D0J9|A4D0J9_NICBE Carbonic anhydrase (Fragment) OS=Nicotiana benthamiana PE=2 SV=1				
15	|Q14RS6|Q14RS6_NICBE 1-deoxy-D-xylulose-5-phosphate reductoisomerase (Fragment) OS=Nicotiana benthamiana GN=dxr PE=2 SV=1	12,16	4,43	247,40	2972033,2
16	|A0A0S4IJL0|A0A0S4IJL0_NICBE Ribulose bisphosphate carboxylase small chain OS=Nicotiana benthamiana GN=rbcS PE=2 SV=1	11,61	4,90	389,20	133350103,1
17	|Q7XAF5|Q7XAF5_NICBE Phosphotransferase OS=Nicotiana benthamiana GN=HXK1 PE=2 SV=1	11,17	6,88	393,10	1285058,0
18	|A0A0H5AWB2|A0A0H5AWB2_NICBE Hydroxymethylglutaryl coenzyme A synthase OS=Nicotiana benthamiana GN=NbHMGS1a PE=2 SV=1	8,40	5,60	310,70	9229228,9
19	|Q52JJ5|Q52JJ5_NICBE Glutamyl-tRNA synthetase OS=Nicotiana benthamiana GN=GRS PE=2 SV=1	7,66	5,11	259,20	2039372,2
20	|C6FFS2|C6FFS2_NICBE Catalase OS=Nicotiana benthamiana GN=CAT1 PE=2 SV=1	7,44	7,16	308,40	2532758,4

Figure 1. Protein rankings and fragments of BPV1 L1 identified by mass spectrometry

Figure 1.A. shows the top 20 proteins identified by mass spectrometry from the L1-infiltrated samples, ranked according to their log probability, with the BPV1 L1 protein shown in pink. **Figure 1.B**. shows the proteins identified in the negative sample.

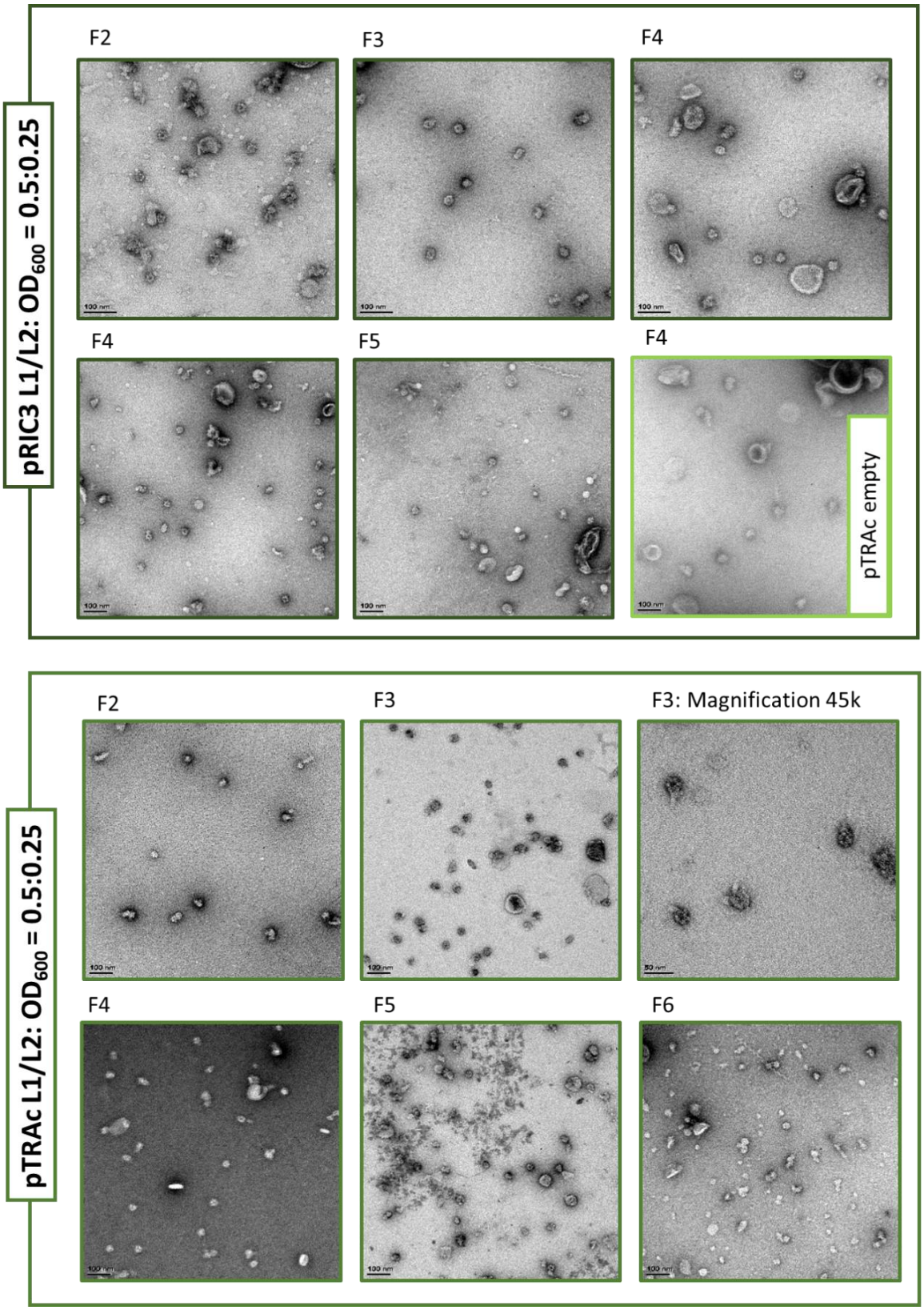

Figure 2. TEM images of pRIC3-L1/L2 and pTRAc-L1/L2 VLPs

Electron micrographs of L1/L2 co-infiltration purifications for pRIC3 and pTRAc. A negative control of plants infiltrated with pTRAc empty vector was included. Magnification was performed at 35,000x and the size bar is indicated in each of the images.

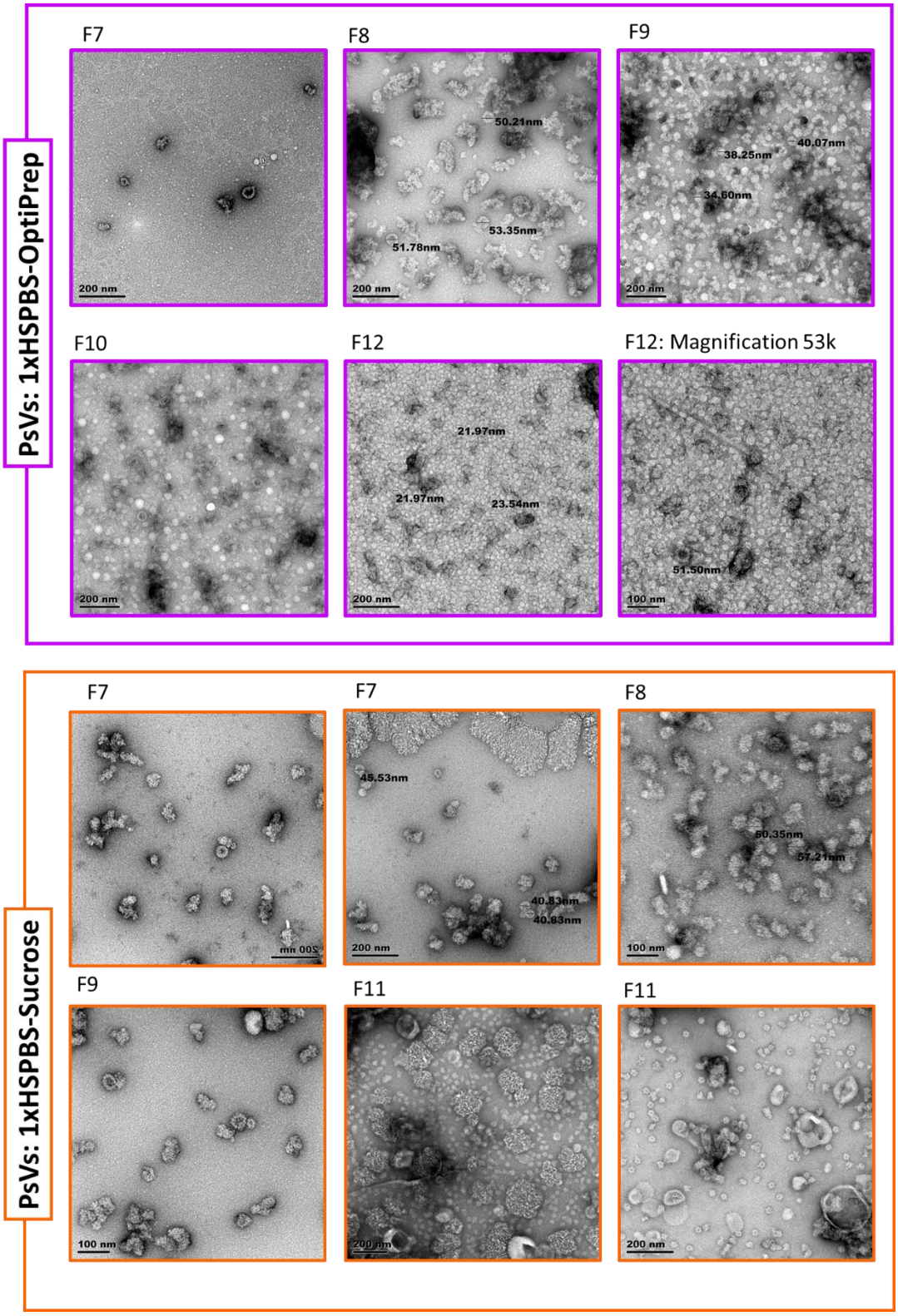

Figure 3. TEM images of sucrose vs. iodixanol purified PsVs in a 1xHSPBS buffer

Magnification was performed at 35,000x, and the size bar is indicated in each of the images. F= Fraction.

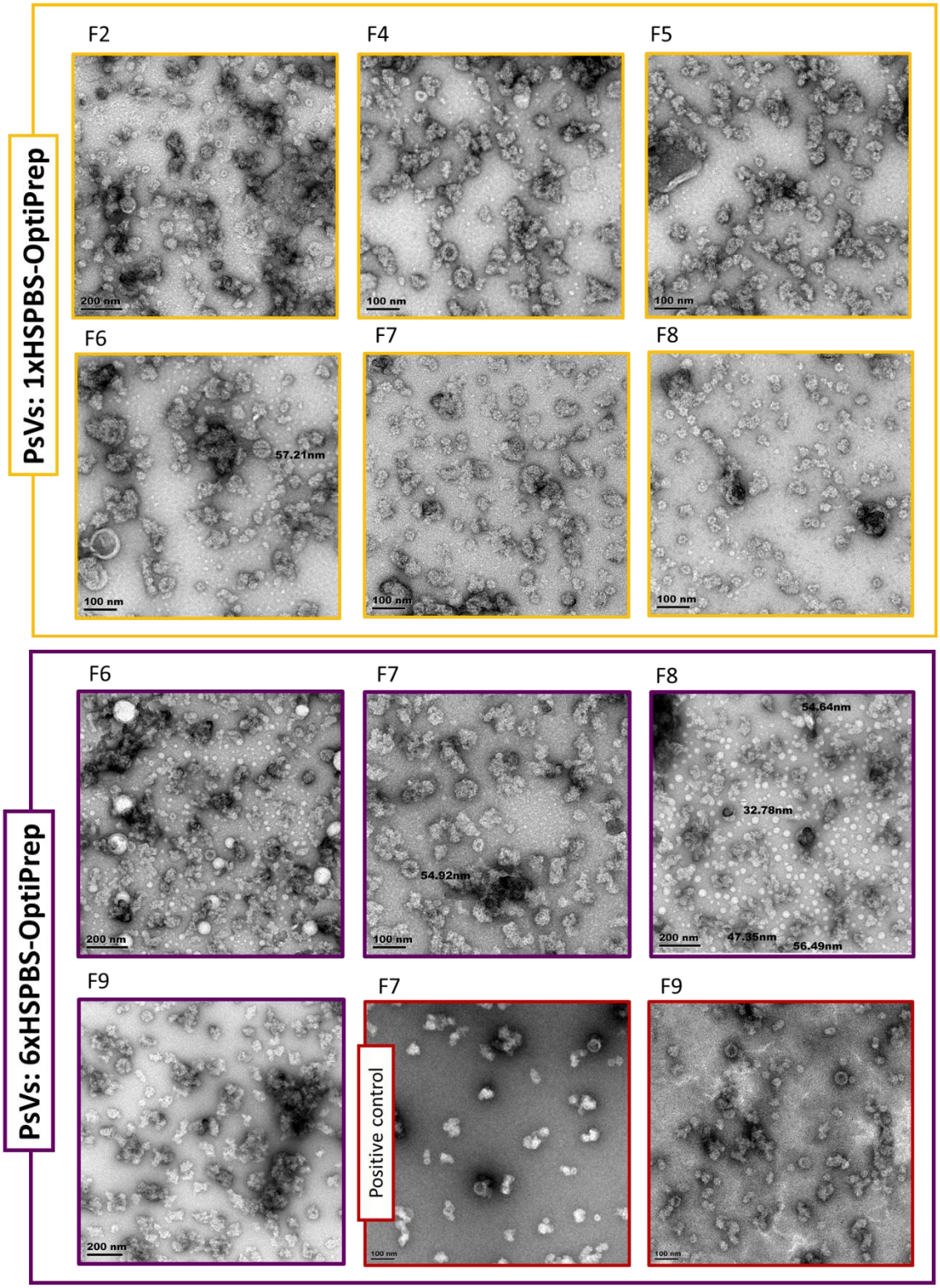

Figure 4. TEM Images of PsVs purified by 1x- or 6-HSPBS iodixanol gradient centrifugation

Positive control = First batch of PsVs purified by 6xHSPBS-iodixanol gradient. Magnification was performed at 35,000x, and the size bar is indicated in each of the images. F=Fraction.

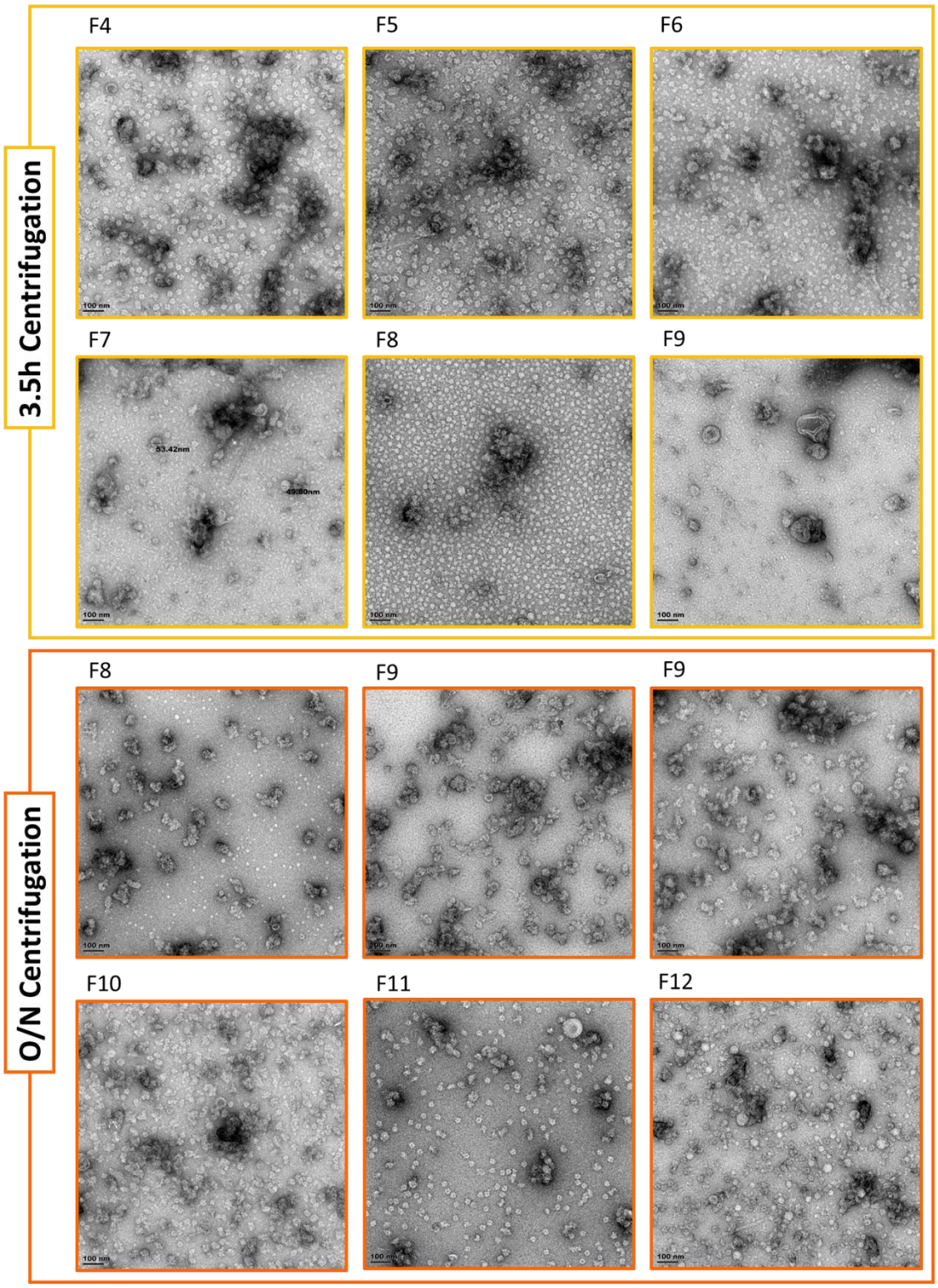

Figure 5. Overnight vs. standard centrifugation of 6xHSPBS-iodixanol purified PsVs

Magnification was performed at 35,000x, and the size bar is indicated in each of the images.

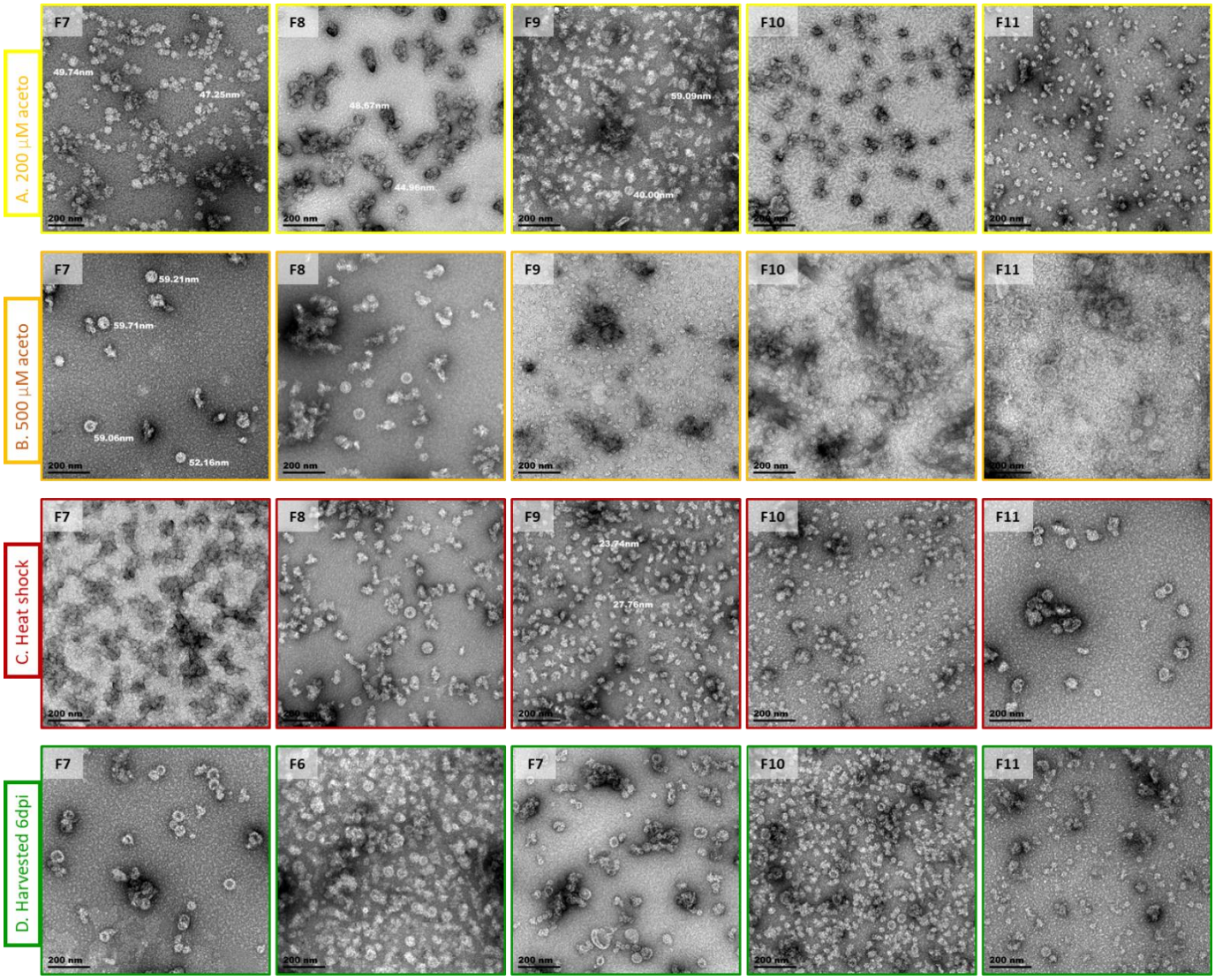

Figure 6. TEM images of expression optimised PsVs

Magnification was performed at 35,000x, and the size bar is indicated in each of the images.